UNIVERSITÀ
DEGLI STUDI
DI PADOVA

UNIVERSITA' DEGLI STUDI DI PADOVA

DIPARTIMENTO DI BIOLOGIA

SCUOLA DI DOTTORATO DI RICERCA IN BIOSCIENZE

INDIRIZZO: GENETICA E BIOLOGIA MOLECOLARE DELLO SVILUPPO

CICLO XXIII

Drosophila melanogaster AS A MODEL TO STUDY MITOCHONDRIAL DISEASES

Direttore della Scuola: Prof. Giuseppe Zanotti
Coordinatore d'indirizzo: Prof. Paolo Bonaldo
Supervisore: Prof. Mauro A. Zordan

Dottorando: Caterina Da Rè

31 gennaio 2011

INDEX

Drosophila melanogaster AS A MODEL TO STUDY MITOCHONDRIAL DISEASES

PART I Functional analysis of d*Surf1* gene using *Drosophila* as a model organism

PART II Characterization of ETHE1, a mitochondrial dioxigenase

PART III Mutations in TTC19 encoding gene cause a severe mitochondrial disease in humans and flies

PART IV Functional characterization of *Drosophila melanogaster* mitochondrial deoxynucleotide transport

UNIVERSITÀ
DEGLI STUDI
DI PADOVA

UNIVERSITA' DEGLI STUDI DI PADOVA

DIPARTIMENTO DI BIOLOGIA

SCUOLA DI DOTTORATO DI RICERCA IN BIOSCIENZE

INDIRIZZO: GENETICA E BIOLOGIA MOLECOLARE DELLO SVILUPPO

CICLO XXIII

Drosophila melanogaster AS A MODEL TO STUDY MITOCHONDRIAL DISEASES

Direttore della Scuola: Prof. Giuseppe Zanotti
Coordinatore d'indirizzo: Prof. Paolo Bonaldo
Supervisore: Prof. Mauro A. Zordan

Dottorando: Caterina Da Rè

31 gennaio 2011

PART I

Morphological and functional characterization of *Surf1* gene post-transcriptional silencing in *Drosophila melanogaster*

Leigh Syndrome (LS) is an early onset progressive mitochondrial encephalopathy usually leading to death within the first decade of life (Leigh 1951). The single most prevalent cause of LS are mutations in the *Surf1* gene. LS patients with mutations in the *Surf1* gene show a marked and specific decrease in the activity of mitochondrial respiratory chain complex IV (cytochrome c oxidase, COX), the terminal enzyme in the respiratory chain. which encodes a protein located in the inner membrane of mitochondria which is thought to be involved in cytochrome c oxidase assembly, (Tiranti et al.1999, Dell'agnello et al. 2007). Since, the molecular mechanism leading to COX deficiency and the pathogenesis of neurodegeneration in human LS are still poorly understood, we had set up a *Drosophila melanogaster* model of this disease based on the post-transcriptional silencing of d*Surf1* (CG9943, the *Drosophila* homolog of h*Surf1*), via transgenic double-stranded RNA interference (Zordan et al. 2006). We used this Drosophila *Surf1*-IR strain to better understand the function(s) of SURF1 since the knockdown model shows wide concordances with the human LS *Surf1*$^{-/-}$ phenotype. Tissue-specific knock down of *Surf1* was produced by exploiting the yeast UAS/GAL4 binary system (Brand and Perrimon 1993). In particular we employed an RU486-sensitive driver to silence *Surf1* specifically in the adult fly, since silencing of *Surf1* during early development generally led to late larval lethality. We thus performed biochemical assays to measure COX activity in these knockdown flies. In addition, we also characterized, from the biochemical point of view, a transgenically "rescued" line in which it is possible to induce the simultaneous activation of d*Surf1*-synonymous expression and dsRNAi silencing of the endogenous *Surf1* gene. The functional characterization of such "rescued" flies shows a complete reversion of biochemical, behavioural and electrophysiological abnormalities which were present in the original knockdown individuals.

INTRODUCTION

1.1 The human *Surf1* gene

Human *Surf1* gene, located on chromosome 9 (9q34.2), is 4696 bp long, and consists of 9 exons encoding for a single 1029 bp transcript which is ubiquitously expressed (figure 1), (Yao & Shoubridge, 1999).

The human *Surf1* gene (GenBank BC071685) encodes a 31 kDa protein located in the inner mitochondrial membrane (Zhu et al. 1998, Tiranti et al. 1998). SURF1 protein is highly conserved from recent prokaryotes to humans (Poyau et al. 1999) and it is characterized by an N-terminal mitochondrial targeting sequence and by two trans-membrane domains (Tiranti et al. 1998, Yao et al. 1999). Most human *Surf1* mutations are of the nonsense type which are predicted to lead to the expression of a prematurely truncated and/or aberrant protein (Pequignot et al. 2001) and are involved in the determination of Leigh syndrome (LS, OMIM 256000). Mammalian *Surf1* belongs to the *surfeit* locus, which comprises a cluster of six non homologous housekeeping genes (*Surf1-6*) (Colombo et al. 1996), showing a strong conservation from birds to mammals, the function of which is relatively little known. *Surf1* is ubiquitously expressed in human tissues, in particular in aerobic tissues such as heart, skeletal muscle, and kidney (Yao and Shoubridge 1999). The SURF1 protein, which is highly conserved from recent prokaryotes to humans (Poyau et al. 1999) is characterized by an N-terminal mitochondrial targeting sequence, by two transmembrane domains and it is actively imported into mitochondria, where it localizes to the inner membrane (Tiranti et al. 1999a, Yao and Shoubridge 1999). More than 50 mutations of human *Surf1* have been reported, most of which are nonsense mutations which are predicted to lead to the expression of a prematurely truncated and/or aberrant protein (Pequignot et al. 2001).

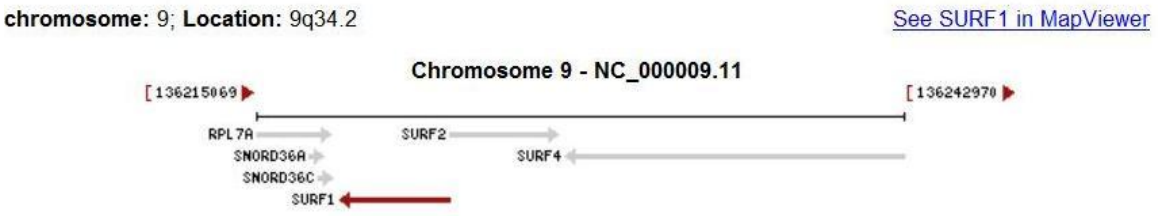

Figure 1.1. The human *Surf1* gene. The *Surf1* gene, (red), belongs to the *Surfeit* locus, which comprise other five *Surf* genes (*Surf2-6)*, in grey. *Surf1* is formed of 9 exons and codes for a single transcript of more or less 1Kb. Its non-coding regions are indicated in blue. http://www.ncbi.nlm.nih.gov.

1.2 The *Drosophila Surf1* gene

The *Drosophila melanogaster Surf1* homolog (CG9943-PA; *Surf1*) maps to chromosome 3L 65D4, and while the vertebrate homolog is part of the *surfeit* gene cluster, Drosophila *Surf* genes are dispersed throughout the genome (Zordan et al. 2006). The *Surf1* gene spans 1200 bp, and the 900-bp coding sequence consists of 4 exons. The inferred 300-aa protein features a 41-aa N-terminal mitochondrial targeting sequence and two transmembrane domains (included between amino acids 62–80 and 296–314, respectively). Following *Surf1* PTS, our findings show that this gene plays a fundamental role in the completion of the pupal-to-adult molt during development as well as in the accomplishment of oculomotor and sensori-neural functions in the adult fly (Zordan et al. 2006).

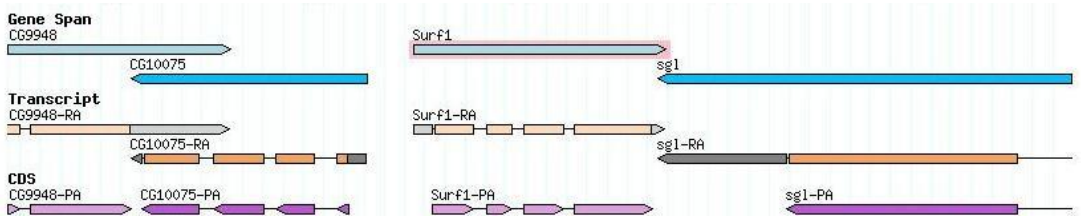

Figure 1.2. The Drosophila *Surf1* gene. *Surf1* Drosophila gene maps to chromosome 3L spans, it spans 1200 bp, and the 900-bp coding sequence consists of 4 exons. (Figure modified by http://flybase.org).

1.3 Leigh Syndrome

In humans, mutations in mitochondrial or nuclear genes encoding mitochondrial components are associated with a wide range of multisystem disorders affecting tissues highly dependent on mitochondrial energy, such as brain, muscle, heart, and the sensori-neural epithelia (Fadic and Johns 1996). An example of such a disorder is Leigh syndrome (LS, OMIM 256000), a progressive mitochondrial encephalopathy characterized by the presence of symmetric necrotizing lesions in subcortical areas of the central nervous system (CNS), including brain stem, cerebellum, diencephalon, and corpus striatum (Leigh 1951, Farina et al. 2002). The disease onset is in infancy, generally after a symptom-free interval of several months. By and large, neurological signs are correlated to the functional anatomy of the brain structures involved in the lesions and include generalized hypotonia, dystonia, ataxia, oculomotor abnormalities, disturbances of swallowing, breathing, and other brain-stem-related neurological functions and less frequently seizures, sensori-neural deafness, and optic atrophy (DiMauro and Schon 2003). The syndrome has a relentlessly progressive course, with death usually occurring within the first decade of life, although protracted cases are known (Tiranti et al. 1998).

The single most prevalent cause of LS are mutations in the *Surf1* gene, which encodes a 31-kDa protein located in the inner membrane of mitochondria (Tiranti et al. 1998, Zhu et al. 1998). Most human *Surf1* mutations are of the nonsense type which are predicted to lead to the expression of a prematurely truncated and/or aberrant protein (Pequignot et al. 2001).

The biochemical hallmark of LS *Surf1* mutant patients is a marked decrease in the activity of mitochondrial respiratory chain complex IV (COX) (Tiranti et al.1999b). COX is the terminal enzyme in both the eukaryotic and prokaryotic respiratory chain, catalyzing the reduction of molecular oxygen to water with concomitant proton pumping from the matrix to the intermembrane space. Studies in human cells (Tiranti et al. 1999a), mice (Agostino et al. 2003) and yeast (Nijtmans et al. 2001) indicate that SURF1 is involved in COX assembly (Coenen et al. 1999, Tiranti et al. 1999a, Hanson et al. 2001).

Cytochrome c oxidase (COX), the terminal enzyme of the mitochondrial respiratory chain (MRC), catalyzes the transfer of electrons from reduced cytochrome c to molecular oxygen (Zhu et al. 1998). COX is composed of 13 protein subunits, the three largest being encoded by mtDNA genes, and the remaining ten are encoded by nuclear DNA genes (Leigh 1951). A number of accessory factors are necessary for the formation of an active holoenzyme complex (Yao et al. 1999), including those involved in synthesis of heme a, incorporation of copper atoms and assembly of the protein backbone (Poyau et al. 1999). One of these factors, SURF1, is a 30 kDa hydrophobic protein embedded in the inner membrane of mitochondria. The absence, or malfunctioning, of SURF1 determines the accumulation of COX assembly intermediates, and a drastic reduction in the amount of fully assembled enzyme, in both yeast (Pequignot et al. 2001) and humans (Farina et al. 2002). As a consequence, profound COX deficiency (Leigh 1951) in multiple tissues of *Surf1* mutant patients (Tiranti et al. 1999a) leads to the development of Leigh syndrome, LS^{COX}, (Agostino et al. 2001).
Mutations in *Surf1* impair the incorporation of subunit II, resulting in a buildup of an early COX assembly intermediate, decrease in other COX subunits and a decrease in COX activity (Tiranti et al, 1999a). COX deficiency may also be complicated by cardiac pathology, including hypertrophic and dilated cardiomyopathies (Marin-Garcia et al. 1999, Holmgren et al. 2003) and conduction defects (DiMauro et al. 1988).

1.3.1 Murine model for LS

In vertebrates *Surf1* is part of the very tight and highly conserved *surfeit* gene cluster, which includes six genes (*Surf1–6*) (Agostino et al. 2003). The reason for long-standing maintenance of such a compact physical organization is obscure, since the corresponding SURF proteins are neither functionally nor structurally related to each

other. The precise function of the SURF1 gene product itself remains unknown, although the results of several studies in yeast and mammals suggest a role for SURF1 protein as an auxiliary chaperone like factor, involved in the early assembly steps of the COX protein backbone (Leigh 1951, Coenen et al. 1999, Tiranti et al. 1999a, Hanson et al. 2001).

To better understand the role of SURF1 and the pathogenesis of LS^{COX}, a constitutive knockout (KO) mouse model was created (Agostino et al. 2003), in which exons 5–7 of the *Surf1* gene were replaced by a neomycin-resistance (NEO) cassette (Nijtmans et al. 2001). Approximately 90% of the $Surf1^{NEO}$ –/– mice died at embryonic stages. The few animals that reached birth partially recapitulated, although to a lesser extent, the biochemical findings, but failed to display the clinical and neuro-pathological features of human LS^{COX} (Agostino et al. 2003).
A second *Surf1* KO model, based on the insertion of a *loxP* sequence in exon 7 of the murine *Surf1* gene ($Surf1^{loxP}$), lead to an aberrant, prematurely truncated and highly unstable protein. The +/+, +/– and –/– genotypes in newborn animals were in agreement with the mendelian distribution, indicating that, rather than to the ablation of *Surf1* itself, the high embryonic lethality observed in the previous $Surf1^{NEO}$–/– model was due to a spurious effect of the NEO cassette on the expression of neighboring genes. Similar to the previous $Surf1^{NEO}$ –/– mice, the $Surf1^{loxP}$ –/– mice displayed mild reduction of COX activity in all tissues, but no lesion resembling LS^{COX} encephalopathy was ever observed. However, when the sensitivity to Ca^{2+} dependent excitotoxicity, induced by exposure to high doses of kainic acid (a glutamatergic epileptogenic agonist), was tested in both $Surf1^{loxP}$ –/– brains and neuronal cell cultures, a virtually complete protection from *in vivo* neurodegeneration was observed. In addition, $Surf1^{loxP}$ –/– mice showed a marked increase in longevity, compared to heterozygous or homozygous wild-type (wt) littermates. These data suggest a role for SURF1 in intracellular Ca^{2+} homeostasis and mitochondrial control of aging which may be independent, at least in part, from those on COX assembly and mitochondrial bioenergetics (Dell'agnello et al. 2007).

1.3.2 Drosophila model for LS

Since, the molecular mechanism leading to COX deficiency and the pathogenesis of neurodegeneration which characterize human Leigh Syndrome are still poorly understood, a *Drosophila melanogaster* model was set up through the generation of functional knockdown (KD) lines for d*Surf1* (CG9943) (Zordan et al. 2006).
Transgenic double-stranded RNA interference was produced by post-transcriptional silencing employing a transgene encoding a dsRNA fragment of the d*Surf1*, activated by the UAS transcriptional activator. The GAL4-UAS binary yeast system (Brand et al. 1993) was exploited to drive the post-transcriptional silencing (PTS) of the target

gene transcript under the control of two alternative promoters: *Actin5C*, an early-expressed housekeeping gene, or *elav*, an early-expressed neuron-specific gene (Yao and White 1994). These drivers, *Actin5C–GAL4* or *elav–GAL4*, were used to induce silencing ubiquitously or pan-neuronally, respectively.

The main phenotypic features following ubiquitous *Actin5C-GAL4* driven d*Surf1* KD were severe impairment of larval development and reduced locomotion, which were likely caused by a generalized defect in respiration and ATP synthesis determined by d*Surf1* silencing. On the other hand, nervous system-wide silencing of d*Surf1* allowed to bypass late larval lethality observed with the ubiquitous driver. Not only did such individuals survive to adulthood, but they showed a strikingly enhanced survival with respect to controls. The larval stages of *elav-GAL4* d*Surf1* PTS individuals were morphologically comparable to controls although they presented slight impairment in locomotor activity and photobehaviour which is reminiscent of the widespread nervous system involvement observed in human mitochondria-related encephalomyopathies. A direct effect of d*Surf1* silencing on mitochondrial respiration was demonstrated by the significant reduction in the histochemical reaction to COX observed in the CNS of the *elav-GAL4* KD adult flies, paralleled by a strong increase in the SDH levels measured in the same tissues, which suggests a compensatory increase in mitochondrial mass. Furthermore, electron microscopic observation showed that in *Actin5C-GAL4* PTS individuals, mitochondria were much larger than normal, with evident morphological alterations, in particular regarding the organization of the internal membranes (Zordan et al. 2006).

Following *Surf1* PTS, these findings show that this gene plays a fundamental role in the completion of the pupal-to-adult molt during development as well as in the accomplishment of oculomotor and sensori-neural functions in the adult fly. The data are also indicative of important functions for SURF1, specifically related to COX activity, suggesting a crucial role of mitochondrial energy pathways in organogenesis and CNS development and function.

Altogether, the above results strongly support the involvement of respiratory deficiency in determining the developmental and functional impairments observed following *dSurf1* PTS in Drosophila individuals. In fact, it has recently been shown that the lethal effects of ubiquitous d*Surf1* PTS in Drosophila could be rescued by the concomitant expression of a *Ciona intestinalis* alternative oxidase (AOX) under the control of an inducible promoter (Fernandez-Ayala et al. 2009). Similarly to COX, AOX is a mitochondrial enzyme which is able to reduce molecular oxygen to water using hydrogen atoms, but differently to COX, this activity is not coupled to proton pumping. To further prove the specificity of *dSurf1* PTS we designed and implemented a rescue construct consisting in a synonymous copy of the d*Surf1* gene in which all the codons were altered so as to escape PTS induced by dsRNA targeting

of the wild type gene. Furthermore, we report of the extreme sensitivity of *Drosophila* adult flies to the lethal effects of acute PTS-mediated depletion of d*Surf1* during adulthood.

RESULTS AND DISCUSSION

3.1 Post transcriptional silencing of d*Surf1* gene

We generated three independent Drosophila transgenic lines, 23.4, 79.10, and 79.1. For each line obtained, the insert map position is given in parentheses: 23.4 (2R, 54BC), 79.1 (3R, 88D) and 79.10 (2R, 50C). Each line carried a single UAS–*Surf1* inverted repeat (IR) autosomal insertion, which allowed the post-transcriptional gene silencing of *Surf1* via dsRNA interference (dsRNAi), following activation by *GAL4*.

The post transcriptional silencing of d*Surf1* was driven first of all ubiquitously, by crossing the IR line with the *Actin5C–GAL4* driver. In this way, KD produced 100% egg-to-adult lethality. The biochemical profile of these *Actin5C* KD larvae showed a significant decrease in the activity of all five respiratory complexes (CI–CV).

In order to obtain further information on the tissue specificity of the effects resulting from the KD of d*Surf1*, we set up genetic crosses which would lead to the silencing of d*Surf1* in all the mesodermal derivates. In this case, post-transcriptional silencing of d*Surf1* is driven by the how^{24B}*–GAL4* driver. *Surf1*(how^{24B}) KD individuals do not develop to adulthood and die during the early steps of pupal metamorphosis (PM) or, sometimes, at slightly later stages. Confocal analysis of GFP-tagged larval muscles revealed the presence of defects in the morphology of the muscle cell nuclei.

Surprisingly d*Surf1* KD limited to the nervous system, by using the pan-neuronal *elav-GAL4* driver, did not cause lethality (Zordan et al., 2006). Contrariwise, such individuals develop to adulthood and additionally live longer than controls, although COX enzymatic activity measured in mitochondrial extracts obtained from the heads of these KD animals is specifically and markedly decreased.

We also performed experiments to silence d*Surf1* in the posterior compartment of the eye-antennal disc, using the specific *GMR–GAL4* driver. In this case we were unable to detect any morphological abnormalities in eye development nor were there any signs of alterations in the developmentally programmed pattern of apoptosis in this compartment.

Finally we employed the *Switch–Act–GAL4* (RU–486 sensitive promoter) driver to induce the ubiquitous silencing of d*Surf1* in a temporally controlled manner, with the objective of specifically silencing *dSurf1* in fully developed adult flies.

3.1.1 Ubiquitous KD of *Surf1*

The *Actin5C* (*Act–GAL4*) driver was used for early, ubiquitous expression of dsRNAi-mediated KD.

Northern blot analysis on the *Act–GAL4 KD* larvae showed the presence of an approximately 2-kb band corresponding to the RNAi d*Surf1* transcript, as well as a smear starting from 0.9 kb, the expected size of the d*Surf1* transcript (clearly visible in the controls on the left in Figure 3.1.A), corresponding to degradation products originating from the post-transcriptional silencing of the d*Surf1* gene transcript (Figure 3.1.A). Controls were larvae and adults from strain w^{1118}, which was used to generate the UAS–*Surf1* IR transgenic lines. The same 2–kb band was visualized by

rehybridization of the blot with a probe complementary to the GFP spacer used in the RNAi d*Surf1* construct (data not shown). Real-time PCR-based quantitative analysis confirmed a drastic reduction of *dSurf1* mRNA (Figure 3.1.B), which corresponded to the virtual absence of dSURF1 protein, as demonstrated by Western blot analysis (Figure 3.1.C).

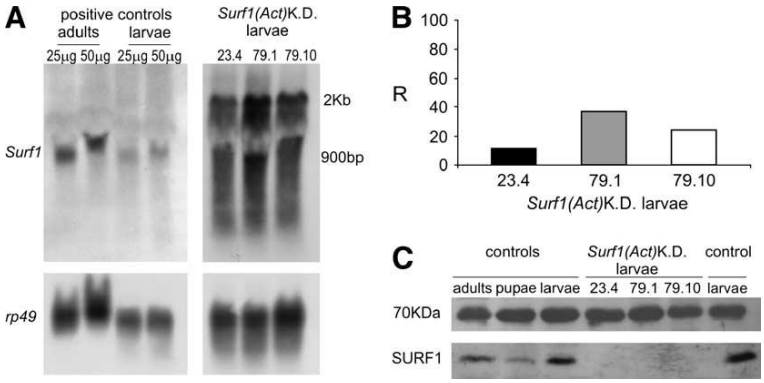

Figure 3.1. Expression analysis in *Actin5C–GAL4* Surf1 KD larvae. (A) Northern blot analysis using as a probe the complete cDNA of the *Surf1* gene. The 2-kb band is relative to the transcription of the hairpin construct while the intense smear, below the band at 0.9 kb (which corresponds to the *Surf1* transcript), is indicative of degradation products resulting specifically from dsRNAi. This pattern of degradation is not seen when the Northern blots are hybridized with a probe against the heterologous GFP spacer which separates the two arms of the IR (data not shown). Signs of very slight a specific mRNA degradation (probably artifactual) are also visible below the 2-kb band, as well as below the rp49 band in the samples collected from larvae, but not in those from adults. Positive controls consisted in mRNA extracted from larvae of the w^{1118} strain, which was used to generate the UAS–*Surf1* inverted repeat transgenic lines, for which two different quantities of mRNA (25 and 50 mg) were loaded on the gels. The experiments with the KD individuals were done using 50 mg of mRNA. In each case a housekeeping gene, i.e., rp49 (which encodes for Drosophila ribosomal protein 49), served as an external reference. **(B)** Real-time PCR estimate of the relative percentage of *Surf1* mRNA in KD individuals from each of the three lines analyzed compared to those of the respective parental lines bearing only the UAS–*Surf1*-inverted repeat (controls). In each case controls are assigned an arbitrary value of 100%. Histograms represent the mean of two independent experiments. Values obtained for each independent experiment were: 32 and 43 for *Act–GAL4* KD 79.1, 12.5 and 36 for *Act–GAL4* KD 79.10, 7.5 and 12.2 for *Act–GAL4* KD 23.4. **(C)** Western blot analysis on KD and control (see B) individuals. The 70-kDa band corresponds to an unknown protein, which was used as a reference signal for the quantization of the SURF1 signal. Controls consisted of mitochondrial protein extracts from larvae, pupae or adults of the w^{1118} strain (Zordan et al. 2006).

All individuals derived from the three transgenic lines in which KD was activted using the *Act–GAL4* driver showed 100% egg-to-adult lethality (Figure 3.2). Most individuals died as larvae, which were very sluggish and showed impaired development. In all three strains, the 7 day old KD larvae appeared smaller than age matched controls, with undersized optic lobes. The *Act–GAL4* KD 23.4 and *Act–GAL4* KD 79.10 individuals had the typical cuticular features of third-stage larvae while in *Act–GAL4* KD 79.1 larvae the morphological features were typical of the second instar stage. Only a few larvae, in particular from the *Act–GAL4* KD 23.4 and *Act–GAL4* KD 79.10 crosses, reached the pupal stage but they did not progress any further in development. Figure 3.2 shows the relative survival percentages of the three different transgenic KD lines and successively Figure 3.3 gives an idea of the

dimensions reached by the *Act–GAL4* KD 79.1 larvae, in fact this KD line shows the most severe phenotype.

In particular, starting from individuals of line 79.1, we genetically introduced into their background a publicly available UAS-GFP transgene by recombining it onto the same chromosome already bearing the interference construct, in order to produce flies having the GFP marker in association with the dsRNAi construct (i.e. following recombination their genotype was: UAS–GFP; 79.1 *Surf1* IR/III), in this manner the KD larvae were distinguishable by their green fluorescence.

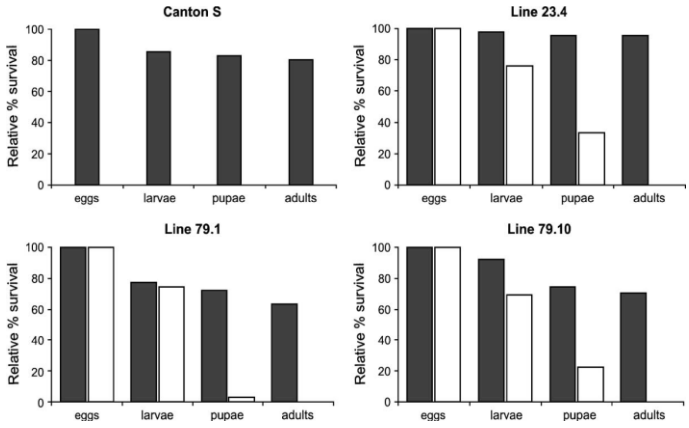

Figure 3.2. Relative percentage of egg-to-adult viability. Percentages were calculated at each of four developmental stages, i.e., eggs, larvae, pupae and adults, in controls (black) and *Actin5C–GAL4*-driven *Surf1* knockdown flies (white). For each line, the control consisted of individuals from the line bearing the non-activated UAS–*Surf1* inverted repeat. CS, Canton S, a reference wild-type strain (Zordan et al. 2006).

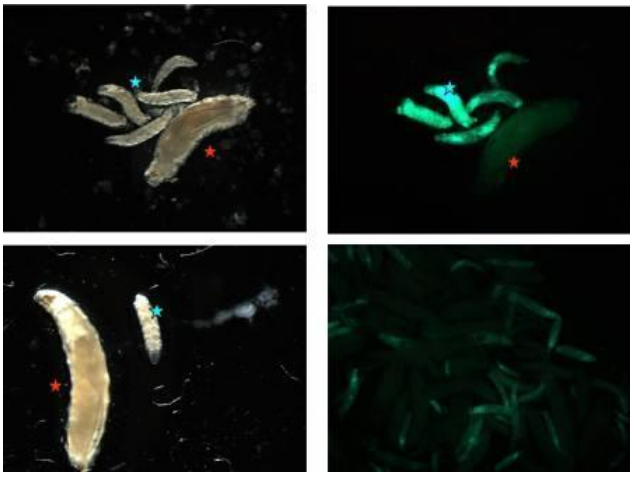

Figure 3.3. Morphology of larvae following ubiquitous knock down of d*Surf1*. Ubiquitous KD organisms were produced by crossing virgin homozygous UAS–*GFP*; 79.1*Surf1* female flies with homozygous *Actin5C–GAL4* male flies. Larvae in which the gene was knocked down (blue star: UAS–GFP/*Act5C-GAL4*; 79.1 *Surf1* IR/III) were easily recognisable because they expressed GFP ubiquitously as well as being sluggish and small. *Actin5C–GAL4* knock down produced 100% egg-to adult lethality with death occurring at the larval stages. The bigger larvae (red star: UAS–GFP/CyO; 79.1 *Surf1*IR /III), the ones which are not fluorescence are used as controls.

Biochemical assays were then performed to check the state of the mitochondrial respiratory chain in control larvae and in the *Act–GAL4*; GFP-79.1 KD individuals (distinguishable by their green fluorescence as shown in Figure 3.3). The enzymatic activities of Complexes I–V and Citrate Synthase were determined as described in (Autore et al., anno) (and see materials and methods). Complexes I–V activities in the larvae tissues are normalized to the activity of Citrate Synthase (CS), both expressed as nmol min^{-1} mg^{-1} and then expressed as a percentage relative to the concurrent wild type controls with the highest activity.

The *Act–GAL4*; GFP-79.1 larvae showed a decrease in Complex IV activity comparable to that of Complexes I, II and III (i.e. an approximately 40% decrease) (Figure 3.4).

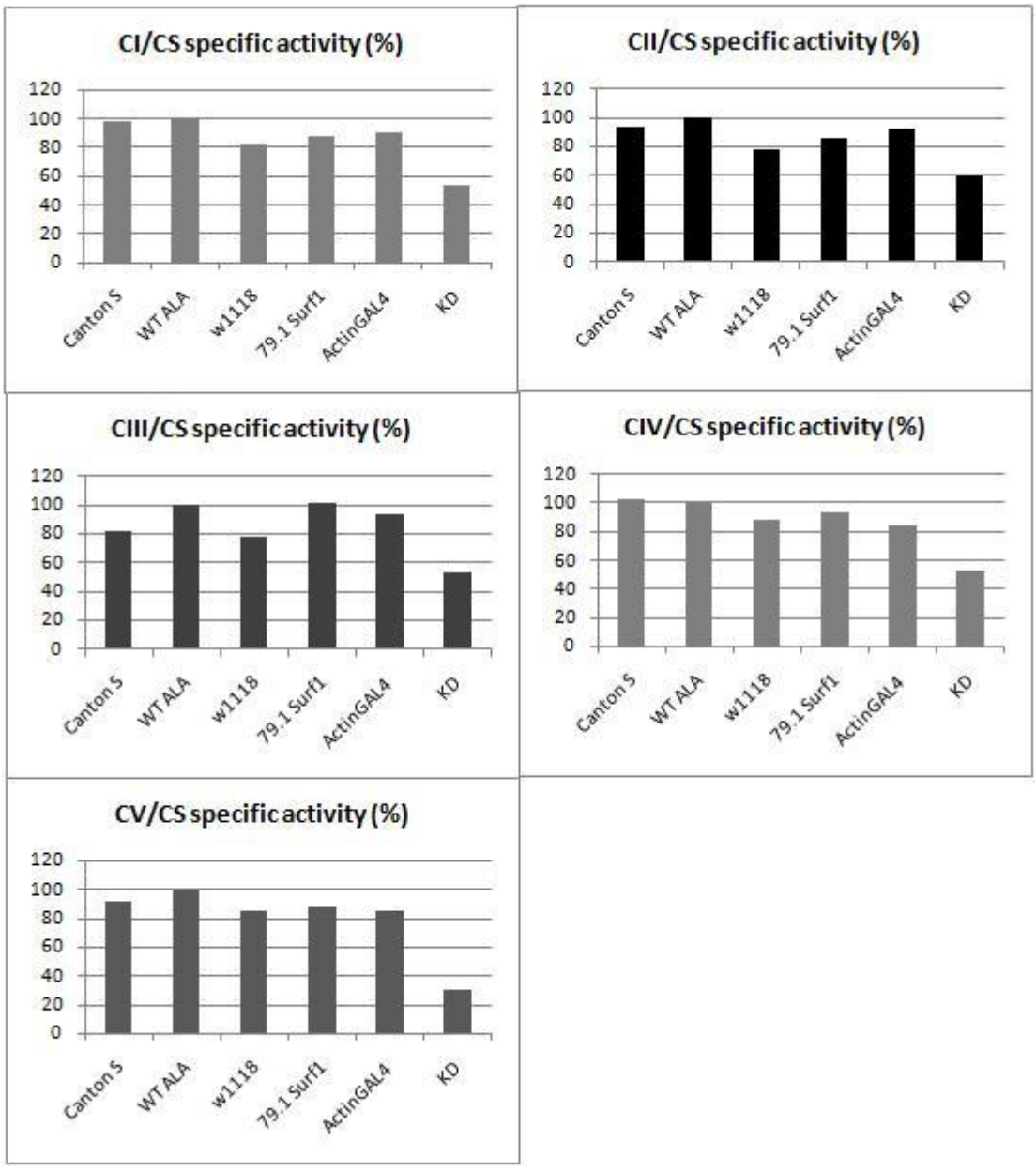

Figure 3.4. Mitochondrial respiratory chain enzymatic activities of control and *Act–GAL4*; GFP-79.1 KD larvae. Complexes I–V activities (all expressed as nmol min^{-1} mg^{-1}) normalized to the activity of Citrate Synthase (CS), are all expressed as percentage of enzymatic activity where WTALA strain's activity is considered as 100%. We measured enzymatic activity in three different wild type lines: Canton S, WT ALA, w^{1118} in the two parental lines: UAS–GFP; 79.1 *Surf1* IR/III, Actin5C-GAL4 and in the KD larvae (obtained by crossing between them the two parental strains). The graphs clearly show that the enzymatic activites in the KD individuals are in all cases markedly lower than the respective controls.

This result is at variance with what is observed in humans with *Surf1* deficiency–related Leigh syndrome (Zhu et al. 1998, Tiranti et al. 1998, Yao and Shoubridge 1999) and in the corresponding mouse model. Both these cases are characterized, at the biochemical level, by an isolated CIV deficiency (Dell'agnello et al. 2007). If the function of Surf1 is related exclusively to its role as a chaperone in the assembly of respiratory Complex IV, the KD of d*Surf1* is not expected to have direct effects on the activity of the other respiratory complexes. It should however be pointed out that, as already noted by (Fernandez-Ayala et al. 2009), the lack of *Surf1* leads to a variety of phenotypes in different organisms. In particular, evidence from yeast (Barrientos et al. 2002) and from mouse models suggests that *Surf1* may not only be involved in COX assembly, but may play a more general role in organization of the respiratory chain complexes and/or that it could also have as yet undescribed functions. Thus, it is possible that in Drosophila larvae, the decrease seen might be due to some form of interdependence of the respiratory complexes so that decreased levels of correctly assembled Complex IV may also causes a reduction in the amount of other mitochondrial complexes.

3.1.2 Central nervous system–restricted KD of d*Surf1* using *elav–GAL4* driver

To bypass the larval lethality caused by *Act–GAL4*-driven KD of *Surf1*, we restricted the expression of the dsRNAi to the CNS by using a pan-neuronal *elav–GAL4* driver. The *elav–GAL4* driver induces dsRNAi in the developing Central and peripheral nervous system and in the eye and antenna disc from early embryogenesis throughout larval development, and continues to be active in the corresponding areas of adult individuals (Yao and White, 1994). *elav–GAL4* KD *Surf1* dsRNAi had no effects on egg-to adult viability. Nonetheless, such KD individuals, show a striking and significant increase in lifespan with respect to controls (Figure 3.5) (Zordan et al. 2006).

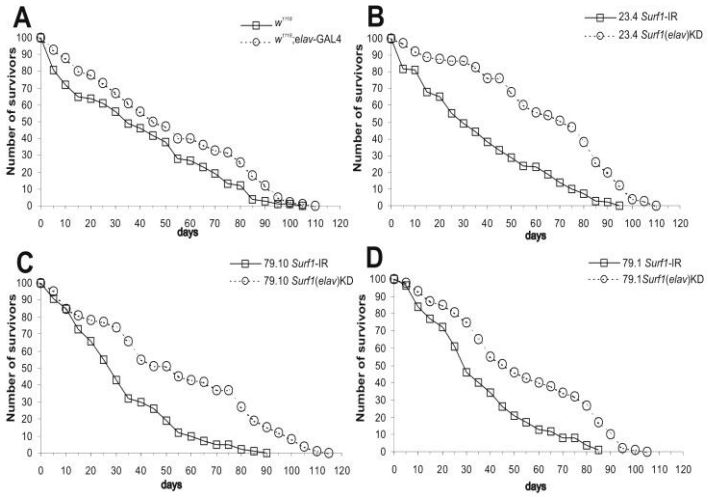

Figure 3.5. *Surf1(elav)*KD adults show enhanced long-term survival. Graphs showing the number of adult flies surviving after up to 115 days. (A) w^{1118} (the background used for transgenesis) and *elav–GAL4* x w^{1118}. (B) 23.4 *Surf1* IR and *Surf1*(*elav*)KD 23.4. (C) 79.10 *Surf1* IR and *Surf1*(*elav*)KD 79.10. (D) 79.1 *Surf1* IR and *Surf1*(*elav*)KD 79.1. For each graph the statistical comparison of the pairs of curves (i.e., KD vs. parental IR line) was done using the Wilcoxon test. (A) P ¼ NS; (B) P ¼ 0.008; (C) P ¼ 0.02; (D) P ¼ NS (Zordan et al. 2006).

Moreover biochemical assays were carried out with control flies and *elav–GAL4* KD flies where, in both lines, the heads were separated from the bodies and the two body parts assayed separately. Figure 3.6 shows Complex I and Complex IV (COX) percentage activities (nmol min^{-1} mg^{-1}) normalized to the activity of citrate synthase (CS), in the indicated tissues. In the heads of *Surf1*(*elav*)KD flies, COX activity was greatly reduced, whereas Complex I (CI) function was not altered in the same tissues. As a control, we also measured the activities of CI and COX in the bodies of the pan neuronal *Surf1* KD flies and we did not observe any differences between the KD and the control individuals.

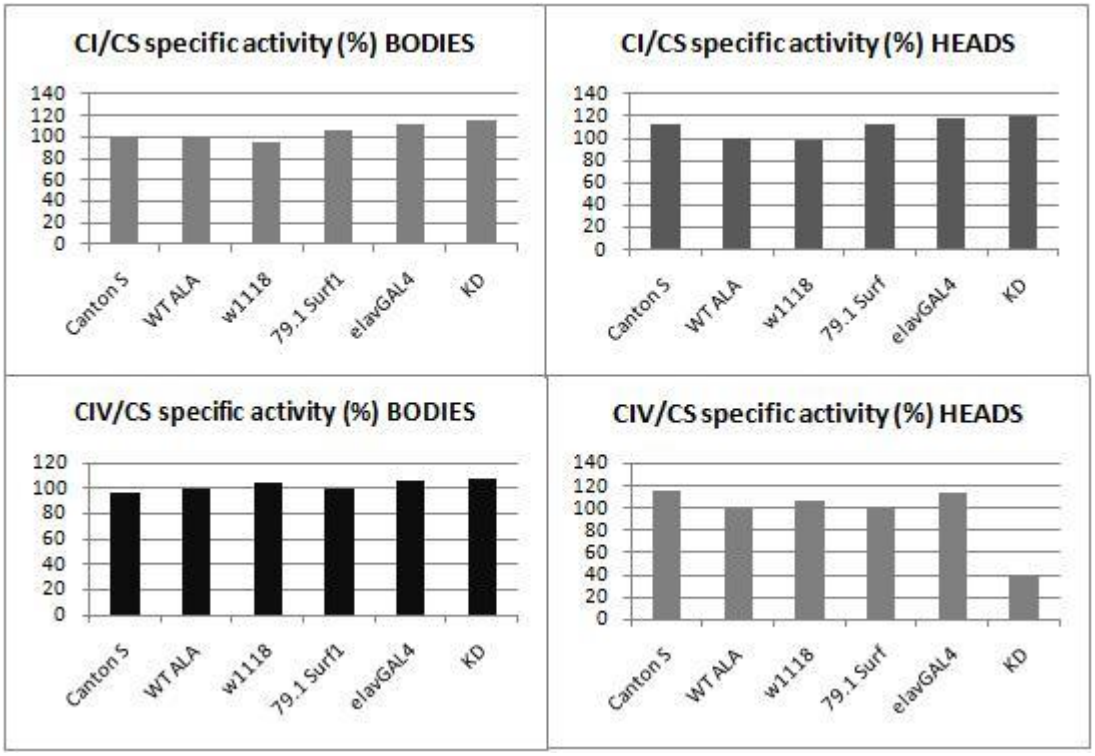

Fig. 3.6. Biochemical assay of Complex I and Complex IV activities in central nervous system-specific *Surf1* knock down adult flies. CI and COX activities, normalized to the activity of CS, are all expressed as percentage of enzymatic activity, where WTALA strain's activity is considered as 100%. Enzymatic activities were measured separately either in bodies or in heads of three different wild type lines: Canton S, WT ALA, w^{1118} ; two parental lines: UAS–GFP; 79.1 *Surf1* IR/III, *elav–GAL4* and in the KD individuals (obtained by crossing the two parental strains). The graphs clearly show that in the heads of *Surf1*(*elav*)KD individuals COX activity is markedly decreased with respect to controls.

3.1.3 Activation of dsRNAi in the mesodermal derivatives

When *Surf1* is post–transcriptionally silenced in all mesodermal derivatives from early embryonic stages to pupal metamorphosis (PM) by the *how*^{24B}*–GAL4* driver, all *Surf1*(*how*^{24B})KD individuals do not develop to adulthood and die during the early steps of PM or, sometimes, at slightly later stages of pupal development. It is clearly visible (Figure 3.7) that whilst in control pupae all developing adult tissues are present, in the KD pupae some of the adult tissues are not present. This is evdenced by the observation that six day-old *Surf1*(*how*^{24B})KD pupae show a void region approximately at the centre of the developing insect body (Figures 3.7, 3.8, 3.9). We monitored pupal development in *Surf1*(*how*^{24B})KD pupae every 24 hours, to try to establish at what time point this kind of "hole" began to appear. We observed that it began to appear already at 24 hours after the beginning of PM (Figure 3.7). By monitoring pupal development in both controls and *Surf1*(*how*^{24B})KD every 15 minutes starting from the beginning of pupal metamorphosis, (24 control and 24 *Surf1*(*how*^{24B})KD pupae), we observed that the "hole" started to appear more or less 3-4 hours after the beginning of PM and that it continued to grow in the following

four hours of monitoring. Figure 3.9 shows six hours of development from a single representative pupa. Finally the "hole" in 24 hours old *Surf1*(*how*^{24B})KD pupae reaches its maximum extension and did not enlarge further in the following days.

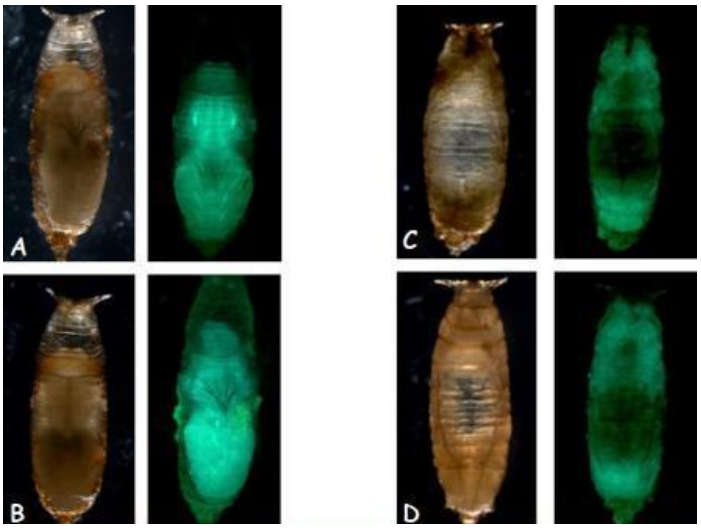

Figura 3.7. Fluorescence microscope images of six day-old control and *Surf1* (*how24B*)KD pupae. A and B are controls (UAS GFP/*how*^{24B}*–GAL4*), whereas C and D are *Surf1*(*how*^{24B})KD.

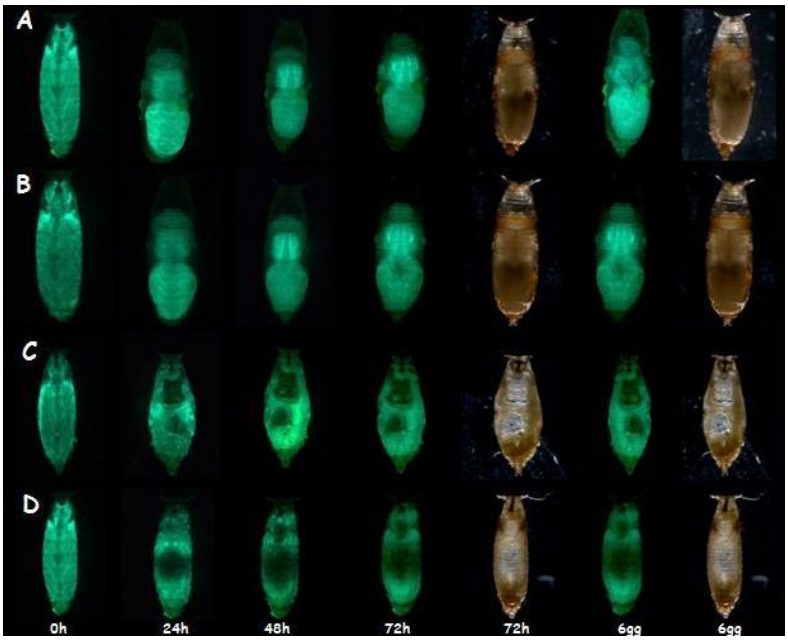

Figura3.8. Six day monitoring of *Surf1 how*^{24B} KD pupal development. We observed the pupal development of two control (panels A and B) and two *Surf1*(*how*^{24B})KD (panels C and D) individuals, checking the developmental state every 24 hours, starting from hour 0 (0h = the beginning of pupal metamorphosis) to 6 days. The region void region (i.e. unstained) is clearly visible in the centre of the *Surf1* (*how*^{24B}*)* KD individual's body.

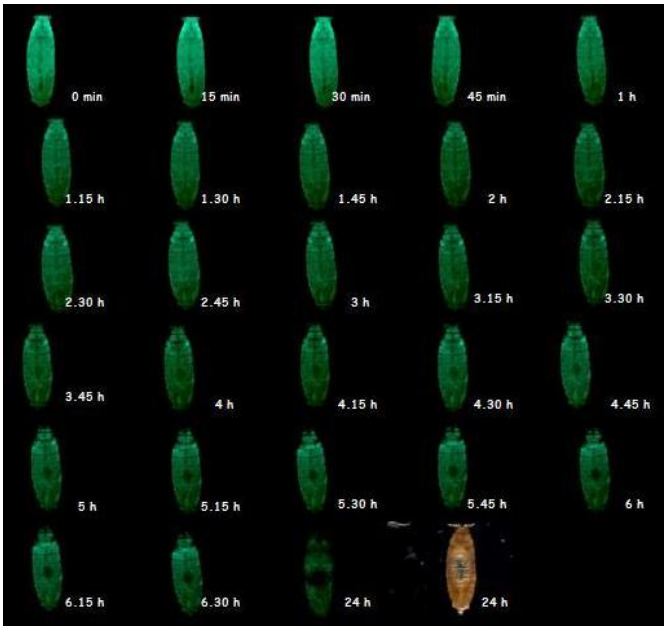

Figure 3.9. Six hour monitoring of *Surf1 how*^{24B} knock down pupae development beginning from 0 minutes of pupal metamorphosis (PM). In this case the void region begins to appear at approximately 3-4 hours of PM.

In order to check the state of the muscle tissue (one of the main mesodermal derivatives) in the *Surf1*(*how*^{24B})KD larvae, we dissected larvae (to obtain body–wall preparations, see material and methods) from ten control larvae (UAS GFP/*how*^{24B}–*GAL4*) and ten *Surf1*(*how*^{24B})KD larvae, after which we subjected these larval preparations to confocal microscope analysis. Figure 3.10 shows a typical example of the results obtained. The main morphological defect which was evidenced by this kind of analysis , was that *Surf1*-KD muscles presented profound alterations in the morphology of the nuclei.

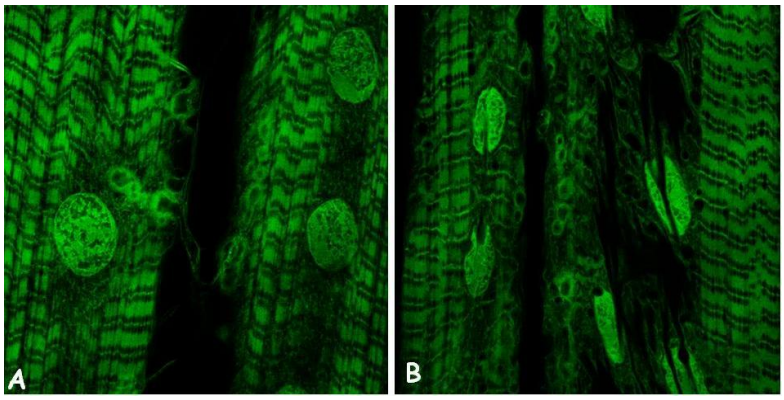

Figure 3.10. Confocal microscope image showing GFP-tagged larval muscle fibres from control (A) and *Surf1how*(*24B*)KD larvae (B).

In attempting to find an explanation for the developmental problems manifested by the *Surf1*(*how*^{24B})KD individuals we thought of trying to establish whether the

defects observed might be due, for instance, to increased levels of apoptosis in the tissue in which *dSurf1* was silenced. In order to test this hypothesis we implemented an approach base on the use of the *GMR-GAL4* driver.

3.1.4 Eye-Antenna disc KD of *Surf1* using the *GMR-GAL4* driver

The *GMR-GAL4* driver targets the expression of *GAL4* to the posterior compartment of the eye-antennal disc. Thus, in our case the use of this driver would lead to the knoc down of *dSurf1* specifically in the developing eye-antennal anlage. It is thus possible to evaluate: (i) whether *Surf1* KD in this compartment induces developmental defects observable as morphological alterations in the strictly geometrical structure of the compound eye; (ii) the levels of apoptosis detectable at the level of the imaginal discs, after staining with acridine–orange. In the latter case, since the GMR driver is specific to the posterior compartment of the imaginal disc, the anterior compartment serves as an internal negative control. However, no signs of developmental anomalies were observed in *GMR–GAL4 Surf1* KD adult flies and following dissection of the larval imaginal discs in the same individuals we did not observed any significant alterations in the pattern of developmentally controlled apoptosis, leading us to conclude that the particular phenotype we observed in the *Surf1*(*how*^{24B})KD pupae is probably not ascribable to apoptotis.

3.1.5 Ubiquitous post–transcriptional silencing of d*Surf1* using the RU486–sensitive inducible driver

In this case our aim was to establish the effects of post transcriptional silencing of d*Surf1* in adult indivuals, since all the drivers employed by us so far, were expressed early during embryonic and/or larval development. To do this we employed an RU–486 sensitive-*Act5C-GAL4* driver (*Switch–Act5C–GAL4*). In this case GAL4 is produced in a ubiquitous pattern determined by the Act5C promoter, but this promoter is subjected to the control of the RU–486 sensitive promoter, which requires the presence of the estrogen RU–486 in order to be active. RU–486 can be simply fed to the individuals bearing such a promoter. Pilot experiments using the *Switch–Act5C–GAL4* showed some promoter leakiness. In our hands this is evidenced by the fact that at room temperature (24-25°C), flies harboring the promoter transgene as well as the d*Surf1*–targeting dsRNAi show late larval lethality in the absence of pharmacological induction of the promoter. Such lethality could be "rescued" simply by growing such larvae at 20°C. Adults allowed to develop at 20°C and then transferred to 25°C show 100% lethality within 48 hours. Apart from the question of the *Switch–Act5C–GAL4* promoter leakiness, these results suggest that Drosophila adults are particularly sensitive to the lack of d*Surf1*.

In order to determine whether adult lethality produced by late activation of d*Surf1* knock-down was paralleled by alterations in the levels of CIV activity, we analyzed respiratory complex levels in *Switch–Act5C–GAL4–*d*Surf1* KD flies. To circumvent the inherent leakiness of the RU–486 sensitive promoter, all experiments were conducted at 20°C. Activation of the driver was thus obtained following transferral of the adult flies to food additioned with RU–486. Under these conditions 100% of the adult flies died within 48 hours of exposure to RU–486.

Figure 3.11 shows, for the different genotypes analyzed, the enzymatic activity ratios, with respect to Citrate synthase, for respiratory Complexes I and IV, respectively. No relevant variations in enzymatic activity, as a function of genotype, were observed for Complex I. On the other hand, a marked variation was evidenced in the case of Complex IV activity (Fig. 3.11). In particular d*Surf1* KD individuals showed an approximately 40% reduction in activity as compared to the controls.

These results point to the elevated sensivity of Drosophila adults to the acute lack of d*Surf1*, during adulthood.

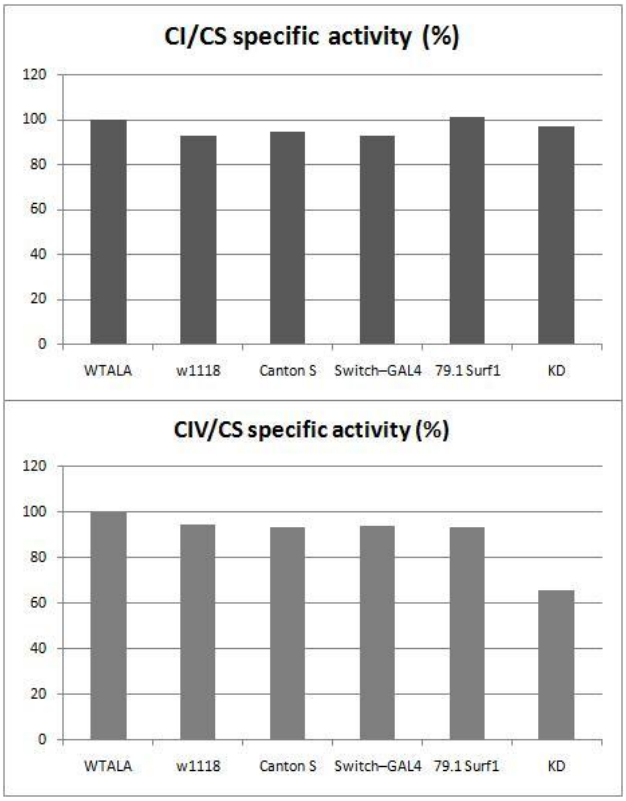

Figure 3.11. Biochemical assay of Complex I and Complex IV activities in *Switch–Act5C–GAL4–*d*Surf1* KD adult flies. CI and COX activities, normalized to the activity of CS, are all expressed as percentage of enzymatic activity where WTALA strain's activity is considered as 100%. Enzymatic activities were measured in three different wild type lines: Canton S, WT ALA, w^{1118} ; two parental lines: UAS–GFP; 79.1 *Surf1* IR/III, *Switch–Act5C–GAL4* and in the KD individuals (obtained by crossing between them the two parental strains). COX activity of KD flies is decreased in respect to controls.

Similarly, when we *Switch–Act5C–GAL4–*d*Surf1* KD larvae are transferred into progesterone additioned food we observed that such larvae reach the pupal stage but they do not develop to adult adulthood. Figure 3.12 shows the pupal phenotype of these KD individuals which arrest their development at the pupal stage.

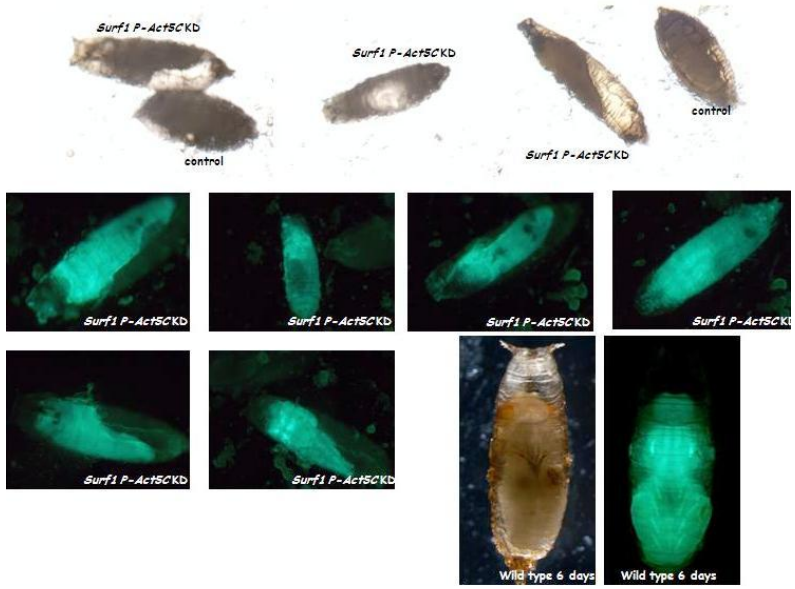

Figure 3.12. *Surf1* ubiquitous KD with the *Switch–Act5C–GAL4* driver at the third stage larva. UAS-GFP; 79.1 *Surf1* IR; *Switch–Act5C–GAL4* larvae were transferred into food containing RU–486. These individuals reach the pupal stage but they die during the early steps of PM.

These results point to the elevated sensitivity of Drosophila adults to the acute lack of d*Surf1*, which could mean that: (i) there is a high turnover of respiratory complexes and their assembly factors (such as d*Surf1*), requiring the continuing expression of d*Surf1* in order to maintain the steady state requirements; (ii) d*Surf1* expression is required constantly for some other vital and as yet unknown process. The fact that acute KD of d*Surf1* leads to isolated CIV deficiency, and not to a more generalized respiratory chain deficiency as occurs in larvae, suggests that there could be important differences in the assembly and/or the organization of the respiratory chain complexes in larvae and adults. Ubiquitous RU-486-mediated KD of d*Surf1* is lethal to larvae (even in the situation in which the *RU-486-GAL4* driver was employed under conditions in which low levels of GAL4 expression were produced through leakiness of the driver construct). This suggests that, as is the case for adults, larvae are sensitive to weak ubiquitous KD of d*Surf1*, as long as the KD is widespread. This is confirmed by the previously reported non-lethal, but weakly deleterious effects, of *elav-GAL4* -driven d*Surf1* KD (throughout the developing nervous system) (Zordan et al. 2006). Furthermore, as previously shown, experiments in which d*Surf1* KD was produced by using an eye-specific *GMR-GAL4* driver confirmed the fact that the KD

do not induce structural anomalies in eye development. In addition, the parallel analysis of the eye-antennal imaginal discs, in such individuals, showed no signs of alterations in the (normal developmentally regulated) pattern of apoptosis (data not shown).

Moreover it should be pointed out that, as already noted by (Fernandez-Ayala et al. 2009), the lack of *Surf1* leads to a variety of phenotypes in different organisms. In particular, evidence from yeast (Barrientos et al. 2002) and from mouse models suggests that *Surf1* may not only be involved in COX assembly, but may play a more general role in organization of the respiratory chain complexes and/or that it could also have as yet undescribed functions.

3.2 Coexpression of a synonymous gene construct rescue targeted d*Surf1* dsRNAi

As a proof of principle, we produced a synthetic form of the *dSurf1* cDNA (in which codons were subject to synonymous substitution) which would not be targeted by the dsRNAi inducing transgene (Kumar et al. 2006). In this way, following introduction of this synthetic transgene into the background of the lines used for dsRNAi, our hope was to be able to rescue the effects produced following the silencing of the endogenous copy of *dSurf1*.

3.2.1 Generation of transgenic lines bearing d*Surf1*–s

d*Surf1*–s was designed to escape native-d*Surf1*–targeted PTS through substitution of each codon triplet in the native d*Surf1* sequence with a synonymous triplet. (Table 3.1, Figure 3.13).

Figure 3.13. *Surf1* synonymous sequence. Bold = Region targeted by RNAi in wild type *dSurf1*. Red = start (atg) and stop (tga) codons, Pink = substituted nucleotides, Yellow = HA-tag sequence.

d*Surf1*	BASE COMPOSITION				%GC IN CODONS		
	A%	T%	C%	G%	FIRST POSITION	SECOND POSITION	THIRD POSITION
NATIVE	24.03	19.49	28.35	28.13	59.14	43.52	66.78
SYNONYMOUS	24.73	20.65	28.06	26.56	60.32	43.23	60.32

Table 3.1. Base composition of the d*Surf1* and d*Surf1*–s genes. For each sequence the table shows the general base composition as well as the proportion of GC nucleotides present in each of the three codon positions.

Following cloning into a pUAST transformation vector, d*Surf1*–s was injected into embryos leading to the obtainment of four transgenic lines: Syn1, Syn2, Syn3, Syn4. Line Syn4 proved to be homozygous lethal and was thus excluded from further analysis. Following production of double homozygote lines (i.e. lines bearing both a Syn transgene as well as an IR construct), these were crossed with the ubiquitous *Act5C–GAL4* driver. Unexpectedly such crosses produced no rescue of the late larval lethality phenotype typically observed following ubiquitous activation of d*Surf1* IR alone.

This result recalls that obtained by (Fernandez-Ayala et al. 2009) in which rescue of d*Surf1* KD by AOX under the control of an *Switch-tub-GAL4* promoter was not obtained at the highest doses of the drug inducer RU-486. On the other hand, in control experiments, at low doses of RU-486, d*Surf1* KD was insufficient to produce complete lethality. At intermediate doses of RU-486, d*Surf1* KD was still lethal or semilethal, and concomitant AOX expression was able to rescue the lethality (Figure 3.14).

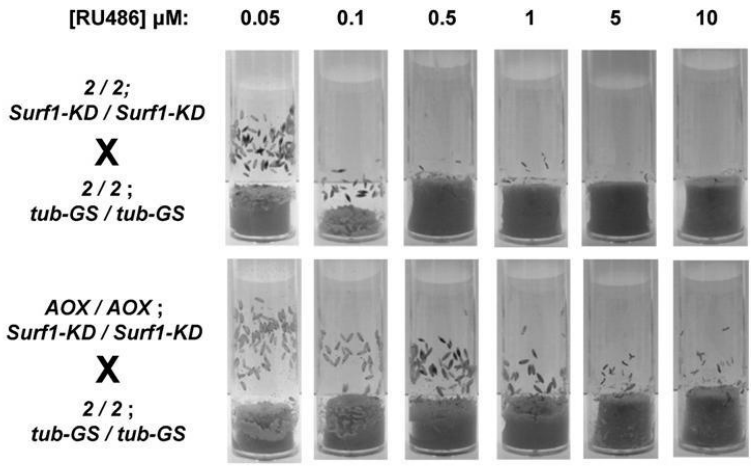

Figure 3.14. Survival of rescued flies. Hemizygous flies for *Surf1*-KD (encoding GAL4-dependent *Surf1*-directed dsRNA) and *tub-GS* transgenes, each on chromosome 3, with or without hemizygous AOX or GFP as an additional GAL4-dependent transgene on chromosome 2, cultured at different doses of the inducing drug RU-486. Image of actual vials is shown above in which AOX-expressing flies consistently reach further in development than nontransgenic flies at any given drug dose (Fernandez-Ayala et al. 2009).

Thus we proceeded to establish whether driving the expression of the KD (IR) and rescue (Syn) constructs in a temporally restricted manner would allow us to find the conditions which would allow to obtain the expected rescue of the larval lethality. To this end, in the experiments which follow, we employed a *hsp70–GAL4* driver.

3.2.2 d*Surf1* knock down using the *hsp70-GAL4* driver

Virgin females homozygous for d*Surf1*–s from lines Syn1, Syn2 and Syn3 were crossed to w; *hsp70–GAL4*/Cyo males. Non–Curly progeny were then collected and subjected to heat shock in order to evaluate the expression of d*Surf1*–s. Total proteins were extracted from 10 adult flies (5 males and 5 females) progeny of the above cross which had been exposed to heat shock (for 60 min at 37°C) 24, 48 or 72 hours after egg laying (AEL). The protein extracts obtained were subjected to Western blot analysis. An example referring to the results obtained following heat shock at 48 hours AEL is shown in Figure 3.15 where dSURF1–s.

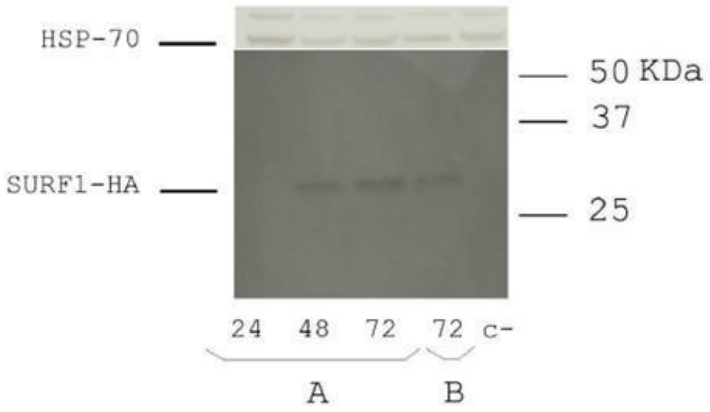

Figure 3.15. Western Blot conducted on 10 adult flies from following lines. (1) w^{1118} (negative control); (2) Syn1 *hsp70-GAL4* ;(3) Syn2 *hsp70-GAL4* ; (4) Syn3 *hsp70-GAL4*, in which expression of d*Surf1*-s was induced by heat shock (1h, 37°C) administered at 48 h after egg laying. The bands indicated in the gel are HSP-70 (the reference protein) and dSURF1-HA.

The presence of SURF1–s protein in the rescued flies bearing the double construct was verified by Western blot (Figure 3.15). The blot shows the band corresponding to the protein encoded by d*Surf1*–s (approx. 34 KD) visible in the lanes loaded with samples from individuals of line Syn2; IR. Semiquantitative estimates (data not shown) of SURF1–s protein on the basis of the optical density of the Western blot bands showed that there was significantly less dSURF1-s protein in individuals exposed to a 60 min. heat shock at 24 hAEL than at 72 h AEL (ANOVA; p=0.021). Experiments were then conducted in order to evaluate whether rescue of lethality, deriving from knock down of native d*Surf1*, could in fact be obtained by coexpressing d*Surf1*–s in the same flies under the control of the *hsp70–GAL4* driver.

We explored various combinations of parameters such as: (i) developmental time at which the heat shock was administered; (ii) duration of the heat shock; (iii) number of heat shock treatments administered during development. In particular all experiments were conducted using lines Syn2–IR and Syn3–IR, which bear both the dsRNAi d*Surf1* and the d*Surf1*–s-expressing transgenes, as well as on the lines bearing either one or the other transgene. Altogether this set of experiments allowed to establish that flies of line IR (those expressing only dsRNA d*Surf1*) did not show the expected late larval lethality, implying that d*Surf1* knock down was not fully activated under the following conditions: (i) a single 60 min. heat shock treatment 24 or 48 h AEL; (ii) a single 30 min. heat shock 72 h AEL; (iii) a double heat shock (30 min. each), administered at 48 or 72 h AEL. In order to avoid the above shortcoming, the progeny from the same crosses as above was exposed to repeated heat shock treatments according to the following schedules: (i) 72, 120 and 168 h AEL, 30 min. each; (ii) 72, 120, 168 and 216 h AEL, 30 min. each. Under these conditions dsRNAi was sufficient to result in the expected late larval lethality. However, this also produced unexpected late larval lethality in the individuals bearing only the d*Surf1*–s transgene, suggesting that the strong overexpression of this transgene is also toxic to the flies. Finally, following a single 60 min. heat shock treatment, 72 h AEL, we obtained the expected late larval lethality in flies expressing only the dsRNAi transgene as well as the partial rescue of the lethal phenotype in the flies expressing both the d*Surf1*–s construct and the dsRNAi d*Surf1* transgene. These results, expressed as percentage survival to adulthood of the different genotypes with respect to the number of eggs laid are shown in Table 3.2.

***hsp70-GAL4* crossed to:**	**Progeny genotype**	**Mean % survivial**
d*Surf1*–IR	IR *hsp70–GAL4*	0
d*Surf1*–s	Syn1 *hsp70–GAL4* Syn2 *hsp70–GAL4*	81.65 $\pm$8.49 64.22 $\pm$ 3.14
d*Surf1*–IR and d*Surf1*–s	Syn1; IR *hsp70–GAL4* Syn2; IR *hsp70–GAL4*	21.16 (17.88) $\pm$ 4.89 18.99 (13.98) $\pm$ 2.73

Table 3.2 Survival to adulthood of rescued flies. Values are expressed as percentages relative to the expected and are average values from three independent replicates (S.D.). The values concerning individuals from lines homozygous for both *Surf1* constructs (Syn1; IR *hsp70-GAL4* and Syn2; IR *hsp70-GAL4*) were corrected for the lethality seen with individuals from lines expressing only the dSurf1-s construct (Syn1 *hsp70-GAL4* and Syn2 *hsp70-GAL4*), respectively. The uncorrected survival values are shown in parentheses.

The above data show that, within the limits of sensitivity afforded by varying the timing of heat shock administration in order to activate the *hsp70-GAL4* driver, that it is possible to produce levels of d*Surf1* KD conducive to larval lethality using various alternative protocols which entail either sustained d*Surf1* KD by repeated short (30 min each) inductions of dsRNAi at different developmental times, or by a single

prolonged (60 min.) induction at 72 h AEL. However, the overexpression of the Syn transcripts (in a wild type background) using the same induction protocols, produced lethality *per se*, in all but the prolonged induction at 72 h AEL. Consequently, it proved particularly difficult to find an experimental condition leading to sufficient KD of the native transcript (to produce the late larval lethal phenotype), while at the same time producing enough Syn transcript to partially rescue flies from the effects of d*Surf1* KD. Rescued individuals reach the adult stages of development, but such individuals represent approximately 20% of the Mendelian expectation. Even if larvae expressing both the Syn and IR constructs, and which are expected to give rise to the rescued adults, could be distinguished from the rest of the larval progeny, only 20% of such larvae would actually reach adulthood. Consequently all analyses regarding rescued individuals were conducted only on the adult flies.
Furthermore, biochemical assays were carried out to determine levels of key respiratory chain enzyme activities only on the rescued adult flies.

3.2.3 Respiratory complex enzymatic activity

The activity of respiratory Complexes I and IV (CI and CIV) and Citrate Synthase (CS) were determined, under various experimental conditions in larvae and adults. In particular, coexpressing the rescue construct (d*Surf1*–s) under the control of a heat-shock driver (*hsp70–GAL4*), in a KD background. Figure 3.16 shows CI/CS and CIV/CS ratios in *hsp70–GAL4* rescue flies. Rescued individuals reached the adult stages of development, but only approximately 20% of rescued larvae actually developed to adulthood. Thus, for reasons previously exposed, respiratory chain complex activities were determined only in the final rescued adult flies, as shown in Figures 3.16. In this case, it is evident that rescued individuals show a complete restoration of CI/CS and CIV/CS activity ratios.

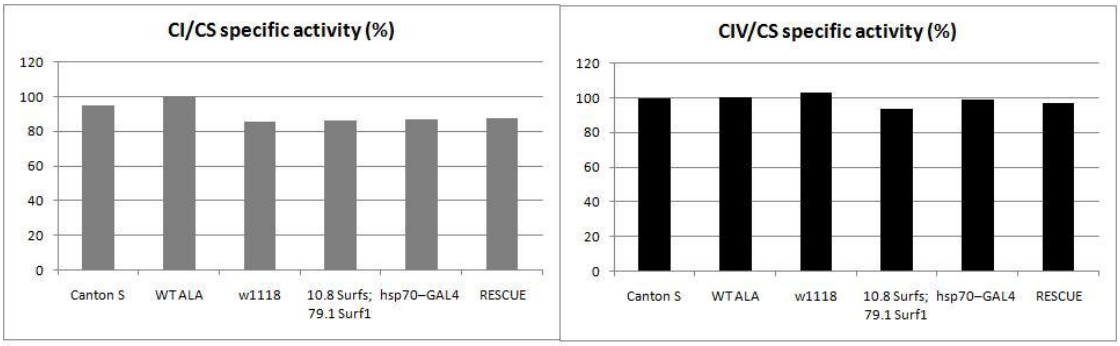

Figure 3.16. Respiratory complex activities in controls and RESCUE adult flies: following d*Surf1* knock down and contemporary activation of the d*Surf1* synonymous construct in adult flies. CI and COX activities, normalized to the activity of CS, are all expressed as percentage of

enzymatic activity where WTALA strain's activity is considered as 100%. Enzymatic activities were measured in three different wild type lines: Canton S, WT ALA, w^{1118}; two parental lines: 10.8 *Surfs*; 79.1 *Surf1* IR/III, *hsp70–GAL4* and in the RESCUE individuals (obtained after coexpression of a synonymous gene construct able to rescue targeted d*Surf1* dsRNAi). COX activity in RESCUE flies is similar to controls.

It is also worth mentioning that the CI/CS and CIV/CS activity ratios are approximately twofold higher in larvae with respect to adults, compare for example, Canton S individuals in figure 3.4). This is further explored in Figure 3.17, which shows the activities of CI, CIV and CS, as determined in larvae and adults of Canton S (wild type) individuals. Here it can be seen that activities of CI and CIV are actually twofold higher in adults with respect to larvae, while the CS activity is almost fivefold higher in adults with respect to larvae. The latter may reflect the lower yield and/or purity of the mitochondrial fraction obtained from larvae with respect to adults but could also imply that larvae have less mitochondria per unit mass of tissue protein. Nonetheless the twofold greater respiratory complex activity in adults suggests that larvae may present an all round lower requirement for oxidative phosphorylation, which would contribute to explain why many Drosophila mutants, defective in respiratory chain function, tend to survive through most of larval development, lethality generally becoming manifest late in larval development or at the larva to pupa transition, see for example: (Zordan et al. 2006, Fernandez-Ayala et al. 2010, Iyengar et al. 1999, Copeland et al. 2009).

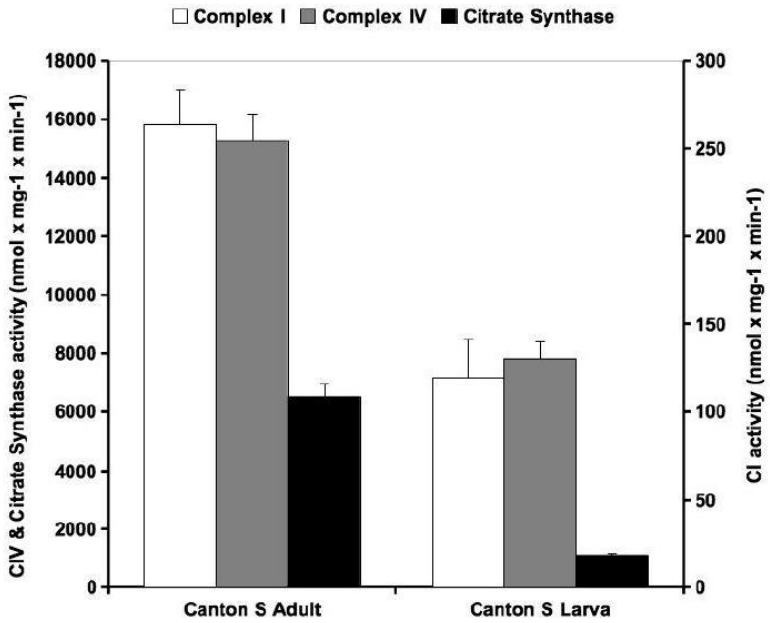

Figure 3.17. Larval versus adult respiratory complex activities. Enzymatic activities of respiratory complexes I and IV and of Citrate Synthase in Canton S (wild type control) larvae and adults.

Concluding, *Drosophila melanogaster* is a widely used model organism in basic and translational research and in many instances such research deals with the characterization of genes involved in mitochondrial function. The data presented here shed new light on the existence of important developmental stage-specific differences in respiratory chain complex activities in this organism, which may have important implications when considering the developmental stage at which phenotypical defects are manifest following the inactivation of the gene(s) of interest. In the case of the gene object of this study, we show the unexpectedly high sensitivity of Drosophila adults to the lack of d*Surf1* and we also provide evidence suggesting that only widespread lack of d*Surf1* is deleterious, while spatially restricted silencing may lead to weak negative effects or to the absence of any identifiable defects.

In the next pages is attached a copy of the paper dealing with the recent results obtained for d*Surf1* gene, currently submitted to *BMC Medical Genetics*.

Synonymous cDNA-mediated rescue of mitochondrial respiratory complex activities following acute dsRNAi of dSurf1 in Drosophila melanogaster.

Clara Benna[1], Caterina Da Re[1], Ester Spadaro[1], Rodolfo Costa*[1], Massimo Zeviani[2] and Mauro A. Zordan[1]

[1]Department of Biology, University of Padova Via U. Bassi 58/B, 35131, Padova, ITALY
[2]Istituto Nazionale Neurologico "Carlo Besta", Milan, ITALY

Email: Clara Benna - costast5@unipd.it; Caterina Da Re - caterina.dare@unipd.it; Ester Spadaro - ester.spadaro@unipd.it; Rodolfo Costa*- rodolfo.costa@unipd.it; Massimo Zeviani - zeviani@istituto-besta.it; Mauro A. Zordan - mauroagostino.zordan@unipd.it;

*Corresponding author

Abstract

Background: Leigh syndrome (LS) is an early onset progressive mitochondrial encephalopathy, usually leading to death within the first decade of life. LS patients with mutations in the *Surf1* gene show a marked and specific decrease in the activity of mitochondrial respiratory chain complex IV (cytochrome c oxidase, COX), the terminal enzyme in the respiratory chain. Experimental evidence suggests that SURF1 is involved in COX assembly. Since, the molecular mechanism leading to COX deficiency and the pathogenesis of neurodegeneration in human LS are still poorly understood, we had previously set up a *Drosophila melanogaster* model based on the post-transcriptional silencing of *dSurf1* (CG9943) via transgenic double-stranded RNA interference. Here, we explored this model further.

Results: We coexpressed a synonymous gene construct encoding for the dSURF1 protein in animals in which the wild type *dSurf1* gene was targeted for dsRNAi-mediated knock down. Under these conditions we show that, in up to 20% of individuals, the synonymous gene could rescue lethality and the respiratory chain Complex IV deficiency, previously shown by us to be a consequence of the post-transcriptional silencing (PTS) of the wild type gene. We also show that the use of an RU-486-sensitive promoter to activate PTS of *dSurf1* in adult flies leads rapidly to isolated respiratory Complex IV deficiency and lethality.

Conclusions: Acute knockdown in parallel with cDNA-mediated rescue of *dSurf1* expression in larvae and/or adults reveals the surprisingly high sensitivity of Drosophila adults to the lack of *dSurf1*. We also provide evidence suggesting that only widespread lack of *dSurf1* is deleterious, while spatially restricted silencing does not lead to detectable defects.

Background

Human *Surf1* encodes a 31 kDa protein located in the inner membrane of mitochondria [1] [2] and it is ubiquitously expressed in human tissues, in particular in aerobic tissues such as heart, skeletal muscle and kidney [3]. SURF1 protein is highly conserved from recent prokaryotes to humans [4], and it is characterized by an N-terminal mitochondrial targeting sequence and by two trans-membrane domains [2] [3]. Most human *Surf1* mutations are of the nonsense type which are predicted to lead to the expression of a prematurely truncated and/or aberrant protein [5] and are involved in the determination of Leigh syndrome (LS, OMIM 256000). LS is a progressive mitochondrial encephalopathy characterized by the presence of symmetric necrotizing lesions in subcortical areas of the CNS, including brainstem, cerebellum, diencephalon and corpus striatum [6]; [7]. The disease onset is in infancy, generally after a symptom-free interval of several months. The syndrome has a relentlessly progressive course, death usually occurring within the first decade of life, although protracted cases are known. LS *Surf1* mutant patients show a marked decrease in the activity of mitochondrial respiratory chain complex IV (cytochrome c oxidase, COX) [2]. COX is the terminal enzyme in the respiratory chain and studies in human cells [8], mice [9] [10] and yeast [11] indicate that SURF1 is involved in COX assembly. Since, the molecular mechanism leading to COX deficiency and the pathogenesis of neurodegeneration which characterize human LS are still poorly understood, we set up a *Drosophila melanogaster* model, by inducing the post-transcriptional silencing of *dSurf1* (CG9943) via transgenic double-stranded RNA interference [12]. The GAL4-UAS binary system [13] was exploited to drive the post-transcritpional silencing (knock down, KD) of the target gene transcript under the control of two alternative promoters, i.e. *Actin5C*, an early-expressed housekeeping gene, or *elav*, an early-expressed neuron-specific gene. The main phenotypic features following ubiquitous *Actin5C-Gal4*-driven *dSurf1* KD were severe impairment of larval

development and reduced locomotion which were likely caused by a generalised defect in respiration and ATP synthesis determined by *dSurf1* silencing. On the other hand, nervous system-wide silencing of *dSurf1* allowed us to bypass late larval lethality observed with the ubiquitous driver. Not only did such individuals survive to adulthood, but they showed a strikingly enhanced survival with respect to controls. The larval stages of *elav-Gal4 dSurf1* KD individuals were morphologically comparable to controls although they presented slight impairment in locomotor activity and photobehaviour which is reminiscent of the widespread nervous system involvement observed in human mitochondria-related encephalomyopathies. A direct effect of *dSurf1* silencing on mitochondrial respiration was demonstrated by the significant reduction in the histochemical reaction to COX observed in the CNS of the *elav-Gal4* KD adult flies, paralleled by a strong increase in the SDH levels measured in the same tissues, which suggests a compensatory increase in mitochondrial mass. Altogether, the above results strongly support the involvement of respiratory deficiency in determining the developmental and functional impairments observed in KD individuals. Indeed, it has recently been shown that the lethal effects of ubiquitous *dSurf1* KD in Drosophila could be rescued by the concomitant expression of a *Ciona intestinalis* alternative oxidase (AOX) under the control of an inducible promoter [14]. Similarly to COX, AOX is a mitochondrial enzyme which is able to reduce molecular oxygen to water using hydrogen atoms, but differently to COX, this activity is not coupled to proton pumping. In this paper we designed and implemented a rescue construct consisting in a synonymous copy of the *dSurf1* gene in which all the codons were altered so as to escape KD induced by dsRNA targeting of the wild type gene. Furthermore, we evaluated the sensitivity of Drosophila larvae or adults to the acute KD of *dSurf1*. Our findings show the unexpectedly extreme sensitivity of Drosophila adult flies to the acute post transcriptional silencing-mediated depletion of *dSurf1* during adulthood, while KD spatially restricted to the developing eye primordia does not appear to cause any detectable negative effects.

Results and Discussion

In this paper we show, the rescue of phenotypes which resulted from the knockdown produced following dsRNAi of *dSurf1*, through the co-expression of a synthetic gene (*dSurf1-s*, (Figure 1) in which codons were subject to synonymous substitution in order to elude targeting by dsRNAi [15].

Generation of transgenic lines bearing dSurf1-s

dSurf1-s was designed to escape native-*dSurf1*-targeted KD through substitution of each codon triplet in the native *dSurf1* sequence with a synonymous triplet. For further details see Materials and Methods and

Table 1. Following cloning into a pUAST transformation vector, *dSurf1-s* was injected into embryos leading to the obtainment of four transgenic lines: Syn1, Syn2, Syn3, Syn4
Line Syn4 proved to be homozygous lethal and was thus excluded from further analysis.
Following production of double homozygous lines (i.e. lines bearing both a Syn transgene as well as a dsRNA-bearing transgene (IR) specifically targeting native *dSurf1*, these were crossed with the ubiquitous *Act5C-Gal4* driver. Unexpectedly such crosses produced no rescue of the late larval lethality phenotype observed following ubiquitous activation of *dSurf1* IR alone. This result recalls that obtained by [14] in which rescue of *dSurf1* KD by AOX under the control of an *Switch-tub-Gal4* promoter was not obtained at the highest doses of the drug inducer RU-486. On the other hand, in control experiments, at low doses of RU-486, *dSurf1* KD was insufficient to produce complete lethality. At intermediate doses of RU-486, *dSurf1* KD was still lethal or semilethal, and concomitant AOX expression was able to rescue the lethality. Thus we proceeded to establish whether driving the expression of the KD (IR) and rescue (Syn) constructs in a temporally restricted manner would allow us to find the conditions which would allow to obtain the expected rescue of the larval lethality. To this end, in the experiments which follow, we employed a *hsp70-Gal4* driver.

dSurf1 knock down using the hsp70-Gal4 driver

Virgin females homozygous for *dSurf1-s* from lines Syn1, Syn2 and Syn3 were crossed to *w;hsp70-Gal4/Cyo* males. Non-*Curly* progeny were then collected and subjected to heat shock in order to evaluate the expression of *dSurf1-s*. Total proteins were extracted from 10 adult flies (5 males and 5 females), progeny of the above cross, which had been exposed to heat shock (for 60 min at 37^{o}C) 24, 48 or 72 hours after egg laying (AEL). The protein extracts were subjected to Western blot analysis. An example referring to the results obtained following heat shock at 48 hours AEL is shown in Figure 2 where dSURF1-s protein from each of the lines assayed is visible as an approximately 34 KiloDalton band.
Since, following heat shock, expression of dSURF1-s was successfully demonstrated in flies of all three crosses analyzed (Syn1 X *hsp70-Gal4*, Syn2 X *hsp70-Gal4* and Syn3 X *hsp70-Gal4*), we crossed the Syn lines to those harboring the *dSurf1* dsRNAi construct in order to produce progeny which, when crossed to the *hsp70-Gal4* line, would express both constructs.
Experiments were then conducted in order to evaluate whether rescue of lethality, deriving from knock down of native *dSurf1*, could in fact be obtained by coexpressing *dSurf1-s* in the same flies under the control of the *hsp70-Gal4* driver. We explored various combinations of parameters such as: (i)

Developmental time at which the heat shock was administered; (ii) Duration of the heat shock; (iii) Number of heat shock treatments administered during development.

In particular all experiments were conducted using lines Syn2-IR and Syn3-IR, which bear both the dsRNAi *dSurf1* and the *dSurf1-s*-expressing transgenes, as well as using the lines bearing either one or the other transgene. Line Syn1; IR was not evaluated further.

Altogether this set of experiments allowed to establish that flies of line IR (those expressing only dsRNA *dSurf1*) did not show the expected late larval lethality, implying that *dSurf1* KD was not fully activated under the following conditions: (i) a single 60 min. heat shock treatment 24 or 48 h AEL; (ii) a single 30 min. heat shock 72 h AEL; (iii) a double heat shock (30 min. each), administered at 48 and 72 h AEL.

In order to attempt to avoid the above shortcoming, the progeny from the same crosses as above was exposed to repeated heat shock treatments according to the following schedules: (i) 72, 120 and 168 h AEL, 30 min. each; (ii) 72, 120, 168 and 216 h AEL, 30 min. each.

Under these conditions dsRNAi was sufficient to result in the expected late larval lethality. However, this also produced unexpected late larval lethality even in the individuals bearing only the *dSurf1-s* transgene.

Finally, following a single 60 min. heat shock treatment, 72 h AEL, we obtained the expected late larval lethality in individuals expressing only the IR transgene as well as the partial rescue of the lethal phenotype in the flies expressing both the Syn construct and the IR transgene. These results, expressed as percentage survival to adulthood of the different genotypes with respect to the number of eggs laid, are shown in Table 2.

The presence of SURF1-s protein in the rescued flies bearing the double construct was verified by Western blot (Figure 3). The blot shows the band corresponding to the protein encoded by *dSurf1-s* (approx. 34 KD) visible in the lanes loaded with samples from individuals of line Syn2; IR. Semiquantitative estimates (data not shown) of SURF1-s protein on the basis of the optical density of the Western blot bands showed that there was significantly less dSURF1-s protein in individuals exposed to a 60 min. heat shock at 24 h AEL than at 72 h AEL (ANOVA; $p=0.021$).

The above data show that, within the limits of sensitivity afforded by varying the timing of heat shock administration in order to activate the *hsp70-Gal4* driver, that it is possible to produce levels of *dSurf1* KD conducive to larval lethality using various alternative protocols which entail either sustained *dSurf1* KD by repeated short (30 min each) inductions of dsRNAi at different developmental times, or by a single prolonged (60 min.) induction at 72 h AEL. However, the overexpression of the Syn transcripts (in a wild type background) using the same induction protocols, produced lethality *per se*, in all but the prolonged

induction at 72 h AEL. Consequently, it proved particularly difficult to find an experimental condition leading to sufficient KD of the native transcript (to produce the late larval lethal phenotype), while at the same time producing enough Syn transcript to partially rescue flies from the effects of *dSurf1* KD. Rescued individuals reach the adult stages of development, but such individuals represent approximately 20%of the Mendelian expectation. Even if larvae expressing both the Syn and IR constructs, and which are expected to give rise to the rescued adults, could be distinguished from the rest of the larval progeny, only 20% of such larvae would actually reach adulthood. Consequently all analyses regarding rescued individuals were conducted only on the adult flies.

Respiratory complex enzymatic activity

The activity of respiratory Complexes I and IV (CI and CIV) and Citrate Synthase (CS) were determined, under various experimental conditions in larvae and adults. In particular, co-expressing the rescue construct (*dSurf1-s*) under the control of a heat-shock driver (*hsp70-Gal4*), in a KD background.
Figure 4 shows CI/CS and CIV/CS ratios in *Act5C-Gal4* KD larvae and in *hsp70-Gal4* rescue flies. Since driving *dSurf1* KD using an *Act5C-Gal4* driver results in larval lethality, respiratory chain complex activities could only be determined in mitochondrial extracts obtained from the larval stages of development, as shown in Figures 4(A, B). In this case *dSurf1* KD larvae show a significant reduction in CI/CS and CIV/CS activities. This result is at variance with what is observed in humans with *Surf1*-deficiency-related Leigh syndrome [1] [2] [3]and in the corresponding mouse model [10]. Both these cases are characterized, at the biochemical level, by an isolated CIV deficiency. It should however be pointed out that, as already noted by [14], the lack of *Surf1* leads to a variety of phenotypes in different organisms. In particular, evidence from yeast [16] and from mouse [10] models suggests that *Surf1* may not only be involved in COX assembly, but may play a more general role in organization of the respiratory chain complexes and/or that it could also have as yet undescribed functions.
For reasons previously explained, Figures 4(C, D) show respiratory chain complex activities which were determined only in the final rescued adult flies. In this case, it is evident that rescued individuals show a complete restoration of CI/CS and CIV/CS activity ratios.
It is also worth mentioning that the CI/CS and CIV/CS activity ratios are approximately twofold higher in larvae with respect to adults (compare, for example, Canton S individuals in panels 4A and 4C). This is further explored in Figure 5, which shows the activities of CI, CIV and CS, as determined in larvae and adults of Canton S (wild type) individuals. Here it can be seen that activities of CI and CIV are actually

twofold higher in adults with respect to larvae, while the CS activity is almost fivefold higher in adults with respect to larvae. The latter may reflect the lower yield and/or purity of the mitochondrial fraction obtained from larvae with respect to adults but could also imply that larvae have less mitochondria per unit mass of tissue protein. Nonetheless the twofold greater respiratory complex activity in adults suggests that larvae may present an all round lower requirement for oxidative phosphorylation, which would contribute to explain why many Drosophila mutants, defective in respiratory chain function, tend to survive through most of larval development, lethality generally becoming manifest late in larval development or at the larva to pupa transition, see for example: [12], [17], [18], [19].

RU-486-Gal4-induced knock down of dSurf1

Pilot experiments using the *Switch-Act5C-Gal4* (RU-486-sensitive promoter) showed some promoter leakiness. In our hands this is evidenced by the fact that flies harboring the promoter transgene as well as the IR transgene show late larval lethality in the absence of pharmacological induction of the promoter. Such lethality could be "rescued" simply by growing such larvae at 20^oC. Adults allowed to develop at 20^oC and then transferred to 25^oC show 100% lethality within 48 hours. Apart from the question of the *Switch-Act5C-Gal4* promoter leakiness, these results suggest that Drosophila adults are particularly sensitive to the lack of *dSurf1*.

In order to determine whether adult lethality produced by late activation of *dSurf1* knock-down was paralleled by alterations in the levels of CIV activity, we analyzed respiratory complex levels in *Switch-Act5C-Gal4-dSurf1* KD flies. To circumvent the inherent leakiness of the RU-486-sensitive promoter, all experiments were conducted at 20^oC. Activation of the driver was thus obtained following transferral of the flies to food additioned with RU-486. Under these conditions 100% of the adult flies died within 48 hours of exposure to RU-486.

Figure 6 (A, B) shows, for the different genotypes analyzed, the enzymatic activity ratios, with respect to Citrate synthase, for respiratory complexes I and IV, respectively. No relevant variations in enzymatic activity, as a function of genotype, were observed for Complex I. On the other hand, a marked variation was evidenced in the case of Complex IV activity (Fig. 6B). In particular *dSurf1* KD individuals showed an approximately 30% reduction in activity as compared to the controls.

These results point to the elevated sensitivity of Drosophila adults to the acute lack of *dSurf1*, which could mean that: (i) There is a high turnover of respiratory complexes and their assembly factors (such as *dSurf1*), requiring the continuing expression of *dSurf1* in order to maintain the steady state requirements;

(ii) *dSurf1* expression is required constantly for some other vital and as yet unknown process.
The fact that acute KD of *dSurf1* leads to isolated CIV deficiency, and not to a more generalized respiratory chain deficiency as occurs in larvae, suggests that there could be important differences in the assembly and/or the organization of the respiratory chain complexes in larvae and adults Ubiquitous RU-486-mediated KD of *dSurf1* is lethal to larvae (even in the situation in which the RU-486-Gal4 driver was employed under conditions in which low levels of Gal4 expression were produced through leakiness of the driver construct). This suggests that, as is the case for adults, larvae are sensitive to weak ubiquitous KD of *dSurf1*, as long as the KD is widespread. This is confirmed by the previously reported non-lethal, but weakly deleterious effects, of *elav-Gal4*-driven *dSurf1* KD (throughout the developing nervous system) [12] . Furthermore, in the course of the present study we also conducted experiments in which *dSurf1* KD was produced by using an eye-specific *GMR-Gal4* driver. In this case we were unable to observe any structural anomalies in eye development. In addition, the parallel analysis of the eye-antennal imaginal discs, in such individuals, showed no signs of alterations in the (normal developmentally regulated) pattern of apoptosis (data not shown).

Conclusions

Drosophila melanogaster is a widely used model organism in basic and translational research. In many instances such research deals with the characterization of genes involved in mitochondrial function. The data presented here shed new light on the existence of important developmental stage-specific differences in respiratory chain complex activities in this organism, which may have important implications when considering the developmental stage at which phenotypical defects are manifest following the inactivation of the gene(s) of interest. In the case of the gene object of this study, we show the unexpectedly high sensitivity of Drosophila adults to the lack of *dSurf1* and we also provide evidence suggesting that only widespread lack of *dSurf1* is deleterious, while spatially restricted silencing may lead to weak negative effects or to the absence of any identifiable defects.

Methods

Production and microinjection of the pP[UAST] dSurf1-s construct.

dSurf1-s was designed so that its nucleotide sequence was sufficiently different from the native sequence as to allow it to escape native-*dSurf1*-targeted KD. This was accomplished by substituting each codon triplet in the native *dSurf1* sequence with a synonymous triplet. Nucleotide substitutions were chosen so as to

maximize differences between *dSurf1* and *dSurf1-s*, while respecting codon bias and avoiding the introduction of new splicing sites (Table 1). On the whole, the *dSurf1-s* nucleotide sequence presents 29.1% differences with respect to *dSurf1*. In addition *dSurf1-s* was also engineered so as to encode an HA tag at the C-terminus. Furthermore, particular attention was dedicated to maintaining a GC content of approximately 60% in the third position of codons in agreement with [20] who report that, in *Drosophila melanogaster*, the most frequently employed codons are characterized by G or C nucleotides in third position. The *dSurf1-s* construct, synthesized by Genscript Corporation, was subcloned into a PUC57 pUAST microinjection vector. Confirmation of the insertion of the synthetic gene into the pUAST vector was obtained by restriction fragment analysis. After EcoRI and XhoI digestion, a 980 pb fragment was obtained which corresponds to the expected size of the *dSurf-s* gene. Further confirmation regarding the nature of the fragments was obtained by direct sequencing.

pUAST *dSurf1-s* was injected into w^{1118} embryos as described in [21]. Embryos which survived microinjection were numbered progressively and crossed with w^{1118} individuals. For each insertion event a single transgenic line was founded. Four transgenic lines were thus obtained: Syn1, Syn2, Syn3, Syn4 Following crosses with balancers, each line was characterized by insertion of pUAST *dSurf1-s* into the following chromosomes: line Syn4 chromosome 3; lines Syn1, Syn2 and Syn3 chromosome 2. From each of the balanced lines, stable homozygous lines were obtained.

Double homozygotes for both the KD and the rescue construct

In order to evaluate whether *dSurf1-s* was able to revert the knockdown phenotype produced by *dSurf1*-IR, it was necessary to obtain transgenic lines bearing both pUAST *dSurf-s*, and pUAST *dSurf1*-IR. Such lines were obtained after appropriate crosses starting from the following lines: lines Syn1, Syn2 and Syn3: bearing pUAST *dSurf-s*. line IR: bearing pUAST *dSurf1*-IR, on the III chromosome (3R, 88D) [12]. In the double homozygote lines thus obtained, the expression of both constructs can be induced using the UAS-GAL4 binary system.

Western blots

Assays were conducted essentially as described in [12]. Briefly: Following extraction of mitochondria, the mitochondrial suspension was sonicated and subjected to 3 freeze/thawing cycles in liquid nitrogen; a protease inhibitor cocktail and detergents were added and the solution was left on ice to allow membrane solubilization. Equal amounts of total proteins ($\sim$ 60 mg) for each sample were resolved on a 12%

SDS-polyacrylamide gel. Following separation and Western blotting onto nitro-cellulose membrane, the membrane was blocked and incubated with the primary followed by secondary antibodies. Positive immunoreactivity was visualized using chemiluminescence.

Adult viability following dSurf1 knock down during adulthood

The following crosses were performed to determine adult survival, of *RU-486-Act5C-Gal4*-driven *dSurf1* KD during the adult stages of development:
(i) Controls = *Uas Gfp/Uas Gfp* X *Switch-Actin5C-Gal4 / TM6B, Tb*; from which the resulting progeny of interest was *Switch-Actin5C-Gal4 / Uas Gfp* (ii) KD indivuals = *Uas Gfp, IR/ Uas Gfp, IR* X *Switch-Actin5C-Gal4 / TM6B, Tb*; from which the resulting progeny of interest was *Switch-Actin5C-Gal4 / Uas Gfp, IR*. Crosses were raised at 20^{o}C on standard sucrose medium. Freshly eclosed flies, both controls (*Switch-Actin5C-Gal4 / Uas Gfp*) and (*Switch-Actin5C-Gal4 / Uas Gfp, IR*) were transferred from RU-486-free food to the food containing RU-486 and kept at a temperature of 20^{o}C. To this end, a 10 mM stock solution of RU-486 (mifepristone; Sigma) in ethanol 80% was added during the preparation of fly medium to a final concentration of 15 μg/ml. A total number of 150 *Switch-Actin5C-Gal4 / Uas Gfp, IR* flies and the same number of control flies were starved and then placed, in groups of 10 into RU-486-containing food.

Respiratory Chain Complex Activity Assays

Mitochondria were extracted in duplicate from samples each containing approximately 200 whole flies or larvae. Each sample was homogenized using a Dounce glass-glass potter and loose fitting pestle. A mannitol-sucrose buffer (pH 7.4), to which 2% BSA was added, was then added to bring the homogenate volume to 25 ml. The samples were then centrifuged at 1500g (Beckman Avanti J-25 Centrifuge, Beckman 2550 rotor) at 4^{o}C for 6 minutes. The pellet was discarded by filtering the sample through a fine mesh, and the supernatant re-centrifuged at 7000g at 4^{o}C for 6 minutes. This supernatant was discarded and the remaining pellet resuspended in 20 ml of mannitol-sucrose buffer without BSA before being centrifuged at 7000g under the same conditions as above. The supernatant was once again discarded and the pellet resuspended in a minimal amount of buffer (approximately 50 μl). Concentration of proteins was determined by the Biuret test before storage at -80^{o}C or immediate use.The extracted mitochondria samples were diluted with hypotonic buffer to the desired concentration - normally a final volume of mitochondria homogenate between 10 and 50μl. Prior to the assays, in order to disrupt the mitochondrial

membranes, the samples were subjected to 3 freeze-thaw cycles using liquid nitrogen.

Complex I activity

was determined by following the oxidation of NADH at 340 nm using ubiquinone-1 as the electron acceptor. The assay buffer consisted of 25mM KH_2PO_4, pH 7.2, 5mM $MgCl_2$ and 2.5mg/ml BSA, to which 2mM KCN, 2 μg/ml antimycin, 97.5 μM ubiquinone, 0.13mM NADH and 50μg mitochondrial proteins were added. As Complex I activity is rotenone-sensitive, activity was measured before and after the addition of rotenone (2μg/ml), the difference between the two then being used to determine actual activity.

Complex IV (cytochrome c oxidase) specific activity

was determined by monitoring the oxidation of cytochrome c at 550 nm. The assay buffer consisted of 100mM K Phosphate pH 7.0, to which 0.1% BSA, 0.8mM Reduced Cytochrome C and 10μg mitochondrial proteins were added. NB Samples used to determine Complex IV activity were treated with n-dodecyl maltoside to disrupt membranes rather than freeze-thawing.

Citrate Synthase activity

was measured by monitoring the reduction of dithio-bis-nitrobenzoic acid (DTNB, colourless) to thionitrobenzoic acid (yellow) with coenzyme A at 412 nm (ϵ = 13,600 M^{-1} cm^{-1}). The assay buffer consisted of 75mM Tris-HCl pH 8, to which 0.4mM acetyl-CoA, 0.1 μM DTNB, 0.5mM oxaloacetate and 5μg mitochondrial proteins were added.

Authors contributions

Clara Benna: Designed the *dSurf1* synonymous construct and performed the molecular biology;
Ester Spadaro: Performed the molecular biology, husbandry of the fly lines and behavioural analyses;
Caterina Da Re: Set up and conducted respiratory complex assays;
Rodolfo Costa: Design of the study, data analysis and discussion;
Massimo Zeviani: Expert on Leigh's syndrome and mammalian models of mitochondrial disease;
Mauro A. Zordan: Design of the study and writing up of the final version of the manuscript.
All the authors read and approved the final manuscript.

Acknowledgements

This work was supported by grants from the Fondazione Telethon-Italy grant number GGP07019 to MZ and RC; and by grants of the Cariparo Foundation; the Ministry of Education and Research; and Progetto Strategico Universita' di Padova "Models of Mitochondrial Disease", to RC.

References

1. Zhu Z, Yao J, Johns T, Fu K, Bie ID, Macmillan C, Cuthbert AP, Newbold RF, Wang J, Chevrette M, Brown GK, Brown RM, Shoubridge EA: **SURF1, encoding a factor involved in the biogenesis of cytochrome c oxidase, is mutated in Leigh syndrome**. *Nat Genet* 1998, **20**(4):337–43.
2. Tiranti V, Hoertnagel K, Carrozzo R, Galimberti C, Munaro M, Granatiero M, Zelante L, Gasparini P, Marzella R, Rocchi M, Bayona-Bafaluy MP, Enriquez JA, Uziel G, Bertini E, Dionisi-Vici C, Franco B, Meitinger T, Zeviani M: **Mutations of SURF-1 in Leigh disease associated with cytochrome c oxidase deficiency**. *Am J Hum Genet* 1998, **63**(6):1609–21.
3. Yao J, Shoubridge EA: **Expression and functional analysis of SURF1 in Leigh syndrome patients with cytochrome c oxidase deficiency**. *Hum Mol Genet* 1999, **8**(13):2541–9.
4. Poyau A, Buchet K, Godinot C: **Sequence conservation from human to prokaryotes of Surf1, a protein involved in cytochrome c oxidase assembly, deficient in Leigh syndrome**. *FEBS Lett* 1999, **462**(3):416–20.
5. Pequignot MO, Desguerre I, Dey R, Tartari M, Zeviani M, Agostino A, Benelli C, Fouque F, Prip-Buus C, Marchant D, Abitbol M, Marsac C: **New splicing-site mutations in the SURF1 gene in Leigh syndrome patients**. *J Biol Chem* 2001, **276**(18):15326–9.
6. Leigh D: **Subacute necrotizing encephalomyelopathy in an infant**. *J Neurol Neurosurg Psychiatr* 1951, **14**(3):216–21.
7. Farina L, Chiapparini L, Uziel G, Bugiani M, Zeviani M, Savoiardo M: **MR findings in Leigh syndrome with COX deficiency and SURF-1 mutations**. *AJNR Am J Neuroradiol* 2002, **23**(7):1095–100.
8. Tiranti V, Jaksch M, Hofmann S, Galimberti C, Hoertnagel K, Lulli L, Freisinger P, Bindoff L, Gerbitz KD, Comi GP, Uziel G, Zeviani M, Meitinger T: **Loss-of-function mutations of SURF-1 are specifically associated with Leigh syndrome with cytochrome c oxidase deficiency**. *Ann Neurol* 1999, **46**(2):161–6.
9. Agostino A, Invernizzi F, Tiveron C, Fagiolari G, Prelle A, Lamantea E, Giavazzi A, Battaglia G, Tatangelo L, Tiranti V, Zeviani M: **Constitutive knockout of Surf1 is associated with high embryonic lethality, mitochondrial disease and cytochrome c oxidase deficiency in mice**. *Hum Mol Genet* 2003, **12**(4):399–413.
10. Dell'Agnello C, Leo S, Agostino A, Szabadkai G, Tiveron C, Zulian A, Prelle A, Roubertoux P, Rizzuto R, Zeviani M: **Increased longevity and refractoriness to Ca(2+)-dependent neurodegeneration in Surf1 knockout mice**. *Hum Mol Genet* 2007, **16**(4):431–44.
11. Nijtmans LG, Sanz MA, Bucko M, Farhoud MH, Feenstra M, Hakkaart GA, Zeviani M, Grivell LA: **Shy1p occurs in a high molecular weight complex and is required for efficient assembly of cytochrome c oxidase in yeast**. *FEBS Lett* 2001, **498**:46–51.
12. Zordan MA, Cisotto P, Benna C, Agostino A, Rizzo G, Piccin A, Pegoraro M, Sandrelli F, Perini G, Tognon G, DeCaro R, Peron S, Kronniè TT, Megighian A, Reggiani C, Zeviani M, Costa R: **Post-transcriptional silencing and functional characterization of the Drosophila melanogaster homolog of human Surf1**. *Genetics* 2006, **172**:229–41.
13. Brand AH, Perrimon N: **Targeted gene expression as a means of altering cell fates and generating dominant phenotypes**. *Development* 1993, **118**(2):401–15.
14. Fernandez-Ayala DJM, Sanz A, Vartiainen S, Kemppainen KK, Babusiak M, Mustalahti E, Costa R, Tuomela T, Zeviani M, Chung J, O'Dell KMC, Rustin P, Jacobs HT: **Expression of the Ciona intestinalis alternative oxidase (AOX) in Drosophila complements defects in mitochondrial oxidative phosphorylation**. *Cell Metab* 2009, **9**(5):449–60.

15. Kumar D, Gustafsson C, Klessig DF: **Validation of RNAi silencing specificity using synthetic genes: salicylic acid-binding protein 2 is required for innate immunity in plants**. *Plant J* 2006, **45**(5):863–8.

16. Barrientos A, Korr D, Tzagoloff A: **Shy1p is necessary for full expression of mitochondrial COX1 in the yeast model of Leigh's syndrome**. *EMBO J* 2002, **21**(1-2):43–52.

17. Fernández-Ayala DJM, Chen S, Kemppainen E, O'Dell KMC, Jacobs HT: **Gene expression in a Drosophila model of mitochondrial disease**. *PLoS ONE* 2010, **5**:e8549.

18. Iyengar B, Roote J, Campos AR: **The tamas gene, identified as a mutation that disrupts larval behavior in Drosophila melanogaster, codes for the mitochondrial DNA polymerase catalytic subunit (DNApol-gamma125)**. *Genetics* 1999, **153**(4):1809–24.

19. Copeland JM, Cho J, Lo T, Hur JH, Bahadorani S, Arabyan T, Rabie J, Soh J, Walker DW: **Extension of Drosophila life span by RNAi of the mitochondrial respiratory chain**. *Curr Biol* 2009, **19**(19):1591–8.

20. Shields DC, Sharp PM, Higgins DG, Wright F: **"Silent" sites in Drosophila genes are not neutral: evidence of selection among synonymous codons**. *Mol Biol Evol* 1988, **5**(6):704–16.

21. Piccin A, Salameh A, Benna C, Sandrelli F, Mazzotta G, Zordan M, Rosato E, Kyriacou CP, Costa R: **Efficient and heritable functional knock-out of an adult phenotype in Drosophila using a GAL4-driven hairpin RNA incorporating a heterologous spacer**. *Nucleic Acids Res* 2001, **29**(12):E55–5.

Figures

Figure 1 - Synonymous construct

Sequence of the cDNA used to produce the transgene expressing the synonymous form of *dSurf1*. Substitutions are shown in pink. The region targeted by dsRNAi is shown in bold. Start and stop codons are shown in red. An HA tag sequence is shown in yellow.

Figure 2 - Western blot of heat shock induced dSURF1-s expression

Western Blot conducted on 10 adult flies from lines: (1) Syn1; *hsp70-Gal4*; (2) Syn2; *hsp70-Gal4*; (3) Syn3; *hsp70-Gal4*, in which expression of *dSurf1-s* was induced by heat shock (1 h, 37^{o}C) administered at 48 h AEL. The bands indicated in the gel are HSP-70 (the reference protein) and dSURF1-HA.

Figure 3 - Western blot of dSURF1-s expression following different heat shock induction protocols

Western blot showing bands corresponding to the reference protein HSP-70 and dSURF1-s. The total protein extracts were obtained from 10 flies of line Syn2; IR *hsp70-Gal4* (A) heat shocked at 24 h AEL (lane 1), 48 h AEL (lane 2), 72 h AEL (lane 3).

Figure 4 (A, B, C, D) - dSurf1 KD vs Rescue Respiratory complex activities

Enzymatic activities of respiratory complexes I and IV, expressed as a ratio of Citrate Synthase activity, in larvae (A and B) and adults (C and D). Canton S = wild type control. IR = parental strain bearing the dsRNAi-expressing construct; *Act5C-Gal4* = parental strain expressing *Gal4* under the control of an

Act5C promoter. *dSurf1* KD = progeny, resulting from the cross of IR X *Act5C-Gal4*, exhibiting knockdown (KD) of *dSurf1*; Syn2. IR = parental strain bearing both the dsRNAi-expressing construct and the recoded synonymous rescue construct. *hsp-70-Gal4* = parental strain expressing *Gal4* under the control of an *hsp-70* promoter. Rescue = progeny, resulting from the cross of IR X *hsp-70-Gal4*, exhibiting rescue of dSurf1. A and B show that in larvae, following ubiquitous KD of *dSurf1*, the activities of both complexes I and IV are significantly reduced with respect to controls. C and D show that in adult individuals, following rescue of ubiquitous *dSurf1* KD, the levels of respiratory complexes I and IV are comparable to those of controls.

Figure 5 - Larval vs adult Respiratory complex activities

Enzymatic actvities of respiratory complexes I and IV and of Citrate Synthase in Canton S (wild type control) larvae and adults.

Figure 6 (A, B) - Respiratory complex activities following dSurf1 KD in adult flies using an RU486-Gal4 driver

Enzymatic activities of: A) respiratory complex I; B) respiratory complex IV, both expressed as a ratio of Citrate Synthase activity, in adults of the following genotypes: Canton S = wild type control. IR = parental strain bearing the dsRNAi-expressing construct. *Switch-Act5C-Gal4* = parental strain expressing *Gal4* under the control of an RU486-inducible *Act5C* promoter. *dSurf1* KD = progeny from the cross of IR X *Switch-Act5C-Gal4*, exhibiting knockdown (KD) of *dSurf1*.

Tables

Table 1 - Base composition of the dSurf1 and dSurf1-s genes.

dSurf1	BASE COMPOSITION				%GC IN CODONS		
	A%	T%	C%	G%	FIRST POSITION	SECOND POSITION	THIRD POSITION
NATIVE	24.03	19.49	28.35	28.13	59.14	43.52	66.78
SYNONYMOUS	24.73	20.65	28.06	26.56	60.32	43.23	60.32

For each sequence the table shows the general base composition as well as the proportion of GC nucleotides present in each of the three codon positions.

Table 2 - Survival to adulthood of rescued flies.

hsp70-Gal4 crossed to:	Progeny genotype	Mean % survivial
dSurf1-IR	IR *hsp70-Gal4*	0
dSurf1-s	Syn1 *hsp70-Gal4*	81.65 ± 8.49
	Syn2 *hsp70-Gal4*	64.22 ± 3.14
dSurf1-IR and *dSurf1-s*	Syn1; IR *hsp70-Gal4*	21.16 (17.88) ± 4.89
	Syn2; IR *hsp70-Gal4*	18.99 (13.98) ± 2.73

Values are expressed as percentages relative to the expected and are average values from three independent replicates (±S.D.). The values concerning individuals from lines homozygous for both *Surf1* constructs (Syn1; IR *hsp70-Gal4* and Syn2; IR *hsp70-Gal4*) were corrected for the lethality seen with individuals from lines expressing only the *dSurf1-s* construct (Syn1 *hsp70-Gal4* and Syn2 *hsp70-Gal4*), respectively. The uncorrected survival values are shown in parentheses.

SURF1 SYNONYMOUS SEQUENCE

cagtgcaaaacggtcttactatcaacttccagttggaaatgtaaataaataaataaatagaaaatttagagcaaa
ataaaagaaagtatgatacgtttggggaaccaaatgtgtcgacaggtcgcgttcaacattcaaacagttttccgg
aatcccggaacggccaataacccccaggttgattacgcgaaaaatgactcagcaacgtcccccggtcaactggacc
actagtatcccgaaccaagccgccaaagataaagaaaaaattgcccccttgggctggtttctgctcctgattccc
gcgacgacattcggattgggatgttggcaggtcaaacggaagatttggaaagaacaattgattaaagatctgaat
aaacaactcagtaccgcccccagtcgcacttcccgatgacctgaccgatttggcgcagatggaatatcggctcgtg
aaaatccgggggtcgatttctacatgataaagaaatgcggctcggaccgcggtcactcattcgcccggacggagtc
gagacgcagggcggcctgttttcccaacgggattccggaaacggatacctttattgttacgccattccaactcgct
gaccgggatgatatcgtcctggtgaaccgtggatgggtctcgcggaaaacaggtcgaaccccgagacgagacccctc
ggacagcagcaagccgaggtcgaactgacggcggtggtccggaagggcgaagcgcggccgcaatttactccggat
cataaaggaaacgtgtacctgtaccgggatttagcccggatgtgtgcggcgactggcgctgcaccagtctttctc
gatgcggtgtatgacccccagactgcagctcacgcacctataggaggccaaactcgggtgacgctccggaatgac
cacctctcctatctcgtcacgtggtttagcctgtcagccgcgacgtcattcctgtggtaccggcagattgtgaaa
agaatcccgtttttacccctacgatgtgcccgattacgcctgaaaaagggaacccaaatcaaacgcact

Bold = Region targeted by RNAi in wild type *dSurf1*.
Red = start (atg) and stop (tga) codons
Pink = substituted nucleotides
Yellow = HA-tag sequence

Figure 1

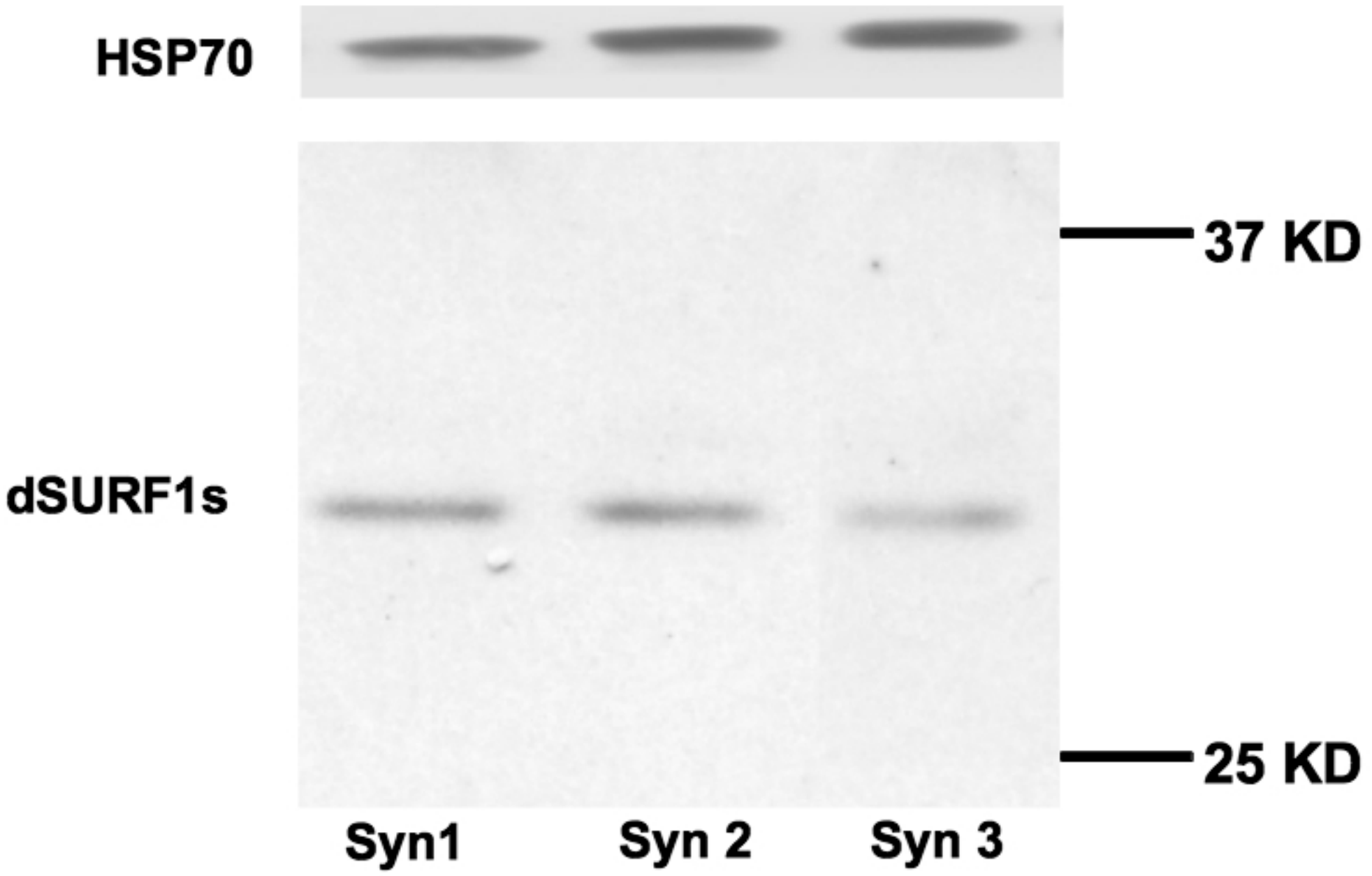

Figure 2

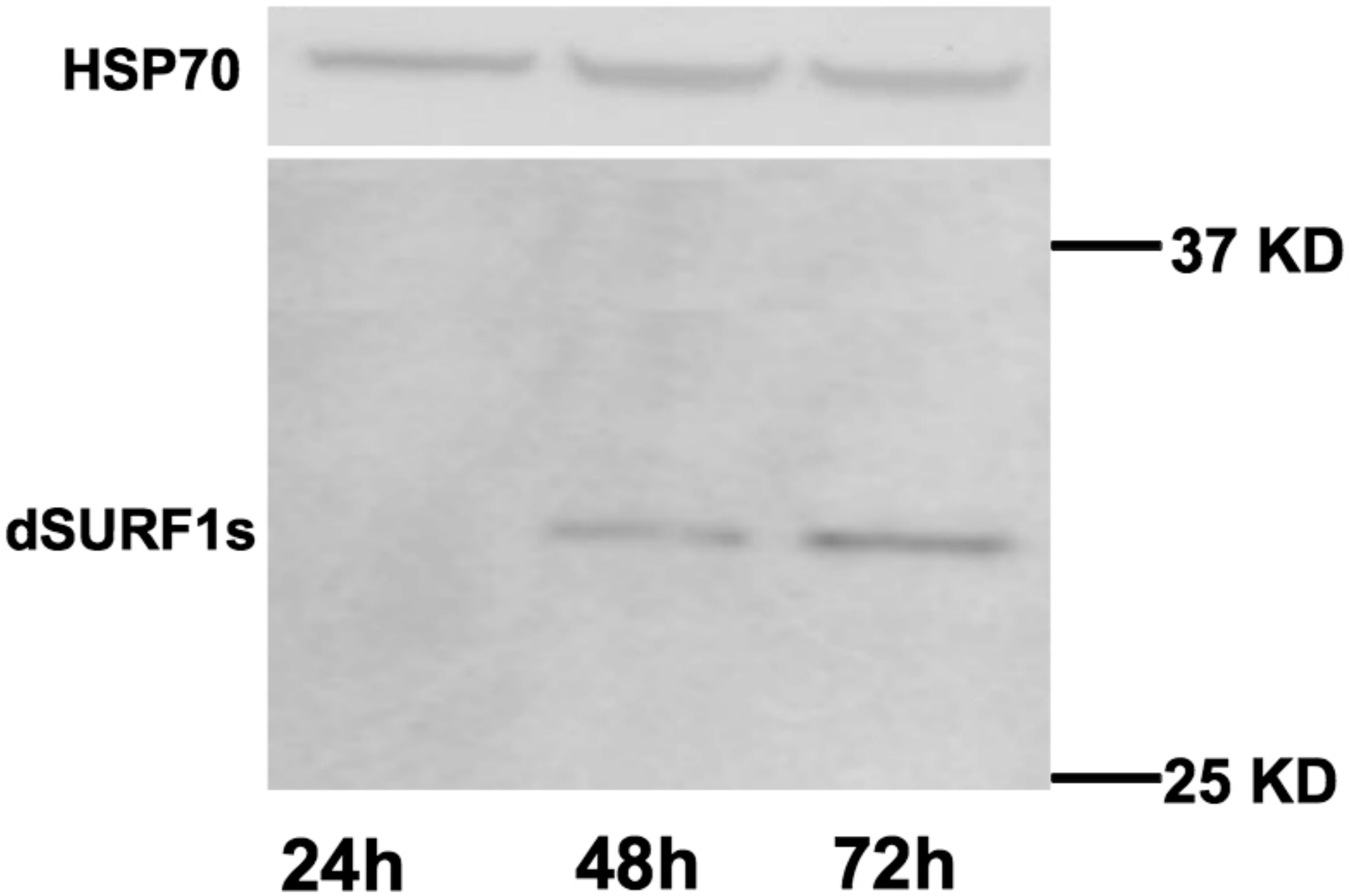

Figure 3

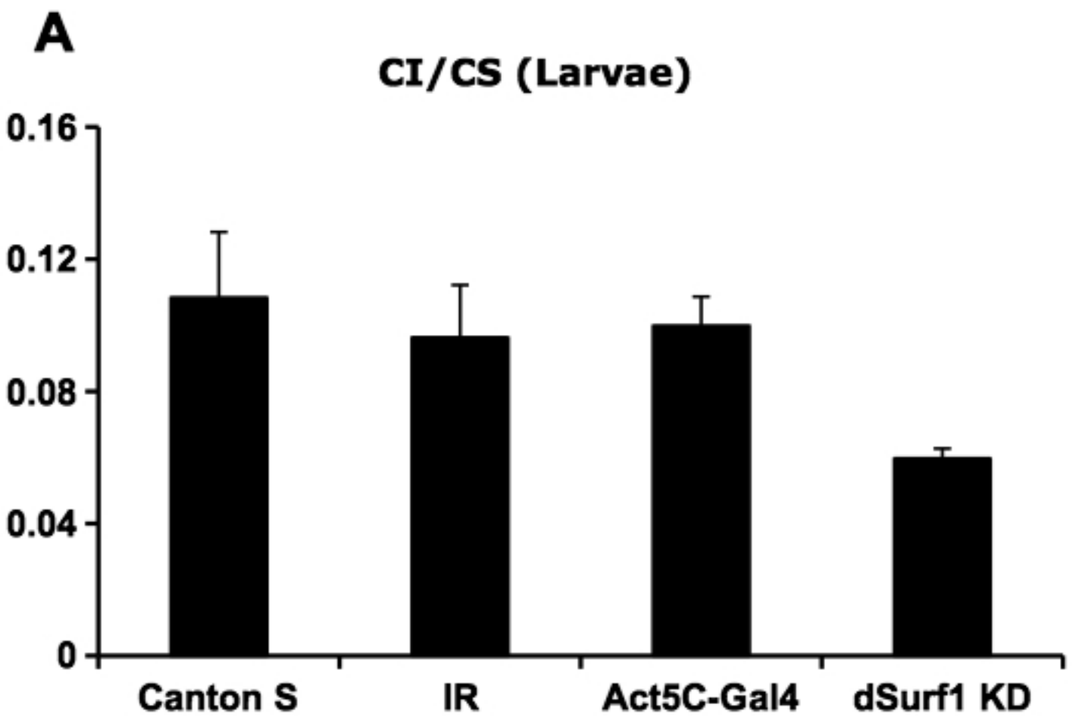
A
CI/CS (Larvae)
0.16
0.12
0.08
0.04
0
Canton S
IR
Act5C-Gal4
dSurf1 KD

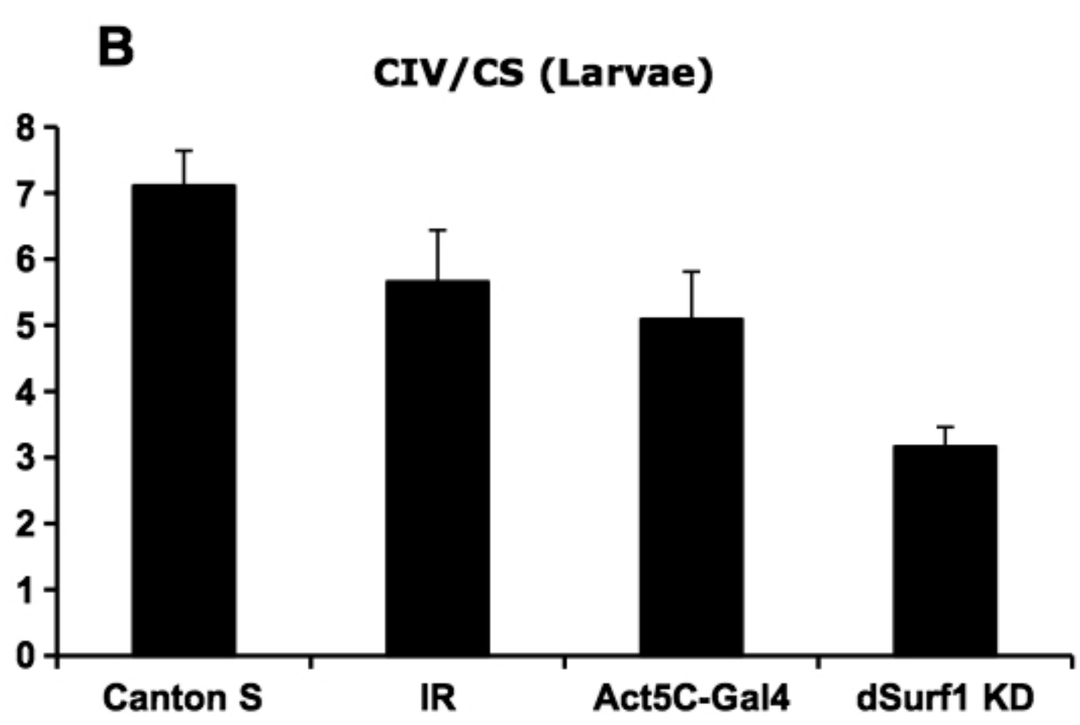
B
CIV/CS (Larvae)
8
7
6
5
4
3
2
1
0
Canton S
IR
Act5C-Gal4
dSurf1 KD

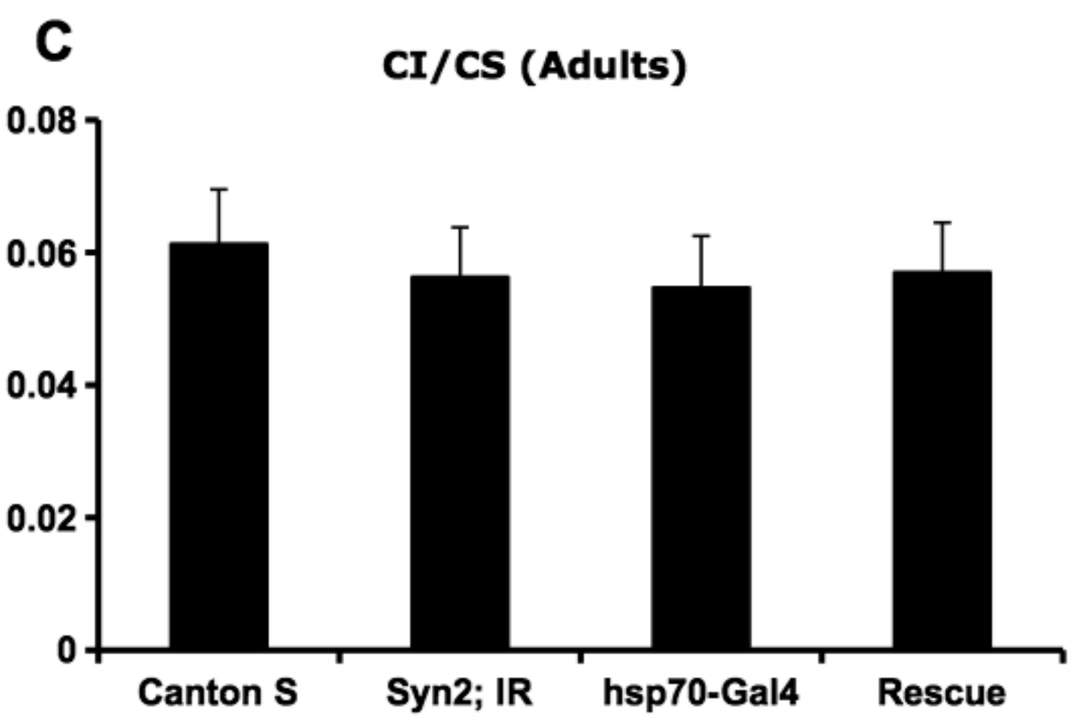
C
CI/CS (Adults)
0.08
0.06
0.04
0.02
0
Canton S
Syn2; IR
hsp70-Gal4
Rescue

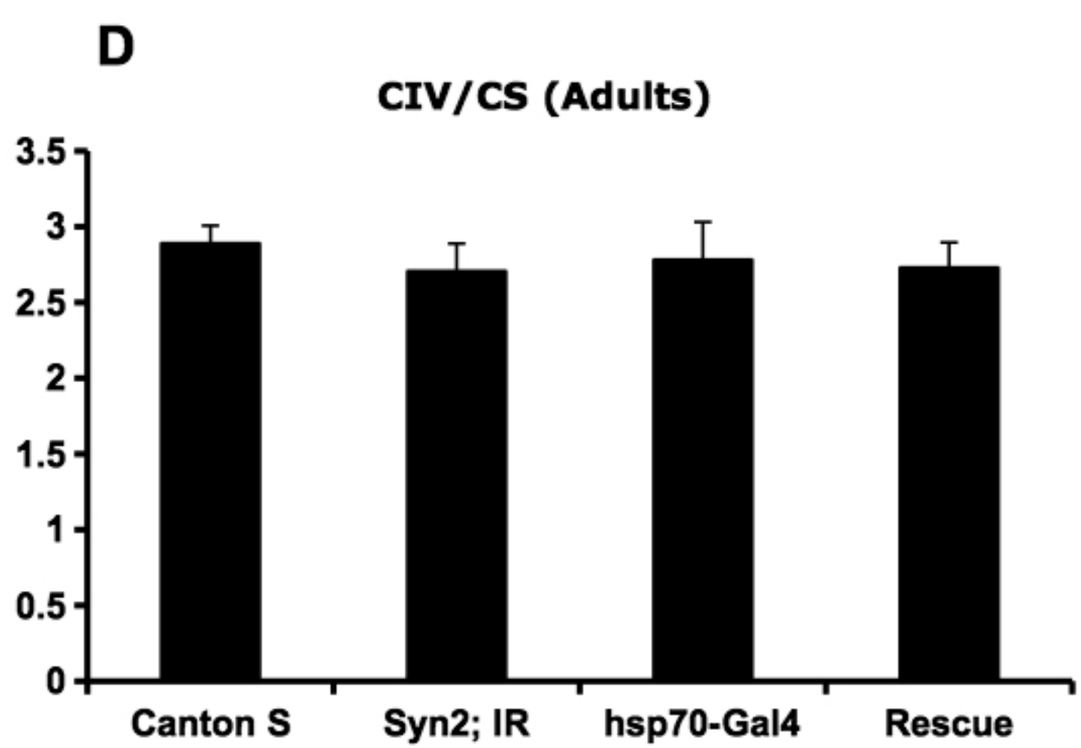
D
CIV/CS (Adults)
3.5
3
2.5
2
1.5
1
0.5
0
Canton S
Syn2; IR
hsp70-Gal4
Rescue

Figure 4

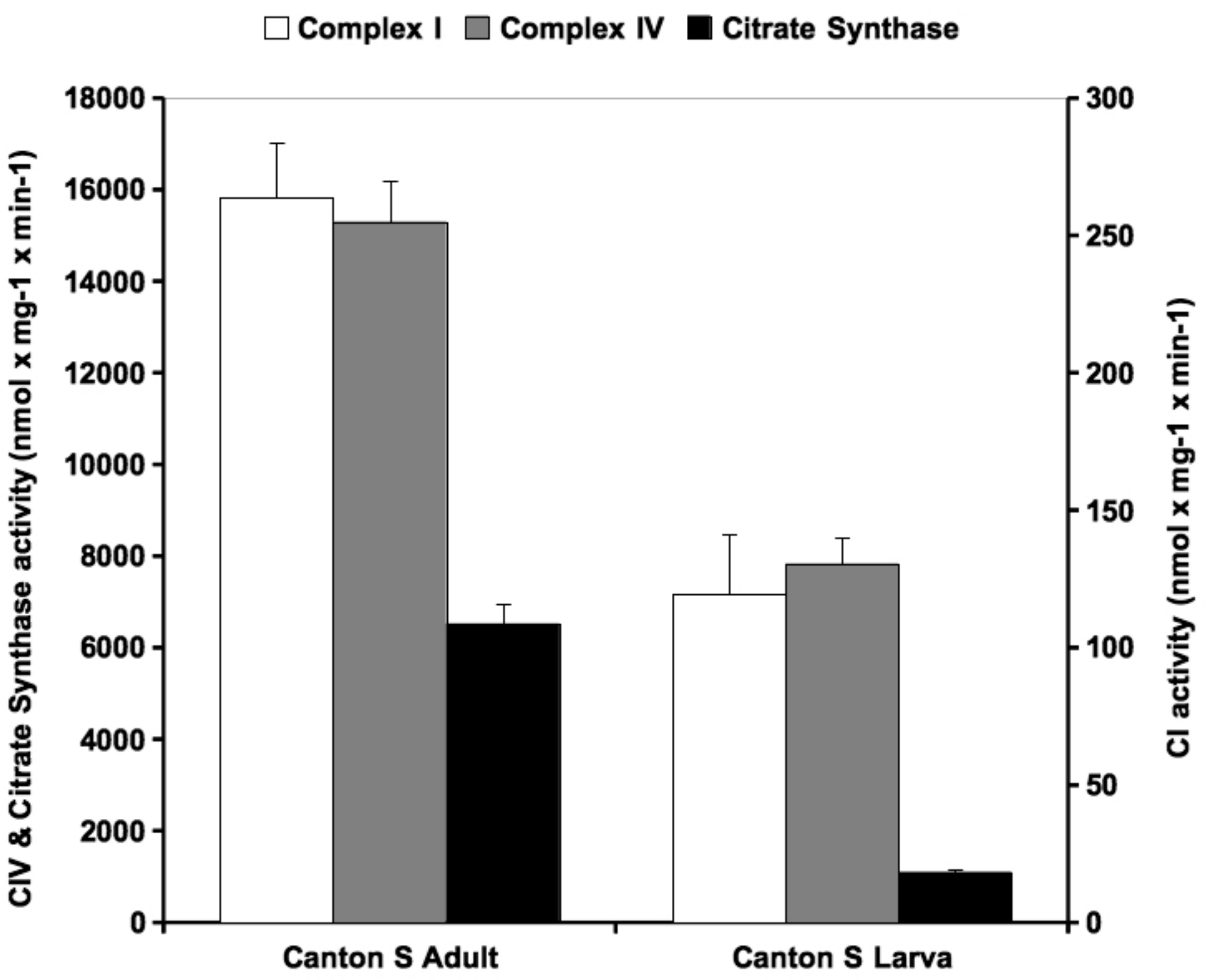
Complex I
Complex IV
Citrate Synthase
CIV & Citrate Synthase activity (nmol x mg-1 x min-1)
CI activity (nmol x mg-1 x min-1)
18000
16000
14000
12000
10000
8000
6000
4000
2000
0
300
250
200
150
100
50
0
Canton S Adult
Canton S Larva

Figure 5

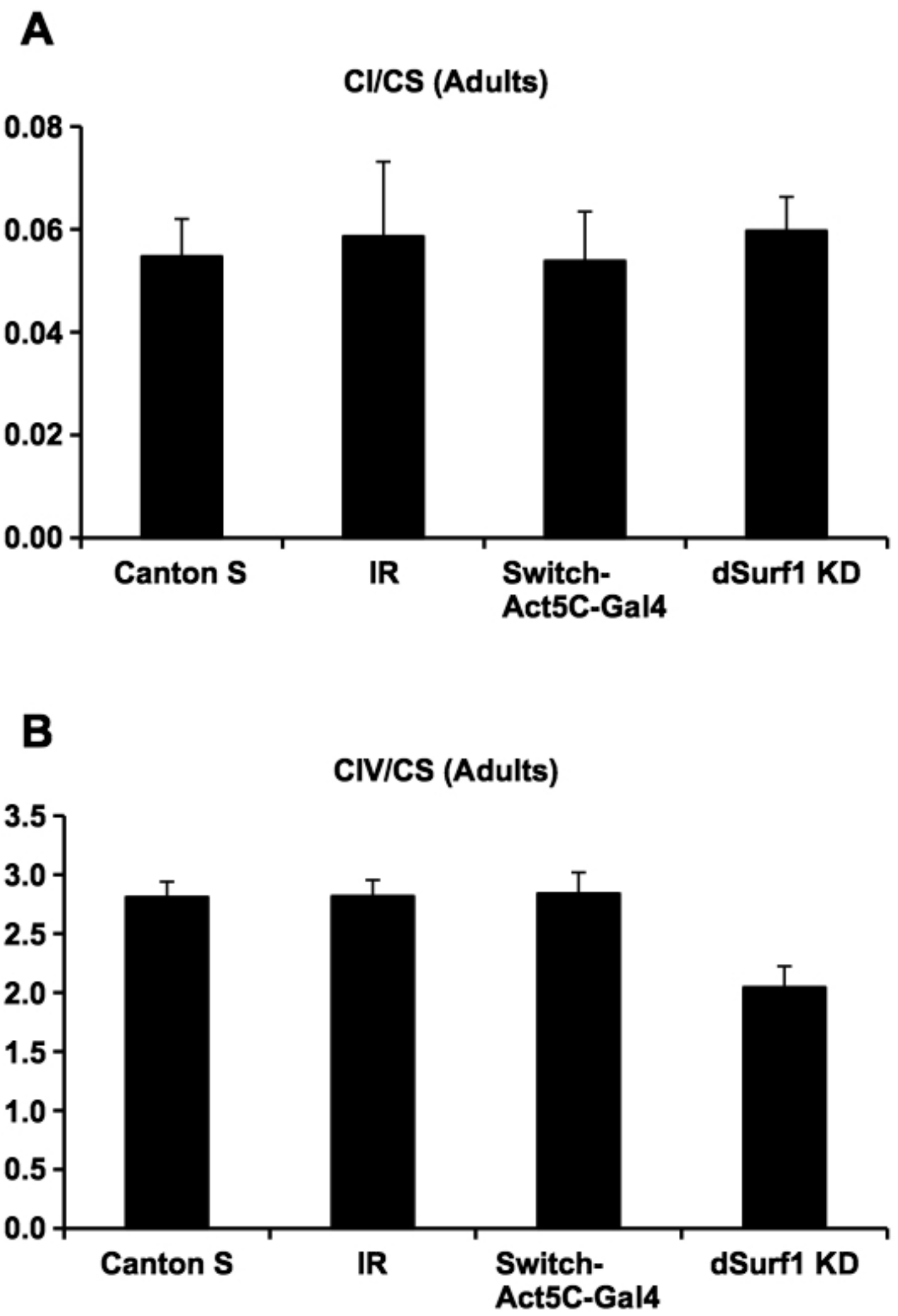
A
CI/CS (Adults)
0.08
0.06
0.04
0.02
0.00
Canton S
IR
Switch-
Act5C-Gal4
dSurf1 KD
B
CIV/CS (Adults)
3.5
3.0
2.5
2.0
1.5
1.0
0.5
0.0
Canton S
IR
Switch-
Act5C-Gal4
dSurf1 KD

Figure 6

PART II

Characterization of ETHE1, a mitochondrial dioxygenase

Ethylmalonic Encephalopathy (EE) is a rare infantile metabolic disorder caused by mutations in *ethe1,* a nuclear gene encoding a mitochondrial sulfur dioxygenase working in tight association with Rhodanese. EE is a disease characterized by an impaired catabolism of inorganic sulfur leading to accumulation of H_2S in key tissues. In mammalian tissues H_2S is a gasotransmitter acting as a signalling molecule, but at supraphysiological concentrations it is a powerful inhibitor of COX with an efficiency similar to that of HCN. The toxic effects of H_2S can account for several features of EE, including ethylmalonic aciduria, COX deficiency, microangiopathy, acrocyanosis and chronic diarrhea (Tiranti et al, 2009). In order to explore the molecular pathogenesis underlying EE, it would be useful to establish a *Drosophila melanogaster* model in which the expression of CG30022 (d*Ethe1*), the *Drosophila Ethe1* homolog, is disrupted or impaired. The *Tilling* technique was used to locate mutations, produced by expousure to EMS, in specific regions of the d*Ethe1* gene. We obtained a number of fly lines carrying different mutations in the d*Ethe1* gene from the FlyTill project (Till et al, 2003). We concentrated our attention on a line harbouring a missense mutation (P157S) localized next to the active site of the putative dETHE1 protein, which is predicted to modify the catalytic activity. We performed an in depth phenotypic analysis of heterozygous individuals for the mutation over a deletion which removes the whole of the d*Ethe1* gene.

We also set up a strategy that provides a way to generate high resolution deletions in the *Drosophila* genome by FLP-FRT recombination. In presence of FLP recombinase, efficient trans-recombination between FRT-bearing transposon elements results in a genomic deletion with precisely defined endpoints. Final confirmation of the deletion ends was provided by specific PCR (Parks et al, 2004). In this way we obtained a number of fly lines lacking the whole of the *Sprite* gene which contains d*ethe1* in one of its introns. Thus the transgenic lines, which were homozygous viable, were deleted for both the *dEthe1* and *Sprite* genes. In order to characterize the phenotype of the knock out flies from the biochemical point of view, we performed biochemical assays on these individuals to measure the enzymatic activities of complexes I and IV of the mitochondrial respiratory chain. We observed that COX activity is markedly decreased in *Ethe1* knock out individuals while complex I is not affected.

We thus demonstrated that in *Drosophila* isolated mitochondria, following *in vitro* exposure to NaHS, COX residual activity decreases as a function of increasing NaHS concentration. NaHS leads to the generation of H_2S. Furthermore, we observed that *Ethe1*$^{-/-}$, *Sprite*$^{-/-}$ flies are more sensitive to the lethal effects of NaHS poisoning. Starting from these "double" knock out lines we are currently producing new lines in which the the *sprite* sequence, cloned into a pUAST vector, will be introduced into the double knock out background in order to obtain individuals bearing only the d*Ethe1* knock out.

INTRODUCTION

1.1 Ethylmalonic encephalopathy: clinical and molecular features

Ethylmalonic encephalopathy (EE [MIM 602473]) is a rare autosomal recessive metabolic disorder which was originally reported in Italian families (Burlina et al. 1991). Most of the patients with EE described thereafter have been, with a few exceptions (Yoon et al. 2001), of Mediterranean (Burlina et al. 1991, 1994; Garavaglia et al. 1994; Garcia-Silva et al. 1997; Grosso et al. 2002) or Arabic (Ozand et al. 1994) descent. EE is characterized by neurodevelopmental delay and regression, prominent pyramidal and extrapyramidal signs, recurrent petechiae, orthostatic acrocyanosis (figure 1*a*), and chronic diarrhea, leading to death in the first decade of life. Symmetrical necrotic lesions in the deep gray matter structures are the main neuropathological features of the disease (figure 1*b*). These lesions may be related to the toxicity of metabolites that accumulate, or they may be secondary to the vascular changes commonly observed in this disorder.
Recently, mutations in *ETHE1*gene, a nuclear gene encoding a mitochondrial sulfur dioxygenase (Tiranti et al. 2009), were proven to be cause of EE (Tiranti et al. 2004; 2006; Mineri et al. 2004). To investigate to what extent *ETHE1* is responsible for EE, this gene was analyzed in 29 patients affected by EE and in 11 patients presenting early onset progressive encephalopathy with ethylmalonic aciduria (non-EE EMA). No *ETHE1* mutations were identified in non-EE EMA patients. Sequence analysis of the *ETHE1* gene revealed the presence of 22 mutations, which were all found in the 29 subjects affected by EE. No mutation was found in the 11 non-EE EMA patients. Sixteen mutations predicted nonsense changes, while six mutations predicted missense changes. The mutations cause truncated proteins or splicing errors (Tiranti et al. 2006).

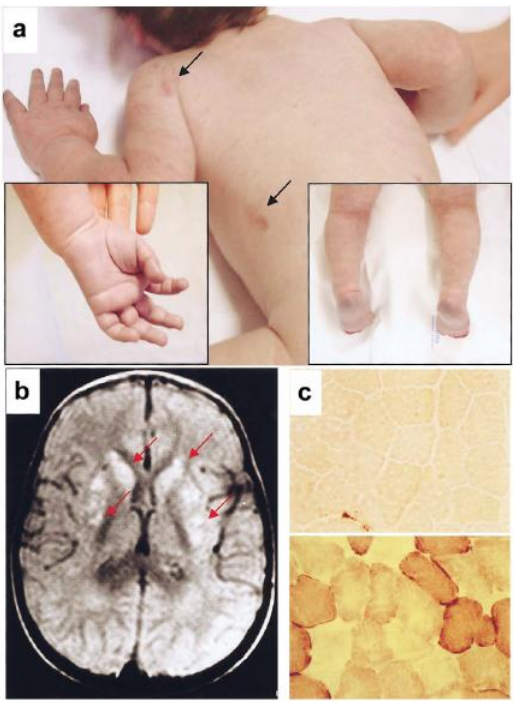

Figure 1.1 Clinical and biochemical features of EE. .
a. Skin areas with petechiae are indicated by arrows The boxed pictures show acrocyanosis of hands and feet.
b. On T2–fluid-attenuated-inversion-recovery (FLAIR) MRI images of a transverse section of the brain, symmetrical, patchy, high-intensity signals are present in the head of nucleus caudatus and in the putamen (arrows). **c**. Histochemical reaction to cytochrome *c* oxidase (COX) in skeletal muscle. The muscle of a patient with EE (*top*) shows a profound and diffuse reduction in COX reactivity, compared with an age-matched control biopsy (*bottom*), (Tiranti et al., 2004).

1.1.1The biochemical profile

EE is characterized by an unusual combination of biochemical findings, which include persistent lactic acidemia, elevated concentrations of C4 and C5 plasma acylcarnitine species, markedly elevated urinary excretion of ethylmalonic acid (EMA), elevated C4–6 acylglycines, notably isobutyrylglycine and 2-methylbutyrylglycine, COX deficiency in muscle and brain (fig. 1*c*) (Burlina et al. 1991).

Ethylmalonic acid derives from α-carboxylation of butyrate, as a consequence of disorders of the ß-oxidation of short-chain fatty acids, however EMA can be also derived from 2-ethylmalonic-semialdehyde, the final product of the R-pathway catabolism of isoleucine (Mamer et al. 1976; Nowaczyk et al. 1998). The differential diagnosis of persistent EMA aciduria is short-chain acyl- CoA dehydrogenase deficiency, including the common variants (Corydon et al. 2001), glutaric acidemia type 2 (sometimes described as ethylmalonic adipic aciduria) (Mantagos et al. 1979), Jamaican vomiting sickness (Tanaka et al. 1976) and EE.

The combination of ethylmalonic aciduria and high C4 and C5 acylcarnitines is the biochemical hallmark of short-chain acyl-CoA dehydrogenase (SCAD) deficiency (Gregersen et al. 1998). Elevated amounts of C4 acylcarnitines, C5 acylcarnitines or both are also present in defects of branched-chain acyl-CoA ß-oxidation, including isobutyryl-CoA dehydrogenase deficiency (Koeberl et al, 2003), 2-α-methylbutyryl-CoA dehydrogenase deficiency (Sass et al. 2008) and isovaleric acidemia (Vockley et al. 2006). However, neither mutations in the genes responsible for, nor impairment of the metabolic pathways affected by these defects were ever detected in ethylmalonic encephalopathy (Garcia-Silva et al. 1994).

In bacteria, *ETHE1*-like sequences are in the same operon of, or fused with, orthologs of TST, the gene encoding rhodanese, a sulfurtransferase. In eukaryotes, both *ETHE1* and rhodanese are located within the mitochondrial matrix. A functional link between ETHE1 and rhodanese has been demonstrated. Levels of sulfur metabolites were measured in both individuals with ethylmalonic encephalopathy and in a mouse model of EE. It was found that thiosulfate was excreted in massive amounts in urine of both *ETHE1*$^{-/-}$ mice and humans with ethylmalonic encephalopathy. High thiosulfate and sulfide concentrations were also present in *ETHE1*$^{-/-}$ mouse tissues (Tiranti et al. 2009).

Sulfide is a colorless gas with a characteristic smell of rotten eggs. In mammalian tissues, H_2S is a gasotransmitter acting as a signaling molecule (Szabo et al. 2004), but at supraphysiological concentrations it is a powerful inhibitor of COX. COX inhibiting concentrations of sulfide are indeed similar to those of cyanide (Leschelle et al. 2005). Sulfide inhibits COX activity and short-chain fatty acid oxidation with vasoactive and vasotoxic effects, that may explain the microangiopathy in

ethylmalonic encephalopathy patients (Tiranti et al. 2009). Sulfide is detoxified by a mitochondrial pathway that includes a sulfur dioxygenase.

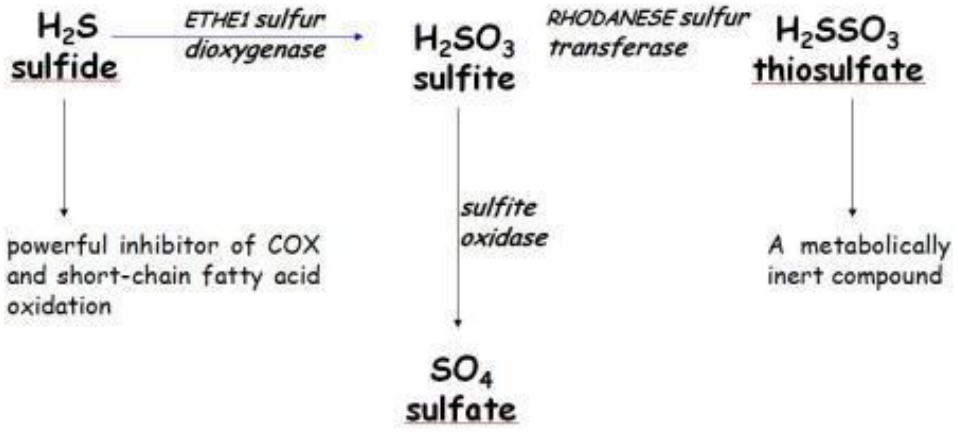

Figure 1.2. Sulfide detoxification pathway. ETHE1 seems to work as a sulfur dioxygenase which converts H_2S, a powerful inhibitor of COX, into sulfite. Then H_2SO_3 is detoxified into a metabolically inert compound: thiosulfate.

1.2 The human *ETHE1* gene

The human *ETHE1* gene, located at chromosome 19q13a (GenBank D83198) encodes a ß-lactamase–like, iron-coordinating metalloprotein which is involved in the sulfur detoxification pathway, acting as a sulfur dioxygenase (Tiranti et al. 2009).

The gene had previously been known as "*HSCO*" (for *hepatoma subtracted clone one*) a gene overexpressed in human hepatoma cell cultures (Higashitsuji et al. 2002). However, in light of its role in EE, the name of the gene has been changed to "*ETHE1*" (Tiranti et al. 2004).

The human *ETHE1* gene is characterized by 20525 bp, it consists of 7 exons encoding for a single 1kb transcript ubiquitously expressed. This transcript encodes an inactive precursor of almost 30 KDa which is imported into the mitochocondrial matrix by an energy-dependent process. Here the precursor is translated in an active 28 KDa form, after the cleavage of the mitochondrial leader peptide (Tiranti et al. 2004).

In bacteria, *ETHE1*-like sequences are in the same operon of, or fused with, orthologs of TST, the gene encoding rhodanese, a sulfurtransferase. In eukaryotes, both *ETHE1* and rhodanese are located within the mitochondrial matrix. Furthermore, *ETHE1*-like gene sequences of several eubacteria are either in the same operon with, or encoded within, genes that code for the sulfurtransferase rhodanese (Tiranti et al. 2009).

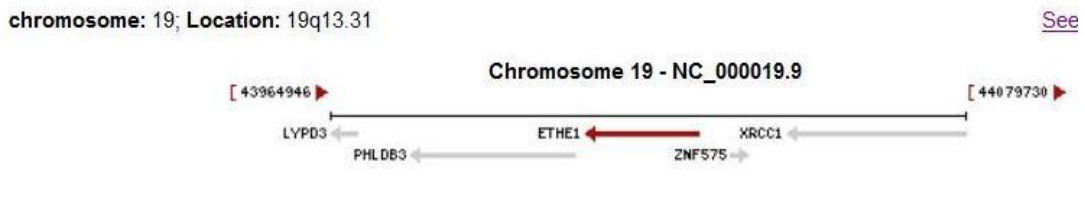

Figure 1.3. The ETHE1 human gene. The human *ETHE1* gene, located at chromosome 19q13a (Figure modified by http://www.ncbi.nlm.nih.gov).

1.3 ETHE1 protein: structure and function

The ETHE1 protein is a phylogenetically conserved protein. A bioinformatic search, with the human ETHE1 predicted protein sequence as a probe, resulted in the identification of highly similar proteins in all metazoan species, in plants, such as *Arabidopsis thaliana*, and in fungi, such as *Saccharomyces cerevisiae* (Tiranti et al. 2004). In contrast with the remaining portion of these protein sequences, the first 20–30 amino acid residues on the N-terminus appear to be poorly conserved. However, when the sequences were analyzed by organellar target–prediction softwares, a high score for mitochondrial targeting was obtained for all of them. This suggests the existence of a distinct family of mitochondrial proteins that is present in all eukaryotes and is structurally, and possibly functionally, similar to the human ETHE1 protein.

The ETHE1 proteins all contain a metallo-ß-lactamase region that, in the ETHE1 protein sequence, encompasses amino acid residues 35–196. A consensus signature sequence, HXHXD(X)H, is conserved throughout the ß-lactamase protein family and is believed to be the Zn(II) ligand (Aravind 1999). In addition, the ETHE1 protein sequences in humans, mice, and other organisms contain the Y residue, which is believed to be part of the binding site for glutathione (Ridderstrom et al. 2000).

The *ETHE1* gene encodes a protein which is demonstrated to be located within the mitochondrial matrix (Tiranti et al. 2004), for most proteins targeted to mitochondria, a canonical mitochondrial leader peptide, which is present at the N-terminus of the full-length ETHE1 protein, targets the protein to the organelle and is cleaved off after internalization in the inner mitochondrial compartment through an energy-dependent process, carried out by mitochondrial processing peptidase (MPP).

The ETHE1 protein also contains an amino (N)-terminal sequence of 24 amino acids, this region is rich in apolar and basic (mostly R) residues, similar to mitochondrial leader peptides (Attardi and Schatz 1988). When analyzed by dedicated software packages available online (Mitoprot-2, PSORT-II, Predotar, and TargetP), the predicted ETHE1 protein sequence showed a very high likelihood of being targeted to mitochondria. This analysis also suggested two potential cleavage sites for (MPP), between either A20 and P21 or R11 and Q12.

The predicted molecular weight of mature ETHE1 protein is 28 kDa. Taken together, these results suggest that, in native conditions, the ETHE1 protein is part of a complex, the size of which is between 28 and 60 kDa.

1.4 dETHE1 the Drosophila homolog

The *Drosophila melanogaster*, ETHE1 homolog is CG30022. This gene is located on chromosome 2R, in the 47F8 region and it spans 1462 bp. The d*Ethe1* gene is localized inside an intronic sequence of the *Sprite* gene (CG30023). The d*Ethe1* 1254-bp coding sequence consists of 4 exons (figure 3) and the single transcript encodes a 279 aa protein (Drysdale et al. 2005), the first 50 aminoacid residues forming the mitochondrial target sequence

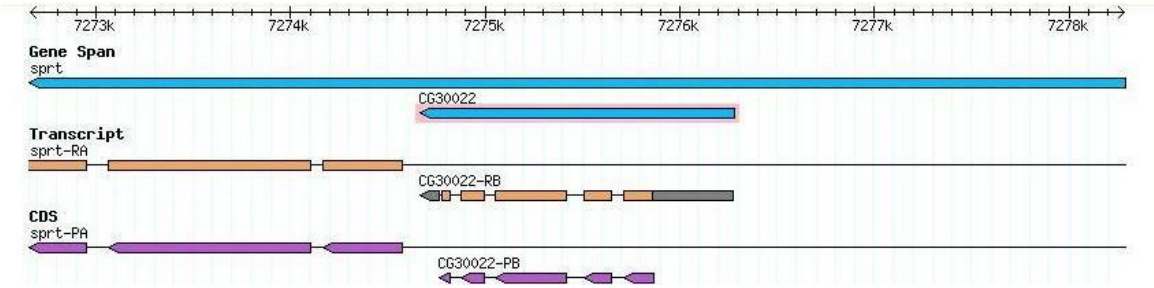

Figure 1.4. CG30022 gene is located at chromosomal region 2R47F8 in correspondence of intronic sequence of *sprt* gene. It consists of 4 exons and it encodes a single 1Kb transcript.(CG30022-PB). (Figure modified by http://Flybase.org).

The comparison between the human and *Drosophila ETHE1* sequences confirm the high conservation of this protein. The human and *Drosophila* sequence share a 58% of identity and 72% similarity. In addition both contain the typical β-lactamase fold and binding site (59-219 aa). In the case of the human protein it is known that five histidines and two aspartate residues interact directly with two zinc ions. All these residues are conserved in dETHE1, strongly suggesting that also this protein can bind two metal ions. In particular, the metal ion ligands are predicted to be H104, H106, and H159 (first metal ion; M1), and D108, H109, and H219 (second metal ion; M2). D179 is predicted to be the residue bridging the two ions. Respectively they correspond to residues H79, H81, H135, D83, H84, H195 e D154 of the human protein (Tiranti et al. 2006).
In addition, it has been demonstrated that the C-terminal region of both ETHE1 and dETHE1 proteins presents three α-helices, which is an invariant feature of enzymes with a β-lactamase fold (Gomes et al. 2002).

RESULTS AND DISCUSSION

3.1 Targeting Induced Local Lesions IN Genome

The Targeting Induced Local Lesions IN Genomes (TILLING) technique is used to locate mutations, produced due to exposure to EMS, in specific regions of the gene of interest.
We obtained a number of fly lines carrying different mutations in the d*Ethe1* gene from the FlyTill project. In particular we obtained 21 mutation-bearing lines, as shown below (table 3.1). Mutations located in the coding regions of d*Ethe1* can be furthermore distinguished as below:
- 7 missense (nonsynonymous) mutations (L65M, D67N, T120S, P157S, P237S, G262S)
- 3 synonymuos mutations (K69, V74, V167)
- 2 frameshift mutations, located in aminoacids D264 e K275

In particular frameshift mutations caused the following substitutions (highlighted) in the aminoacidic sequence:

- dETHE1 protein sequence:
wild type aminoacid sequence:
PYPKKIGGDVNILLYASFTKFNIF

- frameshift mutation in aminoacid D264 of dETHE1:
resulting protein sequence:
PYPKKIGGD**MRSMHITICVFY**

- frameshift mutation in aminoacid K275 of dETHE1:
resulting protein sequence:
PYPKKIGGDVNILLYASFTK**SFICLMARRPTVRSVGCTI**

Further investigations were carried out in the Drosophila lines bearing missense or frameshift mutations localized in the coding region of d*Ethe1*, since the expectation was that in such lines the probability of deleterious defects in the dETHE1 protein function was higher. Seven drosophila lines carrying such mutations in the d*Ethe1* coding sequence were identified and characterized (2952, 6043, 2788, 0242, 0493, 3976, 2770) and are reported in table 3.1.

Nucleotidic substitution	Localization	Mutation	Aminoacidic substitution	Line number
C330A	exon II	missense	L65M	2002
C336A	**exon II**	**missense**	**D67N**	**2952**
C334A	exon II	synonymous	K69=	/
A359G	exon II	synonymous	V74=	/
T445C	intron II	/	/	/
T455GAGA	intron II	/	/	/
C462T	intron II	/	/	/
G483A	intron II	/	/	/
A586T	**exon III**	**missense**	**T120S**	**6043**
C697I	**exon III**	**missense**	**P157S**	**2788**
G729A	exon III	synonymous	V167=	
C991T	**exon IV**	**missense**	**P237S**	**0493**
G1066A	**exon IV**	**missense**	**G262S**	**0242**
G1075ATGCGTAGTATG	**exon IV**	**frameshift**	**D264MRSMHIT ICVFY**	**3976**
T1108TTATA	**exon IV**	**frameshift**	**K275FICLMAR RPTVRSGCTI**	**2700**
C1129T	non coding region	/	/	/
C1134T	non coding region	/	/	/
G1153A	non coding region	/	/	/
A1259T	non coding region	/	/	/
C1304T	non coding region	/	/	/
G1368A	non coding region	/	/	/

Tabella 3.1: List of 21 mutations obtained from TILLING project. Every mutation is described by its nucleotidic substitution (genomic sequence), localization (exonic, intronic or non coding regions). Exonic located mutations are also characterized on the basis of aminoacid substitutions caused, type of mutation (missense, frameshift or synonymous). Drosophila lines used in further investigations are highlighted in bold font.

Lines 2770, 0242, 2952 and 0493, proved to be homozygous lethal. So at this point to evaluate whether the lethal phenotype observed in homozygous individuals belonging to such lines was effectively imputable to mutations in d*Ethe1* and not to other mutations present in the background of the mutagenized genome, we crossed each of these mutated lines with specific Drosophila strains bearing known deletions of varying extent associated with loss of d*Ethe1* gene.

In details we selected the following deletion bearing lines 190, 9344, 8910. The deletions spanned 600Kb, 500 Kb and 470 Kb of DNA respectively, all these deletions involved the loss of d*Ethe1* gene (figure 3.1).

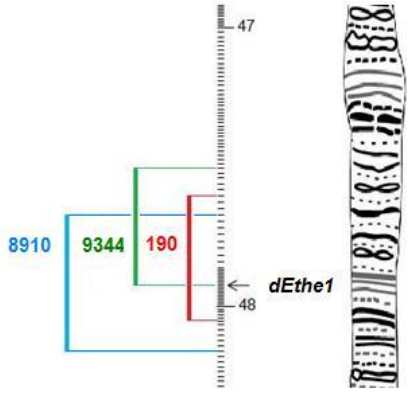

Figure 3.1. Deletions position. Cytological localization of deletions present in lines: 190, 9344 and 8910. Shown deletions extended respectively 600 Kb (line 190), 500 Kb (line 9344) and 470 Kb (line 8910). All these lines are associated with the loss of whole d*Ethe1* gene. Figure modified from http://www.flybase.org.

Therefore we concentrated our attention on line 2788, harbouring a point mutation, in which a single nucleotide is changed, resulting in an amino acid substitution (P157S) . This missense mutation is localized next to the active site of the putative dETHE1 protein (figure 3.2), which is predicted to modify the catalytic activity. In particular, the P157S mutation is placed at the level of the ß–lactamase region. The aminoacidic position 157 needs the presence of a small sized residue, in fact serine is a rather small aminoacid. However the substitution is by a polar aminoacid and this may modify the enzymatic substrate affinity. Furthermore the P157S substitution could induce structural destabilization caused by repulsion forces between neighbouring aminoacids.

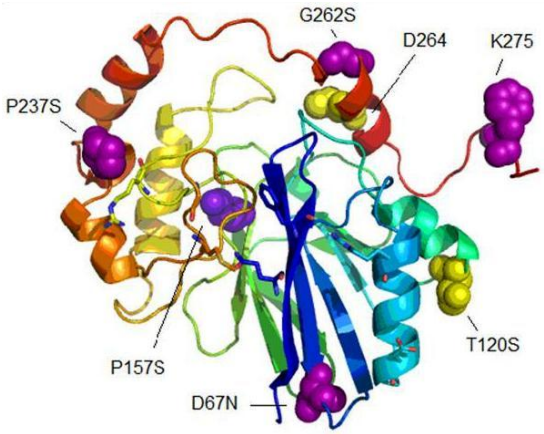

Figure 3.2. Hypothetical 3D structure of dETHE1 protein. The picture shows position of P237S, G262S, T120S, P157S mutations. In particular P157S mutation is located near to the active site, a catalytic center tightly binding a divalent metal cation, Fe^{2+} (Spadaro E. phD thesis).

3.1.1 Biochemical hallmarks

We performed biochemical assays to evaluate functionality of mitochondrial respiratory chain in homozygous (when possible) and hemizygous individuals. Hemizygous mutant flies were obtained by crossing TILLING lines (belonging to lines 2952, 6043, 2788, 2770) with line 190 (bearing a deletion of 600 kb located in proximity of d*Ethe1* gene and including it). The biochemical profile of hemizygous individuals (CI, CII, CII, CIV, CV, CS activities) was comparable to controls in following cases: 2952/190, 6043/190, 2770/190.
Hemizygous 2788/190 and homozygous 2788/2788 flies showed an interesting phenotype from the respiratory chain biochemistry point of view. In particular, both strains were characterized by a marked decrease in Complex IV activity compared to controls (figure 3.3).

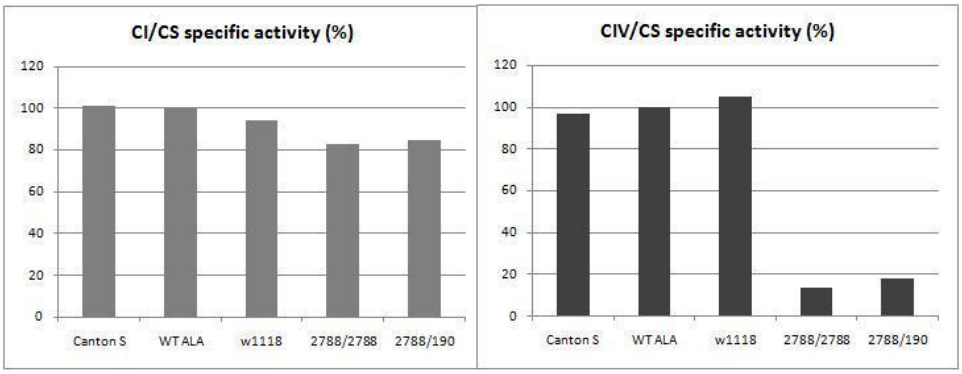

Figure 3.3. Biochemical assay of Complex I and Complex IV activities in control and d*Ethe1* mutant adult flies. Complex I (CI) and Complex IV (COX) activities, normalized to the activity of Citrate Synthase (CS), both expressed as nmol min^{-1} mg^{-1}. Data are means of duplicate experiments from at least 200 flies from each group. The values for the samples are all expressed as percentage of enzymatic activity where WTALA strain's activity is considered as 100%. It is clearly visible in the graphs that in individuals belonging to homozygous (2788/2788) and hemizygous (2788/190) mutant strains, COX activity is dramatically decreased over that of control flies (Canton S, w^{1118}, WT ALA).

3.1.2 Sulfide toxity

As previously discussed in the introductive chapter, ETHE1 is thought to be a mitochondrial sulfur dioxygenase, working in tight functional association with rhodanese and SQR. All three of these enzymes are involved in the catabolism of sulfide (H_2S) which accumulates to toxic levels in ethylmalonic encephalopathy. The product of ETHE1 sulfur dioxygenase is sulfite (H_2SO_3), which is converted into thiosulfate (H_2SSO_3) by rhodanese (see introduction fig. 1.2). Sulfide is a colorless gas, in mammalian tissues it is a gasotransmitter acting as a signalling molecule, but at supraphysiological concentrations it was proved to be a powerful inhibitor of COX and short-chain fatty acid oxidation, with vasoactive and vasotoxic effects that explain the microangiopathy in ethylmalonic encephalopathy patients. The principal role of the system is energetic exploitation of, and detoxification from, inorganic

sulfur compounds, mainly H_2S. According to these findings ethylmalonic encephalopathy is the first example of an inherited mitochondrial disease resulting from toxic inhibition of aerobic energy metabolism (Tiranti et al. 2009).
On the basis of this information we performed a number of experiments in order to characterize the sensitivity of Drosophila to sulfide toxicity. First of all we demonstrated the sulfide inhibiting capacity of COX in Drosophila isolated mitochondria. As shown in figure 3.4 below, following *in vitro* exposure to NaHS, COX residual activity decreases as a function of increasing NaHS concentration. In acqueous solution, NaHS leads to the generation of H_2S. We also demonstrated that COX inhibiting concentrations of NaHS are similar to those of KCN (figure 3.4).

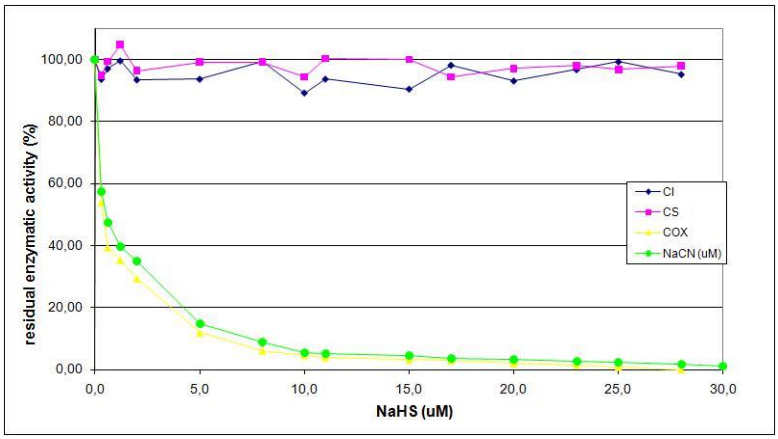

Figure 3.4. H_2S inhibition assay in isolated mitochondria. COX residual activity (%) decreases as a function of increasing NaHS concentration whereas Complex I and Citrate Synthase activities are not affected. NaHS leads to the generation of H_2S. COX inhibiting concentrations of NaHS are indeed similar to those of KCN. The decrease of COX activity observed following *in vitro* treatment of isolated Drosophila mitochondria with NaHS, is not as extreme as that seen with mouse tissues (Tiranti et al. 2009).

The inhibiting capacity of sulfide towards COX shown in isolated Drosophila mitochondria is in agreement with what has already been described for the mouse (Tiranti et al. 2009).
Furthermore, we observed that mutant d*Ethe1* flies show a marked increase in sensitivity to the lethal effects of NaHS poisoning (figure 3.5).

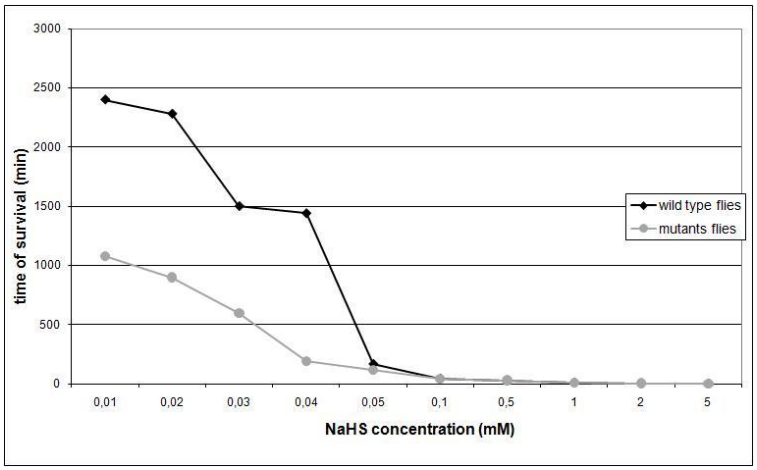

Figure 3.5. Sulfide toxicity in wild type and d*Ethe1* mutants. Canton S flies were used as wild type controls and line 2788 homozygous flies as mutants.

In particular we tested the survival time of both wild type and d*Ethe1* mutants under conditions of sulfide poisoning resulting from exposure to different concentrations of NaHS. As shown in table 3.2, fly survival time decreases as a function of increasing NaHS concentration. At higher NaHS concentrations (0,5-5 mM) both wild type and mutant individuals die within a maximum time of 45 minutes, whereas at lower concentrations of NaHS the response to the poisoning is different between controls and *dEthe1* mutants. In particular the latter die earlier, reflecting the fact that they are more susceptible to sulfide toxicity in comparison to wild type flies (table 3.2).

	NaHS concentration (mM)										
	10 mM	5 mM	2 mM	1 mM	0.5 mM	0.1 mM	0.05 mM	0.04 mM	0.03 mM	0.02 mM	0.01 mM
wild type	2 min	5 min	10 min	30 min	45 min	7 h	24 h	25 h	38 h	40 h	48 h
mutants dethe1	2 min	5 min	10 min	30 min	45 min	5h	8 h	10 h	15 h	18 h	20 h

Table 3.2. NaHS poisoning. Longevity of flies poisoned with sulfide decreases as a function of increasing NaHS concentration. It is quite clear that d*Ethe1* mutants are more susceptible to sulfide toxicity.

The latter experiment suggests that the specific inhibitory effect on COX activity shown by sulfide poisoning in Drosophila is probably reponsible for the lethal effects of sulfide. In fact, biochemical assays to measure residual COX activity in wild type individuals immediately after death from NaHS poisoning, showed that CIV functionality was dramatically reduced, whilst CI activity was not affected by NaHS poisoning (figure 3.6).

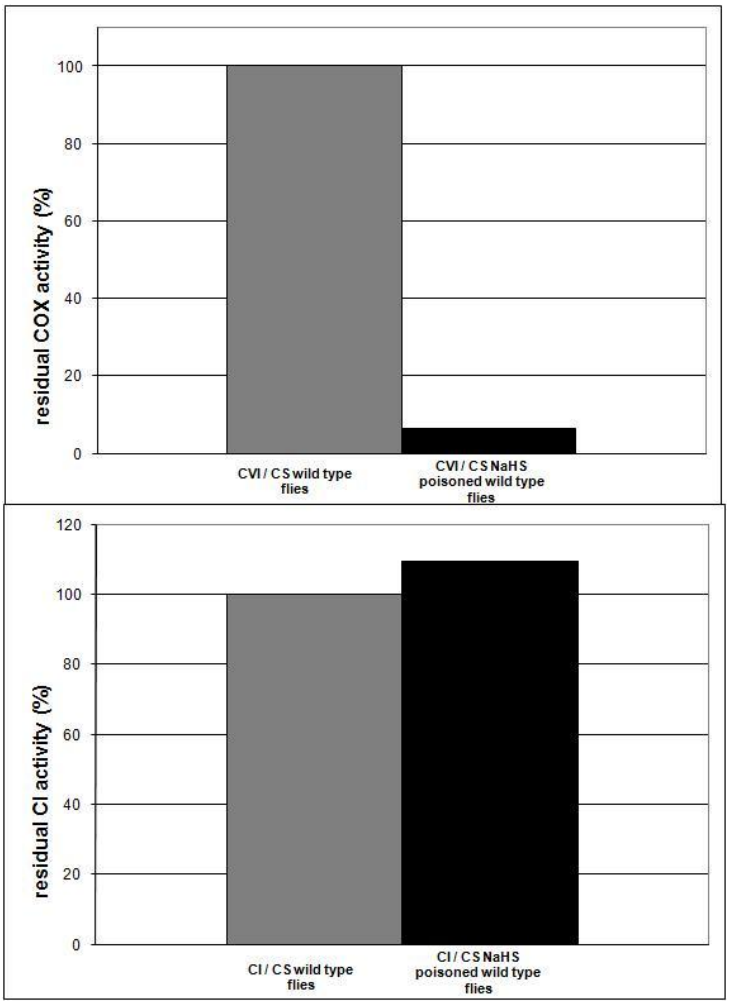

Figure 3.6. Complex IV (COX) and Complex I (CI) activity assay in isolated mitochondria of untreated wild type flies and wild type individuals immediately after death from exposure to 0,1 mM NaHS. Both COX and CI activities, normalized to the activity of CS, are expressed as percentage residual enzymatic activity.

3.2 Generation of the d*Ethe1* knock out line

Although the experiments described above for the *dEthe1* point mutant line 2788 show that the phenotype displayed by such mutants corresponds with the expectation for lack of *dEthe1* function, the fact that the mutant was obtained by chemical mutagenesis leaves the possibility that there might be other unwanted mutations in the genetic background of the strain. This prompted us to adopt a genetic approach to generate a targeted deletion of the *dEthe1* locus, in order to produce a "clean" *dEthe1* deficiency model, which could then be used as a model to explore strategies to modulate the effects of sulfide-induced respiratory chain toxicity.

The knock out strategy used FLP recombinase and the large array of FRT–bearing insertions which provides for the systematic isolation of targeted deletions in the *Drosophila melanogaster* genome (described in Parks et al. 2004).

The P–element insertional lines as well as the FLP recombinase transgene lines used were all from Exelixis (Exelixis, Inc. 170 Harbor Way South San Francisco).

3.2.1 Inverse PCR for recovery of sequences flanking XP elements

The first step before proceeding with the protocol for generating the required targeted deletion consists in ensuring the given positions of insertional elements, required to implement the methodology, by a PCR-based approach. Inverse PCR (iPCR), described by Ochman et al in 1988, is a method for the rapid *in vitro* amplification of DNA sequences that flank a region of known sequence. The method uses the polymerase chain reaction (PCR), but it has the primers oriented in the reverse direction with respect to the usual orientation. The template for the reverse primers is a restriction fragment that has been ligated upon itself to form a circle. Inverse PCR has many applications in molecular genetics, for example, the amplification and identification of sequences flanking transposable elements.

We used this technique to ensure the position of the transposons which were then used to generate the deletion. In particular, regarding P–element d03609, its position was confirmed to be on chromosome 2R; genomic position: 7285475, through the examination of sequences flanking the transposon insertion site, obtained after iPCR. Moreover, at the same time, the position of the second P–element, d00031, was established to be on chromsome 2R; genomic position: 7271757. This proves that both P–elements were in the correct given positions (i.e. flanking the *dEthe1* locus on either side). In our experience, it is highly recommended, to always ensure the location of required transposons before proceeding with the deletion generating protocol, in this manner deletions will occur with the predicted endpoints.

3.2.2 Generation of the Df(47F8) deletion

The Df(47F8) deficiency, in which both CG30022 (d*Ethe1*) and CG30023 (d*Sprite*) are deleted, was generated by following the FLP–FRT–based procedure, as described previously in materials and methods (chapter 2.2). Figure 3.7 below provides a schematic of genetic crosses exploited to generate the FLP-FRT catalyzed deletion. Briefly, P–element line d03609 (inserted at the 3' end of the neighboring CG30022 gene) was crossed to virgin flies carrying an FLP recombinase transgene [genotype: pCaspeR–heat shock–flippase (*hs–flippase*), w^{1118}; II/ *CyO*].

For the next generation (F1), the male progeny carrying both the d03609 and the *hs-flippase* transgenes were selected and mated with virgins carrying the d00031 P–element, inserted close to the 5' end of the CG30023 gene. The sequence included between the two transposons being (2R:7272238..7284935) also includes the CG30022 gene (*Sprite*) (sequence location 2R:7274663..7276282).

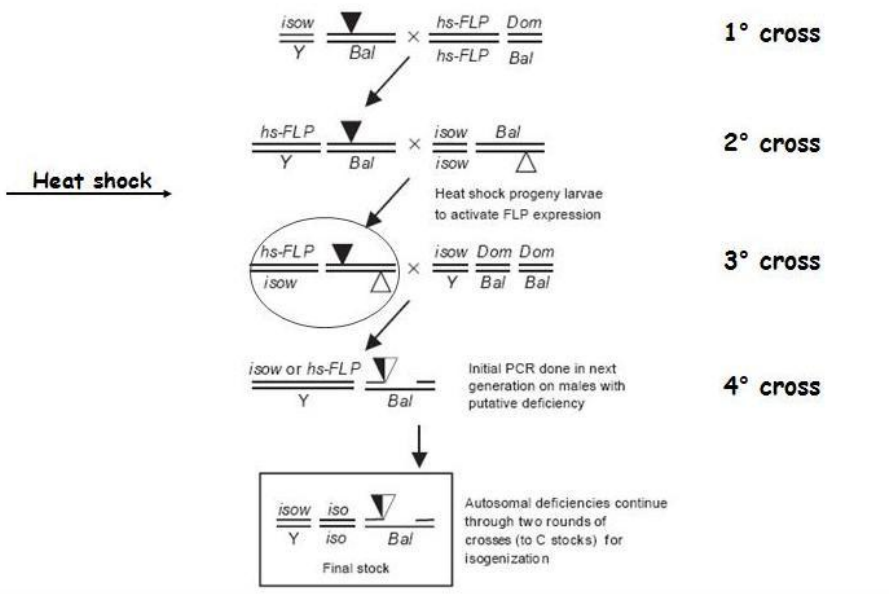

Figure 3.7. Genetic crossing schemes used to generate deletions. Genetic scheme used for FLP-FRT–based deletions. Crosses place two FRT-bearing transposon insertions (triangles) in *trans* in the presence of heat shock–driven FLP recombinase (*hs-FLP*). Activation of FLP recombinase results in the generation of deletions that can be detected by PCR. Deletions are established in isogenized stocks with balancers (*Bal*). *Dom*, dominant visible marker mutation; *iso*, isogenized chromosome; Y, Y chromosome. (Parks et al. 2004). Four crosses are sufficient to obtain the knock out line, further PCR screening is necessary in order to determine whether the deletion is confirmed.

The progeny from the above crosses was heat–shocked at 37°C for 1 hour, 48 hours after egg-laying, and was then heat-shocked for a further 1 hour during each of the following 4 days. In the third generation (F2), the virgin females were collected and crossed to males carrying balancer chromosomes (*w*; *CyO/ScO*). In the fourth generation (F3), individual progeny males (50 progeny from *w+* deletion generation crosses) carrying the Df(47F8) deletion were selected based on their red eye color, and crossed pairwise to virgin females carrying balancer chromosomes to establish individual fly lines and to generate additional progeny to be verified by PCR. The presence of the deletion in these lines was confirmed by PCR analysis of extracted genomic DNA and by DNA sequencing.

Males carrying the Df(48F) deletion balanced with *CyO* were then crossed with virgin females carrying the deletion balanced with *CyO* to balance the stocks in an isogenic background.

The deletion resulted in the complete remove of both the d*Ethe1* and d*Sprite* genes. Using the same approach we also produced another smaller deletion with the use of the piggy Bac–element e01563 (see figure 3.8) and the P–element d03609, but we did not obtain the expected results.

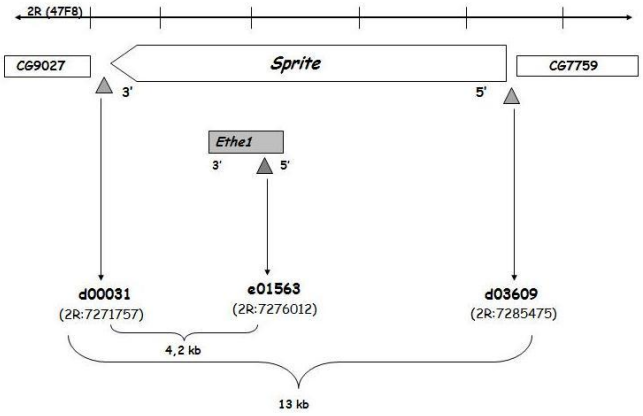

Figure 3.8. Schematics for deficiency generation. We used two different pairwise combinations of Exelixis transposons, harboring FRT sequences, for deletion generation. In the first case we obtained a bigger deletion through the combination of the FRT bearing lines (FRTs located at the extremes of the *Sprite* gene (d00031 and d03609)). Furthermore, we attempted to generate a smaller deletion, comprising *Ethe1* and the 3' part of *Sprite* gene, through recombination, in presence of FLP recombinase, between FRT elements d00031 and e01563 which should have produced a genomic deletion with a single residual element tagging the deletion site.

3.2.3 PCR confirmation of FLP-FRT–based deletions

We carried out all PCR reactions using purified genomic DNA from 50 homogenized flies obtained from each isolate line. In general, it was necessary to test 50 flies for each *w+* deletion. The PCR confirmation strategy (schematics in figure 3.9) used for initial detection of the deletion was carried out with the use of specific primer designed inside the P–elements (XP Reverse and XP Forward; in particular supplementary methods Parks et al. 2004 provide transposon primer sequences and expected fragment sizes for these combinations, as well as additional primer pair sequences for 'two-sided' PCR that may be used for secondary confirmation) and genomic primers chosen using an in-house primer design tool and made by Biosource. The primer sequences use for the PCR screen are shown in (Table 2.2 material and methods).

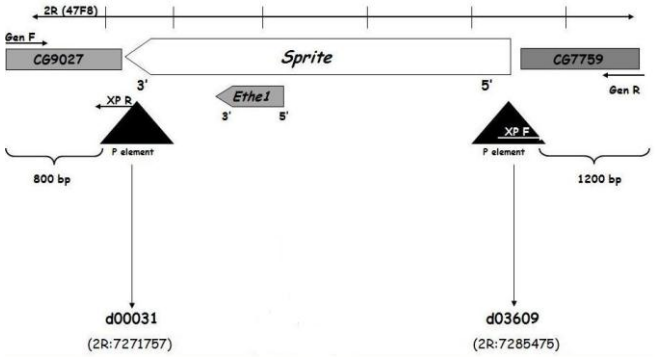

Figure 3.9. PCR primer position. Two-sided PCRs are carried out on both sides of p-element insertions. In particular, the PCR reaction at the level of d00031 P-element is conducted using a specific reverse primer (XP R) located inside the P-element and a genomic primer designed in the neighbouring gene cg9027. On the other hand, at the level of the d03609 P-element we used a pair of

primers: one inside the P-element (XP F) and another chosen in the sequence upstream of the *Sprite* gene (see table 3.3).

PCR screening and successive sequencing of the amplified products confirmed the obtainment of 7 lines carrying the desired deletion. We proceeded to further characterize only three of these KO lines.

Figure 3.10 shows the whole *Ethe1–Sprite* region, with the positions of both the d00031 and d03609 transposons highlighted. In particular, the region sequence begins, following the orientation of the genes (coding direction 5'–3') and not the direction implied by the genomic numeration, in fact it is useful to underline that both d*Ethe1* and d*Sprite* genes are are in orientation which is reversed with respect to the genomic sequence numeration (see figure above). Thus, with reference to the coding orientation of the genes we found in 5' position upstream to the *Sprite* gene sequences corresponding to the cg7759 gene, , followed by the d*Sprite* gene spanning 12697 bp (which includes 1619 bp corresponding to d*Ethe1*) and finally gene cg9027, localized 3' of the *Sprite* gene. The KO lines obtained showed a deletion spanning 13718 bp.

Interestingly the KO line proved to be homozygous viable, so further characterizations were performed in (*Ethe1*, *Sprite*) –/+ and (*Ethe1*, *Sprite*) –/– individuals.

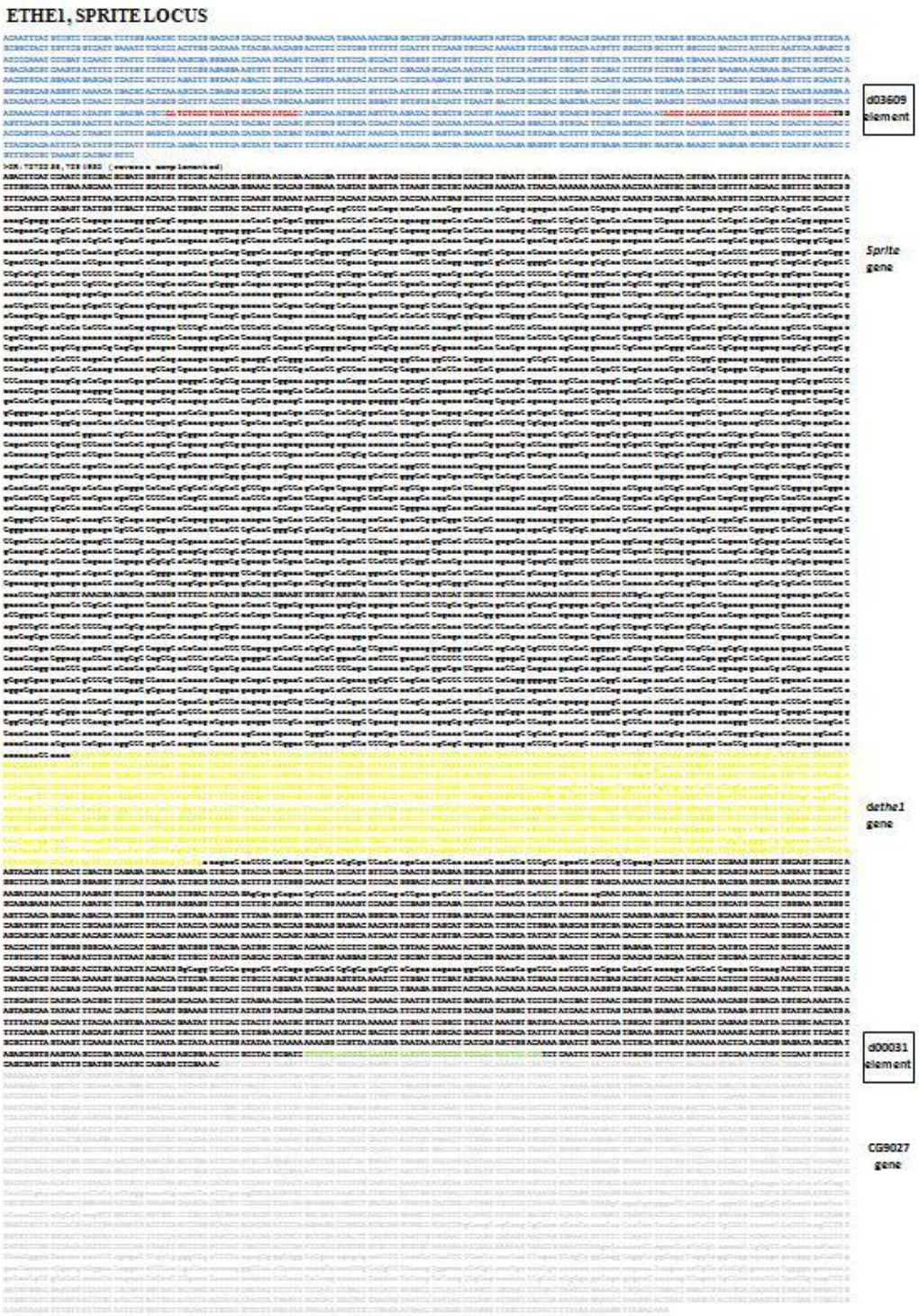

Figure 3.10. The ETHE1, SPRITE locus. Gene order in the 5' to 3' orientation. In blue the sequence upstream of the *Sprite* gene which spans from 2R:7272238 to 7284935**,** contained within the *Sprite* gene sequence is the *Ethe1* gene, in yellow, spanning from 2R:7274663 to 7276282. Finally in grey is gene cg9027 (2R:7267849…7271613**)** located downstream of *Sprite* gene. In addition d03609 5' and 3' flanking sequences are in red, to evidence the location of the P-element, whereas the d00031 3' flanking sequence is in green.

3.2.4 Characterization of KO line

At this point using the P–element lines d00031 and d03609 we obtained a knock out line bearing a deletion of ~13 Kb, which comprises both the d*Sprite* and d*Ethe1* genes.
Starting from these "double" knock out lines we are currently producing new lines in which the the *Sprite* sequence cloned into a pUAST vector will be introduced into the *Sprite*-knock out background in order to obtain individuals bearing only the d*Ethe1* knock out.
However, waiting for the single d*Ethe1* KO line, we tested sulfide–sensibility, mitochondrial respiratory chain state and longevity of these KO individuals.

Biochemical profile

Biochemical assays were performed to evaluate the functionality of the mitochondrial respiratory chain enzymes in double homozygous and double heterozygous KO individuals. Whereas the double homozygous strain is characterized by a marked decrease in Complex IV activity compared to controls, the double heterozygotes do not present any biochemical defects (figure 3.13).

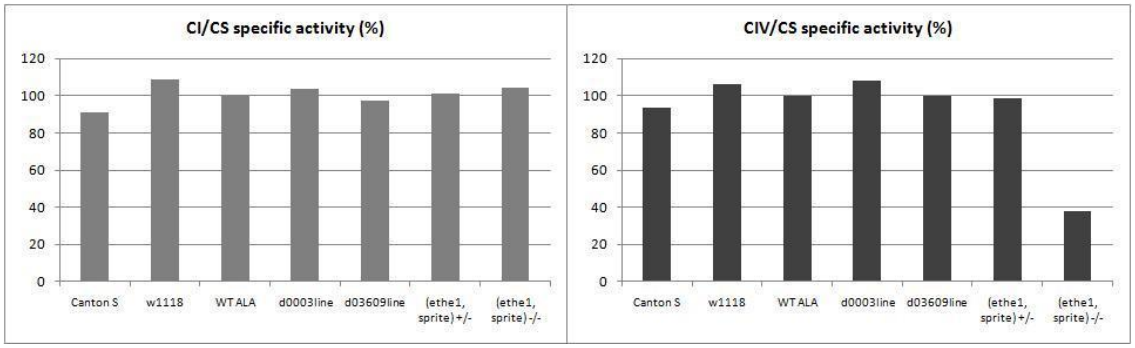

Figure 3.13. Biochemical assay of Complex I and Complex IV activities in control and d*Ethe1* KO adult flies. Complex I (CI) and Complex IV (COX) activities, normalized to the activity of Citrate Synthase (CS), both expressed as nmol min^{-1} mg^{-1}. Data are means of duplicate experiments from at least 200 flies from each group. The values for the samples are all expressed as percentage of enzymatic activity where WTALA strain's activity is considered as 100%. It is clear that double heterozygous KO (*Ethe1*, *Sprite*) flies showed a biochemical profile comparable to controls, whilst double homozygous KO individuals (*Ethe1*, *Sprite*) showed a marked decrease in COX activity in comparison to control flies (Canton S, w^{1118}, WT ALA).

Sulfide–sensitivity

Regarding the sulfide susceptibility we performed the same tests which were carried out in the case of the mutant d*Ethe1* flies, and similarly we observed that longevity of double homozygous KO flies following poisoning with sulfide decreases as a function of increasing NaHS concentration and, in particular, double homozygous KO individuals are more susceptible to sulfide toxicity compared to controls, as described for d*Ethe1* mutants (see figure 3.5).
Double heterozygous (*Ethe1*, *Sprite*) flies showed a behaviour comparable to controls, whereas the response of double homozygous (*Ethe1*, *Sprite*) flies to NaHS poisoning is indeed similar to the d*Ethe1* mutants (figure 3.11).

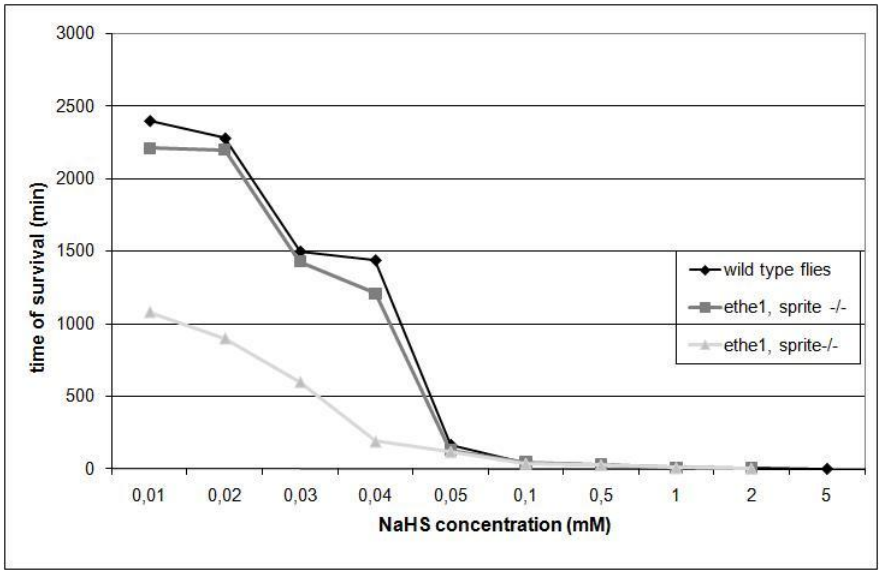

Figure 3.11. Survival time of knock out lines after exposure to NaHS at different concentrations. Sulfide toxicity was measured both in wild type, (*Ethe1*, *Sprite*) –/+ and (*Ethe1*, *Sprite*) –/– flies. Canton S was used as a wild type control.

In addition, biochemical assays were performed to measure the residual COX activity in homozygous KO individuals which had died following NaHS poisoning. We observed that CIV functionality was markedly reduced in the KO flies exposed to NaHS, whilst CI activity was not affected under the same experimental conditions (figure 3.12).

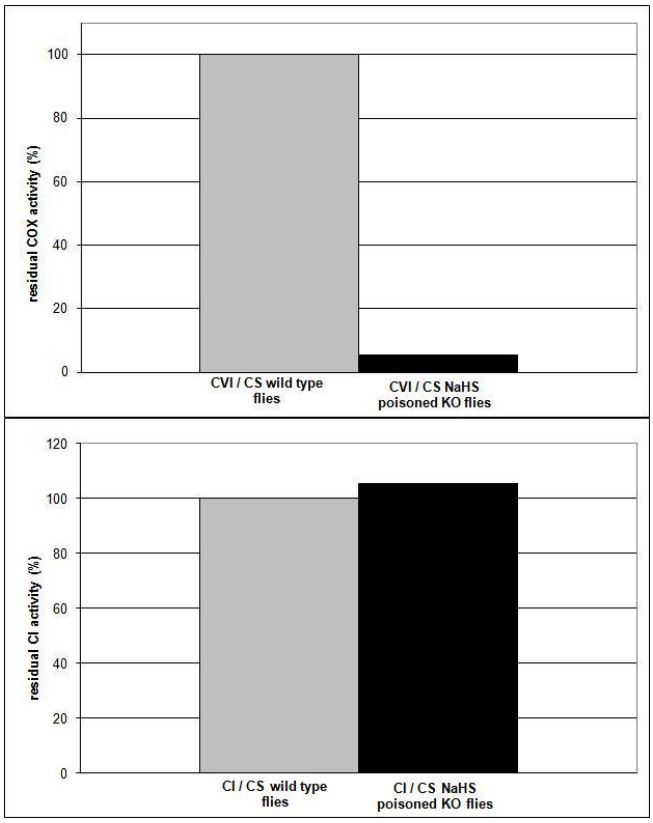

Figure 3.12. Complex IV (COX) and Complex I (CI) activities assayed in isolated mitochondria of not–treated wild type flies and of homozygous KO individuals which had died after exposure to 0,1 mM NaHS. Both COX and CI activities, normalized to the activity of CS, are expressed as percentage residual enzymatic activity.

Survival of adult flies

To investigate the effects of the double ablation of *Ethe1* and *Sprite* on lifespan, we assayed the longevity of female (non virgin) and male flies (see material and methods) in both homozygous and heterozygous lines.

We analyzed longevity of a total of 733 heterozygous KO individuals (354 females and 379 males), 612 homozygous KO individuals (312 females and 302 males) and 615 w^{1118} wild type flies (309 females and 306 males).

The KO homozygous flies exhibited a dramatic decrease in average lifespan over that of control and heterozygous flies (figure 3.14). Average lifespan of homozygous KO flies was decreased by ~60% in both sexes. In particular, control and heterozygous flies reached a maximum age of 110 days whereas the lifespan of homozygous KO individuals was around 45 days.

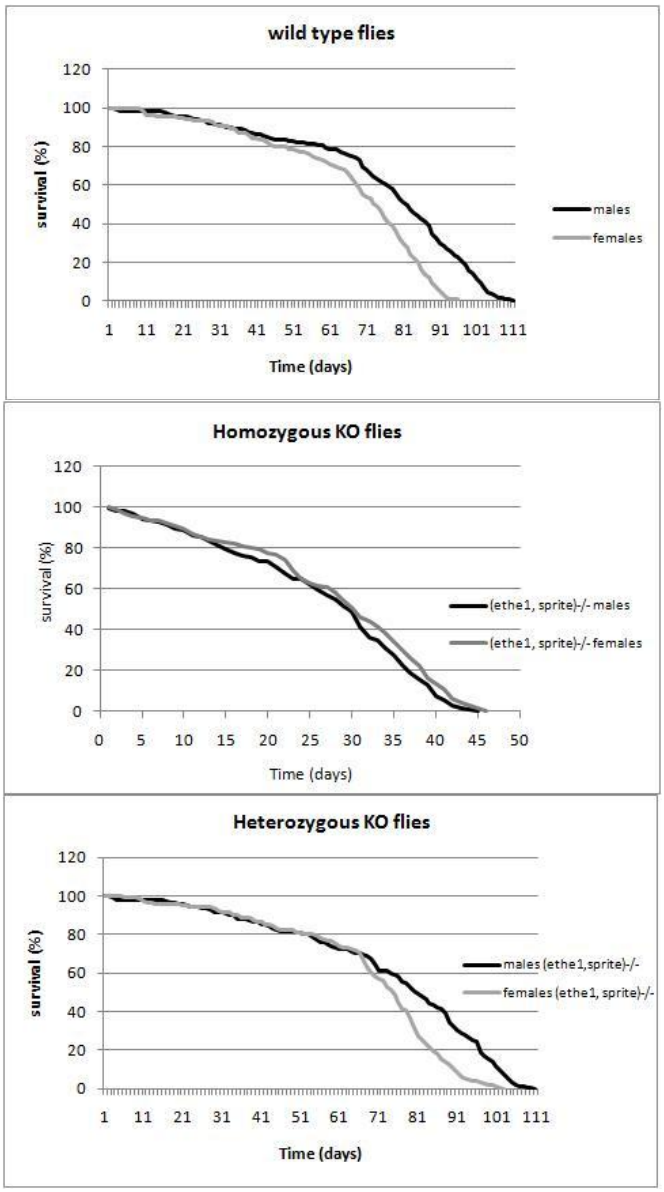

Figure 3.14. Lifespan of control and (*Ethe1, Sprite*) –/+ and (*Ethe1, Sprite*) –/– flies. Survival is expressed as a percentage of flies surviving from the total fly sample present at the start of the experiment.

PART III

Mutations in the TTC19 gene cause a severe mitochondrial disease in humans and flies

The TTC19 gene encodes a member of the tetratricopeptide protein family, a mitochondrial inner membrane protein that physically interacts with, and promotes the assembly of CIII.

In humans a homozygous non-sense mutation in the tetratricopeptide 19 (TTC19)-encoding gene was found in three patients from two families, affected by severe progressive encephalopathy with profound CIII deficiency and accumulation of CIII-specific assembly intermediates. A second homozygous nonsense mutation was later found in an unrelated patient. In all cases these patients were characterized by profound CIII deficiency in skeletal muscle.

We studied a *Drosophila melanogaster* fly line bearing a piggyBac element insertion within the TTC19 coding region. We characterized this insertional *null* mutant in order to evaluate whether it showed any defects in mitochondrial function which might be related to a deficiency in mitochondrial respiration.

The TTC19 knockout fly mutant showed low fertility, severe spontaneous locomotor impairment, and "bang sensitivity", associated with profound CIII deficiency. Thus, the ablation of TTC19 causes a severe mitochondrial disease phenotype linked to CIII impairment in both human patients and flies.

Furthermore, the work done by our group experimentally demonstrated that TTC19 protein is targeted to, and embedded in, the inner mitochondrial membrane We also showed that TTC19 is part of two high-molecular weight complexes, one of which co-migrates with CIII.

TTC19 is a new assembly factor involved in at least one crucial function in mitochondria, that is assembly of CIII, and its absence determines severe neurological abnormalities in both humans and flies.

INTRODUCTION

1.1 Complex III of the mitochondrial respiratory chain

The mitochondrial respiratory chain (MRC) is composed of five multiheteromeric complexes Complex I (CI); Complex II (CII); Complex III (CIII); Complex IV (CIV) or Cytochrome C Oxidase (COX) complex V (CV) or ATP synthase, all embedded in the inner mitochondrial membrane. Four of the five MRC complexes, namely CI, CIII, CIV, CV, contain subunits encoded by the mitochondrial DNA, mtDNA, and synthesized *in situ* by the organellar specific translation machinery (Zeviani and Di Donato 2004). In particular, CIII is a Coenzyme Q (CoQ) Cytochrome *c* (cyt *c*) Oxidoreductase that funnels the electrons fixed into CoQ from different electron donors including 1) oxidated fatty acids, 2) succinate, via CII, or 3) reduced nicotinamide-adenine dinucleotide, NADH+, via CI, to cytochrome *c*, which in turn donates them to COX, and through COX to molecular oxygen. The energy liberated by the electron transfer is exploited by CIII to pump protons from the matrix side to the intermembrane space of mitochondria, thus contributing to the formation of the electrochemical potential across the inner mitochondrial membrane.

Mammalian CIII is composed of 11 subunits, one of which, cytochrome *b*, cyt *b*, is encoded by mtDNA, the remainder being encoded by nuclear DNA genes (Schägger et al. 1986). The latter include the gene encoding the protein component of a second cytochrome, cyt *c1*, the Rieske iron-sulfur protein (RISP), two relatively large "core" subunits, Core 1 (UQCR1) and Core 2 (UQCR2), and 6 additional, smaller proteins (UQCR6-11), the functions of which are unknown. In addition to the protein backbone, prosthetic groups of CIII include the two Fe-containing heme moieties of cyt *b* and *c1*, and the Fe_2S_2 cluster of RISP. The CIII monomer is believed to be a transient form, which quickly converts into a tightly bound, catalytically active homodimer. The latter can also be part of respiratory supercomplexes, together with CI, CIV, or both (Wittig et al. 2006).

Although mammalian CIII contains an additional subunit (subunit 9) compared with that of *S. cerevisiae* (Brandt et al. 1993), in yeast as in humans the assembly of CIII is a dynamic process: dimerization of the complex occurs before the full assembly of CIII monomer has been completed.

1.2 The tetratricopeptide 19 encoding gene

By investigating patients affected by severe progressive encephalopathy with profound CIII deficiency in skeletal muscle and accumulation of CIII-specific assembly intermediates, homozygous non-sense mutations in the gene encoding TTC19 were identified. The TTC19 gene encodes a poorly understood member of the tetratricopeptide (TRP) protein family. Figure 1.1 shows human genomic location of tetratricopeptide repeat domain within chromosome 17.

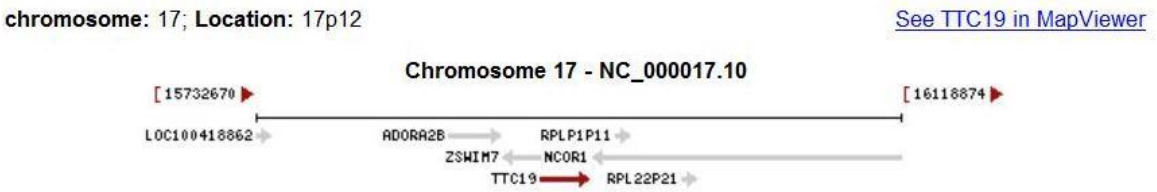

Figure 1.1. The tetratricopeptide repeat domain 19. (Figure modified by http://www.ncbi.nlm.nih.gov).

The TPR motif is a protein-protein interaction module found in multiple copies in a number of functionally different proteins that facilitates specific interactions with partner proteins (Blatch et al. 1999). Three dimensional structural data have shown that a TPR motif contains two antiparallel-helices such that tandem arrays of TPR motifs generate a right-handed helical structure with an amphipathic channel that can accommodate the complementary region of a target protein. The TPR motif may represent an ancient protein-protein interaction module that has been recruited by different proteins and adapted for specific functions. Most TPR-containing proteins are associated with multiprotein complexes, and there is extensive evidence indicating that TPR motifs are important for a number of relevant cell functions. Four major types of complexes that involve TPR proteins have been identified: (i) molecular chaperone; (ii) transcription repression; (iii) anaphase promoting complex; (iv) protein import (Blatch et al. 1999).
A role as co-chaperones has been demonstrated for several TPR proteins, including STI1, Hip and immunophilins CyP40 and HSP56, that act in concert with chaperones HSP70 and HSP90 in a number of important pathways, for instance the maturation of steroid hormone receptors (Kimmins et al 2000). Accordingly, TTC19 was proposed to be a mitochondrial chaperone involved in at least one crucial function, that is, early-step assembly of CIII.

1.3 TTC19 protein

By a series of *in vitro* and *in vivo* experiments, it was proved that TTC19 is a mitochondrial inner membrane protein that physically interacts with, and promotes the assembly of CIII. The ablation of TTC19 causes a severe mitochondrial disease phenotype linked to CIII impairment in both human patients and in a *Drosophila melanogaster* knockout model.
Our research group demonstrated experimentally that the wild-type TTC19 protein is targeted to, and embedded in, the inner mitochondrial membrane. TTC19 is part of two high-molecular weight complexes, one of which co-migrates with CIII. Physical interaction between the protein and CIII was demonstrated by co-immunoprecipitation.

In addition, it was showed that full-length TTC19 protein is a precursor protein that is imported in mitochondria, processed into a shorter mature form and inserted in the inner mitochondrial membrane, where it binds with the CIII holoenzyme in a relatively stable manner.
TTC19 can be described as a new protein involved in the assembly of the mitochondrial respiratory chain of pluricellular animals.

TTC19-like protein sequences are present in all metazoa, but neither in other eukaryotes (plants, fungi), nor in prokaryotes. The putative human *TTC19* ORF (NP_060245) contains two potential AUG initiation codons, translatable in methionine residues, at positions +1 and +122 (M_1, M_{122}). However, since the sequence from M1 to S121 is not conserved among species (Figure 3.2), we considered the 380 aa sequence starting from M_{122} as the real human TTC19 protein (human TTC19).

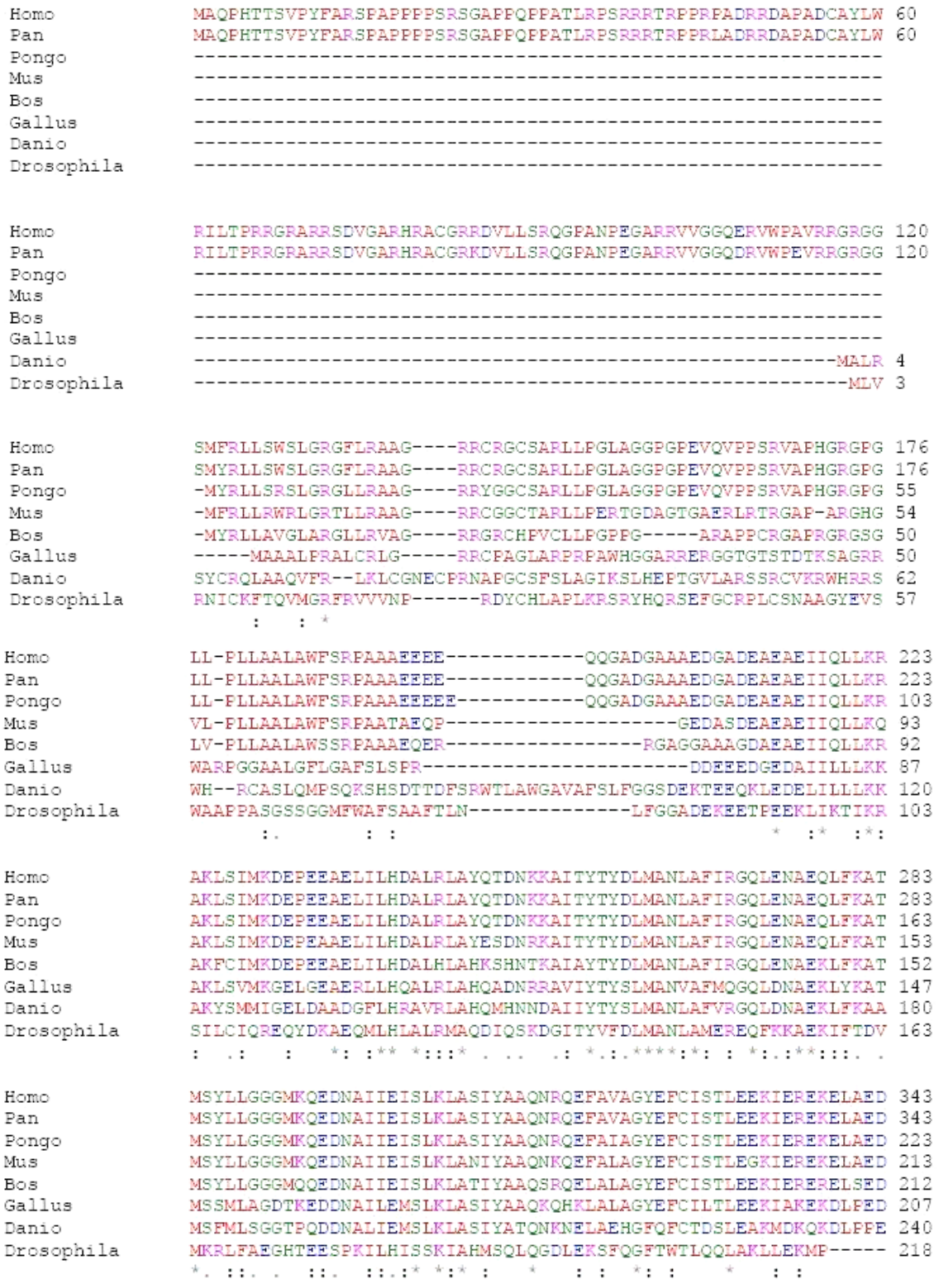
Homo MAQPHTTSVPYFARSPAPPPPSRSGAPPQPPATLRPSRRRTRPPRPADRRDAPADCAYLW 60
Pan MAQPHTTSVPYFARSPAPPPPSRSGAPPQPPATLRPSRRRTRPPRLADRRDAPADCAYLW 60
Pongo
Mus
Bos
Gallus
Danio
Drosophila
Homo RILTPRRGRARRSDVGARHRACGRRDVLLSRQGPANPEGARRVVGGQERVWPAVRRGRGG 120
Pan RILTPRRGRARRSDVGARHRACGRKDVLLSRQGPANPEGARRVVGGQDRVWPEVRRGRGG 120
Pongo
Mus
Bos
Gallus
Danio -MALR 4
Drosophila -MLV 3
Homo SMFRLLSWSLGRGFLRAAG----RRCRGCSARLLPGLAGGPGPEVQVPPSRVAPHGRGPG 176
Pan SMYRLLSWSLGRGFLRAAG----RRCRGCSARLLPGLAGGPGPEVQVPPSRVAPHGRGPG 176
Pongo -MYRLLSRSLGRGLLRAAG----RRYGGCSARLLPGLAGGPGPEVQVPPSRVAPHGRGPG 55
Mus -MFRLLRWRLGRTLLRAAG----RRCGGCTARLLPERTGDAGTGAERLRTRGAP-ARGHG 54
Bos -MYRLLAVGLARGLLRVAG----RRGRCHPVCLLPGPPG-----ARAPPCRGAPRGRGSG 50
Gallus -----MAAALPRALCRLG-----RRCPAGLARPRPAWHGGARRERGGTGTSTDTKSAGRR 50
Danio SYCRQLAAQVFR--LKLCGNECPRNAPGCSFSLAGIKSLHEPTGVLARSSRCVKRWHRRS 62
Drosophila RNICKFTQVMGRFRVVVNP------RDYCHLAPLKRSRYHQRSEFGCRPLCSNAAGYEVS 57
Homo LL-PLLAALAWFSRPAAAEEEE----------QQGADGAAAEDGADEAEAEIIQLLKR 223
Pan LL-PLLAALAWFSRPAAAEEEE----------QQGADGAAAEDGADEAEAEIIQLLKR 223
Pongo LL-PLLAALAWFSRPAAAEEEEE----------QQGADGAAAEDGADEAEAEIIQLLKR 103
Mus VL-PLLAALAWFSRPAATAEQP----------GEDASDEAEAEIIQLLKQ 93
Bos LV-PLLAALAWSSRPAAAEQER----------RGAGGAAAGDAEAEIIQLLKR 92
Gallus WARPGGAALGFLGAFSLSPR----------DDEEEDGEDAIILLLKK 87
Danio WH--RCASLQMPSQKSHSDTTDFSRWTLAWGAVAFSLFGGSDEKTEEQKLEDELILLLKK 120
Drosophila WAAPPASGSSGGMFWAFSAAFTLN----------LFGGADEKEETPEEKLIKTIKR 103
Homo AKLSIMKDEPEEAELILHDALRLAYQTDNKKAITYTYDLMANLAFIRGQLENAEQLFKAT 283
Pan AKLSIMKDEPEEAELILHDALRLAYQTDNKKAITYTYDLMANLAFIRGQLENAEQLFKAT 283
Pongo AKLSIMKDEPEEAELILHDALRLAYQTDNKKAITYTYDLMANLAFIRGQLENAEQLFKAT 163
Mus AKLSIMKDEPEAAELILHDALRLAYESDNRKAITYTYDLMANLAFIRGQLENAEQLFKAT 153
Bos AKFCIMKDEPEEAELILHDALHLAHKSHNTKAIAYTYDLMANLAFIRGQLENAEKLFKAT 152
Gallus AKLSVMKGELGEAERLLHQALRLAHQADNRRAVIYTYSLMANVAFMQGQLDNAEKLYKAT 147
Danio AKYSMMIGELDAADGFLHRAVRLAHQMHNNDAIIYTYSLMANLAFVRGQLDNAEKLFKAA 180
Drosophila SILCIQREQYDKAEQMLHLALRMAQDIQSKDGITYVFDLMANLAMEREQFKKAEKIFTDV 163
Homo MSYLLGGGMKQEDNAIIEISLKLASIYAAQNRQEFAVAGYEFCISTLEEKIERERKELAED 343
Pan MSYLLGGGMKQEDNAIIEISLKLASIYAAQNRQEFAVAGYEFCISTLEEKIERERKELAED 343
Pongo MSYLLGGGMKQEDNAIIEISLKLASIYAAQNRQEFAIAGYEFCISTLEEKIERERKELAED 223
Mus MSYLLGGGMKQEDNAIIEISLKLANIYAAQNKQEFALAGYEFCISTLEGKIERERKELAED 213
Bos MSYLLGGGMQQEDNAIIEISLKLATIYAAQSRQELALAGYEFCISTLEEKIERERELSED 212
Gallus MSSMLAGDTKEDDNAILEMSLKLASIYAAQKQHKLALAGYEFCILTLEEKIAKEKDLPED 207
Danio MSFMLSGGTPQDDNALIEMSLKLASIYATQNKNELAEHGFQFCTDSLEAKMDKQKDLPPE 240
Drosophila MKRLFAEGHTEESPKILHISSKIAHMSQLQGDLEKSFQGFTWTLQQLAKLLEKMP----- 218

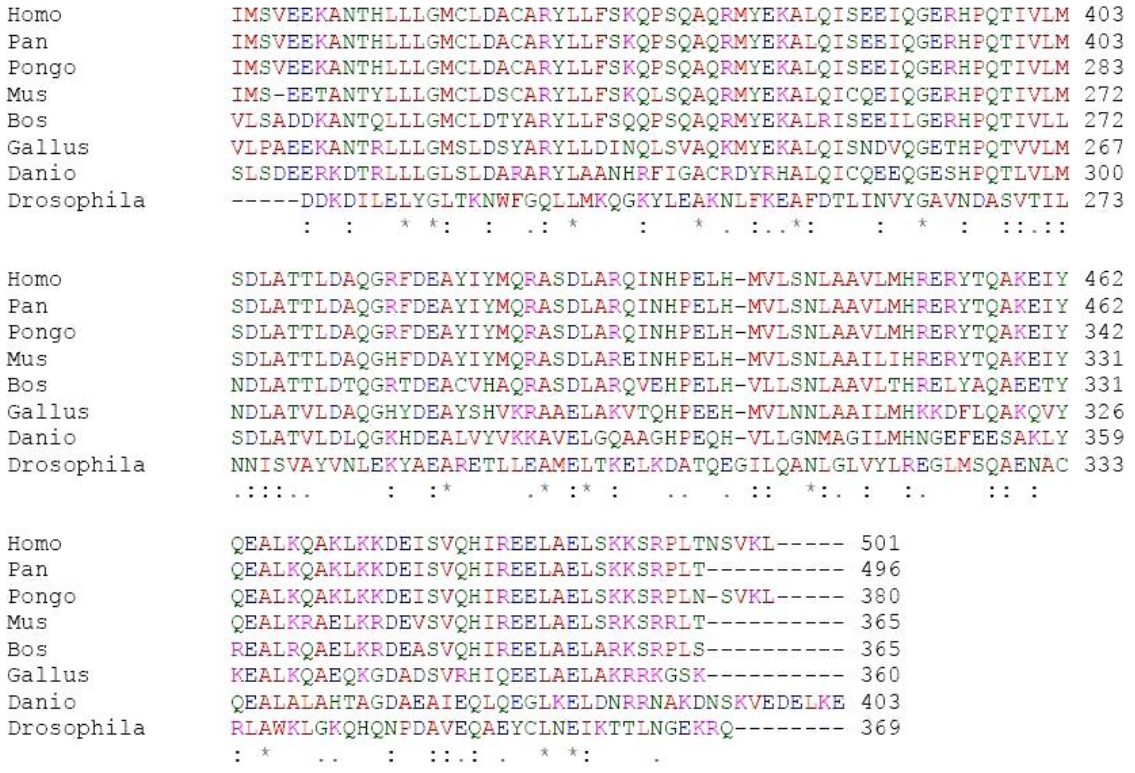

Figure 1.2. Comparative protein sequence analysis of TTC19. Interspecies alignment of TTC19 protein sequences, obtained with ClustalW. Predicted sequences corresponding to the translatable ORF of human TTC19 protein sequence from the first predicted methionine (M_1) to the second methionine (M_{122}). The M_1 is consistently absent in non-human species, with the exception of chimp (Pan) and gorilla (not shown). Homo: *Homo sapiens*, Pan: *Pan troglodytes*, Pongo: *Pongo pygmaeus*, Bos: *Bos Taurus*, Mus: *Mus musculus*,Gallus: *Gallus gallus*, Danio: *Danio rerio*, Drosophila: *Drosophila melanogaster*.

1.4 The *Drosophila TTC19* gene

The *Drosophila melanogaster CG15173* gene (Figure 3.3) is the fly orthologue of the human TTC19. This gene maps to chromosome 2L 37B11 and its gene sequence location is 2L:19043535..19045146. The *CG15173* gene spans 1611 bp, and the 1438 bp coding sequence consists of 4 exons.

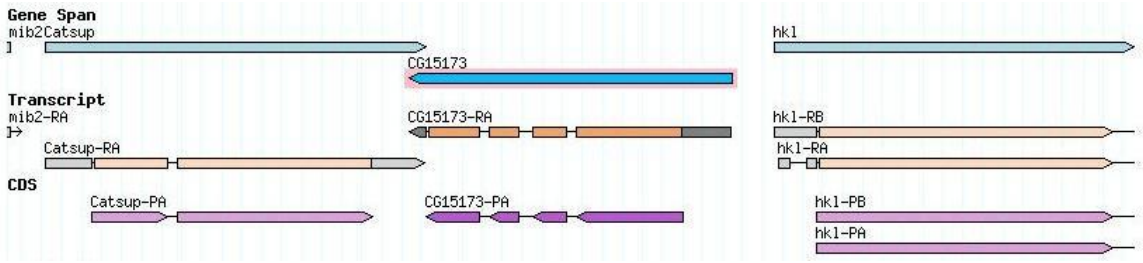

Figure 1.3. The Drosophila *CG15173* gene. This gene is referred to in FlyBase by the symbol Dmel\CG15173 (FBgn0032744). Gene sequence location is 2L:19043535..19045146. (Figure modified from http://flybase.org).

RESULTS AND DISCUSSION

Preliminary considerations

This project began with the identification of TTC19, a poorly understood member of the tetratricopeptide family, as a new protein involved in the assembly of the mitochondrial respiratory chain of pluricellular animals.
We studied the TTC19 encoding gene by investigating mutations, which cause a severe mitochondrial disease, both in humans and flies. Professor Zeviani's group at the Best Neurological Institute in Milan worked on the human gene, whilst the development and characterization of the Drosophila disease model was conducted in our lab.
The work started from the selection of four patients affected by profound isolated deficiency of the mitochondrial respiratory chain Complex III, associated with severe progressive neurodegeneration. Two deleterious non-sense mutations were found in four patients from three unrelated families, all characterized by profound, isolated CIII deficiency in skeletal muscle. SNP-based genome-wide linkage analysis on an index family led to the discovery of a nonsense mutation in the TTC19 gene that resides on human chromosome 17. Next, it was proved by *in vitro* and *in vivo* experiments that the TTC19 protein is targeted to mitochondria, where it is imported and undergoes post-translational maturation into a shorter peptide that is eventually inserted in the inner mitochondrial membrane. Since the defect of Complex III was associated with the accumulation of CIII assembly intermediates, it was hypothesized a role for TTC19 as a chaperone-like assembly factor. To prove this idea, it was demonstrated that TTC19 does in fact physically interact with the CIII homodimer, and then showed that the ablation of TTC19 determines a profound isolated Complex III deficiency not only in humans but also in a *D. melanogaster* recombinant strain. This mutant fly displays a neurological phenotype both spontaneously and under triggering stimuli.
Thus far, only one protein, termed BCS1L, was known to play a specific role in a late step of CIII assembly. Unlike BCS1L, the presence in TTC19-defective tissues of protein intermediates containing early-incorporated proteins such as Core- 1 and Core-2 suggests for TTC19 a role in the early steps of the assembly process. The observation that TTC19 is also present in the fully-assembled 650 kDa dimeric complex, but not in the supercomplex formed by Complex III+IV, suggests for TTC19 an additional role in the stabilization of Complex III. It was found that some TTC19 cross-reacting material is consistently present in an additional, higher molecular weight complex that is detected also in cells that do not have a mitochondrial respiratory chain, suggesting for this protein a third, still undefined, function. TTC19 has been recently reported to interact with, and be part of, the midbody protein repertoire necessary for cytokinesis but, it no trace of TTC19 was found in the midbody, and no evidence of alterations in cytokinesis neither in human TTC19-less cells *in vitro*, nor in spermatids of mutant *Drosophila melanogaster*.
The activity defect found in the four patients, above described, was associated with reduction in the amount of the CIII holoenzyme, and accumulation of low molecular

weight protein species, cross-reacting with Core 1 and Core 2 but not with RISP antibodies. Whilst the former two subunits are assembled early to form CIII, RISP is one of the last subunits to be incorporated (Cruciat et al. 1999), thus suggesting that TTC19 protein is involved in the initial steps of CIII formation.

Here we focus on describing the development and characterization of the Drosophila model of TTC19 deficiency.

3.1 The *Drosophila* knock out model for TTC19

To further corroborate the evidence that TTC19 protein and CIII activity are functionally related, we investigated a *Drosophila melanogaster* knockout strain (line #18843) obtained by the insertion of a >7000bp-long piggyBac element within the ORF region included in the first exon of *CG15173*, the fly orthologue of the gene encoding TTC19 protein (Figure 3.1).

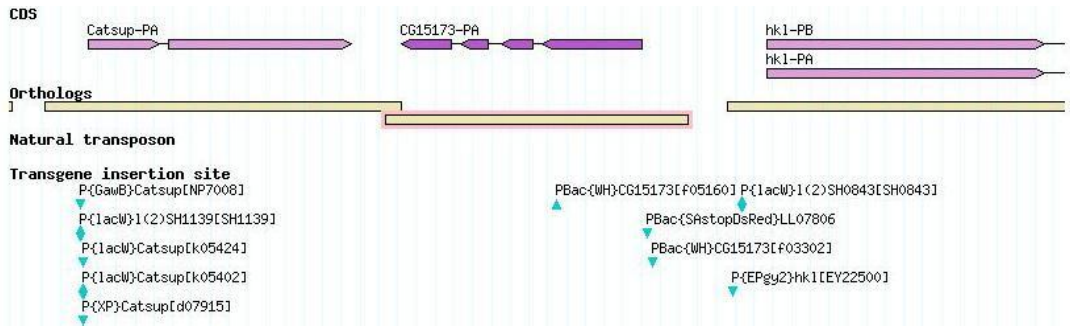

Figure 3.1. Localization of the piggy-back element inside the Drosophila *CG15173* gene. The transgene insertional PBac[WH] CG15173 ^{f05160} (FBti0042429) is localized at 2L:19044446 at the level of the first exon of the gene. The derived cytological map location is 37B11. The associated stock is #18843.

To confirm the piggyBac element insertion location, PCRs on genomic DNA were performed using TTC19-specific primers. Amplifications were carried out by coupling TTC19 and WH piggyBac-element specific primers, as listed in (Table 2 materials and methods). The Exelixis piggyBac WH primers were as reported in (Parks et al. 2004).
We confirmed the piggyBac element insertion location by diagnostic PCR on #18843 genomic DNA using suitable primers (see material and methods chapter 2.4.2).
We showed that this modification causes the interruption of the ORF in both the *CG15173* gene (Supplementary Figure 3.2A) and in the corresponding transcript (Figure 3.2B).

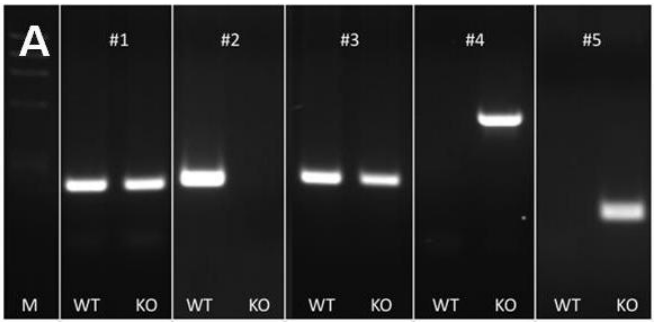

Figure3.2A. Analysis of the insertion of the PiggyBac element within the *CG15173* gene (A) PCR amplification of the *CG15173* gene from genomic DNA obtained from wild-type (WT) and knock-out (KO) flies. Numbers refer to the amplicons reported in table 2.4.2. M: molecular weight markers ΦX174 (HaeIII). Amplicons #4 and #5 are present only in the KO DNA, since they contain the 5' and 3' insertion points of the PiggyBac element respectively, being obtained using primer pairs corresponding to a region of the *cg15173* gene and of the PiggyBac transposable element Amplicon #2 is present only in the WT DNA, being obtained by a primer pair corresponding to 5' and 3' regions of the *CG15173* gene, flanking the transposable element, which is too big to produce a detectable fragment from KO DNA obtained form KO individuals.

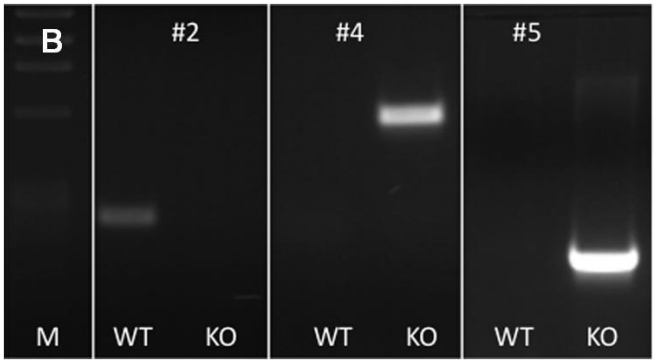

Figure3.2B. Analysis of the insertion of the PiggyBac element within the transcript (B). PCR amplification of the *CG15173* transcript encoding dm.TTC19 from the corresponding cDNA obtained from wild-type (WT) and knock-out (KO) flies. Numbers refer to the amplicons reported in table 2.4.2. M: molecular weight markers ΦX174 (HaeIII). Results are identical to those shown in A and indicate the absence of the normal transcript in the KO flies, which is replaced by an aberrant transcript that includes the transposable element.

3.2 The mitochondrial localization of TTC19

We also showed that like the human TTC19, drosophila TTC19 is targeted to mitochondria in mammalian cells *in vitro* (Figure 3.3).

IF immunodetection of an HA-tagged *CG15173* ORF in COS7 cells using an -HA antibody, clearly demonstrated mitochondrial targeting of TTC19HA overlapping with Mitotracker staining.

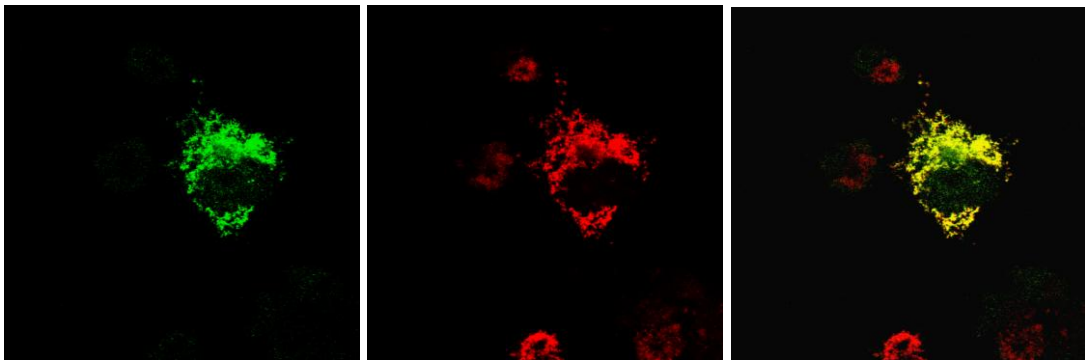

Figure 3.3. Confocal IF images of COS7 cells transfected with *TTC19^{HA}*. The IF signal specific to TTC19HA is in green, whereas the red signal corresponds to MitoTracker, a specific mitochondrial marker (Mitotracker Red, Invitrogen). The figure on the right show the merge of two signals.

3.3 CIII isolated deficiency in TTC19-less flies

We found that the very same biochemical phenotype (i.e. severe isolated CIII deficiency) as found in human patients .

The biochemical activities of MRC CI, CIII and CIV, as well as citrate synthase (CS), were measured in the mitochondria of the *#18843* TTC19-less mutant strain and in two different wild type strains: WTALA (Wild Type, ALto Adige) and Canton S. Both CI and CIV as well as CS activities were similar in controls and mutant flies, whereas CIII activity was markedly reduced in the mitochondria of the mutant compared to wild type adult individuals (Figure 3.4).

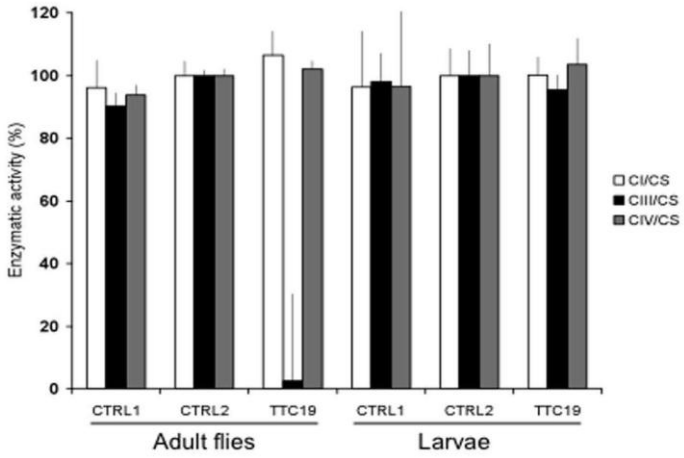

Figure 3.4. Mitochondrial respiratory chain enzymatic activities in adult flies and larvae. Complexes I, CIII and CIV activities (all expressed as nmol min^{-1} mg^{-1}) normalized to the activity of Citrate Synthase (CS), are all expressed as percentage of enzymatic activity where WTALA strain's activity is considered as 100%. Specific activities of MRC complexes were measured in controls (CTRL1= Canton S and CTRL2= WTALA) and TTC19 *null* (TTC19) flies. For each genotype we performed three replicate mitochondrial extractions and for each extraction enzymatic activities were determined from at least 10 replicate reactions.

Interestingly, the CIII deficiency found in the knock out adult flies was not present in mutant larvae, that appeared normal, underwent normal pupation and developed into adult individuals. These data are in agreement with what was observed in humans. In fact the analysis of four patients coming from three different families, reflects the late-disease onset. For instance patient #4 (see attached article) showed a normal psychomotor development with no clinically relevant complaints until the age of 42 years, when he was first examined for a subacute, rapidly progressive neurological syndrome. The patient died at 45 years, two years after the disease onset. The late-disease onset in patient #4 and the normal development and CIII activity of mutant *D. melanogaster* larvae may suggest tissue-specific, age-related, and development-dependent regulation of both TTC19 functions and CIII activity in different cell types and organisms, as already suggested for BCS1L (Kotarsky et al. 2007; Papa et al. 1996).

3.4 Characterization of TTC19 *null* flies

The phenotype of TTC19 homozygote *null* Drosophila mutants consisted of several features, including neurological and non-neurological abnormalities.
These KO flies showed a complex phenotype characterized by severe reduction of fertility, predominance of male individuals in offspring, spontaneous locomotor impairment and bang sensitivity.

3.4.1 Analysis of long term locomotor activity

To evaluate whether TTC19 *null* flies showed any behavioral impairments in addition to the biochemical defect, locomotor activity was measured on the TTC19 KO strain and in controls (Figure 3.5).

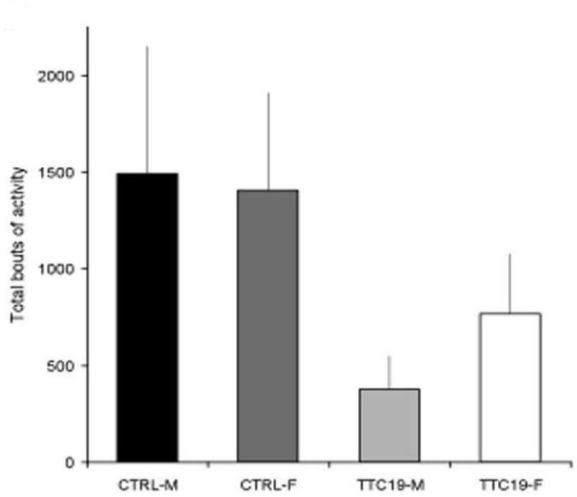

Figure 3.5. Locomotor activity. Spontaneous locomotor activity in *D. melanogaster* Canton S control (Ctrl) and TTC19 *null* (TTC19) flies. In the analysis the flies are divided into males (M) and females (F). Bars indicate SD.

The above graph shows that spontaneous locomotor activity was significantly reduced in both male and female mutant individuals compared to controls.

3.4.2 Bang Test

Seizure sensitivity was then evaluated following intense mechanical stimulation (Bang test) (Glasscock and Tanouye 2005). TTC19 knockout mutants showed a strong delay in the post-mechanical-shock recovery time over that of wild type controls (Figure 3.6).

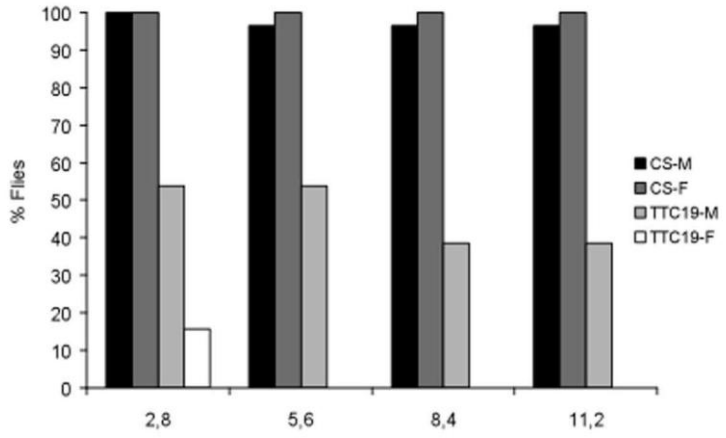

Figure 3.6. Locomotor activity after bang test. Percentage of flies able to reach four selected "end-points", corresponding to 2.8, 5.6, 8.4 and 11.2 cm. CS: Canton S control flies; TTC19: TTC19 *null* flies.

Adult mutant flies displayed strong seizure sensitivity following intense mechanical stimulation. In particular none of the tested mutant females were able to climb further than 5.6 cm from the bottom, and only 40% of the mutant male individuals reached the highest mark placed at 11.2 cm, compared to 100% of the wild type individuals of both sexes

3.4.3 Walking optomotor test

Additionaly to further explore the neurological phenotype of our mutant, the photobehavior of adult TTC19 *null* flies was measured by the optomotor test paradigm. In the optomotor test, which measures locomotor and photobehavioral proficiency, adult control flies normally tend to turn in the direction of the rotating stripes.
TTC19 KO flies turned at random, meaning that they exhibited a number of correct turns which was not significantly different from 50%, indicating an impairment in the capacity to react to the rotating environment (Figure 3.7). Some of the KO flies produced a null response (i.e. were unable to move at all), indicating, in some cases the presence of gross motor impairments.

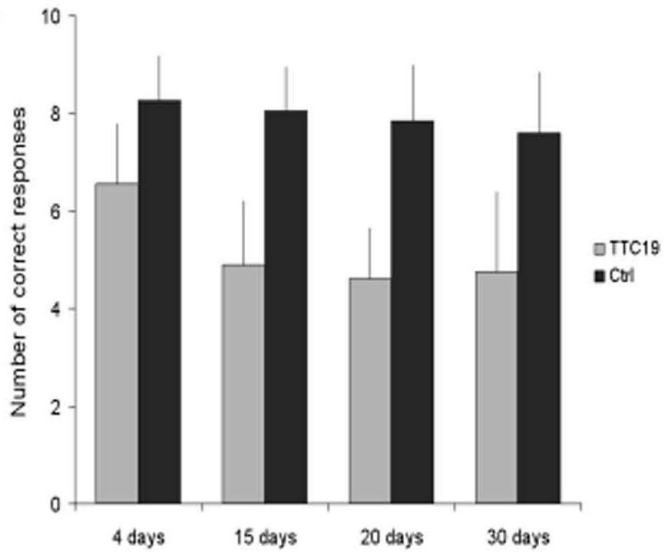

Figure 3.7. Optomotor behavior. Number of correct responses (each fly was given 10 trials, and each time the direction of rotation of the stripes was changed.) to the optomotor test in Canton S control (Ctrl) and TTC19 KO (TTC19) flies, at different days of age.

As can be seen in the graph above, walking optomotor behavior of mutant flies was clearly impaired, suggesting an abnormality in the visual pathway.

3.4.4 Electroretinogram

To verify whether the incorrect response to the optomotor test was due to visual impairment, the response to light of the neuronal retinal pathway was measured by electroretinogram. A normal electroretinogram recording under a photic stimulus is shown in Figure 3.8A. ON/OFF electroretinogram transients are due to synaptic activation of second-order neurons of the visual pathway, while the sustained response is due to photoreceptor light-induced depolarization.
Electroretinograms were recorded extracellularly from 27 day-old adult wild type (Figure 3.8.A) and TTC19-KO (Figure 3.8.B) flies, following white light stimulation. After the onset of a light stimulus, a brief ON transient positive deflection of the trace, corresponding to the activity of *lamina* neurons, is followed by a negative sustained deflection of the trace, determined by photoreceptor response. At the cessation of the light stimulus, an OFF transient, expressed as a negative deflection, is followed by a slow recovery to the pre-stimulus condition. The original responses (3s duration) have been magnified to show both ON and OFF transients. In both wild-type (A) and TTC19-KO (B) electroretinograms, ON and OFF transients are equally present.

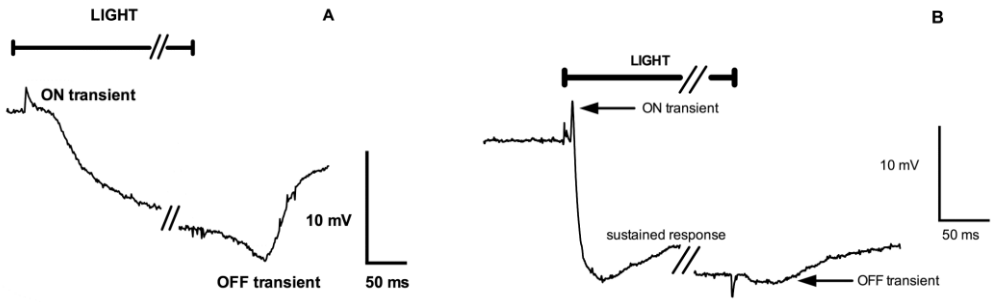

Figure 3.8. Electroretinogram in adult aged flies. Electroretinograms in 27 day-old adult wild type (A) and TTC19-KO (B) flies.

Electroretinogram experiments prove the integrity of the projections from the eye to the visual ganglia of the fly, which correspond to intrinsic retinal neurons in mammals (Borst et al. 2010).

3.4.5 Survival and fertility of TTC19 KO adult flies

The TTC19 *null* adult flies showed reduced lifespan, all being dead by 35-40 days after eclosion, vs. 80-90 days of controls; and poor fertility (≈60% of controls). The

TTC19 *null* flies showed both poor fertility (down to ≈60% of control flies) and a bias in favour of male offspring (≈60% males vs. ≈40% females on a total progeny of 342 individuals).

Given the partial sterility observed for the TTC19 mutants, we also looked for signs of male meiosis impairment. Testis squashes from 4 adult males were prepared and approximately 200 onion stage spermatids were analyzed using phase contrast microscopy. During early spermatid differentiation, mitochondria begin to gather and fuse, forming a spherical mass adjacent to one side of the spermatid nucleus. Later, the individual mitochondria fuse into two giant mitochondria, which are arranged in a densely packed sphere consisting of many layers of wrapped mitochondrial membranes. The spherical mitochondrial derivative is known as the *nebenkern*. At the onion stage of spermatogenesis, spermatid nuclei and *nebenkern* bodies have a regular appearance and show similar sizes. Deviations from such regularity are indicative of failures in the fidelity of meiotic divisions (Fuller 1993; Regan and Fuller 1990; Giansanti et al. 2004).

We failed to find any morphological abnormality in TTC19 mutants, spermatids (Figure 3.9), suggesting that reduced female fitness, rather than altered meiotic maturation of male germ cells, is likely to be responsible of poor fertility.

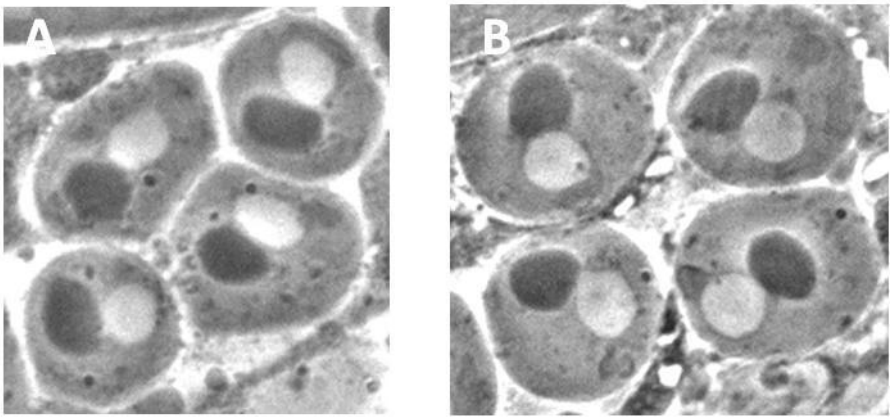

Figure 3.9. **Fly male spermatids.** Phase-contrast 40x images of 4 spermatids from testes of control and TTC19 null flies. The two sections are morphologically normal. A) wild type w^{1118}, B) TTC19 null mutant.

Incidentally, these data provide additional evidence that TTC19 is unlikely to be involved in cytokinesis, at least in the fly, since abnormalities of spermatids are common hallmarks of defects in midbody formation in male flies (Giansanti et al. 2004). The stronger bang sensitivity of females and the lack of female progeny in the mutant lines suggest that the fertility problems may be an indirect consequence of the general impairment of female fitness.

Since we failed to find any evidence of defects in fly male spermids, given the partial sterility observed for the TTC19 mutants, we also looked for morphological abnormality in females ovaries.
We dissected ovaries from ten wild type (w^{1118}) and ten TTC19 null female flies, checking for any sign of impairment. We found that, as clearly visible in Figure 3.10b ovaries from TTC19 KO females showed an impaired phenotype characterized by asymmetry and reduced size over that of controls (Figure 3.10a).

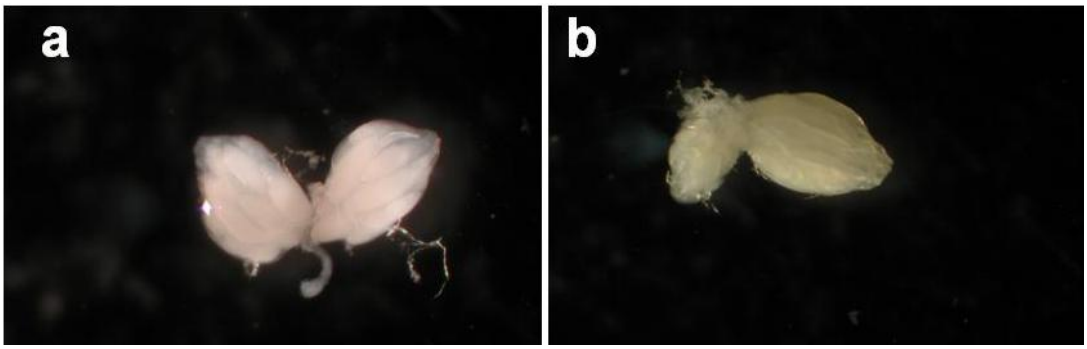

Figure 3.10. Ovaries conformation. Dissected ovaries from 3 day-old a) wild type (w^{1118}) and b) TTC19null females.

3.5 The *Drosophila* knock down model for TTC19

A Drosophila line allowing to produce TTC19 targeted dsRNAi was obtained from the VDRC (Vienna Drosophila RNAi Center): Transformant ID 105382; FlyBase n. CG15173.
dsRNAi of TTC19 was achieved using the GAL4/UAS system to target the RNAi to specific cells in the animal (Dietz et al. 2007). A primer pair specific for the amplification of exons 2/3 (Table 2.3 materials and methods) of *TTC19* cDNA was used for quantitative-PCR, to measure the amount of *TTC19* cDNA. This quantity was then normalized to rp49, a housekeeping cDNA (Figure 3.11) (Zordan et al. 2006).

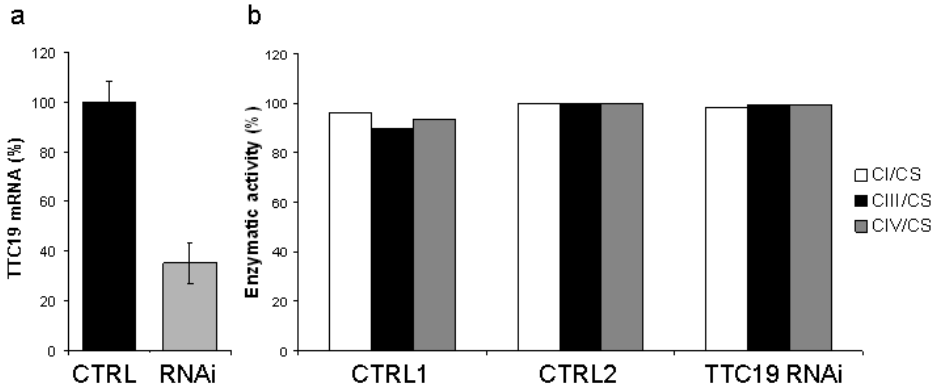

Figure 3.11. Characterization of TTC19 *knock-down* flies. (a) Levels of TTC19 transcript in control (CTRL) and RNAi knock-down (RNAi) flies. Bars indicate SD. (b) Specific activities of MRC Complexes I, III and IV (CI, CIII, CIV) in controls (CTRL1= Canton S and CTRL2= WTALA) and TTC19 RNAi knock-down (TTC19 RNAi) flies, normalized to that of Citrate Synthase (CS).

Ubiquitous activation of dsRNAi, using and Act5C-Gal4 driver produced a ≈65% decrease of *CG15173*-specific mRNA (VDRC ID#105382). However, CIII activity, determined in such individuals, was not different from controls and no neurological phenotype was observed, indicating that ≈35% residual transcript is sufficient to maintain the function of drosophila TTC19.

We thus propose that TTC19 is a new chaperone involved in at least one crucial function in mitochondria, that is, assembly of CIII. This conclusion is supported by the following evidence. First, two deleterious non-sense mutations were found in four patients from three unrelated families, all characterized by profound, isolated CIII deficiency in skeletal muscle. Second, the activity defect was associated with reduction in the amount of the CIII holoenzyme, and accumulation of low molecular weight protein species, cross-reacting with Core 1 and Core 2 but not with RISP antibodies. Whilst the former two subunits are assembled early to form CIII, RISP is one of the latest subunits to be incorporated (Cruciat et al. 1999), thus suggesting that TTC19 is involved in the initial steps of CIII formation. Third, it was shown that full-length human TTC19 protein is a precursor protein that is imported in mitochondria, processed into a shorter mature form and inserted in the inner mitochondrial membrane, where it binds with the CIII holoenzyme in a relatively stable manner, at least in mouse liver and kidney.
Fourth, the very same biochemical phenotype found in patients, i.e. severe isolated CIII deficiency, was also the biochemical hallmark of a knockout fly for TTC19.

Summarizing the characteristics of TTC19 mutant flies we observed that, as in the case of human TTC19, drosophila TTC19 is targeted to mitochondria (Figure 3.3). The drosophila TTC19 *null* adult flies showed reduced lifespan, all being dead by 35-40 days after eclosion, vs. 80-90 days of controls; and poor fertility (≈60% of controls). We failed to find any morphological abnormality in fly spermatids (Figure 3.9), which provides additional evidence that TTC19 is unlikely to be involved in cytokinesis, since abnormalities of spermatids are common hallmarks of defects in midbody formation in male flies (Giansanti et al 2004). However, no multinucleated cells were detected in both human TTC19-less mutant human fibroblasts, and spermatids in the gonads of drosophila TTC19 knockout male flies, indicating that mitosis in human cells and male meiosis in flies proceed normally in the absence of TTC19.
Furthermore adult mutant flies displayed strong bang sensitivity (Glasscock and Tanouye 2005), interestingly, sensitivity to seizures has been observed in *Drosophila* mutants of the *technical knock out* gene (*tko*), as well as in mutants of other genes associated with defects in mitochondrial bioenergy supply, such as *adenine nucleotide translocase* (Zhang et al. 1999), or *citrate synthase knockdown* (Fergestad et al. 2006).
TTC19 *null* adult flies are also characterized by severely reduced spontaneous motor activity, and impaired optomotor activity (Zordan et al. 2006, Borst et al. 2010) (Figure 3.5-3.7). Since an electroretinogram (Figure 3.8) showed the integrity of the projections from the eye to the visual ganglia of the fly, which correspond to intrinsic retinal neurons in mammals (Borst et al. 2010), the impaired response to the optomotor test must be due to abnormalities in the fly brain rather than in the photoreceptive apparatus. For reasons that are presently unknown, a gender bias reduces the reproductive and neurological fitness of mutant females more than that of mutant males (Figures 3.5-3.7).

As previously discussed, CIII activity was markedly reduced in mutant adult flies, whereas CI and CIV activities were normal (Figure 3.4), indicating that the function exerted by TTC19 on CIII activity pre-dates evolutionary divergence between *Arthropoda* and *Chordata*, during the Cambrian age (≈545 Mya).
We obtained the same biochemical results by transferring the mutant allele in a second *D. melanogaster* strain (strain *CyO, GFP*) through suitable crosses, indicating that the phenotype associated with absence of TTC19 is specific, irrespective of the genetic background. However, a strain with ≈65% decrease of *CG15173*-specific mRNA (VDRC ID#105382), obtained by RNA interference, showed normal CIII activity and no neurological phenotype (Figure 3.10), indicating that ≈35% residual transcript is sufficient to maintain the function of TTC19. Importantly, the CIII deficiency found in the KO adult flies was not present in mutant larvae (Figure 3.4), that appeared in fact normal, underwent normal pupation and developed into adult individuals, suggesting the existence of an alternative CIII assembly process in the developing stages of the fly, similar to what has been suggested in humans (Minai et al. 2008).

In conclusion, the identification of TTC19 as a mitochondrial chaperone essential for the formation of the MRC opens several interesting questions, including, for instance, why this protein is absent in non-animal eukaryotes, i.e. plants and fungi, and what is the function of the ≥1MDa TTC19- containing mitochondrial complex. From a mechanistic point of view, whilst the physical interaction of TTC19 with CIII is unequivocally demonstrated by the results of the co-immunoprecipitation experiments, issues that warrant further investigation include which of the CIII subunits constitute the specific target of TTC19, at which specific step of CIII assembly this contact is established, and what is the precise mechanism carried out by TTC19 in the formation of the complex.
Additionally, the late-disease onset in patient #4 and the normal development and CIII activity of mutant *D. melanogaster* larvae may suggest tissue-specific, age-related, and development-dependent regulation of both TTC19 functions and CIII activity.
Last but not least, the presence of a TTC19-containing supercomplex, not associated with any MRC complex, leaves open the possibility of alternative function(s) for this protein in mitochondrial homeostasis. This is also suggested by the clinical phenotype of the *TTC19* knockout fly model that includes, besides neurological abnormalities, hypofertility and embryonic lethality predominantly in female individuals. In any case, the availability of a fly knockout model for TTC19, and the currently underway creation of a *TTC19*-less mouse will constitute important tools to clarify these issues.
In the next pages is attached a copy of the paper dealing with the recent results obtained for d*TTC19* gene, currently accepted for publication in *Nature Genetics*.

Mutations in TTC19 cause mitochondrial complex III deficiency and neurological impairment in humans and flies.

Daniele Ghezzi[1*], Paola Arzuffi[1*], Mauro Zordan[2], Caterina Da Re[2], Costanza Lamperti[1], Clara Benna[2], Pio D'Adamo[3], Daria Diodato[1], Rodolfo Costa[2], Caterina Mariotti[4], Graziella Uziel[5], Cristina Smiderle[6], Massimo Zeviani[1]

[1]Unit of Molecular Neurogenetics, [4]Unit of Laboratory Medicine and [5]Unit of Child Neurology, The Foundation "Carlo Besta" Institute of Neurology, Milan, Italy

[2]Neurogenetics and Behaviour of Drosophila Lab, Dept. of Biology, University of Padova, Italy

[3]Unit of Medical Genetics, Istituto di Ricovero e Cura a Carattere Scientifico, Burlo Garofolo, University of Trieste, Trieste, Italy

[6]Division of Physical Medicine and Rehabilitation, Public Health Hospital, Bassano del Grappa, Italy, Italy

* These Authors contributed equally to the work

Correspondence to:

Massimo Zeviani, MD, PhD

Unit of Molecular Neurogenetics, The "Carlo Besta" Neurological Institute Foundation - IRCCS

via Temolo 4, 20126 Milan, Italy

FAX +39-02-23942619; Phone +39-022394-2630

E-mail: zeviani@istituto-besta.it

ABSTRACT

Although mutations in cytochrome b or BCS1L have been reported in isolated defects of Mitochondrial Respiratory Chain (MRC) complex III (cIII), most of cIII-defective cases remain genetically undefined. We identified a homozygous non-sense mutation in the tetratricopeptide 19 (*TTC19*)-encoding gene in patients from two families, affected by progressive encephalopathy associated with profound cIII deficiency and accumulation of cIII-specific assembly intermediates. A second homozygous nonsense mutation was later found in a fourth patient. We demonstrated that mature TTC19 is embedded into the inner mitochondrial membrane, as part of two high-molecular weight complexes, one of which coincides with cIII. Physical interaction between TTC19 and cIII was then demonstrated by co-immunoprecipitation. Next, we investigated a *Drosophila melanogaster* knockout model for TTC19 that showed low fertility, adult-onset locomotor impairment and bang sensitivity, associated with cIII deficiency. TTC19 is a putative cIII assembly factor that prevents severe neurological abnormalities in humans and flies.

TEXT

MRC cIII (EC1.10.2.2) funnels the electrons fixed onto Coenzyme Q by different donors, e.g. cI and cII, to cytochrome *c* (cyt *c*). The energy liberated by this electron transfer sustains the extrusion of four protons across the inner mitochondrial membrane (IMM), thus contributing to the formation of the electrochemical potential ($\Delta\Psi$). Mammalian cIII is composed of 11 subunits[1]; cytochrome *b*, cyt *b*, is encoded by mtDNA, the remainder being encoded by nuclear DNA genes[2], including a second cytochrome, cyt *c1*, the Rieske iron-sulfur protein, RISP, two "core" subunits, Core1-2, and 6 additional, smaller proteins of unknown function. The cIII monomer is quickly converted into a catalytically active homodimer that takes part in MRC supercomplexes, together with cI, cIV, or both[3]. BCS1L, the only cIII assembly factor thus far known in humans, helps RISP to get inserted into nascent cIII[4], whereas another gene product, HCCS, carries out the insertion of the heme

moieties in both cyt *c* and *c1*[5]. In order to find additional factors affecting cIII assembly and activity, we investigated patients with severe, isolated cIII deficiency, lacking mutations in either cIII subunits or BCS1L.

Patients #1 and #2 are 37 and 24 year-old siblings from reportedly non-consanguineous, healthy parents, originating from the same alpine area of North-Eastern Italy. Both patients are affected by a slowly progressive neurodegenerative (Figure 1a) disorder (Supp Note), with onset in late infancy. A similar course occurred in patient #3, a young lady now 19 yo, the only child from reportedly non-consanguineous healthy parents, originating from the same area of Central Italy. In all three subjects muscle biopsy was morphologically normal, but showed marked isolated reduction of cIII activity (Table 1). Patient #4, born from reportedly non-consanguineous healthy parents from Southern Italy, had no clinically relevant complaint until 42 years, when he developed subacute, rapidly progressive neurological failure (Supp Figure 1), and died three years later. In spite of mild morphological abnormalities (Supp Figure 2), a muscle biopsy showed marked, isolated cIII deficiency (Table 1). A 40% reduction of cIII activity was detected in myoblasts from patient #2. Skin fibroblasts from patients #1, #2 and #3 were biochemically normal in standard conditions, but displayed partial, isolated cIII defect in an OXPHOS-conditioning, galactose-containing medium (Table 1). Oxygen consumption in the same cell lines, measured by a Seahorse FX-96 oxygraph, was significantly decreased, in either glucose (Figure 1b) or galactose medium (not shown), clearly indicating impaired respiration.

Because of the common geographic origin of the parents, we performed genome-wide SNP-based haplotyping in family 1. A continuous 12.8Mb region of homozygosity was found on chr17 in both siblings, containing 265 gene entries. Since the responsible gene was likely to encode a mitochondrial protein, 18 candidates were selected by *in silico* data mining[6], 17 of which failed to show mutations (Supp Table 1). The last candidate gene (*TTC19*) encodes tetratricopeptide repeat domain 19 (NM_017775), a protein present in all metazoa, but neither in other eukaryotes (plants, fungi), nor in prokaryotes. The putative human *TTC19* ORF (NP_060245) contains two potential

AUG initiation codons, translatable in methionines at positions +1 and +122 (M_1, M_{122}). However, since the sequence from M_1 to S_{121} is not conserved among species (Supp Figure 3), we considered the 380aa sequence starting from M_{122} as the real human TTC19 protein (h.TTC19). We found a homozygous c.656T>G nucleotide change in the h.*TTC19* gene, predicting the synthesis of a truncated protein p.L219X, in the two affected siblings #1 and #2, and also in patient #3, whereas a homozygous nonsense mutation c.517C>T, p.Q173X, was found in patient #4 (Supp Figure 4). Since the c.517C>T mutation (patient #4) is only 4 bp upstream from the 3' end of exon 5, the creation of an illegitimate splice site cannot be excluded, predicting a frameshift with a premature stop codon (p.Q173RfsX4). Dense SNP-based intragenic haplotypization demonstrated that patients #1, #2, and #3 carry the same mutant allele (Supp Table 2). Neither mutation was found in 450 alleles from 225 consecutive Italian control DNA samples. We showed that the parents of patients #1 and #2, and those of patient #3 were all heterozygous for the c.656T>G change. Since DNA samples from the parents of patient #4 were not available, we performed a quantitative analysis of the genomic region containing the 517C>T change in the DNA of this patient, demonstrating the presence of two mutated alleles (Supp Figure 5). The amount of *TTC19* mutant transcript was markedly reduced in fibroblasts of patients #1, #2, and #3, in myoblasts of patient #2, and in muscle of patients #2 and #4, suggesting mutation-driven mRNA decay (Figure 1d). No protein was immunodetected with a specific α-TTC19 antibody in mitochondria from fibroblasts of patients #1, #2, and #3 and from myoblasts of patient #2, whereas a normal amount of TTC19 cross-reacting material (CRM) was obtained from fibroblasts of a BCS1L-mutant patient (Figure 1E). The immunofluorescence (IF) confocal pattern of a 3'-in frame, HA-tagged cDNA ($h.TTC19^{HA}$), transiently expressed in COS7 cells, coincided with that of Mitotracker (Figure 2a), indicating that the h.TTC19 protein targets to mitochondria. *In vitro* mitochondrial import assay (Figure 2b) and immunovisualization of native h.TTC19 using an α-TTC19 antibody in cell fractions (Figure 2c,d) demonstrated that (i) TTC19 is a ≈43kDa precursor protein, translocated by a ΔΨ-dependent mechanism into the inner mitochondrial compartment, where its mitochondrial targeting sequence

(MTS) is cleaved off a ≈35kDa mature protein species, which is then embedded in the IMM; (ii) TTC19 is absent elsewhere in the cell; in particular, it is absent in the midbody during cytokinesis, unlike recently suggested[7] (Supp Figure 6). To prove that the loss of h.TTC19 was causally linked to the OXPHOS phenotype, we demonstrated that expression of h.TTC19^{HA} restored oxygen consumption to normal levels in mutant fibroblasts of both patients #1 and #2, and in myoblasts of patient #2 (Figure 1b), as well as cIII activity in galactose-treated fibroblasts of patient #1 (Table 1). We next investigated cIII structure in mutant tissues and cells. A cIII-specific IF signal obtained by using an α-Core1 antibody, decorating the mitochondrial network, was hardly visible in muscle of patients #1 (Figure 3a) and #2 (not shown), and cIII holoenzyme from muscle of patient #2 was markedly low by immunovisualization with α-Core1 on electroblotted 1-dimension (1D) blue-native gel electrophoresis (BNGE) (Figure 3b), suggesting impaired cIII assembly or stability. In yeast, and presumably in mammals too, cIII assembly starts with the formation of three distinct subcomplexes: cytochrome *b*+Qcr7-8; cyt *c1*+Qcr6-9; and Core1+2. They then assemble together to form a cytochrome *bc1* pre-holocomplex, to which the RISP and Qcr10 subunits are eventually added through the action of BCS1L[8,9,10]. We immunodetected lower molecular weight (MW) spots reacting with both α-Core1 and α-Core2 antibodies in mutant muscle, that were absent in control muscle, and were not detected in either sample by an α-RISP antibody (Figure 3c), suggesting accumulation of early cIII assembly intermediates containing Core1-2, but not RISP, a subunit that is incorporated in the last step of cIII assembly. Taken together, these results suggest that the h.TTC19 protein may play a role in the assembly of nascent cIII, its absence being associated with a defect of cIII activity that causes progressive neurological impairment.

Next, we showed that virtually all of the mouse (m).TTC19-CRM was confined to two high-MW spots, corresponding to ≥1MDa and ≈650KDa complexes in both liver (Figure 4a) and kidney (not shown). The cIII dimer is also ≈650KDa in size, raising the possibility that TTC19 physically interacts with cIII. To test this hypothesis, we showed that the material immunoprecipitated by either α-Core1 or α-RISP did also contain m.TTC19; conversely, proteins immunoprecipitated by α-

TTC19 also reacted with α-Core1 and α-RISP. The binding was specific, since neither α-RISP, nor α-Core1, nor α-TTC19 co-immunoprecipitated (substantial amounts of) other components of the IMM, e.g. cII (Figure 4b), or of the mitochondrial matrix, e.g. HSP60 (not shown). Interestingly, isolated mitochondria from cultured human cells showed only the ≥1MDa, but not the ≈650KDa TTC19-containing complex (Figure 4c), suggesting that in actively proliferating human cells the binding of h.TTC19 to cIII is either more labile, transient, or both, compared to mouse solid tissues. The presence of the ≥1MDa TTC19-positive complex suggests for this protein a role in additional functions, unrelated to the MRC, that could nevertheless contribute to the clinical phenotype. In support to this view, we detected the ≥1MDa complex containing h.TTC19 also in 143B-derived rho° cells that lack the four mtDNA-dependent MRC complexes, including cIII (Figure 4c). Although pentatricopeptide mitochondrial proteins are involved in expression of mtDNA genes[11] and penta- and tetra-tricopeptide (TPR) motifs are related to each other[12], we excluded a direct involvement of TTC19 in cyt *b* transcription or translation (Supp Figure 7).

To further test whether TTC19 and cIII are functionally related, we investigated a *Drosophila melanogaster* (dm) strain containing a >7000bp-long piggyBac element within the ORF region of the first exon of *cg15173*, the fly ortholog of *TTC19* (Supp Figure 8). Like h.TTC19, dm.TTC19 is targeted to mitochondria (Supp Figure 9). The dm.TTC19 *null* adult flies showed reduced lifespan, all being dead by 35-40 days after eclosion, vs. 80-90 days of controls; and poor fertility (≈60% of controls). We failed to find any morphological abnormality in fly spermatids (Supp Figure 10), which provides additional evidence that TTC19 is unlikely to be involved in cytokinesis, at least in the fly, since abnormalities of spermatids are common hallmarks of defects in midbody formation in male flies[13].

Adult mutant flies displayed strong bang sensitivity[14], severely reduced spontaneous motor activity, and impaired optomotor test[15,16] (Figure 5A, B, C). Since an electroretinogram (Supp Figure 11) showed the integrity of the projections from the eye to the visual ganglia of the fly, which correspond to intrinsic retinal neurons in mammals[16], the impaired response to the optomotor test

must be due to abnormalities in the fly brain rather than in the photoreceptive apparatus. For reasons that are presently unknown, a gender bias reduces the reproductive and neurological fitness of mutant females more than that of mutant males (Figure 5a-c). The cIII activity was markedly reduced in mutant flies, whereas cI and cIV activities were normal (Figure 5d), indicating that the function exerted by TTC19 on cIII activity pre-dates evolutionary divergence between *Arthropoda* and *Chordata*, during Cambrian. We obtained the same results by transferring the mutant allele in a second *D. melanogaster* strain (strain CyO, GFP) through suitable crosses, indicating that the phenotype associated with absence of dm.TTC19 is specific, irrespective of the genetic background. However, a strain with ≈65% decrease of *cg15173*-specific mRNA (VDRC ID#105382), obtained by RNA interference, showed normal cIII activity and no neurological phenotype (Supp Figure 12), indicating that ≈35% residual transcript is sufficient to maintain the function of dm.TTC19. Importantly, the cIII deficiency found in the KO adult flies was not present in mutant larvae (Figure 5D), that appeared in fact normal, underwent normal pupation and developed into adult individuals, suggesting the existence of an alternative cIII assembly process in the developing stages of the fly, similar to what has been suggested in humans[17].

The TPR motif is a protein-protein interaction module found in multiple copies in a number of functionally diverse proteins that facilitates specific interactions with partner proteins[18]. A role as co-chaperones has been demonstrated for several TPR proteins, including STI1, Hip and immunophilins CyP40 and HSP56, that act in concert with chaperones HSP70 and HSP90 in a number of important pathways[18], e.g. the maturation of steroid hormone receptors[19]. Accordingly, we propose that TTC19 is a mitochondrial chaperone involved in at least one crucial function, that is, early-step assembly of cIII.

Several questions remain open, including why this protein is absent in non-animal organisms, what is the mechanism of TTC19 in cIII formation, and what is the function of the ≥1MDa TTC19-containing mitochondrial complex. Last but not least, the late-disease onset in patient #4 and the normal development and cIII activity of mutant *D. melanogaster* larvae may suggest tissue-specific,

age-related, and development-dependent regulation of both TTC19 functions and cIII activity in different cell types and organisms, as already suggested for BCS1L[20,21].

ACKNOWLEDGMENTS

We are grateful to Dr. Simona Zanotti, PhD, for technical support in preparing myoblast cultures, to Rachele Saccon and Damiano Zanini for helping with the locomotor assays and bang tests. We thank Prof. Maurizio Gatti, "La Sapienza" University, Rome, Italy, for helping with analysis of spermatid development in *D. melanogaster* and Aram Megighian for ERGs studies. The EuroBioBank and Telethon Network of Genetic Biobanks (GTB07001F grant to Dr. M. Mora) are also gratefully acknowledged for providing biological samples. This work was supported by the Pierfranco and Luisa Mariani Foundation Italy; Fondazione Telethon-Italy grant number GGP07019; and grant RF-INN-2007-634163 of the Italian Ministry of Health, to MZ; and by grants of the Cariparo Foundation; the Ministry of Education and Research; and Progetto Strategico Università di Padova "Models of Mitochondrial Disease", to RC.

AUTHOR CONTRIBUTIONS

DG and PA found *TTC19* and characterized the mutations in human cells; CL performed histological analysis of muscle biopsies; M Zordan, CDR, CB and RC carried out the experiments in flies; CM, GU and CS identified the patients and carried out the clinical workout; PD'A performed linkage analysis; DD carried out the mutational screening on patients #3 and #4 and controls; M Zeviani conceived the experimental planning and wrote the manuscript.

COMPETING FINANCIAL INTERESTS

The authors declare no competing financial interests.

FIGURE LEGENDS

Figure 1. Clinical and molecular genetic features of TTC19-mutant patients.

(a) Brain MRI of patient #1.

I. Transverse T2-weighted image of cerebellum and medulla oblongata. The arrows indicate bilateral hyperintense signals in the inferior olives.

II. Transverse T2-weighted image of the supratentorial brain. The arrow shows a hyperintense signal in the right putamen.

III. Median sagittal T1-weighted image showing atrophy of the cerebral cortex and cerebellar vermis (arrow).

IV. Coronal T1-weighted image showing brain atrophy with dilation of the lateral ventricles, atrophy of the caudate nuclei, and bilateral hyperintensities of the substantia nigra (arrows).

(b) Oxygen consumption rate (OCR) of patients fibroblasts (Fb, left panel) and myoblasts (Mb, right panel) before and after (+TTC19) re-expression of wt TTC19. Bars indicate the Standard Deviation for 8-16 technical replicates. *= $p < 0.05$; **= $p < 0.01$. (p values for unpaired, two-tail Student's *t*-test).

(c) Quantitative real-time PCR of TTC19 mRNA relative to GAPDH mRNA in patients and control (Ct) fibroblasts (Fb), myoblasts (Mb) and muscle biopsies (Ms). P1, P2, P3 and P4 correspond to patients #1, 2, 3 and 4, respectively.

(d) Immunoblot analysis of total lysates from myoblasts and fibroblasts using α-TTC19, α-Core1 and α-SDHA antibodies. P1, P2, P3 correspond to patients #1, 2, 3. Fb Bcs1l indicate fibroblasts of a patient with cIII deficiency due to mutations in BCS1L.

Figure 2. TTC19p subcellular localization

(a) Confocal immunofluorescence (IF) of COS7 cells transfected with *h.TTC19*^{HA}. The pattern of the green signal, corresponding to h.TTC^{HA}, coincides with that of the red signal, corresponding to MitoTracker, a mitochondrial marker, in transfected cells, producing a confocalized image in yellow. Bars correspond to 25μm.

(b) Import assay on isolated HeLa cell mitochondria. The in vitro translated h.TTC protein (lane 1), is partially imported and cleaved in the presence of freshly prepared, fully coupled, energized mitochondria (lane 2). The mature protein species is internalized within mitochondria, whereas the precursor protein species, that remains outside mitochondria is digested by proteinase K (PK) (lane 3). Both mature and precursor h.TTC19 proteins are digested when mitochondria are solubilized in Triton-X100 (lane 4). The import is dependent on the integrity of $\Delta\Psi$, since no mature protein is formed when $\Delta\Psi$ is dissipated by valinomycin (lane 5), and is completely digested by PK (lane 6).

(c) Immunoblot analysis of HeLa cell fractions. *iv*T, *in vitro* translated TTC19; Mt, mitochondria; L, cell lysate; PMF, post-mitochondrial fraction; GAPDH (a cytosolic protein) and Core1 (a mitochondrial protein) were used as controls.

(d) Immunoblot analysis of mouse liver mitochondria after treatment with detergent deoxycholate (DOC) or Na_2CO_3. Mt, mitochondrial fraction; MM, mitochondrial matrix, Mb, mitochondrial membrane fraction. HSP60 (mitochondrial matrix protein) and Core1 (a mitochondrial inner-membrane protein) were used as controls.

Figure 3. Protein characterization in *TTC19*-mutant patients

(a) Immunofluorescence images of muscle from a control (Ctrl), a disease control (Ctrl-tRNA) and patient #1 (P1), using α-Core1 antibody. Bars correspond to 25μm.

(b) 1D-BNGE of muscle homogenates from patient#2 (P2) and control (Ctrl). An antibody against the Core 1 subunit was used to detect complex III; an antibody against SDH 70kDa was used for complex II; and an antibody against subunit COX-IV was used for complex IV.

(c) 2D-BNGE of patient#2 (P2) and control (Ctrl) muscle homogenates. Antibodies against Core1, Core2 and RISP protein were used to detect complex III; an antibody against COX-IV was used for complex IV.

Figure 4. Structural analysis of TTC19 interactions

(a) 2D-BNGE on mouse liver mitochondria, using antibodies against TTC19, Core1 and, Core2 . Dotted vertical lines indicate the dimeric form of cIII ($cIII_2$) and the supercomplex composed by cIII and cIV ($cIII_2$+cIV).

(b) Co-immunoprecipitation assays on mouse liver mitochondria. The antibody used for immunoprecipitation (IP) is indicated on top whereas the antibodies used for immunodetection are indicated on the right. SN: supernatant; 2, 5, 10: materials released from beads after treatment with 2, 5, and 10% Triton X-100, respectively.

(c) 2D-BNGE on 143B, 143 rho0 and HeLa cells.

Figure 5. Characterization of dm.TTC19 *null* flies

(a) Spontaneous locomotor activity in *D. melanogaster* CantonS control (Ctrl) and dm.TTC19p *null* (TTC19) flies. The experiment consists in measuring the number of passages of individual flies across an infrared light beam during 30 min. In the analysis the flies are divided into males (-M) and females (-F). Bars indicate SD.

(b) Locomotor activity after Bang test. Percentage of flies able to climb to four selected "end-points", corresponding to 2.8, 5.6, 8.4 and 11.2 cm after vigorous shaking in a test tube by vortexing for 10 sec at maximum speed. CS: CantonS control flies; TTC19: dm.TTC19p *null* flies.

(c) Number of correct responses (taken in 10 trials) to the Optomotor test in CantonS control (Ctrl) and TTC19 KO (TTC19) flies, at different days of age. The stimulus consisted in a black and white striped drum rotating either clockwise or counterclockwise until a response was obtained from individual flies.

(d) Specific activities of MRC complexes in controls (CTRL1= CantonS and CTRL2= WTALA) and dm.TTC19p *null* (TTC19) flies, normalized to that of Citrate Synthase (CS). For each genotype we performed three replicate mitochondrial extractions and for each extraction enzymatic activities were determined from at least 10 replicate reactions. Assays were as described by Bugiani et al (2004)[22].

Table I. Biochemical analysis of OXPHOS activities

Muscle	**CS***	**cI %**	**cII %**	**cIII %**	**cIV %**	**cV %**
Ct value	80-210	70-130	70-130	69-131	61-139	63-137
P1 ms	127	80	103	**19**	65	133
P2 ms	133	92	94	**14**	75	143
P3 ms	108	143	81	**17**	108	106
P4 ms	83	96	69	**8**	121	98
Fibroblasts & Myoblasts	**CS***	**cI %**	**cII %**	**cIII %**	**cIV %**	**cV %**
Ct values	100-200	58-142	64-136	74-126	78-122	73-127
P1 fb	142	nd	nd	77	179	nd
P1 fb (Gal)	148	nd	nd	**63**	205	nd
P1 fb +TTC19	155			74		
P2 fb	143	88	152	81	111	93
P2 fb (Gal)	190	nd	nd	**46**	85	nd
P2 mb	138	nd	nd	**61**	231	nd
P3 fb	184	66	64	89	133	75
P3 fb (Gal)	115	nd	nd	**65**	133	nd

All enzymatic activities are normalized for citrate synthase activity (CS) and expressed as percentage of the mean control value. [a] nmol/min mg; nd: not determined.
fb: fibroblasts; mb: myoblasts; ms: skeletal muscle biopsy. Gal: measurement after growth in galactose medium for 48 hours. +TTC19: measurement after re-expression of wt TTC19, after growth in galactose medium for 48 hours.

URL

Mitoprot (http://ihg2.helmholtz-muenchen.de/ihg/mitoprot.html),

TargetP (http://www.cbs.dtu.dk/services/TargetP),

Predotar (http://urgi.versailles.inra.fr/predotar/predotar.html),

Psort (http://psort.ims.u-tokyo.ac.jp/)

MitoCarta (http://www.broadinstitute.org/pubs/MitoCarta/human.mitocarta.html)

SignalP (http://www.cbs.dtu.dk/services/SignalP)

METHODS

Genetic studies

Samples were genotyped using ILLUMINA 370CNV arrays at CBM Genotyping Core according to manufacturer's protocol and analyzed with Genome studio v.1.1. Homozygosity mapping was performed using PLINK v.1.07 with --homozyg option.

Mutation screening

This study was approved by the Ethics Committee of the "C. Besta" Neurological Institute. Patients or parents signed an informed consent prior to participation in the study. Genomic DNA was extracted by standard methods. The 10 exons and the intron-exon junctions of the human *TTC19* gene were amplified by PCR (primers available upon request); sequenced (Big Dye Terminator System); and analyzed on an ABI Prism 3130XL Genetic Analyzer (Applied Biosystems). Total RNA was isolated from cultured fibroblasts or myoblasts (Rneasy kit, Qiagen) and then transcribed to cDNA (Cloned AMV first-strand cDNA synthesis kit, Invitrogen). Quantitative Real-time PCR was assayed on an ABI Prism 7000 apparatus (Applied Biosystems).

Biochemical assays

Supernatants of 800x g muscle homogenates or digitonin-treated cultured skin fibroblasts were used to measure the activities of MRC complexes and citrate synthase[22]. Oxygen consumption rate (OCR) measurements were carried out as described previously[23] with slight modifications. Cultured fibroblasts and myoblasts were seeded in XF 96-well microplates (Seahorse Bioscience), at $2x10^4$ cells/well, and incubated at 37°C and 5% CO_2 for 24 h. Prior to measurement, the growth medium was replaced with assay medium (Seahorse Bioscience). The OCR measurements were taken every 4 min after a 4-min mix period.

Cloning of TTC19 cDNA

The wild-type *h.TTC19* cDNA from clone IRAUp969G0961D (www.imagenes-bio.de) was 3'-tagged with the sequence encoding an epitope of the haemoagglutinin (HA) of the influenza virus[24]. Tagged or untagged cDNAs were inserted into the eukaryotic-expression plasmid vector pcDNA3.2 (Invitrogen).

Cell culture of COS7 and HeLa Cells

Monkey kidney (COS7) cells, HeLa cells, myoblasts and skin fibroblasts were grown in D-MEM. glucose medium, or, in some experiments, in a galactose-rich (5mM), glucose-free modified D-MEM for 48 hours.

Transfection and lentiviral transduction

Recombinant plasmids were transfected by electroporation in both COS7 cells (for transient expression) and HeLa cells (for stable expression). Stably transfected clones were selected under 800ng/ml Geneticin (G418; Gibco-Invitrogen.). The TTC19HA construct was cloned into the pLenti6 vector and virions were obtained as described by Zhang et al. 2009[25].

Antibodies

The following antibodies were used in the work: mouse monoclonal anti-hemoagglutinin (anti-HA) (Roche) for IF studies and rat anti-HA (Roche) for WB studies; anti-hTTC19 (Sigma); anti-Core1, Core2 and RISP (Invitrogen); anti-SDHA (Invitrogen); anti-mtCOX I and anti-mtCOX IV (Invitrogen); anti-HSP60 (Abcam); anti Aurora B (Abcam), anti-GAPDH (Millipore).

Miscellaneous

Cell fractionation, isolation of mitochondria, mitochondrial *in-vitro* import assay, and immunoblot analysis were performed as described[26]. Muscle biopsies were processed according to standard

histological and histochemical techniques[27,28]. IF was carried out on cells and 10 µm muscle cryostat sections according to standard methods[29].

Quantitative PCR on human samples

We used 10ng of genomic DNA to amplify exons 1, 5 and 10 of the *h.TTC19* gene, and 100ng cDNA, retrotranscribed from total RNA extracted from fibroblasts, myoblasts or skeletal muscle, to amplify two different regions of the *h.TTC19* transcript, with specific primers (Supp. Tables 3 and 4). Cybergreen incorporation was followed in an ABI Taq-Man apparatus. Normalization for genomic quantification was performed using RNAseP, a single-copy gene, and GAPDH for quantification of transcripts, using in both cases the delta-deltaCT mathematical procedure.

Analysis of locomotor activity in mutant vs. control flies

Single flies were placed into glass tubes containing a gel as a source of food and water. Groups of 32 such glass tubes were then loaded into Trikinetics® locomotor activity monitors in an incubator at temp= 25°C, light/dark cycles of 12h, for 3 days. Every time a fly crossed an infrared light beam cast across the glass tube, this was register as a bout of activity. Bouts were collected in 30 min bins.

Bang test analysis in mutant vs. control flies

In order to assay sensitivity to mechanical stimulation[14], on the night before the experiment groups of five CO_2-anesthesized flies of each sex were placed in clean plastic vials containing a strip of moistened tissue paper (to provide a source of hydration). The next day, the paper was removed and each vial was placed in a vortex at the maximum intensity for 10 seconds. The vial containing the vortexed flies was then placed upright into a graduated cylinder in front of a digital webcam connected to a computer. Videotaped activity recorded for a 30 sec. was analyzed to establish the

time taken for each individual to recover from the mechanical shock and climb the vial to reach distance markings along the graduated cylinder.

Analysis of optomotor activity in mutant vs. control flies[15]

Flies were placed in a T-shaped tube with the longer arm painted black, placed in the center of an arena located inside a rotating drum, open at the top. The internal walls of the drum are painted with alternating black and white stripes and the apparatus is illuminated from above with a white light. Attracted by the light, tested flies exit the darkened arm of the T-tube, and will then be exposed to the black & white rotating drum. Normal flies tend to move in the same direction as the rotating environment. The test is repeated 10 times for each fly: five with clockwise and five with counterclockwise, rotations. Each fly is thus scored for the number of correct turns taken in the 10 trials.

Structural analysis by BNGE

BNGE was performed as described on extracts from 25mg of muscle[30] or isolated mitochondria[31]. Fifteen µl of sample were run through a 5-13% non-denaturating gradient (1D-BNGE). For denaturing 2D-BNGE electrophoresis, the 1D-BNGE lane was excised, treated for 1 h at r.t. with 1% SDS and 1% β-mercapto-ethanol and then run through a 16.5% tricine-SDS–polyacrylamide gel, using a 10% spacer gel.

Co-Immunoprecipitation

Mouse liver mitochondria were processed according to manufacturer's instruction (Immunoprecipitation starter Pack, GE Healthcare), using protein G Sepharose 4 Fast Flow and 2µg of specific antibodies. For the dissociation step, the precipitated immune complexes were treated sequentially with 2%, 5% and 10% Triton X-100. The supernatant were analyzed by SDS-PAGE, followed by immunoblotting.

Radiolabeled mitochondrial translation

In vivo analysis of mitochondrial translation and in vitro import were performed as described[32] using a denaturing 15-20% poly-acrylamide gradient gel[33].

Assembly of MRC complexes was investigated on myoblasts preincubated with chloramphenicol 40µg ml^{-1} for 15h. Radiolabeling was carried out as described[32], but using cycloheximide 100µg ml^{-1} instead of emetine. After a 2h pulse period, different chases (0h-3h-16h) were performed in complete cold medium. Cells were collected and processed for BNGE as described by Nijtmans et al.[30].

Mitochondrial Cyt *b* and CoxI transcripts were quantified by Real-time PCR on myoblasts and fibroblasts cDNA from controls and patients. The amount of each transcript was normalized to that of GAPDH transcript.

Genomic analysis of dm.TTC19 mutant flies

A single individual from strain *#18843* (#f05160 Exelixis) was homogenized in 50µl of extraction buffer, 10mM Tris-HCl (pH 8.2), 1mM EDTA and 25 mM NaCl. Proteinase K was added, to a final concentration of 200µg/ml, and the homogenate incubated for 45 min at 37° C. The enzyme was heat inactivated at 95° C for 5 min. Two µl was used as a template in a 25µl PCR reaction mix, containing 1X AccuPrime PCR Buffer I, 5pmol of each primer, 0.5U of AccuPrime *Taq* Polymerase High Fidelity enzyme (Invitrogen). Following a 2min denaturation step at 94°C, 35 rounds of amplification (94°C for 30s, 60°C for 30s, 68°C for 1m and 30s) were performed.

To confirm the piggyBac element insertion location[34], PCRs on genomic DNA were performed. TTC19 specific primers were chosen upstream and downstream the annotated insertion position (458bp downstream the putative ATG start codon). Amplifications were carried out by coupling *dm.TTC19* and WH piggyBac element specific, as listed in Supp Table 5. The Exelixis piggyBac

WH primers were as reported in Parks et al. 2004. The *Drosophila melanogaster TTC19* (*cg15173*) sequence accession number is FBgn0032744 (2L:19043535-19045146).

dm.TTC19 RNAi fly

The knock-down RNAi flies were obtained from VDRC (Vienna Drosophila RNAi Center): Transformant ID 105382; FlyBase n. CG15173.

The knock down of individual *Drosophila* genes was achieved using the GAL4/UAS system to target the RNAi to specific cells in the animal[35]. The primer pair specific for amplicon 3 of *d.TTC19* cDNA was used for quantitative-PCR, to measure the amount of *dm.TTC19* cDNA normalized to rp49, a housekeeping cDNA[15].

Isolation of Drosophila melanogaster mitochondria

Each sample was homogenized using a Dounce glass-glass potter and loose fitting pestle. A mannitol-sucrose buffer (pH 7.4) in 2% BSA was then added to a final volume of 25 ml. Samples were centrifuged at 1500xg (Beckman Avanti J-25 Centrifuge, Beckman 2550 rotor) at 4° for 6 minutes. The pellet was discarded by filtering the sample through a fine mesh, and the supernatant centrifuged at 7000g at 4° for 6 minutes. The pellet was resuspended in 20 ml of mannitol-sucrose buffer without BSA before being centrifuged at 7000 x g under the same conditions as above and resuspended in 50 µl of buffer. Protein concentration was measured by the Biuret test.

REFERENCES

1. Iwata, S. et al. Complete structure of the 11-subunit bovine mitochondrial cytochrome bc1 complex. *Science* **281**, 64-71 (1998).
2. Schägger, H., Link, T.A., Engel, W.D. & von Jagow G. Isolation of the eleven protein subunits of the bc1 complex from beef heart. *Methods Enzymol.* **126**, 224-237 (1986).
3. Wittig, I., Braun, H.P. & Schagger, H. Blue native PAGE. *Nat. Protoc.* **1**, 418-428 (2006).
4. Fernandez-Vizarra, E. et al. Impaired complex III assembly associated with BCS1L gene mutations in isolated mitochondrial encephalopathy. *Hum. Mol. Genet.* **16**, 1241-1252 (2007).
5. Wimplinger, I. et al. Mutations of the Mitochondrial Holocytochrome *c*-Type Synthase in X-Linked Dominant Microphthalmia with Linear Skin Defects Syndrome *AJHG* **79**, 878-889 (2006).
6. Pagliarini, D.J. et al. A mitochondrial protein compendium elucidates complex I disease biology. *Cell* **134**, 112-123 (2008).
7. Sagona, A.P. et al. PtdIns(3)P controls cytokinesis through KIF13A mediated recruitment of FYVE-CENT to the midbody. *Nat. Cell. Biol*. **12**, 362-371 (2010).
8. Brandt, U., Yu, L., Yu, C.A. & Trumpower, B.L. The mitochondrial targeting presequence of the Rieske iron-sulfur protein is processed in a single step after insertion into the cytochrome bc1 complex in mammals and retained as a subunit in the complex *J. Biol. Chem*. **268**, 8387-8390 (1993).
9. Cruciat, C.M., Hell, K., Folsch, H., Neupert, W., & Stuart R.A. Bcs1p, an AAA-family member, is a chaperone for the assembly of the cytochrome *bc*(1) complex. *EMBO J.* **18**, 5226-5233 (1999).
10. Zara, V., Palmisano, I., Conte, L., & Trumpower, B.L. Further insights into the assembly of the yeast cytochrome *bc1* complex based on analysis of single and double deletion mutants lacking supernumerary subunits and cytochrome *b*. *Eur. J. Biochem*. **271**, 1209-1218 (2004).

11. Lightowlers, R.N. & Chrzanowska-Lightowlers, Z.M. PPR (pentatricopeptide repeat) proteins in mammals: important aids to mitochondrial gene expression. *Biochem J.* **416**, e5-6 (2008).
12. Small, I.D. & Peeters, N. The PPR motif - a TPR-related motif prevalent in plant organellar proteins. *Trends Biochem. Sci*. **25**, 46-47 (2000).
13. Giansanti MG, Farkas RM, Bonaccorsi S, Lindsley DL, Wakimoto BT, Fuller MT, Gatti M. Genetic dissection of meiotic cytokinesis in Drosophila males. *Mol. Biol. Cell*. **15**, 2509-22 (2004)
14. Glasscock, E. & Tanouye, M.A. Drosophila couch potato mutants exhibit complex neurological abnormalities including epilepsy phenotypes. *Genetics* **169***, 2137-2149 (200*5**).**
15. Zordan, M.A., et al. Post-transcriptional silencing and functional characterization of the Drosophila melanogaster homolog of human Surf1. *Genetics*, **172,** 229–241 (2006).
16. Borst A, Haag J, Rieff DF. Fly motion vision. *Annu. Rev. Neurosci.* **33**, 49-70 (2010)
17. Minai, L. et al. Mitochondrial respiratory chain complex assembly and function during human fetal development. *Mol Genet Metab.* **94**, 120-126 (2008).
18. Blatch, G.L. & Lassle, M. The tetratricopeptide repeat: a structural motif mediating protein-protein interactions. *BioEssays* **21**, 932-939 (1999).
19. Kimmins, S. & MacRae T.H. Maturation of steroid receptors: an example of functional cooperation among molecular chaperones and their associated proteins. *Cell Stress Chaperones* **5**, 76-86 (2000)
20. Kotarsky, H., et al. BCS1L is expressed in critical regions for neural development during ontogenesis in mice. *Gene Expr. Patterns* **7**, 266-273 (2007).
21. Papa, S. Mitochondrial oxidative phosphorylation changes in the life span. Molecular aspects and physiopathological implications. *Biochim Biophys Acta.* **1276**, 87-105 (1996).
22. Bugiani, M., et al. Clinical and molecular findings in children with complex I deficiency. *Biochim. Biophys. Acta*. **1659**, 136-147 (2004).

23. Wu, M. et al. Multiparameter metabolic analysis reveals a close link between attenuated mitochondrial bioenergetic function and enhanced glycolysis dependency in human tumor cells. *Am. J. Physiol. Cell Physiol.* **292**, C125-C136 (2007).
24. Tiranti, V. et al. Characterization of SURF-1 expression and Surf-1p function in normal and disease conditions. *Hum. Mol. Genet*. **8**, 2533-2540 (1999).
25. Zhang, J.C. et al. Down-regulation of CXCR4 expression by SDF-KDEL in CD34(+) hematopoietic stem cells: an antihuman immunodeficiency virus strategy. *J. Virol. Methods* **16**, 30-37 (2009).
26. Ghezzi, D. et al. Paroxysmal non-kinesigenic dyskinesia is caused by mutations of the MR-1 mitochondrial targeting sequence. *Hum Mol Genet*. **18**, 1058-64 (2009).
27. Heckmatt, J.Z. & Dubowitz, V. Needle biopsy of skeletal muscle. *Muscle Nerve* **7**, 594 (1984).
28. Sciacco, M. & Bonilla, E. Cytochemistry and Immunocytochemistry of Mitochondria in Tissue Sections. *Methods Enzymol*. **264**, 509-521 (1996).
29. Tiranti, V. et al. Mutations of SURF-1 in Leigh disease associated with cytochrome c oxidase deficiency. *Am J Hum Genet*, **63**, 1609-1621 (1998).
30. Nijtmans, L.G., Henderson, N.S. & Holt, I.J. Blue native electrophoresis to study mitochondrial and other protein complexes. *Methods* **26**, 327–334 (2002)
31. Schägger, H. & von Jagow, G. Tricine-sodium dodecyl sulfate-polyacrylamide gel electrophoresis for the separation of proteins in the range from 1 to 100 kDa. *Anal Biochem*. **166**, 368–379 (1987).
32. Fernandez-Silva, P., Acin-Perez, R., Fernandez-Vizarra, E., Perez-Martos, A., & Enriquez, J.A. In vivo and in organello analyses of mitochondrial translation. *Methods Cell Biol*. **80**, 571–588 (2007).
33. Chomyn, A. In vivo labeling and analysis of human mitochondrial translation products. *Methods Enzymol.* **264**, 197–211 (1996).

34. Parks, A.L., Cook, K.R., Belvin, M., Dompe, N.A., Fawcett, R., Huppert, K., Tan, L.R., Winter, C.G., Bogart, K.P., Deal, J.E., et al. Systematic generation of high-resolution deletion coverage of the Drosophila melanogaster genome. *Nat Genet*.**36**, 288-292 (2004).

35. Dietzl, G., Chen, D., Schnorrer, F., Su, K.C., Barinova, Y., Fellner, M., Gasser, B., Kinsey, K., Oppel, S., Scheiblauer, S., Couto, A., Marra, V., Keleman, K., Dickson, B.J. A genome-wide transgenic RNAi library for conditional gene inactivation in Drosophila. *Nature* **448,** 151-156 (2007).

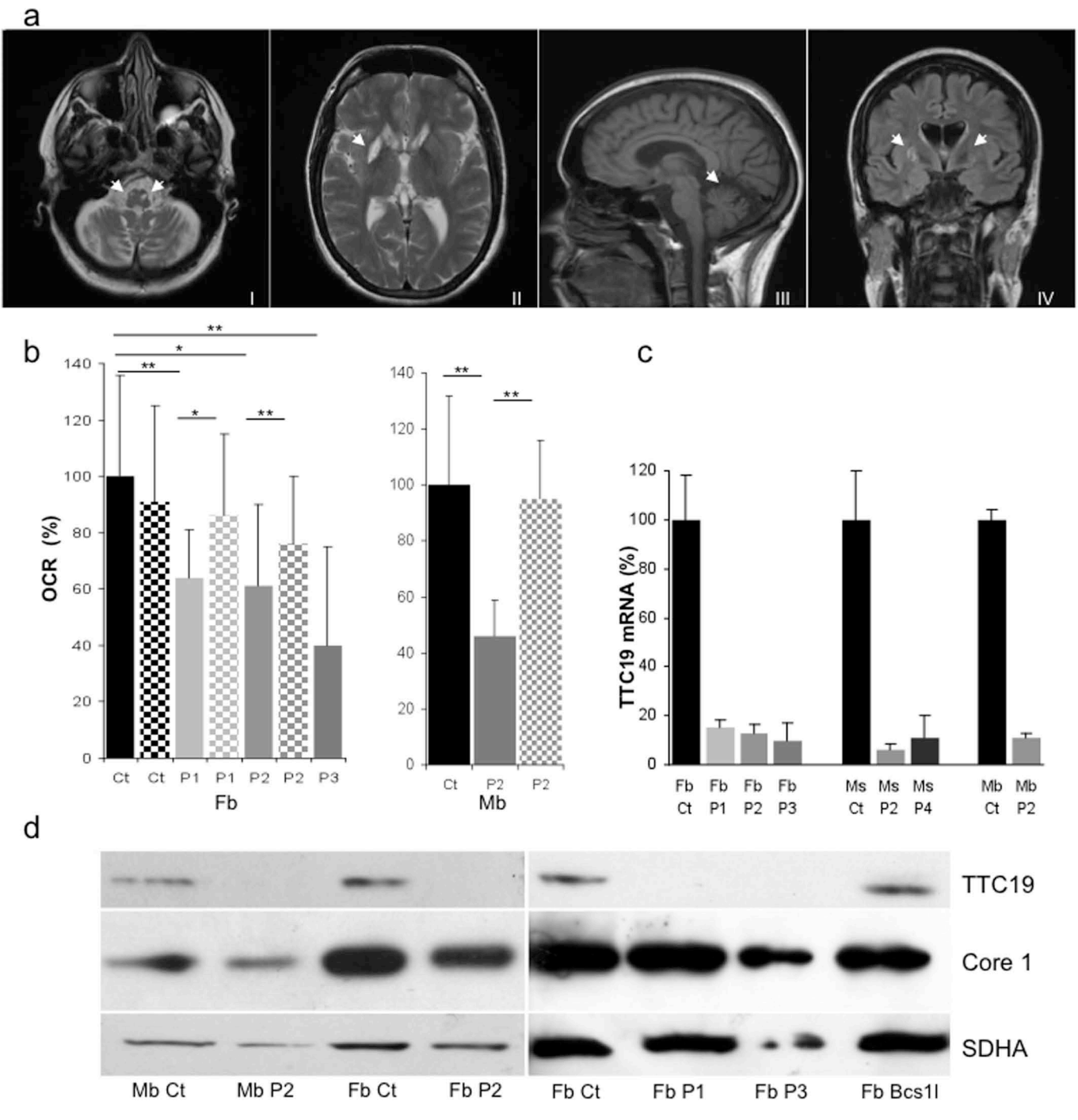
a
I
II
III
IV
b
OCR (%)
Ct Ct P1 P1 P2 P2 P3
Fb
Ct P2 P2
Mb
c
TTC19 mRNA (%)
Fb Ct
Fb P1
Fb P2
Fb P3
Ms Ct
Ms P2
Ms P4
Mb Ct
Mb P2
d
TTC19
Core 1
SDHA
Mb Ct
Mb P2
Fb Ct
Fb P2
Fb Ct
Fb P1
Fb P3
Fb Bcs1l

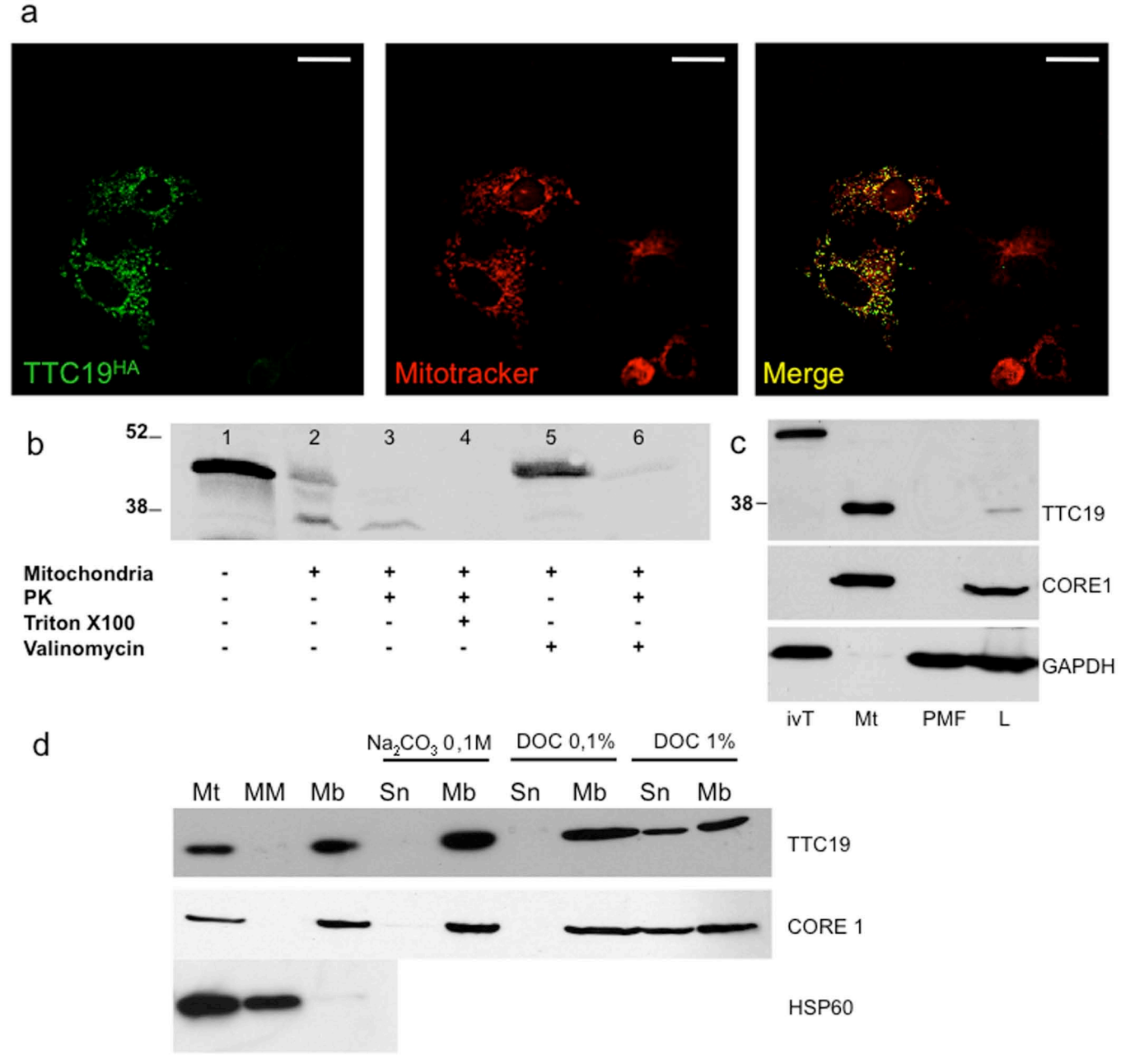
a
TTC19HA
Mitotracker
Merge
b
52
38
1
2
3
4
5
6
Mitochondria - + + + + +
PK - - + + - +
Triton X100 - - - + - -
Valinomycin - - - - + +
c
38
TTC19
CORE1
GAPDH
ivT
Mt
PMF
L
d
Na2CO3 0,1M
DOC 0,1%
DOC 1%
Mt
MM
Mb
Sn
Mb
Sn
Mb
Sn
Mb
TTC19
CORE 1
HSP60

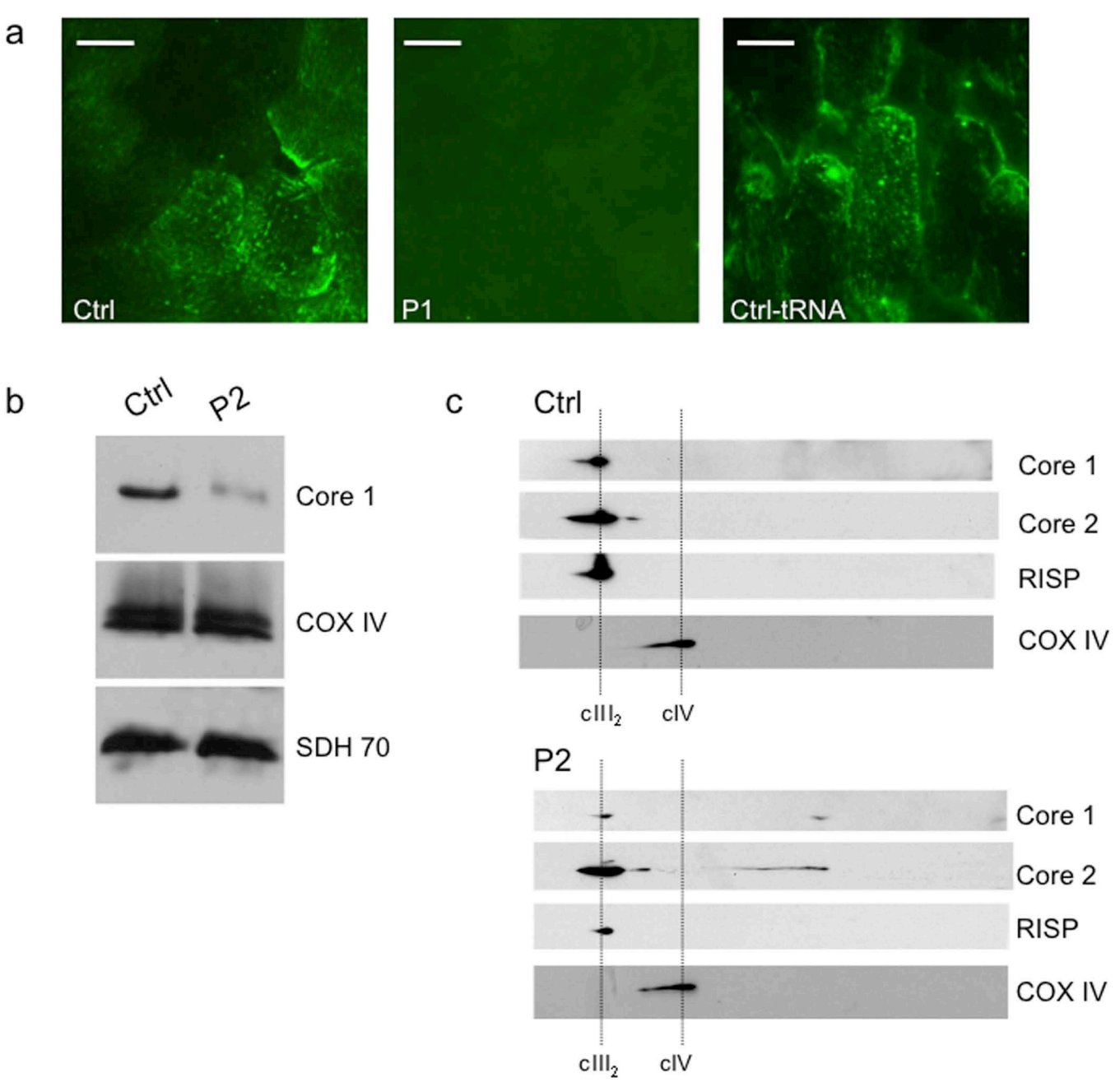
a
Ctrl
P1
Ctrl-tRNA
b
Ctrl
P2
Core 1
COX IV
SDH 70
c
Ctrl
Core 1
Core 2
RISP
COX IV
cIII2
cIV
P2
Core 1
Core 2
RISP
COX IV
cIII2
cIV

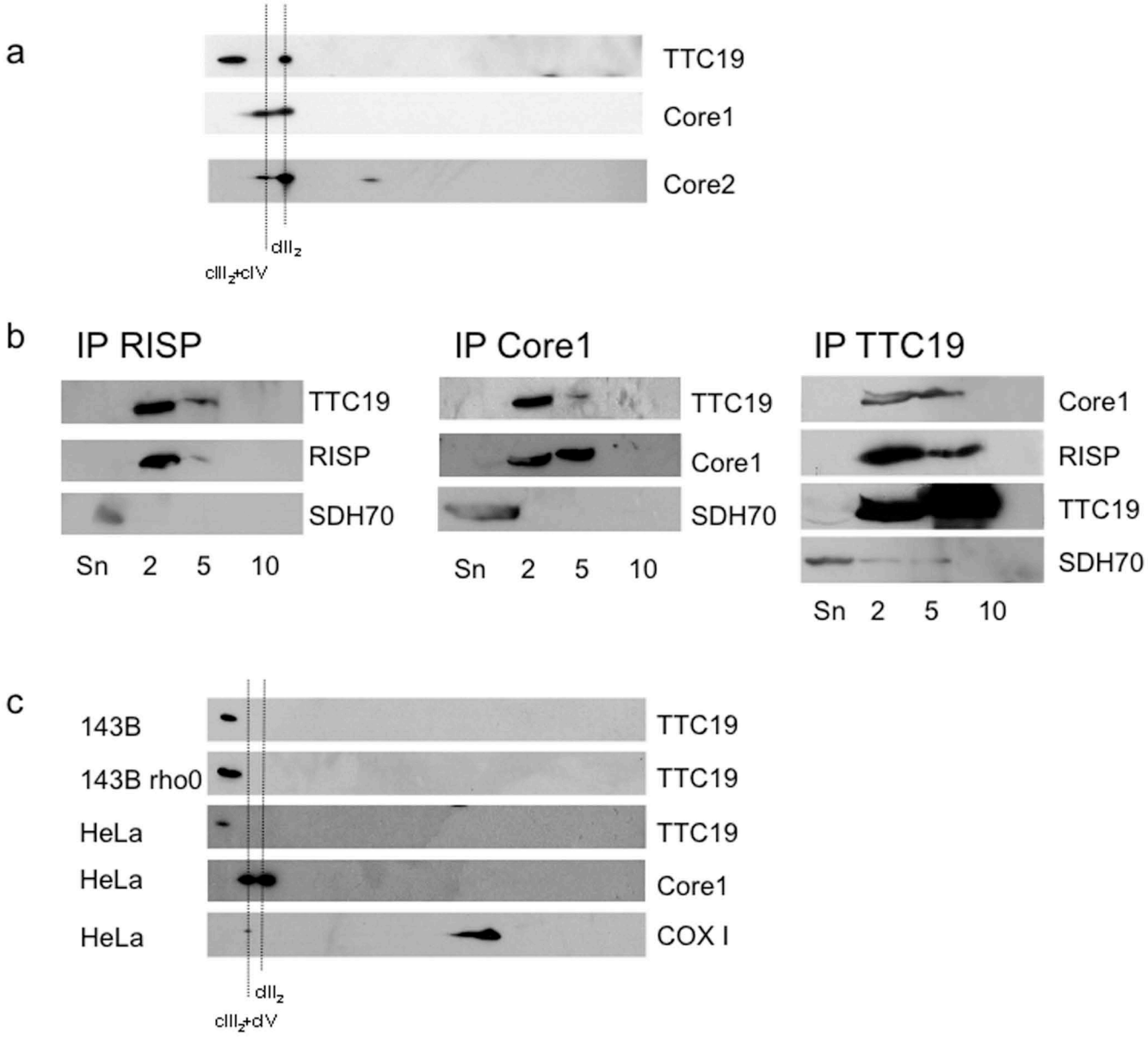
a
TTC19
Core1
Core2
dIII2
cIII2+cIV
b
IP RISP
TTC19
RISP
SDH70
Sn 2 5 10
IP Core1
TTC19
Core1
SDH70
Sn 2 5 10
IP TTC19
Core1
RISP
TTC19
SDH70
Sn 2 5 10
c
143B
143B rho0
HeLa
HeLa
HeLa
TTC19
TTC19
TTC19
Core1
COX I
dIII2
cIII2+cIV

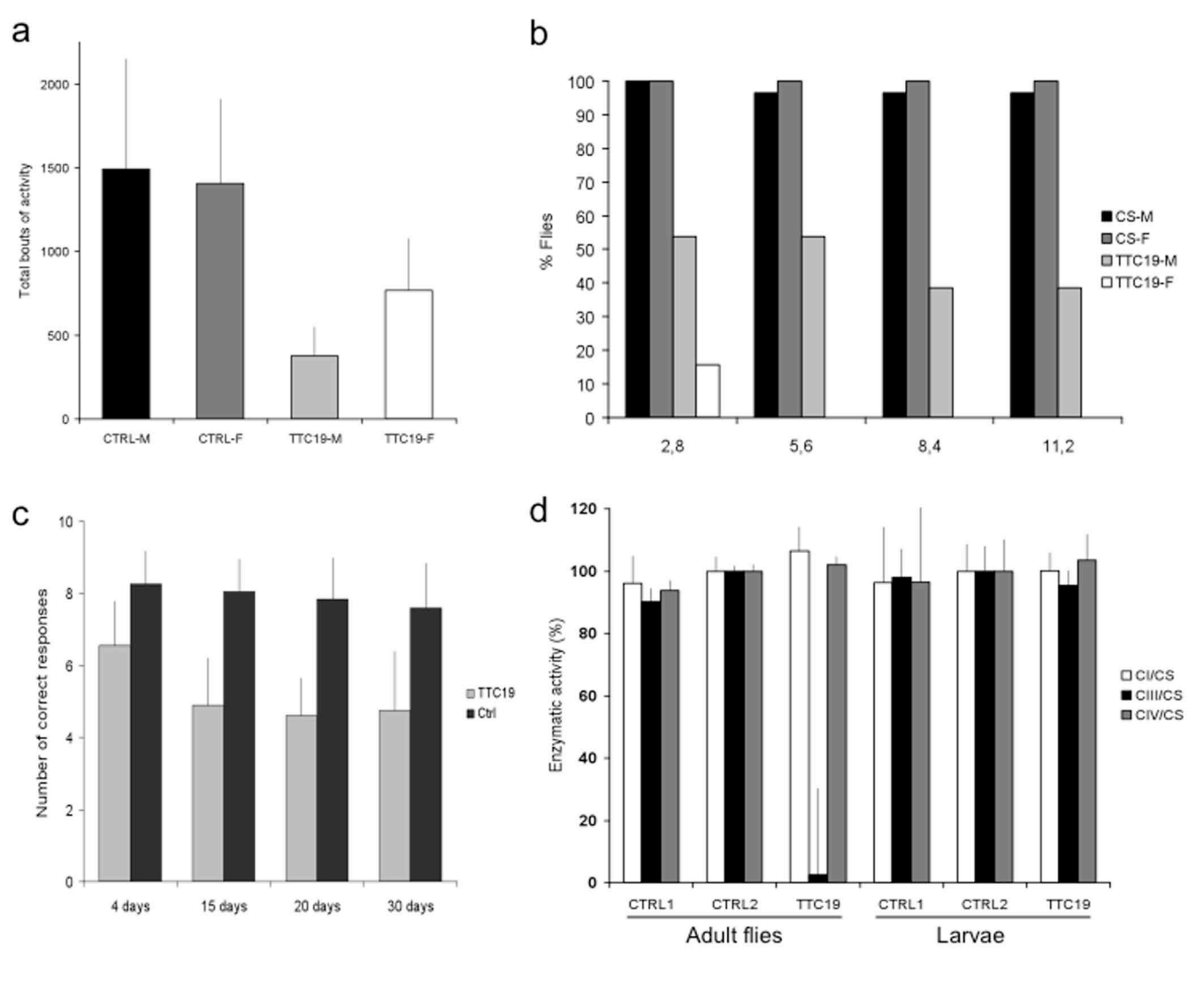
a
Total bouts of activity
2000
1500
1000
500
0
CTRL-M
CTRL-F
TTC19-M
TTC19-F
b
% Flies
100
90
80
70
60
50
40
30
20
10
0
2,8
5,6
8,4
11,2
CS-M
CS-F
TTC19-M
TTC19-F
c
Number of correct responses
10
8
6
4
2
0
4 days
15 days
20 days
30 days
TTC19
Ctrl
d
Enzymatic activity (%)
120
100
80
60
40
20
0
CTRL1
CTRL2
TTC19
CTRL1
CTRL2
TTC19
Adult flies
Larvae
CI/CS
CIII/CS
CIV/CS

PART IV

Functional characterization of *Drosophila melanogaster* mitochondrial deoxynucleotide transport

Structural alterations of the mitochondrial genome or decrease of its copy number have profound consequences on mitochondrial function and cause severe human diseases (Spinazzola and Zeviani 2005). As in the case of nuclear DNA, the maintenance of mitochondrial DNA (mtDNA) depends on the availability of deoxynucleotide precursors for its replication and repair. The precursors must be available in amounts appropriate to the needs of the mtDNA polymerase, and it is essential that the relative proportions among the 4 deoxyribonucleoside triphosphates (dNTPs) be balanced to avoid replication errors and mtDNA mutations. When these conditions are not satisfied the mitochondrial genome is destabilized, with complex consequences on mitochondrial and cellular physiology that are incompletely understood. Until very recently mitochondria were believed to synthesize their own DNA precursors, this view has been challenged by the demonstration that deoxynucleotides move across the inner mitochondrial membrane in both directions. Specific carriers in the mitochondrial inner membrane catalyze the exchange of deoxynucleotides between the two compartments. The RIM2 gene, which encodes for a carrier of pyrimidine nucleotides, was identified in yeast.
On the basis of homology with the *Rim2* gene encoding for a pyrimidine deoxynucleotide carrier in *Saccharomyces cerevisiae*, two genes in humans and one in *Drosophila melanogaster* may code for homologous deoxynucleotide carriers.
We characterized available *Drosophila melanogaster* transgenic lines, harboring a construct encoding for a CG18317/RIM2-specific dsRNA, allowing the targeted silencing of RIM2. In addition we studied *Drosophila* stocks bearing PiggyBac or P-element insertions within the RIM2 coding region. We analyzed both RNAi and insertional mutants in order to evaluate whether they show any defects in mitochondrial function which might be related to a deficiency in mitochondrial nucleotide availability.

Moreover we were also interested in the regulation of a specific mtDNA precursor, deoxyguanosine triphosphate (dGTP). It has been proposed that dGTP accumulates in mitochondria causing impairment of DNA synthesis and repair and serving as a signal for apoptosis (Arpaia et al. 2000). The dGTP pool is presumed to be severely affected in a severe immunodeficiency caused by genetic deficiency for purine nucleoside phosphorylase (PNP), a cytosolic enzyme involved in purine catabolism.
We have so far identified two potential *Drosophila* homologs of human PNP (CG16758 and CG18128). Furthermore, transgenic lines are available which harbor constructs encoding for specific dsRNAs allowing the targeted silencing of each of the PNP *Drosophila* homologs. In addition to the available dsRNAi lines, we also resorted to the production of mutants by inducing the excision of the inserted P- and/or PiggyBac-transposable elements.

INTRODUCTION

1.1 Models for mtDNA diseases

Main theme of this work is the identification of the mechanisms linking genetic defects in enzymes of deoxynucleotide metabolism to specific mitochondrial (mt) diseases in humans. So far only a fraction of the mitochondrial diseases due to depletion or mutation of mtDNA have been attributed to specific biochemical defects, and even in those cases, the molecular mechanisms leading to damage of the mitochondrial genome and impairment of mt oxidative metabolism are largely hypothetical.
To achieve this aim we first preparared by genetic manipulation *Drosophila* strains lacking individual enzymes of deoxynucleotide (dNTP) metabolism or mt deoxynucleotide transporters, then we have bgenu to assess if the inactivation of these proteins affects the mt dNTP pool, impairs mitochondrial functions and induces developmental abnormalities or any other pathological phenotype *in vivo* in *Drosophila*. In parallel, our research group will also evaluate the functional effects of alterations of the dNTP pools due to enzymatic defects or transport abnormalities *in vitro* (isolated organelles) and *in cellula* (mammalian and *Drosophila* cultures).

1.1.1 The mitochondrial (mt) genome stability

Mitochondria are the energy centers of the cell and contain their own genetic information, encoded in a small circular chromosome made of DNA. The maintenance of this DNA requires building blocks that are made both inside mitochondria and in the cytoplasm of the cell. To reach the mitochondrial compartment the latter have to be transported across the mitochondrial membrane by specific carrier proteins.
All the enzymes and carriers involved in these processes are encoded by the nuclear DNA, so that there is a strict interrelation between the nuclear and mitochondrial genomes. Indeed, mutations that inactivate the nuclear genes required for the maintenance of mitochondrial DNA have detrimental effects on the stability of mitochondrial genetic information.
If the mitochondrial genome is altered, the function of mitochondria in energy metabolism may become impaired, with severe cell damage and overt disease. The most affected organs are those with the highest energy consumption, such as skeletal muscle, heart, brain and liver. There are many different human diseases caused by defects of the mitochondrial genome, and in most cases we do not know what causes those defects, or how they appear in association with a given enzymatic deficiency.

1.1.2 Maintenance of mtDNA

The small mitochondrial (mt) genome codes for 13 polypeptides that are essential constituents of the oxidative phosphorylation machinery and for the ribosomal and tRNAs required for their synthesis. Structural alterations or decreased copy number of the mt genome have profound consequences on mt function and cause severe human diseases.
Maintenance of mtDNA depends on the availability of deoxynucleotide precursors, present in appropriate amounts. It is essential that the relative proportions of the 4 deoxyribonucleoside triphosphates (dNTPs) be balanced to avoid replication errors and mtDNA mutations. When these conditions are not satisfied the mt genome is destabilized with complex, still incompletely understood, consequences on mt and cellular physiology. The development of models for mtDNA diseases will be a major step forward in our understanding of how mt dNTP imbalance leads to disease.

1.1.3 Human mtDNA depletions syndromes

Only a minor fraction of human mtDNA depletion syndromes can be accounted for from the etiological point of view. So far inactivating mutations in one of ten nuclear genes have been recognized to cause depletion of the mt genome. Among these, four are directly involved in the metabolism of DNA precursors (the genes coding for mt TK2, dGK, thymidine phosphorylase, a cytosolic enzyme that degrades the deoxynucleosides thymidine and deoxyuridine, and the alternative small subunit of ribonucleotide reductase, p53R2). In the case of the two mt deoxynucleoside kinases and p53R2, mtDNA depletion is probably due to lack of precursors, while in the case of the phosphorylase it would result from accumulation of thymidine triphosphate (dTTP) inside mitochondria (Pontarin et al. 2006). This imbalance of precursors in the mt pool affects the fidelity of mt DNA polymerase causing depletion, point mutations and deletions in the mt DNA of the patients (Nishigaki 2003). Many other cases of disease associated with alteration of the mt genomes remain unexplained. The discovery that normal quiescent cells contain an active ribonucleotide reductase - the R1-p53R2 variant- that is essential for mtDNA maintenance (Hakansson et al. 2006, Pontarin et al. 2007, Bourdon et al. 2007) unexpectedly invalidated the accepted paradigm that de novo synthesis of deoxyribonucleotides only occurs in proliferating cells.

The new data raise a number of questions on how p53R2-dependent *de novo* synthesis complements the intramitochondrial salvage pathway initiated by the two mt deoxynucleoside kinases TK2 and dGK. A puzzling aspect is that genetic mutation in any of these three enzymes leads to mitochondrial disease, but with markedly different target organs.

A common feature, however, is that mt damage occurs in terminally differentiated cells that have stopped dividing. Also on the basis of studies on the dynamics of the mt dNTP pools in cycling and quiescent cells (Pontari et al. 2006, Rampazzo et al. 2004, Ferraro et al. 2005) it appears conceivable that in differentiated cells mitochondria become more dependent on their own pathway of dNTP synthesis because in such cells the cytosolic synthesis of DNA precursors is strongly reduced (Pontarin et al. 2007). Mutations in enzymes involved in the intramitochondrial pathway would therefore become pathogenic only in the absence of other adequate sources of DNA precursors. This hypothesis still does not explain why some tissues and cell types are instead affected by p53R2 deficiency. With the experiments outlined here we wish to answer some of those questions and to extend the knowledge on how mt dNTP pools are regulated. All the work done so far on the mtDNA precursors has dealt with the dTTP pool for two main reasons. First, the mt dTTP pool is affected in two severe mtDNA diseases, TK2-deficiency (a myopathic form of mtDNA depletion syndrome, MDS) (Saada et al. 2001) and thymidine phosphorylase deficiency (which causes a complex mt neurogastrointestinal encephalopathy, MNGIE) (Nishino et al. 1999). Second, the study of Dttp metabolism in intact cells is technically simpler than that of other dNTPs.

1.2 Transport of deoxyribonucleotides

Until very recently mitochondria were believed to synthesize their own DNA precursors by a pathway largely independent of that involved in the production of nuclear DNA precursors (Bogenhagen and Clayton 1976, Zhu et al. 2000). The generally accepted view of a strict compartmentation between mt and cytosolic dNTP pools is supported by the existence of two mt deoxynucleoside kinases [thymidine kinase 2 -TK2- (Berk and Clayton 1973) and deoxyguanosine kinase –dGK– (Arner and Eriksson 1995)] which possess substrate specificities adequate for the phosphorylation of all 4 deoxyribonucleosides (Piskur et al. 2004); and of a series of nucleotide kinases that catalyse the additional steps in the production of the dNTPs. This view has been challenged by the demonstration that deoxynucleotides move across the inner mt membrane in both directions and that influx of precursors made outside mitochondria represents the main source of dNTPs for mtDNA replication in cycling human cells (Pontarin et al. 2003). Thus, carriers in the mt inner membrane must exist which catalyze the exchange of deoxynucleotides between the two compartments. These may include a carrier with specificity for deoxycytidine nucleotides (Bridges et al. 1999) and other putative nucleotide carriers cloned in yeast and characterised in proteoliposomes (Marobbio et al. 2006, Vozza et al. 2004). One such carrier, named DNC, was reported to be expressed in humans (Dolce et al. 2001) but recent studies could not confirm the

finding that the protein was responsible for deoxynucleotide transport into mitochondria (Lam et al. 2005). Consistent with this, the protein was later shown to catalyze the transport of thiamine pyrophosphate (Lindhurst et al. 2006). More likely candidates are two mammalian orthologs of RIM2 that in yeast codes for a carrier for pyrimidine nucleotides. One of the two orthologs was recently reported to be a pyrimidine nucleotide carrier and named PNC-1 (Floyd et al. 2007).

1.3 The pyrimidine deoxynucleotide carrier (RIM2)

Deoxynucleotides are transported across the inner mt membrane and influx of cytosolic precursors is the main source of dNTPs for mtDNA replication in cycling human cells. Thus, carriers in the mt inner membrane catalyze the exchange of deoxynucleotides between the two compartments. To this day, and despite their importance, no mammalian carriers for deoxynucleotides have been unequivocally identified and characterized at the molecular and functional level. On the basis of homology with the *Rim2* gene (Marrobbio et al. 2006) encoding for a pyrimidine deoxynucleotide carrier in *Saccharomyces cerevisiae,* two genes in humans (Floyd et al. 2004) and one in *Drosophila melanogaster* may code for deoxynucleotide carriers. One of the two human orthologs was recently reported to be a pyrimidine nucleotide carrier and named PNC-1 (Floyd et al. 2007). However Thus, to this day no mammalian carrier for deoxynucleotides has been unambiguously identified at the molecular level.

1.3.1 The mitochondrial transporter for pyrimidine nucleotides in *Saccharomyces cerevisiae*

Pyrimidine (deoxy)nucleoside triphosphates are required in mitochondria for the synthesis of DNA and the various types of RNA present in these organelles. In *Saccharomyces cerevisiae,* these nucleotides are synthesized outside the mitochondrial matrix and must therefore be transported across the permeability barrier of the mitochondrial inner membrane. A RIM2 protein has been identified as a yeast mitochondrial pyrimidine nucleotide transporter (Marobbio et al. 2006). RIM2 (Replication In Mitochondria 2) is a member of the mitochondrial carrier protein family having some special features. It transports the pyrimidine (deoxy)nucleoside tri- and di-phosphates and, to a lesser extent, pyrimidine (deoxy)nucleoside monophosphates, by a counter-exchange mechanism.

The main physiological role of RIM2 is proposed to be to transport (deoxy)pyrimidine nucleoside triphosphates into mitochondria in exchange for intramitochondrially generated (deoxy)pyrimidine nucleoside monophosphates (Marobbio et al. 2006).

The protein encoded by *Rim2* belongs to the mitochondrial carrier family. In fact, the RIM2 amino acid sequence displays three repeats, each containing two putative Trans Membrane Sequences (TMSs) and the signature sequence motif PXD/EXXR/K. However, RIM2, consisting of 377 residues, is longer than the great majority of mitochondrial carriers (molecular mass 30–34 kDa) and shorter than the Ca^{2+}-activated mitochondrial carriers (molecular mass 50–60 kDa) (Palmieri 2004, Fiermonte et al. 2004). A major difference between RIM2 and most members of the mitochondrial carrier family is that the N-terminal extension, the matrix loop between TMS I and II and the cytosolic loop between TMS IV and V of RIM2 are longer than usual. Another typical feature of RIM2 is the presence of a tryptophan residue (PIWLIK) instead of the acidic residue in the signature motif of the second repeat.

1.3.2The human mitochondrial pyrimidine nucleotide carriers

The two putative nucleotide transporters of the inner mt membrane, SLC25A33 and SLC25A36 are encoded by genes orthologous to the *Rim2* gene, that in budding yeast has been shown to be essential for the maintenance of mtDNA and involved in the exchange of pyrimidine nucleotides between mitochondria and cytosol. One of the two human orthologs of yeast *Rim2* gene, named PNC-1, was recently characterized (Floyd et al. 2007). Like yeast RIM2 (Marobbio et al. 2006), the carrier transports pyrimidine nucleotides and was designated PNC-1 (Pyrimidine Nucleotide Carrier-1). PNC-1 is a mitochondrial pyrimidine nucleotide carrier, which shares significant identity with the essential yeast mitochondrial carrier RIM2.

PNC-1 was described to be a UTP carrier, in fact when the carrier was downregulated in whole cells only mt UTP was found reduced. So it is likely that reduced availability of UTP in PNC1-deficient cells could impair mtDNA transcription (Floyd et al. 2007).

A comparison of both the human and mouse sequences with those in the EMBL nucleotide sequence database showed that PNC1 cDNA encoded a member of the mitochondrial carrier family (Palmieri et al. 1994, Kunji 2004). These carriers have three homologous repeats, each containing a signature motif, typically P-X-[DE]-X-X-[KR] (Figure 1.1).

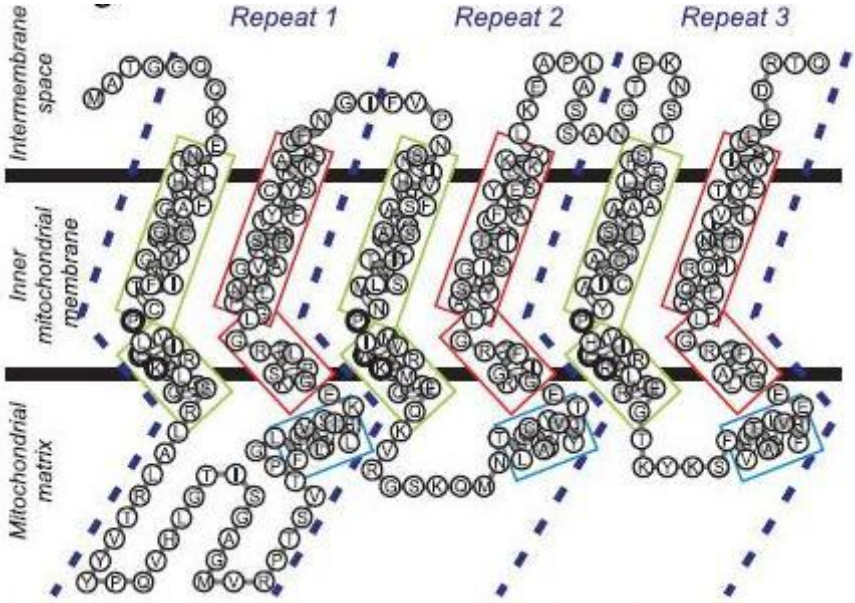

Figure1.1. The predicted protein topology of the mitochondrial pyrimidine transporter PNC-1. The prediction is based on the homology to the bovine ADP/ATP carrier (Pebay-Peyroula et al. 2003) showing the six transmembrane helices, the three fold sequence repeats, the conserved signature motifs, the positions of the α-helices and the signature motifs (box) (Floyd et al. 2007).

The main structural fold is a six α-helical bundle with pseudothreefold symmetry as exemplified by the structure of the bovine ADP/ATP carrier (Pebay-Peyroula et al. 2003). This gene is located on human chromosome 1 (1p36.22), and its product (Q9BSK2) has another isoform (Q96CQ1) with 60% identity that is located on chromosome 3. It is also identical in sequence to a previously reported human carrier of unknown function huBMSC-MCP that was assigned to chromosome 11 (Wang et al. 2004). Both isoforms have homologues in mice, Q921P8 and Q922G0 with 91 and 61% shared identity with PNC-1, respectively. These carriers contain a variation in the signature motif of the second repeat, where the negatively charged amino acid has been replaced by a tryptophan (P-I-W-M-V-K), but the basic residue of the interacting salt bridge is retained. The electrons of the aromatic residues form a negatively charged face, which can interact electrostatically with positively charged residues (Dougherty, 1996) The human mitochondrial carrier is also closely related to three carriers from yeast—RIM2 or Pyt1p (Marobbio et al. 2006), Ndt1p, and Ndt2p (Todisco et al. 2006)—that share an identity of 29.5, 23.4, and 24.0%, respectively.

1.3.3 *Drosophila* gene homolog of yeast *Rim2*

Drosophila represents an ideal system to study the physiological function of mt dNTP carriers. In *Drosophila* only one gene shows significant similarity to *Rim2*, suggesting that in this species all dNTPs share the same mt transporter. Thus,

Drosophila would represent an ideal model system to study the physiological function of mt deoxynucleotide carriers because it would not pose problems of functional redundancy among different gene products.

The *Drosophila melanogaster CG183173* gene (Figure 1.2) is the fly orthologue of the yeast *Rim2* gene (Marobbio et al. 2006) and of the two human PNC-1 genes (Floyd et al. 2004), AAL13964.

The *Drosophila* gene maps on chromosome 2 (position 22B1) and its gene sequence location is 2L:1716888..1724391. The *CG18317* gene spans 7503 bp, and the 1776 bp coding sequence consists of 6 exons, the related polypeptide consisted on 365 aa (40.5 kDa).

Figure 1.2. Drosophila *Rim2* gene. This gene is referred to in FlyBase by the symbol Dmel\CG18317 (FBgn0031359). It is a protein coding gene from *Drosophila melanogaster*. Based on sequence similarity, it is predicted to have molecular function: transmembrane transporter activity. An electronic pipeline based on InterPro domains suggests that it is involved in the biological process: transmembrane transport; mitochondrial transport. 10 alleles are reported. No phenotypic data is available. It has one annotated transcript and one annotated polypeptide. Protein features are: Mitochondrial brown fat uncoupling protein; Mitochondrial substrate carrier; Mitochondrial substrate/solute carrier. Gene sequence location is 2L:1716888..1724391. (Figure modified by http://flybase.org/).

There is currently no information available concerning the function of the probable *Drosophila* homolog of RIM2, although the putative protein shows domains which are typical of mitochondrial transporter proteins. One objective is to test experimentally if the single *Drosophila* gene homologue of the budding yeast RIM2 gene is involved in the exchange of deoxynucleotides between mitochondria and cytoplasm, and to study the effect of its inactivation on the stability of the mt genome.

1.4 Purine nucleoside phosphorylase deficiency

Genetic deficiency of purine nucleoside phosphorylase (PNP) results in severe immunodeficiency in man (Cohen et al. 1978). A PNP knock-out mouse shows similar symptoms (Arpaia et al. 2000). In both cases T lymphocytes are more severely affected than B lymphocytes due to a preferential accumulation of dGTP. *In vitro* the T-lymphocytes showed increased apoptosis and higher sensitivity to γ-irradiation. It was proposed that dGTP accumulates in mitochondria causing impairment of DNA synthesis and repair and serving as a signal for apoptosis (Arpaia et al. 2000). It is, however, not clear why the accumulation should preferentially occur in mitochondria and the published data on this point are not very convincing.

1.4.1 A *Drosophila* model of PNP deficiency

The possibility of obtaining a new animal model of PNP deficiency is clearly of great interest and it was very interesting to produce such a model in *Drosophila*. On the basis of the presence of a nucleoside-phosphorylase-family-2 signature domain, we have so far identified two potential *Drosophila* homologs of human PNP: CG16758 and CG18128. The former shows a 51% identity, while the latter shows a 37% identity to human PNP. There is no information available concerning the function of either gene in *Drosophila*. We characterized dsRNA bearing strains available from the VDRC (Vienna *Drosophila* RNAi Center) (Tanaka et al. 2000), which allow the temporally and/or spatially targeted silencing of each of the *Drosophila* homologs of PNP.

Figure 1.3. Drosophila *PNP* gene. This gene is referred to in FlyBase by the symbol Dmel\CG16758 (FBgn0035348). It is a protein coding gene from *Drosophila melanogaster*. Based on sequence similarity, it is predicted to have molecular function: purine-nucleoside phosphorylase activity. An electronic pipeline based on InterPro domains suggests that it is involved in the biological process: nucleoside metabolic process. One allele is reported. No phenotypic data is available. It has 4

annotated transcripts and 4 annotated polypeptides. Protein features are: Inosine guanosine/xanthosine phosphorylase; Nucleoside phosphorylase domain; Purine nucleoside phosphorylase I, inosine/guanosine-specific; Purine phosphorylase, family 2. Gene sequence location is 3L:2498704..2503584. (Figure modified by http://flybase.org/).

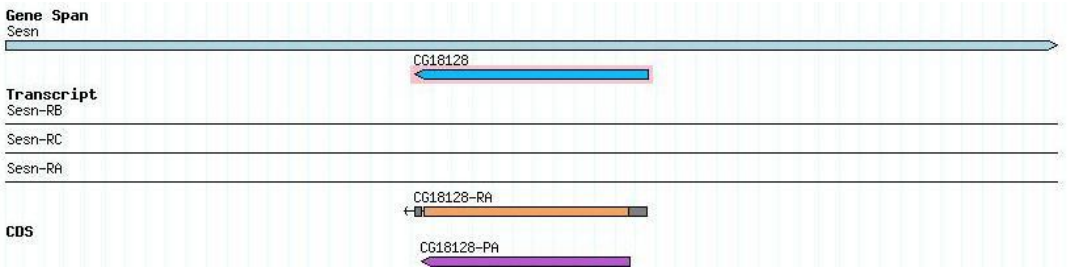

Figure 1.4. Drosophila *PNP* gene. This gene is referred to in FlyBase by the symbol Dmel\CG18128 (FBgn0034898). It is a protein coding gene from *Drosophila melanogaster*. Based on sequence similarity, it is predicted to have molecular function: purine-nucleoside phosphorylase activity. An electronic pipeline based on InterPro domains suggests that it is involved in the biological process: nucleoside metabolic process. 2 alleles are reported. No phenotypic data is available. It has one annotated transcript and one annotated polypeptide. Protein features are: Inosine guanosine/xanthosine phosphorylase; Nucleoside phosphorylase domain; Purine phosphorylase, family 2. Gene sequence location is 2R:19606320..19607459. (Figure modified by http://flybase.org/).

RESULTS AND DISCUSSION

3.1 d*Rim2* post transcriptional silencing

We started with characterization of the *CG18317* drosophila gene, homolog of the yeast *RIM2* gene, by post transcriptional silencing. We obtained from the Vienna Drosophila RNAi Center (VDRC) transgenic lines, harboring a construct encoding for a CG18317/RIM2-specific dsRNA, which allows the targeted silencing of d*Rim2* (Trasformant ID #44203 and #44202).

The ubiquitous activation of dsRNAi with these lines produced no alterations in fertility or viability. Furthermore, ubiquitous dsRNA knock down of d*Rim2* with a third transgenic line, which was later made available by the VDRC collection (line 100807), produced the same results in terms of adult viability, although, differently from the other dsRNAi lines characterized, in this case a significant decrease of d*Rim2* transcripts was shown by RT-PCR. In particular, three independent real time experiments, confirmed an interference of the d*Rim2* gene of approximately 70%. These data suggests that 30% of gene activity is sufficient to allow the development of mutant flies to adulthood.

In addition real time experiments evidenced an over-expression of *CG18317* gene in mutant line e01575 (for a description of this mutant, see following paragraph) (Figure 3.1).

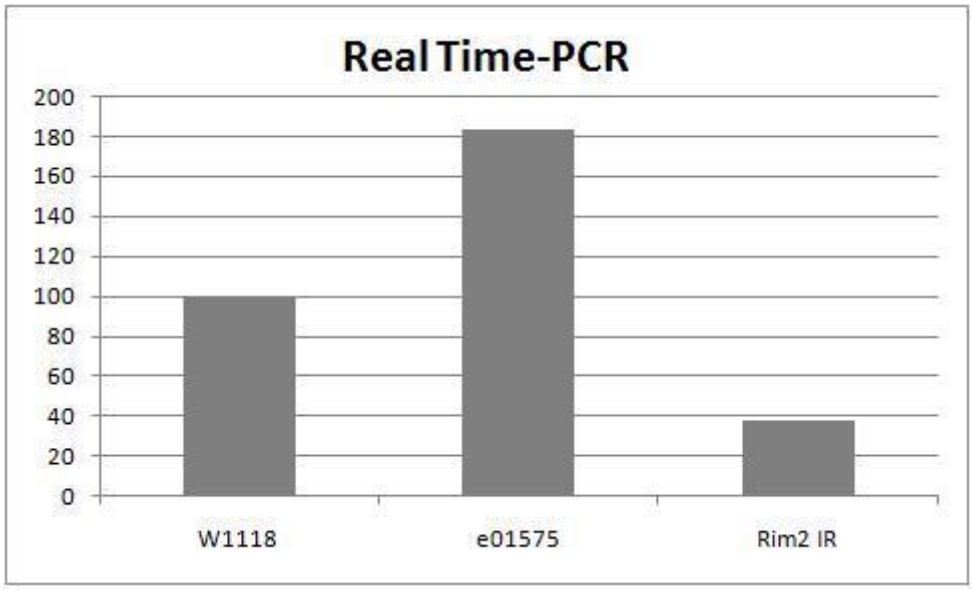

Figure 3.1. Real-time PCR-based quantitative analysis. RT-PCR estimate of the relative percentage of *CG18317* mRNA in KD individuals from line 100807 compared to those of w^{1118} controls and mutant line e01575. In each case controls are assigned an arbitrary value of 100%. Histograms represent the mean of three independent experiments (SD??). Real-time PCR-based quantitative analysis confirmed a reduction *CG18317* mRNA in KD line 100807 and an over-expression of CG18317 gene in mutant line e01575.

3.2 Generation of *Drosophila Rim2Δ* strain, lacking the putative deoxynucleotide transporter RIM2

Using the same technique previously described for *Ethe1*, based on targeted deletion of the region spanning d*Rim2* (see material and methods) (Parks et al. 2004), we isolated a knock out (KO) line for d*Rim2*.

We obtained from the Bloomington Drosophila stock center, transgenic lines bearing insertional elements localized at the boundaries of the CG18317/RIM2 gene. In particular, line PBac[RB] CG18317^{e01575} (FBti0047179) harbors a piggyBac element at the 5' level of the gene, in position. The other insertional line PBac[RB] CG18317^{e00041} harbors a piggyBac element at the 3' portion of the gene (Figure 3.2).

We obtained a whole gene deletion of through the combination of the FRT bearing lines (e01575, e00041) in presence of FLP recombinase, which should produce a genomic deletion with a single residual element tagging the deletion site.

Additionally, we also characterized pBac insertional line e01575 (used for the deletion generation) which proved to be homozygous lethal. The insertion of the pBac element in the 5' region of the d*Rim2* gene appears to de-regulate gene expression, mimicking a KO condition.

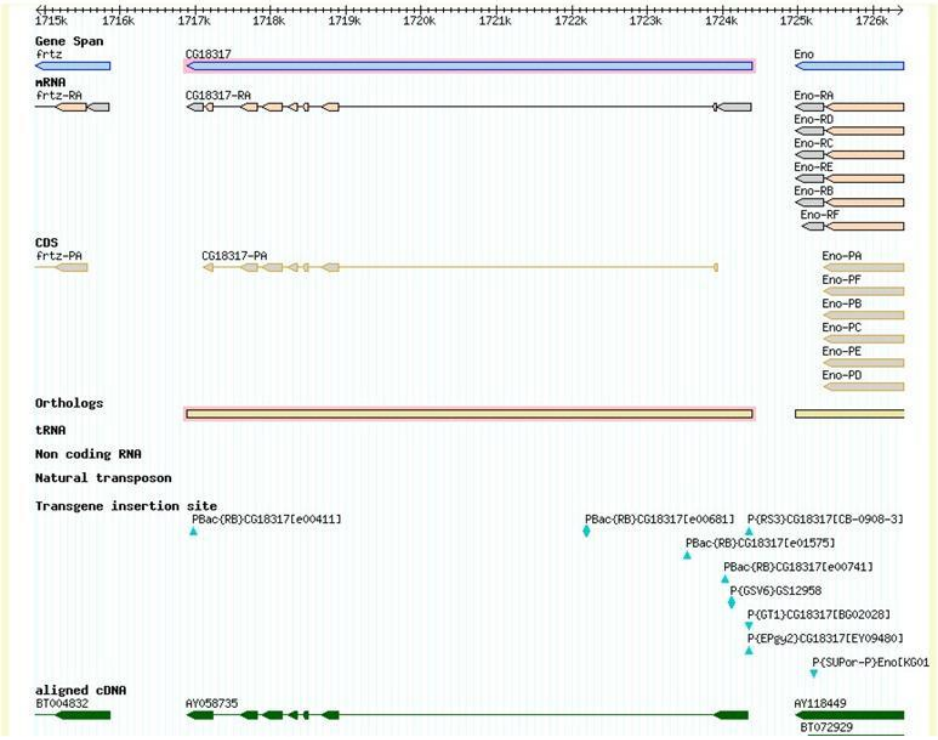

Figure 3.2. Localization of the piggy-Bac elements in the Drosophila *CG181317 locus*. The transgene insertional PBac[WH] CG18317 ^{e00041} is localized in the 3' region of the gene, in position 2L:1716977, the other line PBac[RB] CG18317^{e01575} harbors a piggyBac element in the 5' region of the gene, in position 2L:17253536.

3.2.1 PCR confirmation of FLP-FRT–based deletions

We carried out all PCR reactions using purified genomic DNA from 50 homogenized flies obtained from each isolate line. In general, it was necessary to test 50 flies for each *w+* deletion. The PCR confirmation strategy used for initial detection of the deletion was carried out with the use of specific primer designed inside the P–Bac elements. The primer sequences use for the PCR screen are shown in Table xx (material and methods).

3.3 Characterization of the knock out line

3.3.1 Survival of d*Rim2* KO flies

Characterization of the knock out line shows that, although KO individuals survive through the larval stages of development, 100% of homozygous d*Rim2* deletion-bearing larvae die at the pupal stage. Moreover, the KO larvae are smaller compared to both *dRim2* deletion heterozygotes and wild type larvae (Canton S strain).
The heterozygous KO line obtained was balanced with *CyO*-GFP so that it allowed us to discriminate between homozygous (non GFP-fluorescent) and heterozygous (GFP-fluorescent) larvae (Figure 3.3).

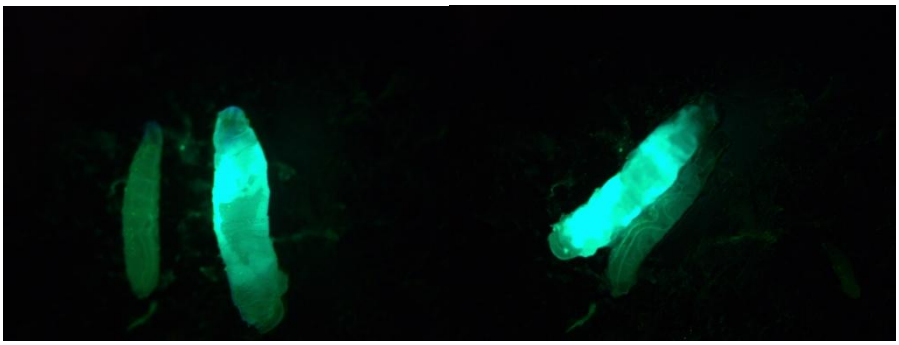

Figure 3.3. d*Rim2* KO larvae. Heterozygous knock out larvae d*Rim2*/CyO-GFP were easily recognisable because they expressed GFP, whilst homozygous knock out larvae d*Rim2* are the smaller ones which are not fluorescence.

3.3.2 Biochemical profile of d*Rim2* KO flies

Based on the expectation that d*Rim2* might be specifically involved in the exchange of deoxynucleotides between the mitochondria and the cytoplasm, we reasoned that defects in d*Rim2* function might result in damage to mitochondrial genome integrity, which would then lead to pupal death in the KO individuals. In order to establish

whether this might be the case, we first of all determined whether the activities of each of the mitochondrial respiratory chain complexes (MRCC) were in any way affected.

Biochemical assays were performed to check the state of the mitochondrial respiratory chain in control larvae, in heterozygous and homozygous individuals (distinguishable by their green fluorescence as shown in Figure 3.3).

The results show that there were no significant variations in the activity of any of the MRCC (I, II, III, IV, V) in the KO larvae with respect to controls (Figure3.4).

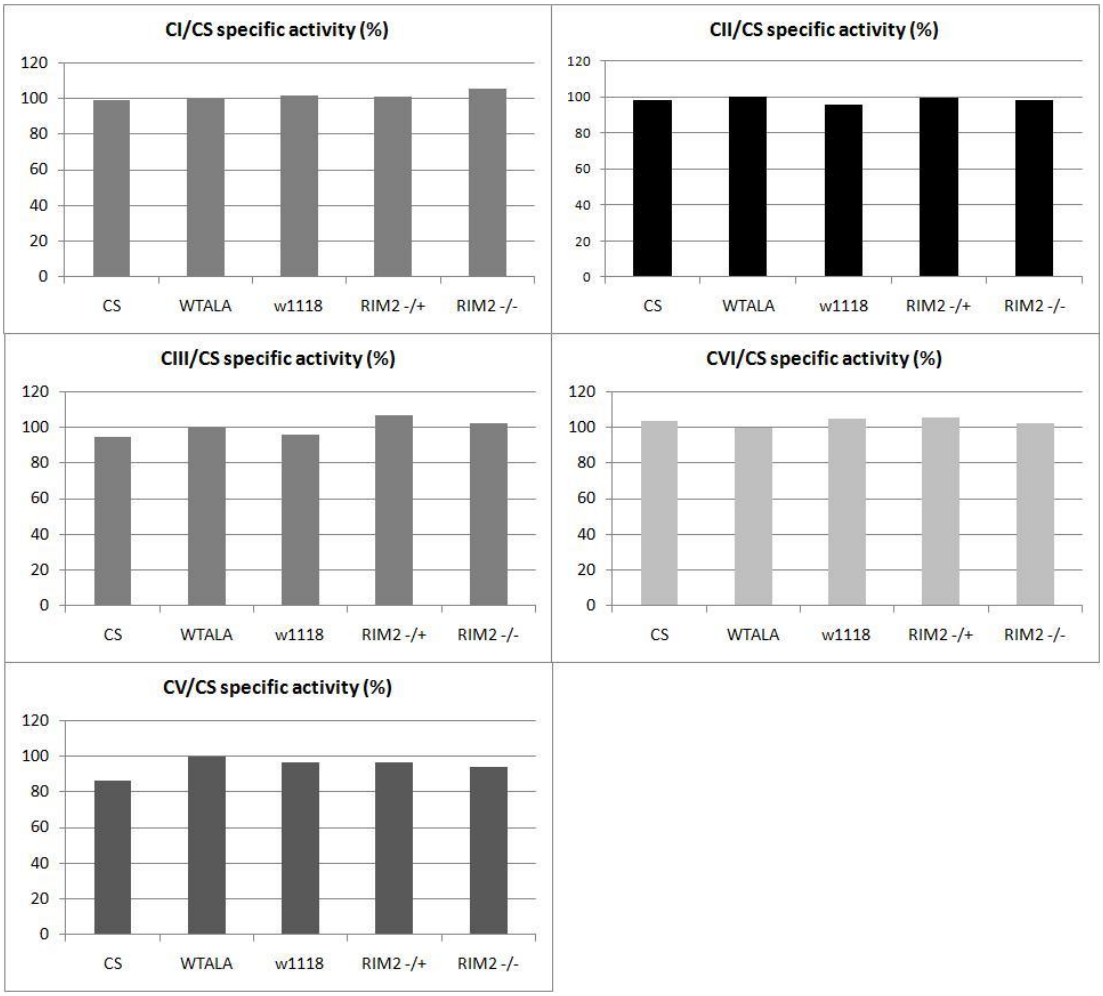

Figure 3.4. Mitochondrial respiratory chain enzymatic activities of control and *RIM2 -/+*, *RIM2 -/-* larvae. Complexes I–V activities (all expressed as nmol min^{-1} mg^{-1}) normalized to the activity of Citrate Synthase (CS), are all expressed as percentage of enzymatic activity where WTALA strain's activity is considered as 100%. We measured enzymatic activity in three different wild type lines: Canton S, WT ALA, w^{1118} in the two KO lines: RIM2 homozygous and heterozygous larvae. The graphs clearly show that the enzymatic activites in the KO individuals are in all cases comparable to that of controls.

Moreover we tested the mitochondrial respiratory chain's functionality in adult mutants. We performed biochemical assays in adult heterozygous KO flies (d*Rim2*/CyO) and in the heterozygous adult flies belonging to the insertional mutant line e01575. In both mutant strains analyzed, the activities of respiratory chain complexes (CI, CII; CIII; CIV; CV) compared with controls, were not affected in any case.

3.4 Rescue of the KO phenotype

In order to further validate the KO model we tried to rescue the phenotype observed in knock out individuals. We rescued the pupal lethality through the expression of an exogenous copy of d*Rim2*, a pUAST-d*Rim2*-FLAG construct.
In parallel we also produced constructs bearing the human isoforms of *Rim2*, (SLC25A33 and SLC25A36) in pUAST vectors, in order to produce transgenic lines which, following appropriate genetic crosses, were used to evaluate the capacity of the human *Rim2* isoforms to rescue the Drosophila KO. These constructs were microinjected and the progeny of the injected individuals were screened for the presence of transgenic flies.
Constructs carrying the human isoforms of *Rim2* were a gift from Professor Bianchi's lab in Padova, which collaborates with our group in the characterization of RIM2 function.

3.4.1 Rescue with the d*Rim2* expressing construct

First of all, we microinjected the w^{1118} drosophila line with a pUAST construct bearing the wild type sequence of d*Rim2* under the control of a UAS promoter, which allows the expression of the cDNA after activation by a GAL4 protein.
We then rescued the knock out phenotype by crossing the fly line expressing the pUAST-d*Rim2* construct with flies from the d*Rim2* knock out strain. In this way we produced progeny bearing both the *Rim2* deletion and the pUAST-d*Rim2* construct. Both constructs were activated by the use of an *Actin5C-GAL4* driver present in the final progeny background.
Out of three lines bearing the rescue construct, only one was able to rescue the phenotype of the *dRim2* KO. As expected, "rescued" individuals developed to adults and they did not show defects in fertility or viability.

3.4.2 Rescue with the human *Rim2* constructs

In addition, we also wished to explore the ability of human *Rim2* isoforms to rescue the Drosophila KO by expressing the human *Rim2* gene in the described Drosophila KO background. In particular, we performed the rescue of d*Rim2* KO by expressing

constructs bearing each one of the two human isoforms of *Rim2* cloned into pUAST vectors.

We designed two different constructs each carrying one of the two human *Rim2* isoforms (SLC25A33 and SLC25A36).

After appropriate crossing, as described above, we obtained four fly lines resulting from the expression of four different insertions of the SLC25A33 cDNA_bearing transgenes, in a *Rim2* KO background and seven lines resulting from the expression of seven different insertions of the SLC25A36 cDNA-bearing transgenes in a *Rim2* KO background.

Through analysis of the lines expressing the human isoform (SLC25A33) of *Rim2* we did not observed any rescue of pupal lethality which characterized the KO individuals. Since, the function of human SLC25A33 has not been described in literature we cannot further speculate about the meaning of this result, although we can only suppose that, since there are two *Rim2* isoforms in humans, they may have developed non overlapping functions. Thus it may be that, SLC25A33 is not involved in the transport of pyrimidine nucleotides, and as such cannot complement the lack of dRim2 function.

On the other hand, the line expressing the human SLC25A36 isoform was able to revert the KO phenotype. From the literature, SLC25A36 is the human *Rim2* isoform described in (Floyd et al. 2007) and named PNC-1 and it was recently characterized as a mitochondrial pyrimidine nucleotide carrier. In particular PNC-1 was described to be a UTP carrier (see introduction chapter 1.3.2).

There are evidences in literature (Floyd et al.2007) that the human mitochondrial pyrimidine nucleotide carrier (PNC-1) is linked with the mTOR pathway , essential for the survival and growth of normal cells. This pathway together with insulin/insulin-like growth signaling seems to be linked with regulation of mitochondrial function, but how this occurs, is incompletely understood. It has been demonstrated that IGF-I and insulin induce rapid transcription of the mitochondrial pyrimidine nucleotide carrier PNC-1. PNC1 expression is dependent on PI-3 kinase and mTOR activity and is higher in transformed fibroblasts, cancer cell lines, and primary prostate cancers than in normal tissues. Overexpression of PNC-1 enhances cell size, whereas suppression of PNC-1 expression causes reduced cell size and retarded cell cycle progression and proliferation. Cells with reduced PNC-1 expression have reduced mitochondrial UTP levels, but while mitochondrial membrane potential and cellular ATP are not altered, cellular ROS levels are increased. Overall the data indicate that PNC-1 is a target of the IGF-I/mTOR pathway that is essential for mitochondrial activity in regulating cell growth and proliferation. (Floyd et al.2007).

Insulin and insulin-like growth factor-I (IGF-I) regulate metabolism and cell survival, growth, and proliferation through the insulin or IGF-I receptors (IR or IGF-IR) and their downstream signaling pathways.

A direct role for mTOR signaling in enhancing mitochondrial oxidative phosphorylation has also recently been described (Schieke et al. 2006) as well as a role for mTOR in regulating the production of mitochondrial-derived reactive oxygen species (ROS) that are thought to be causative in ageing (Schieke and Finkel, 2006). Although much evidence points to altered mitochondrial physiology in cancer cells, the interactions between growth factor signaling and mitochondrial function in regulating cell survival and proliferation remain to be fully elucidated.

In our particular case, many question still remain open, for istance (i) is *Drosophila Rim2* responsible for mitochondrial deoxynucleotide transport, (ii) does the depletion of *Rim2 in vivo* affect the integrity of the mitochondrial (mt) genome.

To answer these questions we need to implement approaches aimed at determining the integrity of the mitochondrial DNA (mtDNA) in these animals. Thus we are setting up different techniques which entail the determination of: (a) mtDNA copy number depletion; (b) mtDNA macroscopic deletions; (c) mtDNA point mutations.

In order to check for mtDNA copy number depletion we designed primers to amplify the mitochondrial encoded cytochrome c oxidase (MRRC IV) *CoxII* subunit gene, and by using a QRT-PCR approach, we quantified the amount of *CoxII* present in the KO larvae with respect to controls. Pilot experiments carried out in KO individuals showed a 15% reduction in the number of copies of *CoxII*, which is probably too small a reduction to justify the lethal effects observed in our *dRim2* KO model.

In order to check for the presence of macroscopic deletions in the mtDNA of the KO larvae we designed primers suitable to allow the amplification of most of the mtDNA (i.e. a 10 Kb fragment, corresponding to approximately 52% of the total mt genome) from single individuals through the use of a Long-PCR (Reynier et al. 1995) protocol. Application of this protocol, led to the amplification of a single product of the expected size in both controls and KO larvae, suggesting the integrity of the corresponding mtDNA.

To establish whether lack of dRIM2 function might result in an increase in the point mutation rate in the mtDNA of the KO individuals we set up an approach based on the amplification of 1 Kb sequence of mtDNA from single individuals. The amplified products were then cloned and sequenced. We have so far sequenced 10 fragments from 5 controls (2 cloned fragments from each individual) and 9 fragments from 3 d*Rim2* KO larvae (3 cloned fragments from each individual). The comparison of the sequences obtained so far has not evidenced any differences.

In addition, by using a FLAG tagged wild type *dRim2* cDNA-bearing construct we intend to perform protein complex immunoprecipitation followed by Maldi-Tof-Tof mass spectrometry (facility currently available at the Venetian Institute of Molecular Medicine) in order to attempt to identify interacting partners of d*Rim2*.

MATERIALS AND METHODS

2.1 Fly Stocks and Maintenance

Flies were raised on a standard yeast–glucose–agar medium (Roberts and Standen 1998) and were maintained at 18° C, 70% relative humidity, on a 12h light: 12h dark cycle.

2.2 Functional characterization of d*Surf1* gene post-transcriptional silencing

2.2.1 Fly strains

The w^{1118} strain was microinjected with the transformation plasmid. The dominantly-marked, multiply-inverted balancer chromosomes w; CyO/Sco; MKRS/TM6B stock was used for determining the chromosomal locations of the transgenes and for subsequent manipulations of the transgenic lines. Previously work done in our laboratory generated three independent Drosophila transgenic lines, 23.4, 79.10, and 79.1. For each line obtained, the insert map position is given in parentheses: 23.4 (2R, 54BC), 79.1 (3R, 88D) and 79.10 (2R, 50C). Each line carried a single UAS–*Surf1* inverted repeat (IR) autosomal insertion, which allowed the post-transcriptional gene silencing of *Surf1* via dsRNA interference (dsRNAi), following activation by GAL4 (Zordan et al. 2006).
The following GAL4 lines, obtained from Bloomington Stock Center were used to drive the expression of the UAS–*Surf1*–IR construct:

- ***elav C155 GAL4*** [genotype: P{GawB}elav^{C155} GAL4] expressed in all tissues of the embryonic nervous system beginning at stage 12. elav–GAL4 driver is used to drive the post transcriptional silencing of d*Surf1* pan neuronally, (Bloomington number B.N. 458);

- **w;; *how^{24B} GAL4*** [genotype: w^{*}; P{GawB}how^{24B} GAL4] in embryonic mesoderm, (B.N. 1767);

- ***Switch–Actin5C–GAL4* /TM6B, Tb** [genotype: P{hsFLP}22, y^{1} w^{*}; P{UAS-GFP.S65T}T2; P{Act5C(–FRT)GAL4.Switch.PR}3/TM6B, Tb^{1}]. Expresses a progesterone–inducible GAL4 in all cells, **(**B.N. 9431);

- **y, w;; *Act5C–GAL4*/CyO** [genotype: y^{1} w^{*}; P{Act5C–GAL4}25FO1/CyO, y^{+}]. Ubiquitous expression of GAL4, (B.N. 4414);

- **y, w;; *Act5C–GAL4*/TM6B, Tb** [genotype: y^1 w^*; P{Act5C–GAL4} 17bFO1/TM6B, Tb^1]. Ubiquitous expression of GAL4, (B.N. 3954);

- ***Hsp70 GAL4*** [genotype: w^1; sna^{Sco}/CyO, P{GAL4–Hsp70.PB}TR1, P{UAS–GFP.Y}TR1]. Heat shock inducible GAL4, (B.N. 5702);

- ***GMR-GAL4*** [genotype: y^1 w^{1118}; P{GAL4–ninaE.GMR}12; P{UAS–InR.A1325D}3]. glass enhancer driving GAL4 in the eye disc, provides strong expression in all cells behind the morphogenetic furrow. (B.N. 8440);

2.2.2 Production and microinjection of the p[UAST] d*Surf1*-s construct

d*Surf1*–s was designed so that its nucleotide sequence was sufficiently different from the native sequence as to allow it to escape native–d*Surf1*–targeted PTS. This was accomplished by substituting each codon triplet in the native d*Surf1* sequence with a synonymous triplet. Nucleotide substitutions were chosen so as to maximize differences between d*Surf1* and d*Surf1*–s, while respecting codon bias and avoiding the introduction of new splicing sites. On the whole, the d*Surf1*–s nucleotide sequence presents 29.1% differences with respect to d*Surf1*. In addition d*Surf1*–s was also engineered so as to encode an HA tag at the C–terminus. Furthermore, particular attention was dedicated to maintaining a GC content of approximately 60% in the third position of codons in agreement with (Shields et al. 1988) who report that, in *Drosophila melanogaster*, the most frequently employed codons are characterized by G or C nucleotides in third position. The d*Surf1*–s construct, synthesized by Genscript Corporation, was subcloned into a PUC57 pUAST microinjection vector. Confirmation of the insertion of the synthetic gene into the pUAST vector was obtained by restriction fragment analysis. After *Eco*RI and *Xho*I digestion, a 980 pb fragment was obtained which corresponds to the expected size of the d*Surf1*–s gene. Further confirmation regarding the
nature of the fragments was obtained by direct sequencing. pUAST d*Surf1*–s was injected into w^{1118} embryos as described in (Piccin et al. 2001). Embryos which survived microinjection were numbered progressively and crossed with w^{1118} individuals. For each insertion event a single transgenic line was founded. Four transgenic lines were thus obtained: Syn1, Syn2, Syn3, Syn4. Following crosses with balancers, each line was characterized by insertion of pUAST d*Surf1*–s into the following chromosomes: line Syn4 chromosome 3; lines Syn1, Syn2 and Syn3 chromosome 2. From each of the balanced lines, stable homozygous lines were obtained.

2.2.3 Double homozygotes for both the KD and the rescue construct

In order to evaluate whether d*Surf1*–s was able to revert the knockdown phenotype produced by d*Surf1*–IR, it was necessary to obtain transgenic lines bearing both pUAST d*Surf1*–s, and pUAST d*Surf1*–IR. Such lines were obtained after appropriate crosses starting from the following lines: lines Syn1,Syn2 and Syn3: bearing pUAST d*Surf1*–s. line IR: bearing pUAST d*Surf1*–IR, on the III chromosome (3R, 88D) (Zordan et al. 2006). In the double homozygote lines thus obtained, the expression of both constructs can be induced using the UAS–GAL4 binary system.

2.2.4 Western blots

Assays were conducted essentially as described in (Zordan et al. 2006). Briefly: Following extraction of mitochondria, the mitochondrial suspension was sonicated and subjected to 3 freeze/thawing cycles in liquid nitrogen; a protease inhibitor cocktail and detergents were added and the solution was left on ice to allow membrane solubilization. Equal amounts of total proteins (60 mg) for each sample were resolved on a 12% SDS–polyacrylamide gel. Following separation and Western blotting onto nitro-cellulose membrane, the membrane was blocked and incubated with the primary followed by secondary antibodies. Positive immunoreactivity was visualized using a chemiluminescent system.

2.2.5 Adult viability following d*Surf1* knock down during adulthood

The following crosses were performed to determine adult survival, following RU–486-*Act5C–GAL4*–d*Surf1* knock down during the adult stages of development: (i) Controls = UAS GFP / UAS GFP X *Switch–Actin5C–GAL4* /TM6B, Tb; from which the resulting progeny of interest was *Switch-Actin5C–GAL4* /UAS GFP (ii) KD indivuals = UAS GFP, IR/ UAS GFP, IR X *Switch–Actin5C–GAL4* /TM6B, Tb; from which the resulting progeny of interest was *Switch–Actin5C–GAL4* /TM6B, Tb /UAS GFP, IR Crosses were raised at 20°C on standard sucrose medium. Freshly eclosed flies, both controls (Switch-*Actin5C–GAL4* / UAS GFP) and (*Switch–Actin5C–GAL4* /TM6B, Tb / UAS GFP, 79.1 *Surf*) were transferred from RU–486-free food to the food containing RU–486 and kept at a temperature of 20°C, to this end, a 10 mM stock solution of RU–486 (mifepristone; Sigma) in ethanol 80% was added during the preparation of fly medium to a final concentration of 15 µg/ml. A total number of 150 *Switch–Actin5C–GAL4* /TM6B, Tb /UAS GFP, IR flies and the same number of control flies were starved and then placed, in groups of 10 into RU–486–positive food.

2.3 Analysis of d*Ethe1* gene

2.3.1 Fly stocks

Previous work done in our laboratory led to the obtainment of fly lines carrying different mutations in the d*Ethe1* gene from the FlyTill project. In particular 7 mutations located in the coding sequence of the gene were obtained, each of which is correlated to a different mutagenic (sai cos'e' il significato di mutagenic??? E' lo stesso di mutageno.....quindi si tratta di mutant line , casomai.
Fly stocks obtained by tilling project are the following:
- TILLING line **2002** nucleotide substitution **C330A**, localization exon II, missense mutation, aminoacidic substitution L65M;

- TILLING line **2952** nucleotide substitution **C336A**, localization exon II, missense mutation, aminoacidic substitution D67N;

- TILLING line **6043** nucleotide substitution **A586T**, localization exon III, missense mutation, aminoacidic substitution T120S

- TILLING line **2788** nucleotide substitution **C697I**, localization exon III, missense mutation, aminoacidic substitution P157S;

- TILLING line **0493** nucleotide substitution **C991T**, localization exon IV, missense mutation, aminoacidic substitution P237S;

- TILLING line **3976** nucleotide substitution **G1075ATGCGTAGTATG**, localization exon IV, frameshift mutation, aminoacidic substitution D264MRSMHITICVFY;

- TILLING line **2700** nucleotide substitution **T1108TTATA**, localization exon IV, frameshift mutation, aminoacidic substitution K275FICLMARRPTVRSGCTI.

Moreover in the present work we implemented a protocol for the generation of a targeted deletion of the *Ethe1* gene, described in chapter 2.3.3. Fly strains necessary for the achievement of the knock out are: a line expressing the FLP recombinase transgene, two FRT-bearing P–element insertional lines and a balancer line (described in Parks et al. 2004).
In particular, Drosophila stocks used in the generation of deletion were the following:

- **d00031:** XP–element insertional fly line, chromosomal location is 2R (47F8), sequence location (2R:7,271,757..7,271,757);

- **d03609**: XP–element insertional fly line, chromosomal location is 2R (47F8), sequence location (2R:7,285,475..7,285,475);

- **Heat shock-flippase:** carrying an FLP recombinase transgene under the control of a heat shock promoter [genotype: pCaspeR–heat shock–flippase (hs–flippase), w^{1118}; II/ CyO];

- **balancer line:** *w;* CyO*/Sco;* MKRS/TM6B, Bloomington stock number 2475.

The P–element insertional lines as well the FLP recombinase transgene line were all from (Exelixis, Inc. 170 Harbor Way South San Francisco).

2.3.2 Targeting Induced Local Lesions IN Genomes

The approach that determines the function of genes first defined by DNA sequence analysis is referred to as reverse genetics.
Targeting Induced Local Lesions IN Genomes (TILLING) is a general reverse genetic technique that uses traditional chemical mutagenesis methods to create libraries of mutagenized individuals that are later subjected to high-throughput screens of pooled PCR products for the discovery of mutations in a target gene (Till et al. 2003). TILLING is reliable and widely applicable. TILLING is used to locate mutations, produced due to exposure to EMS, in specific regions of the gene that are of interest, resulting in the isolation of missense and nonsense mutant alleles of the targeted genes. TILLING technique produces an allelic series of mutations including hypomorphic alleles that are useful for genetic analysis. In this case the organism was *Drosophila melanogaster*.
In concordance with the TILLING technique it was decided to locate mutations in a specific region which comprises 1458 bp covering the whole extension of the d*Ethe1* gene. Following are reported the primer sequences used to screen the drosophila mutagenized library, searching any mutations in the interest region (2R:7,274,663...7,276,282).

d*Ethe1* TILLING Forward 5'-CGAGGCAAATAATTACAC-3'
d*Ethe1* TILLING Reverse 5'-GGTACTGGCAGTCTCCTG-3'

Library screening and identification of mutations in d*Ethe1* were carried out by the "Fly-TILL" service (http://tilling.fhcrc.org:9366), following the method described by (Till et al. 2003).
A number of fly lines carrying different mutations in the d*Ethe1* gene were obtained from the FlyTill project. In particular 21 mutations were obtained, each of which is corresponds to a different strain. In particular, we concentrated our attention on lines

carrying missense or frameshift mutations in the coding regions of d*Ethe1* gene. We selected seven lines with mutations located in exons, four of these (2770, 0242, 2952 and 0493) were proved to be homozygous lethal. Further investigations were conducted in these lines.
We initially concentrated our attention on a line harbouring a missense mutation (P157S) localised next to the active site of the putative dETHE1 protein, which may modify the catalytic activity. The adult flies we analyzed are hemizygous for the mutation because they carried the P157S mutation over a deletion which removes the whole of the *Ethe1* gene.

2.3.3 Generation of deletion: knock out of d*Ethe1*

2.3.3.1 Inverse PCR

Inverse PCR (IPCR), described by Ochman et al in 1988, is a method for the rapid in vitro amplification of DNA sequences that flank a region of known sequence. The method uses the polymerase chain reaction (PCR), but it has the primers oriented in the reverse direction of the usual orientation. The template for the reverse primers is a restriction fragment that has been ligated upon itself to form a circle. Inverse PCR has many applications in molecular genetics, for example, the amplification and identification of sequences flanking transposable elements.
Here we used the inverse PCR technique to ensure the position of P-element by recovering sequences flanking the XP elements. This protocol is an adaptation of "Inverse PCR and Cycle Sequencing Protocols" by E. Jay Rehm Berkeley Drosophila Genome Project.
The protocol starts with the digestion of genomic DNA with two different enzyme *Sau3A* I and *HinP1* I, done separately. *Sau3A* I digests are for 5' and 3' iPCR, whereas *HinP1* I digests are for 3' iPCR only **.**

Genomic DNA (~0.5 fly)	10.0 µl
10X buffer (NEB *Sau3A*I or NEB 2)	2.0 µl
10X BSA (*Sau3A*I only)	2.0 µl
*Sau3A*I or HinPI	4 units *Sau3A*I or 5 units *Hin*PI
ddH_2O	add to 20 µl total

Then the reaction mix is incubated at 37°C for 1 hour and successively at 65°C for 20 min. to heat inactivate. Consequently the ligation protocol per reaction is as follow:

Digested genomic DNA (~0.075 fly)	3.0 µl
NEB 10X T4 DNA Ligase Buffer (w/ 10mM ATP)	1.0 µl
ddH_2O	6.0 µl
NEB T4 DNA Ligase (200 Weiss units)	0.5 µl

If doing PCR immediately following ligation; it is necessary to incubate at room temperature for 30 min and aliquot for the first round of PCR.

First round iPCR: 20.0 µl reaction

Ligated genomic DNA (~0.035 fly)	5.0 µl
10X dNTP (2mM each)	2.0 µl
forward primer (10 µM)	0.4 µl
reverse primer (10 µM)	0.4 µl
10X PE AmpliTaq buffer w/ 15mM $MgCl_2$	2.0 µl
ddH_2O	9.9 µl
PE AmpliTaq (2 units)	0.3 µl

Do 1:10 dilution of first round PCR by adding 180 µl H_2O.

Second round iPCR: 20.0 µl reaction.

1:10 diluted first round DNA	5.0 µl
10X dNTP (2mM each)	2.0 µl
forward primer (10 µM)	0.4 µl
reverse primer (10 µM)	0.4 µl
10X PE AmpliTaq buffer w/ 15mM $MgCl_2$	2.0 µl
ddH_2O	9.9 µl
PE AmpliTaq (2 units)	0.3 µl

Primers for first and second round iPCR:

Primer Name	PCR Round	XP-element end	Primer Sequence 5' to 3'
51A	1st	5’ end	5'-AATGATTCGCAGTGGAAG GCT-3'
51B	1st	5’ end	5'-CACCCAAGGCTCTGC TCCCACAAT-3'
52A	2nd	5’ end	5'-TACCAGTGGGAGTAC ACAAAC-3'
52B	2nd	5’ end	5'-TTTACTCCA GTCACAGCTTTG-3'
31A	1st & 2nd	3’ end	5'-CGACACTCAGAATACTATTCC-3'
31B	1st & 2nd	3’ end	5'-AATTTGCGAGTACGCAAAGC-3'

Pre-Sequencing Preparation

Strong and unique bands as well as smears from the iPCRs can be directly sequenced without extensive purification. Prior to sequencing, we use the USB ExoSAP-IT kit to clean up an aliquot of the second round reactions. This kit uses Exonuclease I (degrades primers) and Shrimp Alkaline Phosphatase (degrades unincorporated nucleotides) to prepare the template for sequencing.
The protocol per reaction is as follows:

ExoSAP protocol

Make a master mix per reaction of:

Exonuclease I (10U/µl)	1 µl
Shrimp Alkaline Phosphatase (2U/µl)	1 µl
ddH_2O	3 µl

Remove 5 µl second round iPCR and add to 5 µl SAP mix (to make 10 µl total).
Run on "SAP" program on tetrad using heated lid.
SAP 1) 37°C 30min. 2) 85°C 15min. 3) 4°C hold

Sequencing Primers:

Primer Name	XP-element End	Sequence 5' to 3'
XP-5SEQ	5' end	5'-ACACAACCTTTCCTCTCAACAA-3'
XP-3SEQ	3'end	5'-TACTATTCCTTTCACTCGCACTTATTG-3'

2.3.3.2 Generation of the Df(47F8) deletion

After confirmation with iPCR of the correct position of the transposable elements we started the protocol for the generation of the targeted knock out.
In fruit fly research, up until now, chromosomal deletions were generated by irradiation or chemical mutagenesis. These methods are labor-intensive, generate random breakpoints and result in unwanted secondary mutations that can confound phenotypic analyses. Most of the existing deletions are large and have molecularly undefined endpoints. Furthermore, the existence of haplolethal or haplosterile loci

makes the recovery of deletions of certain regions exceedingly difficult by traditional methods, resulting in gaps in coverage. In this case we employed a method (Parks et al. 2004), that addresses these problems by providing for the systematic isolation of targeted deletions in the *D. melanogaster* genome.

The strategy used FLP recombinase and the large array of FRT-bearing insertions (described in Parks et al. 2004) to generate 519 isogenic deletions with molecularly defined endpoints. The Exelixis deletion collection provides 56% genome coverage so far. The methodology enables the generation of small custom deletions with predictable endpoints throughout the genome and should make their isolation a simple and routine task. As described by (Thibault et al.2004) Exelixis generated a large isogenic collection of *P* and *piggyBac* insertion lines containing FRT sites. In the presence of FLP recombinase, FRT-bearing transposon insertions can be used to efficiently isolate deletions with precisely defined endpoints. We used this method to generate a set of isogenic deletions as described below. The Exelixis deletion series is based on three of the four classes of transposon constructs described in Parks et al. , 2004). These transposon insertions contain FRT sites of 199 bp either 5′ (in XP and WH transposons) or 3′ (in *RB* transposons) of the *white+* transgene (*w+*; figure 2.1).

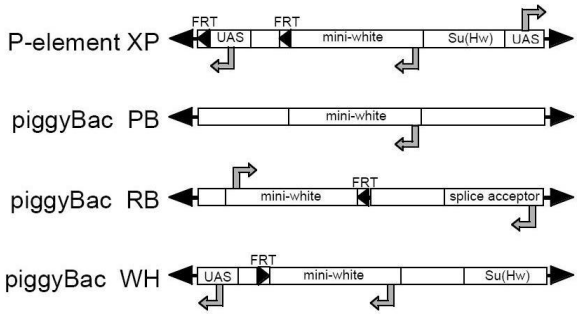

Figure 2.1. FRT-bearing transposons. Schematic of the three transposon types used in FLP-FRT–based deletions. FRT sites, UAS-containing sequences and the gene *white* are indicated. See Thibault et al. for details. FRT orientation is indicated by the direction of the arrowheads (FRT sites must be in the same orientation for deletion generation). (Parks et al. 2004).

In the presence of FLP recombinase, efficient *trans*-recombination between FRT elements results in a genomic deletion with a single residual element tagging the deletion site (figure. 2.2).

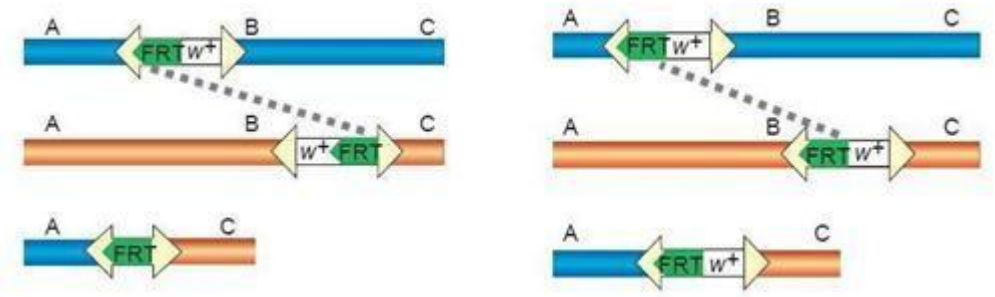

Figure 2.2. Schematics for deficiency generation. In the scheme on the left is shown the recombination strategy using FLP-FRT to generate *w*– deficiencies from Exelixis transposon insertions. On the right, the second scheme represents the FLP-FRT recombination to generate *w*+ deficiencies from Exelixis transposon insertions. (Parks et al. 2004).

In deletions generated using XPs, which contain tandem FRT sites, the *cis*-recombination event occurs earlier than that in *trans*. Depending on the pair of starting insertions, their genomic orientation and the relative position of *w*+ with respect to the FRTs, some deletions can initially be detected in the progeny by a loss of the *w*+ marker (table 2.1).

Lower coordinate tn1 (strand)	Higher coordinate tn2 (strand)	*w*+/–	Initial PCR confirmation method	UAS remaining?
RB (–)	*RB* (–)	*w*+	Two-sided	No
RB (–)	*WH* (+)	*w*+	Hybrid	No
RB (+)	*RB* (+)	*w*+	Two-sided	No
RB (+)	*WH* (–)	*w*+	Hybrid	Yes
RB (+)	*XP* (+)	*w*+	Two-sided*	Yes
WH (–)	*RB* (+)	*w*+	Hybrid	No
WH (–)	*WH* (–)	*w*+	Two-sided	Yes
WH (–)	*XP* (+)	*w*+	Two-sided*	Yes
WH (+)	*RB* (–)	*w*+	Hybrid	Yes
WH (+)	*WH* (+)	*w*+	Two-sided	Yes
XP (–)	*RB* (–)	*w*+	Two-sided*	Yes
XP (–)	*WH* (+)	*w*+	Two-sided*	Yes
XP (–)	*XP* (–)	*w*+	Two-sided	Yes
XP (+)	*XP* (+)	*w*+	Two-sided	Yes
XP (+)	*RB* (+)	*w*–	Hybrid	No
XP (+)	*WH* (–)	*w*–	Hybrid	Yes
RB (–)	*XP* (–)	*w*–	Hybrid	No
WH (+)	*XP* (–)	*w*–	Hybrid	Yes

*Hybrid PCR, though not tested by us, should also work for these deletion types.

Table 2.1. Allowable pairwise combinations of Exelixis transposons for deletion generation. (Parks et al. 2004).

The necessary crosses are outlined in figure 2.3 and allow the efficient recovery of deletions in four generations. Progeny are screened for the presence of the residual element by PCR detection of a resulting hybrid element (XP:WH) using element-specific primers, or by detection of residual element ends using paired element-specific and genome-specific primers (figure 2.4). Final confirmation of the deletion ends can be provided by PCR or sequencing with genome-specific primers. In

general, PCR screening of five *w*– individual progeny from *w*– deletion generation crosses, or 50 progeny from *w*+ deletion generation crosses, resulted in four confirmed deletions. In addition to deletions, tandem duplications could also be isolated using these insertions and an appropriately designed PCR strategy.

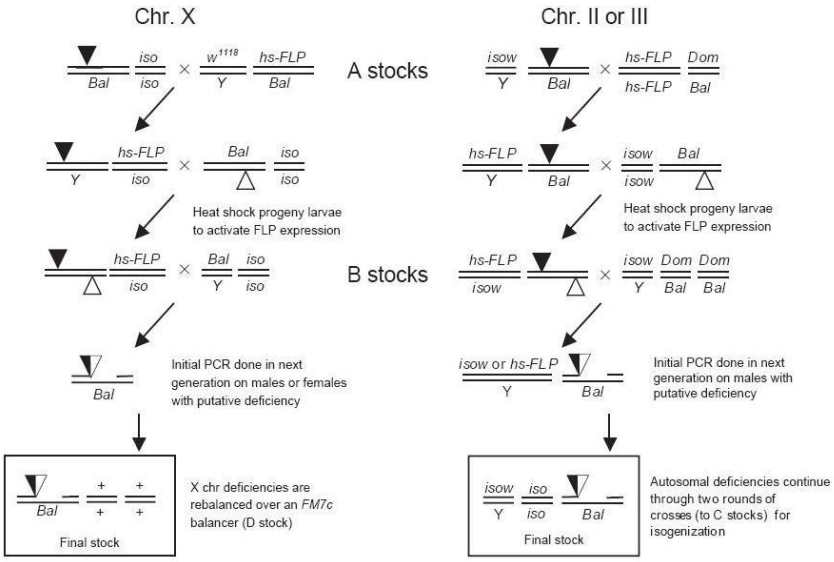

Figure 2.3. Genetic crossing schemes used to generate deletions. Genetic scheme used for FLP-FRT–based deletions. Crosses place two FRT-bearing transposon insertions (triangles) in *trans* in the presence of heat shock–driven FLP recombinase (*hs-FLP*). Activation of FLP recombinase results in the generation of deletions that can be detected by PCR. Deletions are established in isogenized stocks with balancers (*Bal*). *Dom*, dominant visible marker mutation; *iso*, isogenized chromosome; Y, Y chromosome. (Parks et al. 2004).

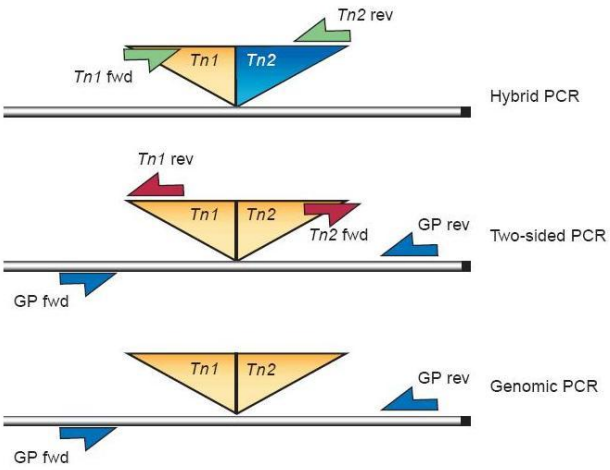

Figure 2.4. PCR strategies used in FLP-FRT–based deletions. For transposon combinations that generate a recombinant hybrid element (composed of two different element types), transposon-specific primers were used to generate a fragment of known size across the newly formed hybrid (hybrid PCR). For transposon combinations that regenerate an intact element, a genomic primer in combination with a transposon-specific primer for each end of the transposon was used (two-sided PCR). We also carried out PCR using only genomic primers for additional confirmation (genomic PCR). (Parks et al. 2004).

The PCR confirmation strategy used for initial detection of the deletion was carried out with the use of specific primer designed inside the P–elements (XP Reverse and XP Forward; in particular supplementary methods Parks et al. 2004 provide transposon primer sequences and expected fragment sizes for these combinations, as well as additional primer pair sequences for 'two-sided' PCR that may be used for secondary confirmation) and genomic primers chosen using an in-house primer design tool and made by Biosource. The primer sequences use for the PCR screen are shown in table 3.3.
For products longer than 3 kb we carried out PCR using TaKaRa La Taq (Takara Bio). For products less than 3 kb, we used AmpliTaq Gold (Applied Biosystems). We used a standard touchdown program with both systems. Genomic primers were chosen using an in-house primer design tool and made by Biosource.

LEFT ISOLATE	RIGHT ISOLATE	LEFT PRIMER	RIGHT PRIMER	PRODUCT SIZE
XP5' plus	**Gen F**	TTTACTCCAGTCACAGCTTTG	AACCAGTTACCGCAAAAACG	800 bp
Gen R	**XP3' plus**	CTCTTCGATTCTCCGCATTC	TACTATTCCTTTCACTCGCACTTATTG	1200 bp

Table 2.2. Primers for screening FLP/FRT deletion stocks by PCR. Two-sided PCR (Transposon-specific primers facing outward).

In summary, this method describes the highest resolution deletion coverage in the *D. melanogaster* genome in an efficient and straightforward manner.

2.3.4 H_2S determinations

Biochemical assays performed to characterize NaHS inhibition in drosophila isolated mitochondria were carry out as previously described. In particular, for H_2S inhibition assays, we measured Complex IV (COX), Complex I (CI) and Citrate Synthase (CS) activities, in wild type isolated mitochondria, in duplicate after having added increasing concentrations of NaHS or NaCN (5–30 μM). In this way we obtained a clear decreas in COX residual activity (%) in the presence of increasing concentrations of NaHS.
Then we tested the survival time of wild type, d*Ethe1* mutant and (d*Ethe1*, *Sprite*) -/- KO poisoned with different sulfide concentrations. We exposed flies to NaHS at

different concentrations (from 0,01 to 10 mM) and we monitored longevity under these conditions.
In addition we extracted mitochondria from a large number of flies which had died following exposure to NaHS 0,1 mM and we tested inhibiting capacity of sulfide by measuring CI, COX and CS enzymatic activities in such individuals.

2.4 Characterization of TTC19 deficiency

2.4.1 Drosophila strains

The *Drosophila melanogaster CG15173* is the fly orthologue of the gene encoding TTC19 [sequence accession number is FBgn0032744 (2L:19043535-19045146)]. We studied a fly line bearing a piggyBac element insertion within the TTC19 coding region. The knockout strain was originally obtained by the insertion of a piggyBac element within the ORF region included in the first exon of CG15173.
The transgene insertional PBac[WH] $CG15173^{f05160}$ (FBti0042429) is located at 2L:19044446 at the level of the first exon of the gene. The associated stock was obtained from Bloomington is #18843.
We also investigated another insertional line PBac[WH] $CG15173^{f03302}$ harboring the insertion of a piggyBac element at the level of the 5' portion of the gene, located at 2L:19044958.
Furthermore, to investigate the effects of CG15173 knock-down, RNAi flies were obtained from VDRC (Vienna Drosophila RNAi Center):Transformant ID #105382. Gene specific knock down was achieved using the GAL4/UAS system to target the RNAi to specific cells in the animal (Dietz et al. 2007). The primer pair specific for amplicon 3 of drosophila *TTC19* cDNA was used for quantitative-PCR, to measure the amount of drosophila *TTC19* cDNA normalized to rp49, a housekeeping cDNA as in (Zordan et al. 2006).

2.4.2 Genomic analysis of TTC19 mutant flies

A single individual from Bloomington strain #18843 (#f05160 Exelixis) was homogenized in 50µl of extraction buffer, 10mM Tris-HCl (pH 8.2), 1mM EDTA and 25 mM NaCl. Proteinase K was added, to a final concentration of 200µg/ml, and the homogenate incubated for 45 min at 37° C. The enzyme was heat inactivated at 95° C for 5 min. Two µl of this preparation was used as template for a 25µl PCR reaction mix, containing 1X AccuPrime PCR Buffer I, 5pmol of each primer, 0.5U of AccuPrime *Taq* Polymerase High Fidelity enzyme (Invitrogen). Following a 2min denaturation step at 94°C, 35 rounds of amplification (94°C for 30s, 60°C for 30s,

68°C for 1m and 30s) were performed. To confirm the piggyBac element insertion location, PCRs on genomic DNA were performed. TTC19 specific primers were chosen upstream and downstream the annotated insertion position (458bp downstream the putative ATG start codon). Amplifications were carried out by coupling TTC19 and WH piggyBac element specific, as listed in Table 2.3. The Exelixis piggyBac WH primers were as reported in (Parks et al. 2004). The *Drosophila melanogaster TTC19* (CG15173) sequence accession number is FBgn0032744 (2L:19043535-19045146).

Exon and position relative to the PBac insertion	**Seq. left primer**	**Seq. right primer**	**size (cDNA)**	**size (genomic)**
Exon1, upstream insertion	**TTC19_1F** GCAAGTTTACGCAAGTTATGGG	**TTC19_1R** AGTGAAAGCAGCGGAAAATG	218	218
Exon1 flanking insertion	**TTC19_2F** AGGAAACTCCGGAGGAAAAA	**TTC19_2R** GGCAAAAAGCCGTTTCATAA	239	239
Exon2/3, downstream insertion	**TTC19_3F** CCCGACGACAAGGACATACT	**TTC19_3R** ATGGTTACAGAGGCGTCGTT	164	234
Exon1 upstream from and within PiggyBac	**WH5' plus** TCCAAGCGGCGACTGAGATG	**TTC19_1F** GCAAGTTTACGCAAGTTATGGG	~500	~500
Exon1 downstream from and within PiggyBac	**WH3' plus** CCTCGATATACAGACCGATAAAAC	**TTC19_2R** GGCAAAAAGCCGTTTCATAA	~150	~150

Table 2.3. Amplicons and primers used for the analysis of Drosophila mutant TTC19.

2.4.3 Bang test analysis

In order to assay sensitivity to mechanical stimulation, on the night before the experiment, groups of five CO_2-anesthesized flies of each sex were placed in clean plastic vials containing a strip of moistened tissue paper (to provide a source of hydration). The next day, the paper was removed and each vial was placed in a vortex at the maximum intensity for 10 seconds. The vial containing the vortexed flies was then placed upright into a graduated cylinder in front of a digital webcam connected to a computer. The activity of the flies was videotaped for a maximum of 30 seconds. The videos were analyzed to establish the time taken for each individual to recover from the mechanical shock and climb the vial reaching established markings on the graduated cylinder.

2.4.4 Microscopic analysis of male meiosis

Testes from young adults were dissected in testis buffer, TB (7mM K_2HPO_4, 80mM KCl, 16mM NaCl, 5mM, MgCl2, 1% PEG 6000) and transferred to a 2µl drop of TB on a clean non siliconized coverslip. The testes were then torn open using very thin forceps. A clean glass slide was then placed over the coverslip, without pressing, and the sandwich inverted. Preparations were observed and photographed at 40x under a phase-contrast microscope.

2.5 Functional characterization of mitochondrial deoxynucleotide transport

2.5.1 Fly strains

We started with characterization of the *CG18317* drosophila gene, homolog of the yeast RIM2 gene, by post transcriptional silencing the in order to ascertain whether they show any defects in mitochondrial function which might be related to a deficiency in mitochondrial nucleotide availability.. We ordered from VDRC (Dietzl et al. 2007) two available transgenic lines, harboring a construct encoding for a CG18317/RIM2-specific dsRNA, which allows the temporally and/or spatially targeted silencing of the *Drosophila* homolog of RIM2 (Trasformant ID #44203, #44202 and #100807).

In addition, using the same technique previously described for *Ethe1*, we performed the knock out of CG18317/RIM2. We obtained from Bloomington transgenic lines bearing insertional elements localized at the boundaries of CG18317/RIM2 gene. In particular, line PBac[RB] CG18317^{e01575} (FBti0047179) harbors a piggyBac element at the 5' level of the gene, in position 2L:17253536. The other insertional line PBac[RB] CG18317^{e00041} (FBti0046412) harbors a piggyBac element at the 3' portion of the gene, located at 2L:1716977.
In addition we also characterized the PBac[RB] CG18317^{e01575} stock bearing PiggyBac insertion within the coding region of RIM2 just to evaluate whether this insertion caused a de-regulation of the gene transcription.

2.5.2 Generation of *Drosophila Rim2* KO strain, lacking the putative deoxynucleotide transporter *Rim2*

We obtained available stocks bearing PiggyBac insertions (PBac[RB] CG18317^{e01575} and PBac[RB] CG18317^{e00041}) within the RIM2 locus in order to achieved the *Rim2*

gene deletion through the specific recombination between the FRT element within the PBac elements (Parks et al. 2004). The KO technique we carried out is the same already described in chapter 2.3.3 for the achievement of d*Ethe1* knock out. The obtained KO lines were further used to evaluate whether they show any defects in mitochondrial function which might be related to a deficiency in mitochondrial nucleotide availability. In table 2.4 are reported the primer sequences used to screen the putative knock out individuals, in particular we use the "two sided PCR" method (Parks et al. 2004), with primer designed in the PBac insertional element (given by supplementary materials Parks et al. 2004) and in the *Rim2* genomic region.

LEFT ISOLATE	RIGHT ISOLATE	LEFT PRIMER	RIGHT PRIMER	PRODUCT SIZE
RB5' plus	**Gen F**	ATTTCGCCTCACAGCTTTG	GATGACAAAGTGCACCATCG	150 bp
Gen R	**RB3' plus**	CTCTTCGATTCTGGGCATTC	TACTATTCCTTTCACTCGCACTTATTG	238 bp

Table 2.4. Primers for screening FLP/FRT deletion stocks by PCR. Two-sided PCR (Transposon-specific primers facing outward).

2.5.3 RNA extraction and real-time PCR

RNA was treated with RQ1RNAse-freeDNAse (Promega,Madison,WI) and a cleaning step with 1:1 phenol-chloroform. For each sample, 1 mg of RNA was used for the first-strand cDNA synthesis, employing oligonucleotides dT-20 and M-MLV Reverse Transcriptase Rnase H Minus, Point Mutant (Promega) according to the manufacturer's instructions. The primers used for the realtime PCR were designed with the Primer 3 Software available at (http://www.basic.nwu.edu/biotools /Primer3.html).
Real-time PCR was performed on a Rotor Gene 3000 (Corbett Research) by using the following primers for *Rim2* mRNA:

TATGATACGTTTGGGGAACC
ACCATCCCAAAGGAGCTATC

and for the housekeeping rp49 mRNA

ATCGGTTACGGATCGAACAA
GACAATCTCCTTG CGCTTCT

The primers used for *Rim2*, were designed so as not to amplify the ds interfering RNA. SYBR Green (Applied Biosystems, Foster City, CA) fluorescent marker was used to generate semiquantitative data. PCR premixes containing all reagents except for target cDNAs were prepared and aliquoted by a Robotic Liquid Handling System (CAS-1200, Corbett Robotics) into PCR tubes (Corbett Research). The PCR reaction was carried out following the program: 95°C for 30 sec, 60°C for 30 sec, 72°C for 45 sec, for 40 cycles, followed by a final 10 min at 72°C. The amplification efficiencies ($E= 10^{-1/slope}$) for each sample were calculated on the basis of the results of three amplification reactions, each with a different quantity of the template (6, 18, or 54 ng of total reverse transcribed RNA), according to (Pfaffl 2001). Each reaction was performed in duplicate. The amplification efficiency, obtained for each sample, was used to estimate the relative level of expression between the normal sample we chose as the ‘‘calibrator’’ (w^{1118} larvae or parental line) and the silenced samples (called ‘‘X conditions’’): $R = Et^{\Delta Ct}/Eh^{\Delta Ch}$ where Et is the amplification efficiency of *Rim2* mRNA; Eh is the amplification efficiency of rp49 mRNA; ΔCt=Ctc-Ctx is the difference between cycle threshold (Ct) of the calibrator and the Ct of X condition for *Rim2* mRNA; ΔCh= Ctc-Ctx is the difference between Ct of the calibrator and the Ct of X condition for rp49 mRNA.

2.6 Respiratory chain complex activity assays

Mitochondria were extracted in duplicate from samples each containing approximately 200 whole flies or larvae. Each sample was homogenized using a Dounce glass–glass potter and loose fitting pestle. A mannitol–sucrose buffer (pH 7.4), to which 2% BSA was added, was then added to bring the homogenate volume to 25 ml. The samples were then centrifuged at 1500 g (Beckman Avanti J–25 Centrifuge, Beckman 2550 rotor) at 4°C for 6 minutes. The pellet was discarded by filtering the sample through a fine mesh, and the supernatant re–centrifuged at 7000 g at 4°C for 6 minutes. This supernatant was discarded and the remaining pellet resuspended in 20 ml of mannitol–sucrose buffer without BSA before being centrifuged at 7000 g under the same conditions as above. The supernatant was once again discarded and the pellet resuspended in a minimal amount of buffer (approximately 50 ml). Concentration of proteins was determined by the Biuret test before storage at –80°C or immediate use. The extracted mitochondria samples were diluted with hypotonic buffer to the desired concentration – normally a final volume of mitochondria homogenate between 10 and 50µl. Prior to the assays, in order to disrupt the mitochondrial membranes, the samples were subjected to 3 freeze–thaw cycles using liquid nitrogen.

The enzymatic activities of Complexes I–V and Citrate Synthase measured, were obtained as described in Methods in Cell Biology Vol.80, 2008.

Complex I (NADH: ubiquinone reductase) activity

The activity of NADH: ubiquinone reductase was determined by following the oxidation of NADH at 340 nm (Ɛ= 6220 M^{-1} cm^{-1}) using ubiquinone–1 as the electron acceptor. The assay buffer consisted of 25 mM KH_2PO_4, pH 7.2, 5mM $MgCl_2$ and 2.5 mg/ml BSA, to which 2 mM KCN, 2 µg/ml antimycin, 97.5 µM ubiquinone, 0.13 mM NADH and 50 µg mitochondrial proteins were added. As Complex I activity is rotenone–sensitive, activity was measured before and after the addition of rotenone (2µg/ml), the difference between the two then being used to determine actual activity.

Complex II (ubiquinone succinate dehydrogenase)

The activity of ubiquinone succinate dehydrogenase was measured as the decrease in absorbance due to the reduction of 2,6–dichloroindophenol (DCIP), the electron acceptor, at 600 nm (Ɛ= 21,000 M^{-1} cm^{-1}), coupled to the reduction of ubiquinone. The assay buffer consists of 100 mM KH_2PO_4 pH 7, to which 0.1 mM DCIP, 1.5 mM KCN, 16 mM succinate (the electron donor), 50 µM coenzyme Q_1 and 50 µg mitochondrial proteins were added.

Complex III (ubiquinol: cytochrome c reductase)

Complex III activity was determined by following the oxidation of decylubiquinol at 550 nm (Ɛ= 18,500 M^{-1} cm^{-1}) with cytochrome *c* as the electron acceptor.
The assay buffer consists of 50 mM KH_2PO_4 pH 7.4, to which 0.1% BSA, 2 µg/ml rotenone, 50 µM decylubiquinol, 2 mM NaN_3 50 µM cytochrome *c*, 0.001% Antymicine A and 5 µg mitochondrial proteins were added. Each sample was measured without and with Antimycine A (specific inhibitor for complex III). Complex III activity was expressed as the antimycin A–sensitive rate.

Synthesis of decylubiquinol

Decylubiquinol was synthesized according to the method of (Gudz et al. 1997) and all procedures were carried out in subdued light. Decylubiquinone (10 µM) was dissolved in 2 ml ethanol + water (1 + 1 v/v; pH 2) and reduced to the corresponding alcohol by addition of $NaBH_4$. The decylubiquinol was twice extracted from the aqueous ethanol using 1 ml of diethylether + isooctane (2 + 1; v/v). The organic phases were combined, then washed with 2 ml of 2 M NaCl and evaporated to dryness at room temperature under a stream of nitrogen. The product was dissolved

in ethanol (990 µl), acidified by addition of 10 µl of 0.1 M HCl and transferred to a storage vial. After flushing the airspace of the vial with nitrogen, the vial was securely capped and the decylubiquinol solution kept at –80 °C in darkness.

Complex IV (cytochrome c oxidase) activity

Cytochrome c oxidase was determined by monitoring the oxidation of cytochrome c at 550 nm (Ɛ= 18,500 M^{-1} cm^{-1}). The assay buffer consisted of 100mM K Phosphate pH 7.0, to which 0.1% BSA, 0.8 mM reduced cytochrome c and 10 µg mitochondrial proteins were added. Samples used to determine complex IV activity were treated with n–dodecyl maltoside to disrupt membranes rather than freeze–thawing.

Complex V (ATP synthase) activity

Complex V activity was measured by monitoring the oxidation of NADH at 340 nm, in a LDH catalysed reaction. The assay buffer consists of hepes–Mg buffer pH 8.0, to which 0.3mM NADH, 2.5mM P–enol pyruvate, 2µg antimycin A, 19µg pyruvate kinase, 22µg lactic dehydrogenase and 5 µg mitochondrial proteins were added.

Citrate Synthase activity

Citrate Synthase activity was measured by monitoring the reduction of dithio-bis-nitrobenzoic acid (DTNB, colourless) to thionitrobenzoic acid (yellow) with coenzyme A at 412 nm (Ɛ= 13,600 M^{-1} cm^{-1}). The assay buffer consisted of 75mM Tris-HCl pH 8, to which 0.4mM acetyl-CoA, 0.1 µM DTNB, 0.5mM oxaloacetate and 5µg mitochondrial proteins were added.

2.7 Single–fly genomic DNA preps for PCR

Flies are anesthetized with CO_2 and placed singly into an eppendorf vial (0,5 ml). 50 µl Buffer A are added (10 mM TrisHCL pH 8.2, 2 mM EDTA, 25mM NaCl) to each sample. Each fly is then homogenized using a Sigma Homogenizer and 1 µl proteinase K (10 mg/ml) added. The mixture is the incubated at 37°C for 45 minutes and successively at 100°C for 3 minutes to inactivate pK. The vial is the quickly spun to pull down any pellet and the supernatant transferred to a new vial.
Storage samples at –80°C.

2.8 Survival of adult flies

The fruit fly *Drosophila melanogaster* is a wellsuited model for ageing studies as it has a relatively short lifespan. Procedures for lifespan studies were conducted as in (Broughton et al. 2005).
Briefly, all flies were reared at standard low density, and virgins were collected and handled with CO_2 anesthesia. Adults of the same sex were kept at a density of 10 per vial. Flies were transferred to fresh medium, without anesthesia, and deaths were scored five times per week. The survival of all genotypes was compared with the wild type stock.

2.9 Walking optomotor test

The optomotor response was tested as in (Sandrelli et al. 2001), with modifications as in (Zordan et al. 2006). Flies are placed in a T-shaped tube with the longer arm painted black. The T with the fly inside is placed in the centre of an arena located inside a rotating drum which is open at the top. The internal walls of the drum are painted with alternating black and white stripes and the apparatus is illuminated from above with a white light. The fly will be attracted by the light to exit the darkened arm of the T-tube, and will then be confronted with the rotating environment. In most cases, wild type flies will tend to move in the same direction as the rotating environment. The test is repeated 10 times for each fly; five trials with the drum rotating from right to left and five trials in the opposite direction. Each fly is thus scored for the number of correct turns taken in the 10 trials.

2.10 Analysis of long term locomotor activity

Single flies were placed into glass tubes containing a gel as a source of food and water. Groups of 32 such glass tubes were then loaded into Trikinetics® locomotor activity monitors. The monitors were placed into an incubator in which temperature and light ambient conditions are under control (temp= 25°C, light= 12h Light: 12h Dark cycles) for 3 days. During this time, every time a fly crossed an infrared light beam cast across the glass tube, the monitor registered this as a bout of activity. Bouts of activity were collected in 30 min bins.

2.11 Electroretinogram

All experiments were done as described in (Zordan et al. 2005). Recorded signals were amplified with an intracellular amplifier (705; WPI Instruments), fed to a signal conditioner (CyberAmp; Axon Instruments), lowpass filtered (3 kHz), and then fed to a

personal computer through an A/D converter (Digidata 1200; Axon Instruments). For each fly, the amplitude of the first two electroretinogram (ERG) responses was measured using appropriate software (PClamp 6.04; Axon Instruments). Data were analyzed for statistical significance using one-way ANOVA tests.

REFERENCES

Agostino A, Invernizzi F, Tiveron C, Fagiolari G, Prelle A, Lamantea E, Giavazzi A, Battaglia G, Tatangelo L, Tiranti V, Zeviani M (2003). **Constitutive knockout of *Surf1* is associated with high embryonic lethality, mitochondrial disease and cytochrome c oxidase deficiency in mice.** *Hum Mol Genet*, **12**(4):399{413.

Angelin A, Tiepolo T, Sabatelli P, Grumati P, Bergamin N, Golfieri C, Mattioli E, Gualandi F, Ferlini A, Merlini L, Maraldi NM, Bonaldo P and Bernardi P (2007). **Mitochondrial dysfunction in the pathogenesis of Ullrich congenital muscular dystrophy and prospective therapy with cyclosporins**. *Proc Natl Acad Sci USA* **104,** 991–996.

Aravind L (1999). **An evolutionary classification of the metallo ß-lactamase fold proteins.** *In Silico Biol* **1**, 69–91.

Arner ES and Eriksson S (1995). **Mammalian deoxyribonucleoside kinases.** *Pharmacol Ther* **67,** 155–186.

Arpaia E, Benveniste P, Di CA, Gu Y, Dalal I, Kelly S, Hershfield M, Pandolfi PP, Roifman CM and Cohen A (2000). **Mitochondrial basis for immune deficiency. Evidence from purine nucleoside phosphorylase-deficient mice**. *J Exp Med* **191,** 2197–220.8.

Attardi G, Schatz G (1988). **Biogenesis of mitochondria.** *Annu Rev Cell Biol* **4**, 289–333.

Barrientos A, Korr D, Tzagoloff A (2002). **Shy1p is necessary for full expression of mitochondrial COX1 in the yeast model of Leigh's syndrome**. *EMBO J* **21**, (1-2):43{52.

Berk AJ and Clayton DA (1973). **A genetically distinct thymidine kinase in mammalian mitochondria. Exclusive labeling of mitochondrial deoxyribonucleic acid**. *J Biol Chem* **248**, 2722–2729.

Bianchi V, Pontis E and Reichard P (1987). **Regulation of pyrimidine deoxyribonucleotide metabolism by substrate cycles in dCMP deaminasedeficient V79 hamster cells**. *Mol Cell Biol* **7**, 4218–4224.

Blatch GL and Lassle M (1999). **The tetratricopeptide repeat: a structural motif mediating protein-protein interactions.** *BioEssays* **21**, 932–939.

Bogenhagen D and Clayton DA (1976). **Thymidylate nucleotide supply for mitochondrial DNA synthesis in mouse L-cells. Effect of 5-fluorodeoxyuridine and methotrexate in thymidine kinase plus and thymidine kinase minus cells**. *J Biol Chem* **251,** 2938–2944.

Bogenhagen D, Clayton DA (1974). **The number of mitochondrial deoxyribonucleic acid genomes in mouse L and human HeLa cells. Quantitative isolation of mitochondrial deoxyribonucleic acid.** *J Biol Chem* **49**, 7991.

Borst A, Haag J, Rieff DF (2010). **Fly motion vision.** *Annu. Rev. Neurosci.* **33**, 49-70.

Bourdon A, Minai L, Serre V, Jais JP, Sarzi E, Aubert S, Chretien D, de LP, Paquis-Flucklinger V, Arakawa H, Nakamura Y, Munnich A and Rotig A (2007). **Mutation of RRM2B, encoding p53-controlled ribonucleotide reductase (p53R2), causes severe mitochondrial DNA depletion**. *Nat Genet* **39,** 776–780.

Bradshaw HDJ and Deininger PL (1984). **Human thymidine kinase gene: molecular cloning and nucleotide sequence of a cDNA expressible in mammalian cells.** *Mol. Cell. Biol.* **4,** 2316–2320.

Brand AH, Perrimon N (1993).**Targeted gene expression as a means of altering cell fates and generating dominant phenotypes**. *Development*, 118(2):401{15.

Brandt U, Yu L, Yu CA and Trumpower BL (1993). **The mitochondrial targeting presequence of the Rieske iron–sulfur protein is processed in a single step after insertion into the cytochrome bc1 complex in mammals and retained as a subunit in the complex**. *J Bio Chem* **268**, 8387–8390.

Bridges EG, Jiang Z and Cheng YC (1999). **Characterization of a dCTP transport activity reconstituted from human mitochondria**. *J Biol Chem* **274,** 4620–4625.

Bugiani M, Invernizzi F, Alberio S, Briem E, Lamantea E, Carrara F, Moroni I, Farina L., Spada M, and Donati MA (2004). **Clinical and molecular findings in children with complex I deficiency**. *Biochim Biophys Acta* **1659**, 136-147.

Burlina AB, Dionisi-Vici C, Bennet MJ, Gibson KM, Servidei S, Bertini E, Hale DE, Schimidt-Sommerfeld E, Sabetta G, Zacchello F, Rinaldo P (1994) **A new syndrome with ethylmalonic aciduria and normal fatty acid oxidation in fibroblasts.** *J Pediatr* **124**, 79–86.

Burlina AB, Zacchello F, Dionisi-Vici C, Bertini E, Sabetta G, Bennet MJ, Hale DE, Schimidt-Sommerfeld E, Rinaldo P (1991). **New clinical phenotype of branched-chain acyl-CoA oxidation defect**. *Lancet* **338**, 1522–1523.

Chabes A and Thelander L (2000). **Controlled protein degradation regulates ribonucleotide reductase activity in proliferating mammalian cells during the normal cell cycle and in response to DNA damage and replication blocks.** *J Biol Chem* **275,** 17747–17753.

Chomyn A (1996**). In vivo labeling and analysis of human mitochondrial translation products**. *Methods Enzymol* **264**, 197–211.

Coenen M, van den Heuvel LP, Nijtmans LG, Morava E, Marquardt I (1999). **SURFEIT-1 gene analysis and twodimensional blue native gel electrophoresis in cytochrome coxidase deficiency.** *Biochem Biophys Res Commun* **265**, 339–344.

Cohen A, Hirschhorn R, Horowitz SD, Rubinstein A, Polmar SH, Hong R and Martin DW, Jr. (1978). **Deoxyadenosine triphosphate as a potentially toxic metabolite in adenosine deaminase deficiency**. *Proc Natl Acad Sci U S A* **75,** 472–476.

Corydon MJ, Vockley J, Rinaldo P, Rhead WJ, Kjeldsen M, Winter V, Riggs C, Babovic-Vuksanovic D, Smeitink J, De Jong J, Levy H, Sewell AC, Roe C, Matern D, Dasouki M, Gregersen N (2001). **Role of common variant alleles in the molecular basis of short-chain acyl-CoA dehydrogenase deficiency**. *Pediatr Res* **49**, 18–23.

Cruciat CM, Hell K, Folsch H, Neupert W and Stuart RA (1999). **Bcs1p, an AAA-family member, is a chaperone for the assembly of the cytochrome *bc*(1) complex.** *EMBO J* **18**, 5226–5233.

Dell'agnello C, Leo S, Agostino A, Szabadkai G, Tiveron C, Zulian A, Prelle A, Roubertoux P, Rizzuto R, Zeviani M (2007). **Increased longevity and refractoriness to Ca($^{2+}$)-dependent neurodegeneration in *Surf1* knockout mice**. *Hum Mol Genet* **16**(4), 431{44.

Deng WB, Feng YP (1997). **Effect of dilbutylphthaline on brain edema in rats subjected to focal cerebral ischemia.** *Chi Med Sci J* **12**, 102.

Deng Y and Nicholson RA (2005). **Block of electron transport by surangin B in bovine heart mitochondria.** *Pestic Bioch and Physiol* **81** 39–50

Dietzl G, Chen D, Schnorrer F, Su KC, Barinova Y, Fellner M, Gasser B, Kinsey K, Oppel S, Scheiblauer S, Couto A, Marra V, Keleman K and Dickson BJ (2007). **A genome-wide transgenic RNAi library for conditional gene inactivation in Drosophila**. *Nature* **448,** 151–156.

DiMauro S and Schon EA (2003). **Mitochondrial respiratorychain diseases.** *New Engl J Med* **348**, 2656–2668.

DiMauro S and Schon EA (2008). **Mitochondrial Disorders in the Nervous System** *Annu Rev Neurosci* **31**, 91-123.

DiMauro S, Moraes CT, Shanske S, Lombes A, Nakase H, Mita S, Tritschler HJ, Bonilla E, Miranda AF and Schon EA (1991). **Anomalous intensity-dependent vibrational distributions of oxygen molecules in a nonresonant laser field: A molecular perspective.** *Rev Neurologiq* **147**, 443–449.

DiMauro S, Zeviani M, Rizzuto R, Lombes A, Nakase H, Bonilla E, Miranda A and Schon E (1988). **Molecular defects in cytochrome c oxidase in mitochondrial diseases.** *J Bioenerg Biomembr* **20**, 353–364.

Dolce V, Fiermonte G, Runswick MJ, Palmieri F and Walker JE (2001). **The human mitochondrial deoxynucleotide carrier and its role in the toxicity of nucleoside antivirals**. *Proc Natl Acad Sci U S A* **98,** 2284–2288.

Dougherty DA (1996). **Cation-pi interactions in chemistry and biology: a new view of benzene, Phe, Tyr, and Trp.** *Science* **271**, 163–168.

Drysdale RA, Crosby MA, The flybase consortium (2005). ***FlyBase*: genes and gene models.** *Nucleic Acids Research* **33**, 390–395.

Fadic R and Johns DR (1996). **Clinical spectrum of mitochondrial diseases.** *Semin Neurol* **16**, 11–20.

Farina L, Chiapparini L, Uziel G, Bugiani M and. Zeviani M (2002). **MR findings in Leigh syndrome with COX deficiency and Surf-1 mutations**. *AJNR Am J Neuroradiol*. **23**, 1095–1100.

Fergestad T, Bostwick B and Ganetzky B (2006). **Metabolic disruption in Drosophila bangsensitive seizure mutants**. *Genetics* **173**,1357-1364.

Fernandez-Ayala DJM, Sanz A, Vartiainen S, Kemppainen KK, Babusiak M, Mustalahti E, Costa R, Tuomela T, Zeviani M, Chung J, O'Dell KMC, Rustin P, Jacobs HT (2009). **Expression of the Ciona intestinalis alternative oxidase (AOX) in Drosophila**

complements defects in mitochondrial oxidative phosphorylation. *Cell Metab* **9**(5), 449–60.

Fernandez-Vizarra E, Bugiani M, Goffrini P, Carrara F, Farina L, Procopio E, Donati A, Uziel G, Ferrero and Zeviani M. (2007). **Impaired complex III assembly associated with BCS1L gene mutations in isolated mitochondrial encephalopathy**. *Hum. Mol. Genet.* **16,** 1241–1252.

Ferraro P, Nicolosi L, Bernardi P, Reichard P and Bianchi V (2006). **Mitochondrial deoxynucleotide pool sizes in mouse liver and evidence for a transport mechanism for thymidine monophosphate**. *Proc Natl Acad Sci U S A* **103,** 18586–18591.

Ferraro P, Pontarin G, Crocco L, Fabris S, Reichard P and Bianchi V (2005). **Mitochondrial deoxynucleotide pools in quiescent fibroblasts: a possible model for mitochondrial neurogastrointestinal encephalomyopathy (MNGIE).** *J Biol Chem* **280,** 24472–24480.

Fiermonte G, De Leonardis F, Todisco S, Palmieri L, Lasorsa FM and Palmieri F (2004). **Identification of the mitochondrial ATP-Mg/Pi transporter. Bacterial expression, reconstitution, functional characterization, and tissue distribution**. *J Biol Chem* **279**, 30722–30730.

Floyd S, Favre C, Lasorsa FM, Leahy M, Trigiante G, Stroebel P, Marx A, Loughran G, O'Callaghan K, Marobbio CM, Slotboom DJ, Kunji ER, Palmieri F and O'Connor R (2007). **The insulin-like growth factor-I-mTOR signaling pathway induces the mitochondrial pyrimidine nucleotide carrier to promote cell growth.** *Mol Biol Cell* **18,** 3545–3555.

Fuller MT (1993). **Spermatogenesis. In The Development of Drosophila**, (M. Martinez-Arias and M. Bate, eds.) Cold Spring Harbor Press, Cold Spring Harbor, New York. pp.71-147.

Garavaglia B, Colamaria V, Carrara F, Tonin P, Rimoldi M, Uziel G (1994). **Muscle cytochrome c oxidase deficiency in two Italian patients with ethylmalonic aciduria and peculiar clinical phenotype.** *J Inher Metab Dis* **17**, 301–303.

García-Silva MT, Campos Y, Ribes A, Briones P, Cabello A, Santos Borbujo J, Arenas J, Garavaglia B. (1994). **Encephalopathy, petechiae, and acrocyanosis with ethylmalonic aciduria associated with muscle cytochrome c oxidase deficiency**. *J Pediatr* **125**, 843–844.

Garcia-Silva MT, Ribes A, Campos Y, Garavaglia B, Arenas J (1997). **Syndrome of encephalopathy, petechiae, and ethylmalonic aciduria**. *Pediatr Neurol* **17**, 165–170.

Gazziola C, Ferraro P, Moras M, Reichard P and Bianchi V (2001). **Cytosolic high k(M) 5'-nucleotidase and 5'(3')-deoxyribonucleotidase in substrate cycles involved in nucleotide metabolism.** *J BiolChem* **276,** 6185–6190.

Giansanti MG, Farkas RM, Bonaccorsi S, Lindsley DL, Wakimoto BT, Fuller MT and Gatti M (2004). **Genetic dissection of meiotic cytokinesis in Drosophila males**. *Mol Biol Cell* **15**, 2509-2522.

Glasscock E and Tanouye MA (2005). **Drosophila couch potato mutants exhibit complex neurological abnormalities including epilepsy phenotypes**. *Genetics* **169**, 2137-2149.

Gomes CM, Frazao C, Xavier AV, Legall J, Teixeira M (2002). **Functional control of the binuclear metal site in the metallo-beta-lactamase-like fold by subtle amino acid replacements**. *Protein Science* **11**, 707–712.

Gregersen N, Winter VS, Corydon MJ, Corydon TJ, Rinaldo P, Eiberg H (1998). **Identification of four new mutations in the short-chain acyl-CoA dehydrogenase (SCAD) gene in two patients: one of the variant alleles, 511C-T, is present at an unexpectedly high frequency in the general population, as was the case for 625G-A, together conferring susceptibility to ethylmalonic aciduria.** *Hum Mol Genet* **7**, 619–627.

Grosso, S, Mostardini R, Farnetani MA, Molinelli M, Berardi R, Dionisi-Vici C, Rizzo C, Morgese G, Balestri P (2002). **Ethylmalonic encephalopathy, further clinical and neuroradiological characterization**. *J Neurol* **249**, 1446–1450.

Gudz TI, Tserng KY, Hoppel CL (1997). **Direct inhibition of mitochondrial respiratory chain complex III by cellpermeable ceramide**, *J. Biol. Chem.* **272** 24154–24158.

Hakansson P, Hofer A and Thelander L (2006). **Regulation of mammalian ribonucleotide reduction and dNTP pools after DNA damage and in resting cells**. *J Biol Chem* **281,** 7834–7841.

Hanson BJ, Carrozzo R, Piemonte F, Tess A, Robinson BH (2001). **Cytochrome c oxidase-deficient patients have distinct subunit assembly profiles**. *J Biol Chem* **276**, 16296–16301.9.

Haslbrunner E, Tuppy H and Schatz G. (1964). **Deoxyribonucleic Acid Associated with Yeast Mitochondria**. *Biochem Biophys Res Commun* **15**, 127–132.

Heckmatt L and Dubowitz V (1984). **Needle biopsy of skeletal muscle.** *Muscle Nerve* **7**, 594.

Herrmann JM and Funes S (2005). **Biogenesis of cytochrome oxidase-sophisticated assembly lines in the mitochondrial inner membrane.** *Gene* (*Amst*) **354**, 43–52.

Higashitsuji H, Nagao T, Nonoguchi K, Fujii S, Itoh K, Fujita J (2002). **A novel protein overexpressed in hepatoma accelerates export of NF-*K*B from the nucleus and inhibits p53-dependent apoptosis**. *Cancer Cell* **2** ,335–346.

Holmgren D, Wahlander H, Eriksson BO, Oldfors A, Holme E and Tulinius M (2003). **Cardiomyopathy in children with mitochondrial disease, clinical course and cardiological findings**. *Eur Heart J* **24**, 280–288.

Holt IJ, Harding AE, Morgan Hughes JA (1988). **Deletions of muscle mitochondrial DNA in patients with mitochondrial myopathies**. *Nature* **331**, 717–719.

Irwin WA, Bergamin N, Sabatelli P, Reggiani C, Megighian A, Merlini L, Braghetta P, Columbaro M, Volpin D, Bressan GM, Bernardi P and Bonaldo P (2003). **Mitochondrial dysfunction and apoptosis in myopathic mice with collagen VI deficiency.** *Nat Genet* **35,** 267–271.

Johansson M and Karlsson A (1997). **Cloning of the cDNA and chromosome localization of the gene for human thymidine kinase 2.** *J Biol Chem* **272,** 8454–8458.

Jordan A and Reichard P (1998). **Ribonucleotide reductases.** *Annu Rev Biochem* **67,** 71–98.

Kauffman MG and Kelly TJ (1991). **Cell cycle regulation of thymidine kinase: residues near the carboxyl terminus are essential for the specific degradation of the enzyme at mitosis.** *Mol Cell Biol* **11,** 2538–2546.

Kicska GA, Long L, Horig H, Fairchild C, Tyler PC, Furneaux RH, Schramm VL and Kaufman HL (2001). **Immucillin H, a powerful transition-state analog inhibitor of purine nucleoside phosphorylase, selectively inhibits human T lymphocytes**. *Proc Natl Acad Sci U S A* **98,** 4593–4598.

Kimmins S and MacRae TH (2000). **Maturation of steroid receptors: an example of functional cooperation among molecular chaperones and their associated proteins.** *Cell Stress Chaperones* **5**, 76-86

Koeberl DD, Young SP, Gregersen NS, Vockley J, Smith WE, Benjamin DK Jr, An Y, Weavil SD, Chaing SH, Bali D, McDonald MT, Kishnani PS, Chen YT, Millington DS (2003). **Rare disorders of metabolism with elevated butyryl- and isobutyrylcarnitine detected by tandem mass spectrometry newborn screening.** *Pediatr Res* **54**, 219–223.

Kotarsky H., (2007). **BCS1L is expressed in critical regions for neural development during ontogenesis in mice.** *Gene Expr. Patterns* **7**, 266-273

Kumar D, Gustafsson C, Klessig DF (2006). **Validation of RNAi silencing specificity using synthetic genes: salicylic acid-binding protein 2 is required for innate immunity in plants**. Plant J, **45**(5):863{8.

Kunji ER (2004). **The role and structure of mitochondrial carriers**. *FEBS Lett* **564,** 239–244.

Lam W, Chen C, Ruan S, Leung CH and Cheng YC (2005). **Expression of deoxynucleotide carrier is not associated with the mitochondrial DNA depletion caused by anti-HIV dideoxynucleoside analogs and mitochondrial dNTP uptake**. *Mol Pharmacol* **67,** 408–416.

Lash LH, Jones DP (1993). **Mitochondrial Dysfuntion**. *Meth in Toxicol. Academic Press*, Vol. I: San Diego.

Leigh D. (1951). **Subacute necrotizing encephalomyelopathy in an infant.** *J Neurol Neurosurg Psychiatr* **14**, 216–221.

Leonard JV and Schapira AVH (2000a). **Mitochondrial respiratory chain disorders I: mitochondrial DNA defects.** *Lancet* **355**, 299–304.

Leonard JV and Schapira AVH (2000b). **Mitochondrial respiratory chain disorders II: neurodegenerative disorders and nuclear gene defects.** *Lancet* **355**, 389–94.

Leschelle X, Goubern M, Andriamihaja M, Hervé M. Blottière HM, Couplan E, Gonzalez-Barroso M, Petit C, Pagniez A, Chaumontet C, Mignotte B, Bouillaud F and Blachier F**.** (2005). **Adaptative metabolic response of human colonic epithelial cells to the adverse effects of the luminal compound sulfide**. *Biochim Biophys Acta* **1725**, 201–212.

Lesnefsky EJ, Gudz IT, Moghaddas S, Migita CT, Ikeda-Saito M, Turkaly PJ and Hoppel CL (2001). **Aging decreases electron transport complex III activity in heart interfibrillar mitochondria by alteration of the cytochrome *c* binding site** *J Mol Cell Cardiol* **33**, 37–47

Lightowlers RN and Chrzanowska-Lightowlers ZM (2008) **PPR (pentatricopeptide repeat) proteins in mammals: important aids to mitochondrial gene expression**. *Biochem J* **416**, 5-6.

Lindhurst MJ, Fiermonte G, Song S, Struys E, De LF, Schwartzberg PL, Chen A, Castegna A, Verhoeven N, Mathews CK, Palmieri F and Biesecker LG (2006). **Knockout of Slc25a19 causes mitochondrial thiamine pyrophosphate depletion, embryonic lethality, CNS malformations, and anemia**. *Proc Natl Acad Sci U S A* **103,** 15927–15932.

Mamer OA, Tjoa SS, Scriver CR, Klassen GA (1976). **Demonstration of a new mammalian isoleucine catabolic pathway yielding an R series of metabolites**. *Biochem J* **160**, 417–426.

Mantagos S, Genel M, Tanaka K (1979). **Ethylmalonic-adipic aciduria: in vivo and in vitro studies indicating deficiency of activities of multiple acyl-CoA dehydrogenases.** *J Clin Invest* **64**, 1580–1589.

Marin-Garcia J, Goldenthal MJ, Pierpont EM, Ananthakrishnan R and Perez-Atayde A **Is age a contributory factor of mitochondrial bioenergetic decline and DNA defects in idiopathic dilated cardiomyopathy?** (1999). *Cardiovasc Pathol* **8**, 217– 222.

Marobbio CM, Di Noia MA and Palmieri F (2006). **Identification of a mitochondrial transporter for pyrimidine nucleotides in Saccharomyces cerevisiae: bacterial expression, reconstitution and functional characterization**. *Biochem J* **393,** 441–446.

Minai L, Martinovic J, Chretien D, Dumez F, Razavi F, Munnich A, Rötig A (2008). **Mitochondrial respiratory chain complex assembly and function during human fetal development**. *Mol Genet Metab.* **94**, 120-126.

Mineri R, Rimoldi M, Burlina AB, Koskull S, Perletti C, Heese B, von Döbeln U, Mereghetti P, Di Meo I, Invernizzi F, Zeviani M, Uziel G, Tiranti V (2008). **Identification of new mutations in the ETHE1 gene in a cohort of 14 patients presenting with ethylmalonic encephalopathy**. *J Med Genet* **45**, 473–478.

Moore A and Golden A (2009). **Hypothesis: Bifunctional Mitochondrial Proteins Have Centrosomal Functions.** *Environmental and Molecular Mutagenesis* **50**, 637-648.

Morrow G and Tanguay RM (2008). **Mitochondria and ageing in *Drosophila.*** *Biotechnol J* **3,** 728–739.
Nakano K, Balint E, Ashcroft M and Vousden KH (2000). **A ribonucleotide reductase gene is a transcriptional target of p53 and p73**. *Oncogene* **19,** 4283–4289.

Nass MM and Nass S (1963). **Intramitochondrial Fibers with DNA characteristics**. *J Cell Biol Bd* **19**, 593–629.

Neupert W (1997). **Protein import into mitochondria**. *Annu Rev Biochem* **66**, 863–917.

Nijtmans LG, Henderson NS and Holt IJ (2002**). Blue native electrophoresis to study mitochondrial and other protein complexes.** *Methods* **26,** 327–334.

Nijtmans LG, Sanz MA, Bucko M, Farhoud MH, Feenstra M, Hakkaart GA, Zeviani M, Grivell LA (2001). **Shy1p occurs in a high molecular weight complex and is required for efficient assembly of cytochrome c oxidase in yeast.** *FEBS Lett* **498**, 46–51.

Nishigaki Y, Marti R, Copeland WC and Hirano M (2003). **Site-specific somatic mitochondrial DNA point mutations in patients with thymidine phosphorylase deficiency**. *J Clin Invest* **111,** 1913–1921.

Nishino I, Spinazzola A and Hirano M (1999). **Thymidine phosphorylase gene mutations in MNGIE, a human mitochondrial disorder**. *Science* **283,** 689–692.

Nobrega FG, Nobrega MP and Tzagoloff A (1992). **BCS1, a novel gene required for the expression of functional Rieske iron–sulfur protein in *Saccharomyces cerevisiae*.** *EMBO J* **11**, 3821–3829.

Nowaczyk MJ, Lehotay DC, Platt BA, Fisher L, Tan R, Phillips H, Clarke JT (1998). **Ethylmalonic and methylsuccinic aciduria in ethylmalonic encephalopathy arise from abnormal isoleucine metabolism**. *Metabolism* **47**, 836–839.

Ozand PT, Rashed M, Millington DS, Sakati N, Hazzaa S, Rahbeeni Z, Al Odaib A, Youssef N, Mazrou A, Gascon GG, Brismar (1994). **Ethylmalonic aciduria: an organic acidemia with CNS involvement and vasculopathy.** *Brain Dev* **16**, 12–22.

Pagliarini DJ, Calvo SE, Chang B, Sheth SA, Vafai SB, Ong SE, Walford GA, Sugiana C, Boneh A, Chen WK (2008). **A mitochondrial protein compendium elucidates complex I disease biology**. *Cell* **134**, 112–123.

Palmieri F (2004). **The mitochondrial transporter family (SLC25): physiological and pathological implications.** *Pflueger's Arch* **447**, 689–709.

Palmieri L, Runswick MJ, Fiermonte G, Walker JE and Palmieri F (2000). **Yeast mitochondrial carriers: bacterial expression, biochemical identification and metabolic significance.** *J Bioenerg Biomembr* **32**, 67–77.

Papa S (1996). **Mitochondrial oxidative phosphorylation changes in the life span. Molecular aspects and physiopathological implications.** *Biochim Biophys Acta* **1276**, 87-105

Parks AL. Cook KR, Belvin M, Dompe NA, Fawcett R, Huppert K, Tan LR, Winter CG, Bogart KP, Deal JE (2004). **Systematic generation of high-resolution deletion coverage of the *Drosophila melanogaster* genome.** *Nat Genet* **36**, 288-292.

Pebay-Peyroula E, Dahout-Gonzalez C, Kahn R, Trezeguet V, Lauquin GJ and Brandolin G (2003). **Structure of mitochondrial ADP/ATP carrier in complex with carboxyatractyloside.** *Nature* **426**, 39–44.

Pequignot MO, Desguerre I, Dey R, Tartari M, Zeviani M, Agostino A, Benelli C, Fouque F, Prip-Buus C, Marchant D, Abitbol M, Marsac C (2001). **New splicing-site mutations in the SURF1 gene in Leigh syndrome patients.** *J Biol Chem* **276**(18), 15326{9.

Pfaffl MW (2001). **A new mathematical model for relative quantification in real-time RT-PCR**. *Nucleic Acids Res* **29**, e45.

Piccin A, Salameh A, Benna C, Sandrelli F, Mazzotta G, Zordan M, Rosato E, Kyriacou CP, Costa R (2001). **Efficient and heritable functional knock-out of an adult phenotype in Drosophila using a GAL4-driven hairpin RNA incorporating a heterologous spacer**. *Nucleic Acids Res* **E55**, 12–29.

Piskur J, Sandrini MP, Knecht W and Munch-Petersen B (2004). **Animal deoxyribonucleoside kinases: 'forward' and 'retrograde' evolution of their substrate specificity**. *FEBS Lett* **560,** 3–6.

Pontarin G, Ferraro P, Hakansson P, Thelander L, Reichard P and Bianchi V (2007). **p53R2-dependent ribonucleotide reduction provides deoxyribonucleotides in quiescent human fibroblasts in the absence of induced DNA damage**. *J Biol Chem* **282,** 16820–16828.

Pontarin G, Ferraro P, Valentino ML, Hirano M, Reichard P and Bianchi V (2006). **Mitochondrial DNA depletion and thymidine phosphate pool dynamics in a cellular model of mitochondrial neurogastrointestinal encephalomyopathy**. *J Biol Chem* **281,** 22720–22728.

Pontarin G, Gallinaro L, Ferraro P, Reichard P and Bianchi V (2003). **Origins of mitochondrial thymidine triphosphate: Dynamic relations to cytosolic pools**. *Proc Natl Acad Sci USA* **100,** 12159–12164.

Poyau A, Buchet K, Godinot C (1999). **Sequence conservation from human to prokaryotes of *Surf1*, a protein involved in cytochrome c oxidase assembly, deficient in Leigh syndrome**. *FEBS Lett* 462(3):416{20.

Rampazzo C, Fabris S, Franzolin E, Crovatto K, Frangini M and Bianchi V (2007). **Mitochondrial thymidine kinase and the enzymatic network regulating thymidine triphosphate pools in cultured human cells**. *J Biol Chem* **282,** 34758–34769.

Rampazzo C, Ferraro P, Pontarin G, Fabris S, Reichard P and Bianchi V (2004). **Mitochondrial Deoxyribonucleotides, Pool Sizes, Synthesis, and Regulation**. *J Biol Chem* **279,** 17019–17026.

Rampazzo C, Gallinaro L, Milanesi E, Frigimelica E, Reichard P and Bianchi V (2000). **A deoxyribonucleotidase in mitochondria: involvement in regulation of dNTPs pools and possible link to genetic disease.** *Proc. Natl. Acad. Sci. USA* **97,** 8239–8244.

Regan C and Fuller MT (1990). **Interacting genes that affect microtubule function in Drosophila melanogaster: two classes of mutations revert the failure to complement between haync2 and mutations in tubulin genes.** *Genetics* **125**, 77–90.

Ridderstrom M, Saccucci F, Hellman U, Bergman T, Principato G, Mannervik B (1996). **Molecular cloning, heterologous expression, and characterization of human glyoxalase II.** *J Biol Chem* **271**, 319–323.

Roberts DB and Standen GN (1998). **The elements of Drosophila biology and genetics, pp. 1–54 in Drosophila**: A Practical Approach, edited by D. B. Roberts. IRL Press, Oxford.

Rosenberg MJ, Agarwala R, Bouffard G, Davis J, Fiermonte G, Hilliard MS, Koch T, Kalikin LM, Makalowska I, Morton DH (2002). **Mutant deoxynucleotide carrier is associated with congenital microencephaly.** *Nat. Genet.* **32,** 175–179.

Rouslin W (1983). **Mitochondrial complexes I, II, III, IV, and V in myocardial ischemia and autolysis.** *Am. J. Physiol* **244**, H743-H748.

Rouslin W, Millard RW (1981). **Mitochondrial inner membrane enzyme defects in porcine myocardial ischemia.** *Am J Physiol***240**, H308-H313.

Rouslin W, Ranganathan S (1983). **Impaired function of mitochondrial electron transfer complex I in canine myocardial ischemia: loss of flavin mononucleotide.** *J Mol Cell Cardiol* **15**, 537-542.

Saada A, Shaag A, Mandel H, Nevo Y, Eriksson S and Elpeleg O (2001). **Mutant mitochondrial thymidine kinase in mitochondrial DNA depletion myopathy**. *Nat Genet* **29,** 342–344.

Sagona AP, Nezis IP, Pedersen NM. Liestøl K, Poulton J, Rusten TE, Skotheim RI, Raiborg C and Stenmark H (2010). **PtdIns(3)P controls cytokinesis through KIF13Amediated recruitment of FYVE-CENT to the midbody**. *Nat Cell Biol* **12**, 362-371.

Sandrelli F, Campesan M, Rossetto G, Benna C, Zieger E (2001). **Molecular dissection of the 59 region of no-on-transientA of *Drosophila melanogaster* reveals cis-regulation by adjacent dGpi sequences**. *Genetics* **157**, 765–775.

Sass JO, Ensenauer R, Röschinger W, Reich H, Steuerwald U, Schirrmacher O, Engel K, Häberle J, Andresen BS, Mégarbané A, Lehnert W, Zschocke J (2008). **2-Methylbutyryl-coenzyme A dehydrogenase deficiency: functional and molecular studies on a defect in isoleucine catabolism**. *Mol Genet Metab* **93**, 30–35.

Schägger H and von Jagow G (1987). **Tricine-sodium dodecyl sulfate-polyacrylamide gel electrophoresis for the separation of proteins in the range from 1 to 100 kDa**. *Anal Biochem* **166**, 368–379.

Schägger H, Link TA, Engel WD and von Jagow G (1986). **Isolation of the eleven protein subunits of the bc1 complex from beef heart.** *Methods Enzymol* **126**, 224–237.

Schon EA (2000). **Mitochondrial genetics and disease**. *Trends Biochem Sci* **5**, 555–560.

Sciacco M and Bonilla E (1996). **Cytochemistry and immunocytochemistry of mitochondria in tissue sections**. *Methods Enzymol* **264**, 509–521.

Shields DC, Sharp PM, Higgins DG, Wright F (1988).**"Silent" sites in Drosophila genes are not neutral: evidence of selection among synonymous codons**. *Mol Biol Evol*, **5(6)**, 704–716.

Small ID and Peeters N (2000). **The PPR motif a TPR-related motif prevalent in plant organellar proteins**. *Trends Biochem. Sci.* **25**, 46–47.

Smeitink J, van den Heuvel L and DiMauro S (2001). **The genetics and pathology of oxidative phosphorylation.** *Nat Rev Genet* **2**, 342–352.

Smeitink JA (2003). **Mitochondrial disorders: clinical presentation and diagnostic dilemmas**. *J Inher Metab Dis* **26**, 199–207.

Solans A, Zambrano A and Barrientos A (2004). **Cytochrome c oxidase deficiency: from yeast to human.** *Preclinica*, **2**, 1–13.

Spinazzola A and Zeviani M (2005). **Disorders of nuclear-mitochondrial intergenomic signaling**. *Gene* **354,** 162–168.

Szabo C (2007). **Hydrogen sulphide and its therapeutic potential.** *Nat Re. Drug Discov* **6**, 917–935.

Tanaka H, Arakawa H, Yamaguchi T, Shiraishi K, Fukuda S, Matsui K, Takei Y and Nakamura Y (2000). **A ribonucleotide reductase gene involved in a p53- dependent cell-cycle checkpoint for DNA damage**. *Nature* **404,** 42–49.

Tanaka K, Ramsdell HS, Baretz BH, Keefe MB, Kean EA, Johnson B (1976). **Identification of ethylmalonic acid in urine of two patients with the vomiting sickness of Jamaica**. *Clin Chim Acta* **69**, 105–112.

Thibault ST, Singer AM, Miyazaki YW, Milash B, Dompe AN, Singh MC,Buchholz R, Demsky M, Fawcett R, Francis-Lang LH, Ryner L (2004). **A complementary transposon toolkit for *Drosophila melanogaster*.** *Nat. Genet*. advance online publication, 22 February (doi:10.1038/ng1314).

Till BJ, Colbert T, Tompa R, Enns LC, Codomo CA, Johnson JE, Reynolds SH, Henikoff JG, Greene EA, Steine MN, Comai L, Henikoff S (2003). **High-throughput TILLING for functional genomics.** *Methods Mol Biol* **236**, 205–220.

Tiranti V, Briem E, Ferrari G, Lamantea E, Papaleo E, De Gioia L, Rinaldo P, Dickson P, Abu-LibdeH B, Heberle L, Owaidha M, Jack RM,,Christensen E, Zeviani M. (2006). ***Ethe1*** **mutations are a prevalent cause of Ethylmalonic Encephalopathy.** *J Med Genet* **43**, 340–346.

Tiranti V, Galimberti C, Nijtamns L, Bovolenta S, Perini MP and Zeviani M (1999a). **Characterization of SURF-1 expression and Surf-1p function in normal and disease conditions.** *Hum Mol Genet* **8**, 2533–2540.

Tiranti V, Hoertnagel K, Carrozzo R, Galimberti C, Munaro M, Granatiero M, Zelante L, Gasparini P, Marzella R, Rocchi M (1998). **Mutations of SURF-1 in Leigh disease associated with cytochrome c oxidase deficiency.** *Am J Hum Genet* **63**, 1609-1621.

Tiranti V, Viscomi C, Hildebrandt T, Di Meo I, Mineri R, Tiveron C, Levitt MD, Prelle A, Fagiolari G, Rimoldi, Zeviani M (2009). **Loss of *Ethe1*, a mitochondrial dioxygenase, causes fatal sulfide toxicity in ethylmalonic encephalopathy.** *Nat Med* **15**, 200–205.

Tiranti V, D'Adamo P, Briem E, Ferrari G, Mineri R, Lamantea E, Mandel H, Balestri P, Garcia-silva MT, Vollmer B, Rinaldo P, Hahn SH, Leonard J, Rahman S, Dionisi-VicI C, Garavaglia B, Gasparini P, Zeviani M (2004). **Ethylmalonic encephalopathy is caused by mutations in *Ethe1*, a gene encoding a mitochondrial matrix protein**. *Am J Hum Genet* **74**, 239–252.

Tiranti VM, Jaksh S, Hofman C, Galimberti K, Hoertnagel C (1999b). **Loss-of-function mutations of SURF1 are specifically associated with Leigh syndrome with cytochrome c oxidase deficiency**. *Ann Neurol* **46**, 161–166.

Todisco S, Agrimi G, Castegna A and Palmieri F (2006). **Identification of the mitochondrial NAD-transporter in *Saccharomyces cerevisiae*.** *J Biol Chem* **281**, 1524–1531.

van den Ouweland JM, Lemkes HH, Ruitenbeek W, Sandkuijl LA, de Vijlder MF, Struyvenberg PA, van de Kamp JJ, Maassen JA (1992). **Mutation in mitochondrial tRNA(Leu)(UUR) gene in a large pedigree with maternally transmitted type II diabetes mellitus and deafness.** *Nat Genet* **1**, 368–71.

Vockley J and Ensenauer R (2006). **Isovaleric acidemia: new aspects of genetic and phenotypic heterogeneity.** *J Med Genet* **142**, 95–103.

Vozza A, Blanco E, Palmieri L and Palmieri F (2004). **Identification of the mitochondrial GTP/GDP transporter in Saccharomyces cerevisiae**. *J Biol Chem* **279,** 20850–20857.

Wallace DC (1999b). **Mitochondrial diseases in man and mouse**. *Science*, **283**, 1482–8.

Wallace DC, Brown MD, Lott MT. (1999). **Mitochondrial DNA variation in human evolution and disease.** *Gene* **238**, 211–30.

Wallace DC, Zheng X, Lott MT, Shoffner JM, Hodge JA, Kelley RI, Epstein CM, Hopkins LC, (1988). **Familial mitochondrial encephalomyopathy (MERRF): genetic, pathophysiological, and biochemical characterization of a mitochondrial DNA disease**. *Cell* **55**, 601–610.

Wang B, Li N, Sui L, Wu Y, Wang X, Wang Q, Xia D, Wan T and Cao X (2004). **HuBMSC-MCP, a novel member of mitochondrial carrier superfamily, enhances dendritic cell endocytosis.** *Biochem Biophys Res Commun* **314**, 292–300.

Wang L, Munch-Petersen B, Herrstrom-Sjoberg A, Hellman U, Bergman T, Jornvall H and Eriksson S (1999). **Human thymidine kinase 2: molecular cloning and characterization of the enzyme activity with antiviral and cytostatic nucleoside substrates.** *FEBS Lett.* **443,** 170–174.

Wiedemann, N., Frazier, A.E., and Pfanner, N. (2004). **The protein import machinery of mitochondria.** *J Biol Chem* **279**, 14473–14476.

Wiesner RJ, Ruegg JC, Morano I (1992). **Counting target molecules by exponential polymerase chain reaction, copy number of mitochondrial DNA in rat tissues.** *Biochim Biophys Acta* **183** (2): 553–559.

Wimplinger I, Morleo M, Rosenberger G, Iaconis D, Orth U, Meinecke P, Lerer I, Ballabio A, Gal A, Franco B, and Kutsche K (2006). **Mutations of the Mitochondrial Holocytochrome *c*–Type Synthase in X-Linked Dominant Microphthalmia with Linear Skin** Defects Syndrome AJHG 79, 878-889.

Wittig I, Braun HP and Schagger H (2006). **Blue native PAGE**. *Nat Protoc* **1**, 418–428.

Wu M, Neilson A, Swift AL, Moran R, Tamagnine J, Parslow D, Armistead S, Lemire K, Orrell J, Teich J, Chomicz S and Ferrick DA (2007). **Multiparameter metabolic analysis reveals a close link between attenuated mitochondrial bioenergetic function and**

enhanced glycolysis dependency in human tumor cells. *Am J Physiol Cell Physiol* **292,** C125–C136.

Xu F, Ackerley C, Maj MC, Addis JBL, Levandovskiy V, Lee J, MacKay N, Cameron J M and Robinson BH (2008). **Disruption of a mitochondrial RNA-binding protein gene results in decreased cytochrome b expression and a marked reduction in ubiquinol–cytochrome c reductase activity in mouse heart mitochondria.** *Biochem J* **416**, 15–26.

Yao J, Shoubridge EA (1999). **Expression and functional analysis of SURF1 in Leigh syndrome patients with cytochrome c oxidase deficiency.** *Hum Mol Genet*, **8**(13), 2541{9.

Yao KM, and. White K (1994). **Neural specificity of *elav* expression: defining a Drosophila promoter for directing expression to the nervous system.** *J Neurochem* **63**, 41–51.

Yoon HR, Hahn SH, Ahn YM, Jang SH, Shin YJ, Lee EH, Ryu KH, Eun BL, Rinaldo P, Yamaguchi S (2001). **Therapeutic trial in the first three Asian cases of ethylmalonic encephalopathy: response to riboflavin**. *J Inherit Metab Dis* **24**, 870–873.

Young P, Leeds JM, Slabough MB and Mathews C (1994). **Ribonucleotide reductase: evidence for specific association with HeLa cell mitochondria.** *Biochem Biophys Res Commun* **203,** 9300–9304.

Zara V, Palmisano I, Conte L and Trumpower BL (2004). **Further insights into the assembly of the yeast cytochrome *bc1* complex based on analysis of single and double deletion mutants lacking supernumerary subunits and cytochrome *b*.** *Eur J Biochem* **271**, 1209–1218.

Zeviani M and Di Donato S (2004). **Mitochondrial disorders**. *Brain* **127**, 2153–2172.

Zhang JC, Sun L, Nie QH, Huang CX, Jia ZS, Wang JP, Lian JQ, Li XH, Wang PZ, Zhang Y (2009). **Down-regulation of CXCR4 expression by SDF-KDEL in CD34(+) hematopoietic stem cells: an antihuman immunodeficiency virus strategy.** *J Virol Methods* **16**, 30-37.

Zhang YQ, Roote J, Brogna S, Davis AW, Barbash DA, Nash D and Ashburner M (1999). ***Stress sensitive B* encodes an adenine nucleotide translocase in *Drosophila melanogaster*.** *Genetics* **153**, 891-903.

Zhu C, Johansson M and Karlsson A (2000). **Incorporation of nucleoside analogs into nuclear or mitochondrial DNA is determined by the intracellular phosphorylation site**. *J Biol Chem* **275,** 26727–26731.

Zhu Z, Yao J, Johns T, Fu K, Bie ID, Macmillan C, Cuthbert AP, Newbold RF, Wang J, Chevrette M, Brown GK, Brown RM, Shoubridge EA (1998). **SURF1, encoding a factor involved in the biogenesis of cytochrome c oxidase, is mutated in Leigh syndrome**. *Nat Genet*, **20**(4):337{43.

Zordan M.A, Massironi M, Ducato MG, Te Kronnie G, Costa R (2005). **Drosophila CAKI/CMG protein, a homolog of human CASK, is essential for regulation of neurotransmitter vesicle release**. *J Neurophysiol* **94**, 1074–1083.

Zordan MA, Cisotto P, Benna C, Agostino A, Rizzo G, Piccin A, Pegoraro M, Sandrelli F, Perini G, Tognon G, DeCaro R, Peron S, Kronni TT, Megighian A, Reggiani C, Zeviani M, Costa R (2006). **Post-transcriptional silencing and functional characterization of the Drosophila melanogaster homolog of human *Surf1*.** *Genetics* **41**, 172–229.